ZooKeys 1061: 1–9 (2021)
doi: 10.3897/zookeys.1061.73114
https://zookeys.pensoft.net

RESEARCH ARTICLE

A peer-reviewed open-access journal
ZooKeys
Launched to accelerate biodiversity research

First record of the lac-producing species *Kerria nepalensis* Varshney (Hemiptera, Kerriidae) from China, with a key to Chinese species

Nawaz Haider Bashir[1], Weiwei Wang[1], Juan Liu[1], Wei Wang[1], Hang Chen[1,2]

1 *Research Institute of Resource Insects, Chinese Academy of Forestry, Kunming, China* **2** *The Key Laboratory of Cultivating and Utilization of Resources Insects, State Forestry Administration, Kunming, China*

Corresponding author: Hang Chen (stuchen6481@gmail.com)

Academic editor: Roger Blackman | Received 17 August 2021 | Accepted 30 August 2021 | Published 28 September 2021

http://zoobank.org/77FEE74A-62DD-44D4-944B-130BEE3EC3E2

Citation: Bashir NH, Wang W, Liu J, Wang W, Chen H (2021) First record of the lac-producing species *Kerria nepalensis* Varshney (Hemiptera, Kerriidae) from China, with a key to Chinese species. ZooKeys 1061: 1–9. https://doi.org/10.3897/zookeys.1061.73114

Abstract

Lac insects include astonishing species responsible for lac production. Lac is composed of resins, dyes, and shellac wax with significant economic importance. Previously, 11 species of the genus *Kerria* were reported from China, with the highest species diversity in Yunnan province. Another lac-producing species of the genus *Kerria*, namely *Kerria nepalensis* Varshney, is recorded for the first time in Yunnan province, China, on *Dalbergia cochinchinensis* Pierre ex Laness. (Fabaceae), a new host plant. In addition, a key to the 12 *Kerria* species recorded in China is also given.

Keywords

Coccoidea, lac insects, Oriental China, taxonomy

Introduction

Scale insects (Hemiptera, Coccoidea) are classified into 35 extant families, with more than 8300 described species to date (García Morales et al. 2016). These are phytophagous insects found in all zoogeographical realms except Antarctica (Ahmad et al. 2014). Lac insects belong to family Kerriidae, which is comprised of nine genera and 101 species worldwide (García Morales et al. 2016). Currently, the genus *Kerria* contains 29 species known in Asia (Table 1) and distributed in tropical and subtropical regions

(Varshney and Sharma 2020). More than 20 species of *Kerria* have been described and recorded from India, Myanmar, Nepal, Pakistan, and Thailand. So far, 11 species of the genus *Kerria* have been reported from China (Varshney 1976; Chen et al. 2011), with *K. ruralis* (Wang, Yao, Teui & Liang) and *K. yunnanensis* (Ou & Hong) being endemic species (Chen et al. 2013).

Lac insects are fully depending on their host plant and till now, more than 400 host plants have been recorded (Sharma 2017). Ber (*Ziziphus mauritiana* Lam.: Rhamnaceae), Kusum (*Schleichera oleosa* Lour.: Sapindaceae), and Palas (*Butea monosperma* Lam.: Fabaceae) are the common host plants for the production of lac in India (Bhatnagar et al. 2020), whereas *Acacia catechu* Willd., *A. nilotica* Willd. ex Delile (Fabaceae), *Butea monosperma*, *Samanea saman* (Jacq.) Merr., (Fabaceae), and *Ziziphus mauritiana* are potential lac host plants in Bangladesh (Ferdousee et al. 2010). Lac host plants in China are *Dalbergia szemaoensis* Prain, *D. assamica* Benth, *D. obtusifolia* Prain, *Pueraria tonkinensis* Gagn. (Fabaceae), *Ficus altissima* Blume, and *F. racemosa* L. (Moraceae) (Chen et al. 2010, 2011).

Herein, we redescribe and illustrate *K. nepalensis* Varshney, a species recorded for the first time from Yunnan province and China. We also provide a key to the 12 Chinese species of *Kerria*.

Table 1. Worldwide distribution of the genus *Kerria*.

No.	Species	Distribution	Reference
1	*Kerria albizziae* (Green, 1911)	India, Myanmar, Sri Lanka	Varshney 1976; Chen et al. 2013
2	*Kerria brancheata* Varshney, 1966	India	Varshney 1976
3	*Kerria canalis* Rajgopal, 2021	India	Rajgopal et al. 2021
4	*Kerria chamberlini* Varshney, 1966	Bhutan, China, India, Myanmar, Nepal, Thailand	Varshney 1976; Chen et al. 2013
5	*Kerria chinensis* (Mahdihassan, 1923)	Bhutan, Cambodia, China, India, Myanmar, Nepal, Thailand, Vietnam	Chen et al. 2011, 2013; Varshney and Sharma 2020
6	*Kerria communis* (Mahdihassan, 1923)	India	Varshney 1976
7	*Kerria destructor* Talukder & Das, 2020	India	Talukder and Das 2020
8	*Kerria dubeyi* Ahmad & Ramamurthy, 2013	India	Ahmad et al. 2013a
9	*Kerria ebrachiata* (Chamberlin, 1923)	India, Myanmar, Nepal, Pakistan	Varshney 1976; Chen et al. 2013
10	*Kerria fici* (Green, 1903)	China, India, Pakistan, Thailand	Varshney and Sharma 2020
11	*Kerria greeni* (Chamberlin, 1923)	China, Philippine, Thailand	Chen et al. 2013
12	*Kerria indicola* (Kapur, 1958)	India	Varshney 1976
13	*Kerria javana* (Chamberlin, 1925)	India, Indonesia, Malaysia	Chamberlin 1925; Chen et al. 2013
14	*Kerria lacca* (Kerr, 1782)	Azerbaijan, Bangladesh, China, Georgia, Guyana, India, Malaysia, Myanmar, Nepal, Pakistan, Sri Lanka, Thailand	Chen et al. 2013; Varshney and Sharma 2020
15	*Kerria maduraiensis* Ahmad & Ramamurthy, 2013	India	Ahmad et al. 2013b
16	*Kerria manipurensis* Ahmad & Ramamurthy, 2013	India	Ahmad et al. 2013b
17	*Kerria mengdingensis* Zhang, 1993	China	Zhang 1993
18	*Kerria meridionalis* (Chamberlin, 1923)	China, Philippines, Thailand	Chen et al. 2013
19	*Kerria nagoliensis* (Mahdihassan, 1923)	Bangladeshi, India, Pakistan	Varshney 1976; Chen et al. 2013
20	*Kerria nepalensis* Varshney, 1976	China, India, Myanmar, Nepal	Varshney 1976; Chen et al. 2011
21	*Kerria pennyae* Ahmad & Ramamurthy, 2013	India	Ahmad et al. 2013a
22	*Kerria pusana* (Misra, 1930)	India, Indonesia, Malaysia, Myanmar	Varshney 1976; Chen et al. 2013, 2011;
23	*Kerria rangoonensis* (Chamberlin, 1925)	China, India, Indonesia, Myanmar, Thailand	Chamberlin 1925; Varshney 1976; Chen et al. 2013
24	*Kerria ruralis* (Wang, Yao, Teui & Liang, 1982)	China	Chen et al. 2011
25	*Kerria sharda* Mishra & Sushil, 2000	India	Varshney and Sharma 2020
26	*Kerria sindica* (Mahdihassan, 1923)	Bangladesh, China, India, Pakistan	Chen et al. 2011, 2013
27	*Kerria thrissurensis* Ahmad & Ramamurthy, 2013	India	Ahmad et al. 2013b
28	*Kerria varshneyi* Ahmad & Ramamurthy, 2013	India	Ahmad et al. 2013a
29	*Kerria yunnanensis* (Ou & Hong, 1990)	China	Chen et al. 2011

Materials and methods

Twigs bearing *K. nepalensis* (new record) were collected by Dr Juan Liu from roadside *Dalbergia cochinchinensis* trees at Mengzi city (22°56'N, 103°32'E), Yunnan province, China, on 15 September 2020. Fresh samples of adult females were preserved in 75% ethanol. Specimens were placed in 10% KOH for few hours and rinsed in 5–8 changes of distilled water for preparation of permanent slides as described previously (Chen et al. 2008). The photographs and measurements were taken with a Keyence VHX-1000 digital microscope. Terminology mainly follows Kondo and Gullan (2007) and Ahmad et al. (2013b). All specimens are deposited in the museum of Research Institute of Resource Insects, Kunming, China (**RIRI-CAF**).

More than 10 individuals were selected for observation under electron microscope. The dehydration of specimens was accomplished by passing through a series of increasing alcohol concentrations as 30%, 50%, 70%, 80%, 90%, and 95% alcohol (Mehdizadeh et al. 2014). They were placed on a conductive resin and gilded for 60 sec in an ion plating machine (JS-1600, Beijing Htcy Technology Co., Ltd, China) and then observed under an electron microscope (TM3000, Hitachi High-Technologies Corporation, Japan). Photographs were arranged by using Adobe Photoshop 8.0.

Taxonomy

Class Insecta Linnaeus, 1758
Order Hemiptera Linnaeus, 1758
Suborder Sternorrhyncha Amyot & Audinet-Serville, 1843
Superfamily Coccoidea Handlirsch, 1903
Family Kerriidae Lindinger, 1937
Genus *Kerria* Targioni Tozzetti, 1884

***Kerria nepalensis* Varshney, 1976**
Figures 1, 2

Material examined. China: Yunnan: Mengzi city, 22°56'N, 103°32'E, 15.IX.2020, coll. Juan Liu, *Dalbergia cochinchinensis* (Fabaceae), 5 slides (10 adult ♀♀).

Diagnosis. Adult female: body generally large globular to elongate in shape, 1.7–3.87 mm long, 1.16–2.42 mm wide (Fig. 1F, G).

***Dorsum*.** Anal tubercle well developed, elongate, 320–1100 μm long, 170–680 μm wide, apparently two-segmented (Figs 1A, 2B) and bearing 6–15 anal ring setae, each 80–90 μm long (Fig. 2A); supra anal plate heavily sclerotized, a little longer than broad, with few small setae on each side (Fig. 2B); brachia oval, elongate (Figs 1B, 2E), heavily sclerotized; brachial plate nearly circular, broader than long; brachial crater circular and small, 80–160 μm long, 70–130 μm wide, 0.03–0.07 mm^2 in center; brachial tube 210–460 μm long, dimples inconspicuous, uncountable due to thick sclerotiza-

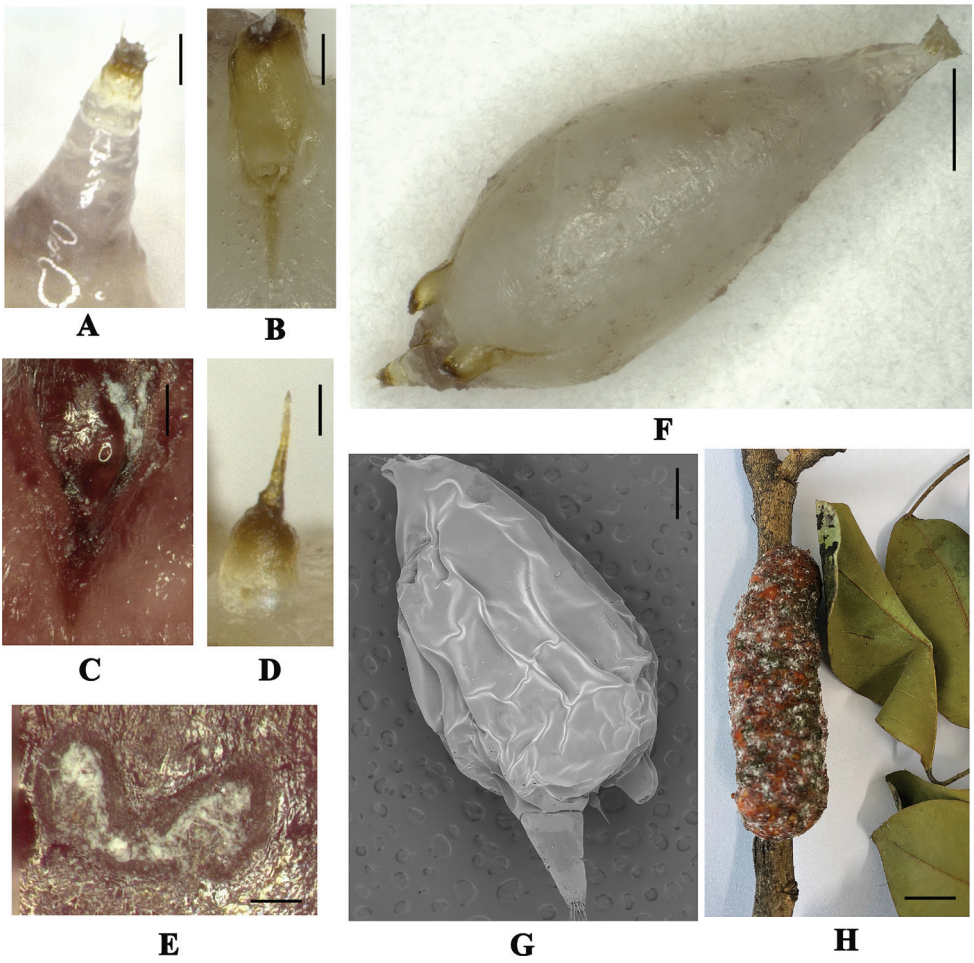

Figure 1. *Kerria nepalensis*. **A** anal tubercle **B** brachia **C** anterior spiracle **D** dorsal spine **E** marginal duct cluster **F, G** body **H** lac tests, ex *Dalbergia cochinchinensis* (**A–F, H** Light micrographs **G** Scanning electron micrographs). Scale bars: 1000 µm (**A**), 200 µm (**B–G**), 1 cm (**H**).

tion (Fig. 2F); anterior spiracles widely separated (Figs 1C, 2G), 220–400 µm away from brachial plate, canellar bands below anterior spiracles as a chitinous extension 150–300 µm long (Fig. 1B, C); dorsal spine 170–190 µm long, pedicel longer and tubular in shape 80–160 µm long, 70–130 µm wide at widest point (Figs 1D, 2K).

Venter. Antennae very small, conical shaped, probably one segmented, with 4 fleshy and 2 short hair-like setae (Fig. 2J); mouthparts with labium length 600–780 µm, width 70–180 µm, post oral lobes each 75–140 µm wide (Fig. 2L); legs vestigial; posterior spiracles much smaller with fine pores on each side; perivulvar pores 14–31 in number on each side of anal tubercle (Fig. 2C, D); marginal duct clusters convoluted (Figs 1E, 2H), 6 in number, each with 30–36 ducts (Fig. 2I); ventral duct clusters with 3 pairs, irregular in shape.

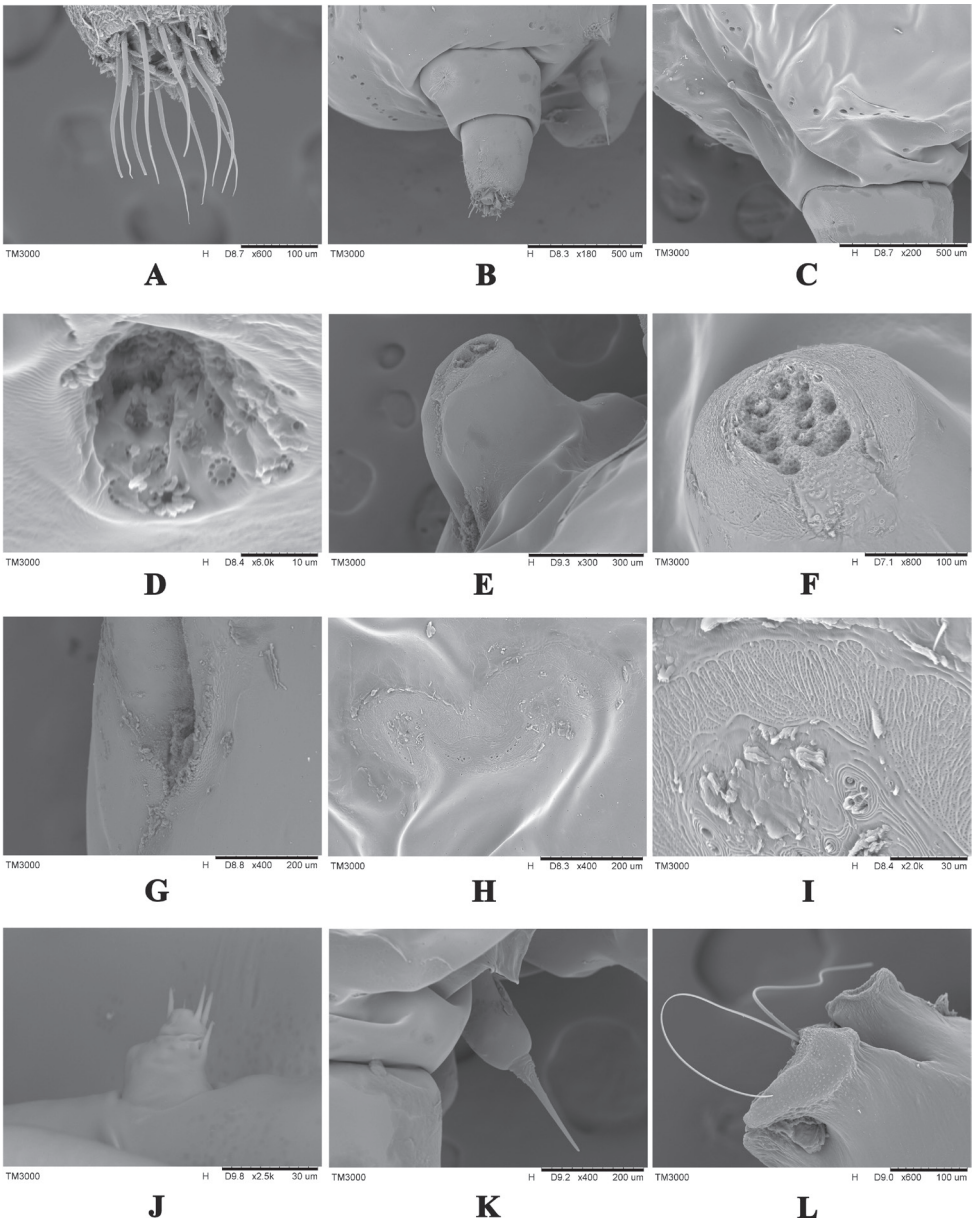

Figure 2. *Kerria nepalensis* scanning electron micrographs **A** anal ring setae **B** anal tubercle and dorsal spine **C** perivulvar pore cluster **D** magnified single perivulvar pore **E** brachia **F** brachial plate with dimples **G** anterior spiracle **H** a marginal duct cluster **I** a magnified marginal duct cluster **J** antenna **K** dorsal spine **L** mouthparts. Scale bars: 10 μm (**D**), 30 μm (**I, J**), 100 μm (**A, F, L**), 200 μm (**G, H, K**), 300 μm (**E**), 500 μm (**B, C**).

Distribution. India, Myanmar, Nepal (Varshney and Sharma 2020), China (Yunnan).

Host plants. *Dalbergia cochinchinensis* (specimens collected in this study), *Litchi chinensis* (Varshney 1976), and *Ficus* sp. (Chen et al. 2011).

Key to species of the genus *Kerria* from China

1 Anal tubercle (supra anal plate) elongate, distinctly longer than broad **2**
– Anal tubercle (supra anal plate) abbreviated, length subequal to width or broader than long **6**
2 Canellar pore bands present as a chitinous extension below anterior spiracles.... **3**
– Canellar pore bands absent **4**
3 Canellar pore bands below anterior spiracles short, 150–300 μm long; dorsal spine 170–190 μm long ..... ***K. nepalensis* Varshney**
– Canellar pore bands below anterior spiracles very long, 300–500 μm long; dorsal spine 190–240 μm long ..... ***K. chinensis* (Mahdihassan)**
4 Length of brachia subequal or shorter than length of supra anal plate ..... ***K. chamberlini* Varshney**
– Length of brachia distinctly greater than length of supra anal plate **5**
5 Supra anal plate smooth; brachial plate with 10–12 distinct dimples; each marginal duct cluster with 25–30 ducts..... ***K. lacca* (Kerr)**
– Supra anal plate hispid; brachial plate with 8–15 indistinct dimples; each marginal duct cluster with 30–36 ducts..... ***K. yunnanensis* (Ou & Hong)**
6 Each marginal duct cluster with 70–75 ducts; distance between anterior spiracle and brachial plate 17–34 μm..... ***K. mengdingensis* Zhang**
– Each marginal duct cluster with more than 20 ducts; distance between anterior spiracle and brachial plate greater than 34 μm..... **7**
7 Brachial plate diameter equal or greater than length of supra anal plate..... **8**
– Brachial plate diameter distinctly less than length of supra anal plate **10**
8 Brachial tube 65–90 μm long; anterior spiracles 180–260 μm long..... ***K. ruralis* (Wang, Yao, Teui & Liang)**
– Brachial tube 170–340 μm long; anterior spiracles 130–180 μm long..... **9**
9 Brachial crater not in center of plate, found near the margin; dimples obscure and small; crater rim open ..... ***K. sindica* (Mahdihassan)**
– Brachial crater in center of plate; dimples large and distinct; crater rim closed .... ***K. fici* (Green)**
10 Brachial crater not well defined; number of perivulvar pore clusters 68–70 ..... ***K. rangoonensis* (Chamberlin)**
– Brachial crater well defined; number of perivulvar pore clusters less than 60.... **11**
11 Marginal duct clusters duplex, with large nuclear ducts; number of perivulvar pore clusters 58 ..... ***K. greeni* (Chamberlin)**
– Marginal duct clusters simplex, no large nuclear ducts present; number of perivulvar pore clusters less than 50 ..... ***K. meridionalis* (Chamberlin)**

Discussion

Kerria nepalensis was identified and described on host *Litchi chinensis* from India and Nepal by Varshney (1976). Later it was also recorded from Myanmar (Chen et al.

2011), where it was used for commercial lac production. This species is present in tropical monsoon climates with an average annual precipitation of 800–1000 mm, temperature of 23–29 °C, and at low elevations about 200 m (Chen et al. 2011). *Litchi chinensis* (Sonn.) and *Ficus* sp. were the known host plant of *K. nepalensis* (Chen et al. 2011; Varshney and Sharma 2020). We here report *Dalbergia cochinchinensis* as a host of *K. nepalensis*. *Dalbergia cochinchinensis* Pierre ex Laness. is commonly known as Siam Rosewood or Rosewood (Sriudorn and Benchawattananon 2018). It prefers sandy-clay soil, where the mean annual rainfall is 1200–1650 mm and the temperature ranges from 20–32 °C (So et al. 2010; Phunchaisri et al. 2019). It is a perennial tree and distributed in China (Yunnan province), Cambodia, Laos, Thailand, and Vietnam (He 2014; Liu et al. 2016).

The presence of *K. nepalensis* in Yunnan province increases the number of known *Kerria* species in China that could be used for lac production. The natural lac-plant resources are abundant in Yunnan Province (Chen et al. 2010). The Chinese diversity of the genus *Kerria* needs further investigation, and taxonomic studies particularly in Oriental China promise to find new species and new country records of this genus.

Acknowledgements

This project is funded by the National Natural Science Foundation of China (grant no. 31772542) and the Program of Innovative Team of Yunnan Province (202005AE160011).

References

Ahmad A, Ramamurthy VV, Sharma KK, Mohanasundaram A, Vidyarthi AS, Ramani R (2013a) Three new species of *Kerria* (Hemiptera: Coccoidea: Tachardiidae) from India. Zootaxa 3734(4): 442–452. https://doi.org/10.11646/zootaxa.3734.4.2

Ahmad A, Ramani R, Sharma KK, Vidyarthi AS, Ramamurthy VV (2014) Distinction of Indian commercial lac insect lines of *Kerria* spp. (Homoptera: Coccoidea) based on their morphometrics. Journal of Insect Science 14(263): 1–10. https://doi.org/10.1093/jisesa/ieu125

Ahmad A, Sharma KK, Ramamurthy VV, Vidyarthi AS, Ramani R (2013b) Three new species of *Kerria* (Hemiptera: Sternorrhyncha: Coccoidea: Tachardiidae), a redescription of *K. yunnanensis* Ou & Hong, and a revised key to species of *Kerria*. Zootaxa 3620(4): 518–532. https://doi.org/10.11646/zootaxa.3620.4.2

Bhatnagar P, Prajapati S, Lodhi B, Bhalawi R, Aarmo BS (2020) Studies on lac host plant occurrence in different agro-climatic zones of Madhya Pradesh. International Journal of Ecology and Environmental Sciences 2(4): 197–204.

Chamberlin JC (1925) Supplement to a monograph of the Lacciferidae (Tachardiinae) or lac insects (Homopt., Coccidae). Bulletin of Entomological Research 16(1): 31–41. https://doi.org/10.1017/S0007485300056121

Chen H, Chen XM, Feng Y, Yang H, He R, Zhang WF, Yang ZX (2013) Molecular phylogeny and biogeography of lac insects (Hemiptera: Kerriidae) inferred from nuclear and mitochondrial gene sequences. Molecular Biology Reports 40(10): 5943–5952. https://doi.org/10.1007/s11033-013-2701-5

Chen H, Chen XM, Feng Y, Yang ZX (2008) Cladistic analysis of phylogenetic relationships among 7 species of lac insects (Homoptera: Tachardiidae). Forest Research 21(5): 599–604.

Chen XM, Chen H, Feng Y, He R, Yang ZX (2011) Status of two species of lac insects in the genus *Kerria* from China based on morphological, cellular, and molecular evidence. Journal of Insect Science 11(106): 1–14. https://doi.org/10.1673/031.011.10601

Chen YQ, Li Q, Chen YL, Wang SM, Yang YC (2010) Lac-production, arthropod biodiversity and abundance, and pesticide use in Yunnan Province, China. Tropical Ecology 51(2): 255–263.

Ferdousee N, Nayen MJ, Hoque ATMR, Mohiuddin M (2010) Lac production and its economic return to rural economy in Rajshahi Division, Bangladesh. In: Proceedings of the International Conference on Environmental Aspects of Bangladesh, Japan, 4 September 2010, 69–72.

García Morales M, Denno B, Miller DR, Miller GL, Ben-Dov Y, Hardy NB (2016) ScaleNet: a literature-based model of scale insect biology and systematics. Database. http://scalenet.info. https://doi.org/10.1093/database/bav118 [accessed 22 April 2021]

He L (2014) Present situation on cultivation and utilization of precious and rare timber tree species in Xishuangbanna. Tropical Agriculture Science and Technology 37(3): 40–42.

Kondo T, Gullan PJ (2007) Taxonomic review of the lac insect genus *Paratachardina* Balachowsky (Hemiptera: Coccoidea: Kerriidae), with a revised key to genera of Kerriidae and description of two new species. Zootaxa 1617(1): 1–41. https://doi.org/10.11646/zootaxa.1617.1.1

Liu RH, Wen XC, Shao F, Zhang PZ, Huang HL, Zhang S (2016) Flavonoids from heartwood of *Dalbergia cochinchinensis*. Chinese Herbal Medicines 8(1): 89–93. https://doi.org/10.1016/S1674-6384(16)60014-X

Mehdizadeh KA, Tahermanesh K, Chaichian S, Joghataei MT, Moradi F, Tavangar SM, Mousavi NAS, Lotfibakhshaiesh N, Pour BS, Fazel AYA, Abed SM (2014) How to prepare biological samples and live tissues for scanning electron microscopy (SEM). Galen Medical Journal 3(2): 63–80.

Phunchaisri T, Wachrinrat C, Meunpong P, Tangmitcharoen S (2019) Environmental factors related to the site index of Siamese rosewood plantations in Thailand. Journal of Tropical Forest Research 3(2): 17–28.

Rajgopal NN, Mohanasundaram A, Sharma KK (2021) A new species of lac insect in the genus *Kerria* Targioni Tozzetti (Hemiptera: Coccomorpha: Tachardiidae) on *Samanea saman* (Fabaceae) from India. Zootaxa 4938(1): 60–68. https://doi.org/10.11646/zootaxa.4938.1.2

Sharma KK (2017) Lac insects and host plants. In: Omkar (Ed.) Industrial Entomology. Springer, Singapore, 157–180. https://doi.org/10.1007/978-981-10-3304-9_6

So T, Theilade I, Dell B (2010) Conservation and utilization of threatened hardwood species through reforestation–an example of *Afzelia xylocarpa* (Kruz.) Craib and *Dalbergia cochinchinensis* Pierre in Cambodia. Pacific Conservation Biology 16(2): 101–116. https://doi.org/10.1071/PC100101

Sriudorn N, Benchawattananon R (2018) Morphology and anatomy of Rosewood (*Dalbergia cochinchinensis*) and relationship between its elemental components and soil properties for identification of endemic species. International Journal of Agricultural Technology 14(7): 1977–1986.

Talukder B, Das BK (2020) A new invasive species of *Kerria* Targioni-Tozzetti (Hemiptera: Coccomorpha: Kerriidae) on rain tree, *Albizia saman* (Fabaceae) from India. Oriental Insects 54: 1–15. https://doi.org/10.1080/00305316.2020.1759467

Varshney RK (1976) Taxonomic studies on lac insects of India (Homoptera: Tachardiidae). Oriental Insects 10(5): 1–97. https://doi.org/10.1080/00305316.1976.11745227

Varshney RK, Sharma KK (2020) Lac Insects of the World–an Updated Catalogue and Bibliography. Indian Council of Agricultural Research, Indian Institute of Natural Resins and Gums, Ranchi, 84 pp.

Zhang ZS (1993) Four new species of lac insects of the genera *Metatachardia* and *Kerria* from China (Homoptera: Tachardiidae). Oriental Insects 27(1): 273–286. https://doi.org/10.1080/00305316.1993.10432279

ZooKeys 1061: 11–22 (2021)
doi: 10.3897/zookeys.1061.67458
https://zookeys.pensoft.net

RESEARCH ARTICLE

A peer-reviewed open-access journal
ZooKeys
Launched to accelerate biodiversity research

Cotesia cassina sp. nov. from southwestern Colombia: a new gregarious microgastrine wasp (Hymenoptera, Braconidae) reared from the pest species *Opsiphanes cassina* Felder & Felder (Lepidoptera, Nymphalidae) feeding on *Elaeis* oil palm trees (Arecaceae)

Geraldo Salgado-Neto[1], Consuelo Alexandra Narváez Vásquez[2], Dillon S. Max[3], James B. Whitfield[3]

1 *Pós-graduação em Agronomia, Departamento de Defesa Fitossanitária, Universidade Federal de Santa Maria, 97105-900, Santa Maria, RS, Brazil* **2** *Pós-graduação em Entomologia, Departamento de Entomologia/BIOAGRO, Universidade Federal de Viçosa, 36570-900, Viçosa, MG, Brazil* **3** *Department of Entomology, 320 Morrill Hall, 505 South Goodwin Ave., University of Illinois at Urbana-Champaign, Urbana, IL 61801, USA*

Corresponding author: James B. Whitfield (jwhitfie@life.illinois.edu)

Academic editor: J. Fernandez-Triana | Received 16 April 2021 | Accepted 12 July 2021 | Published 28 September 2021

http://zoobank.org/8208BB83-731B-4F97-90F2-8515638EC124

Citation: Salgado-Neto G, Vásquez CAN, Max DS, Whitfield JB (2021) *Cotesia cassina* sp. nov. from southwestern Colombia: a new gregarious microgastrine wasp (Hymenoptera, Braconidae) reared from the pest species *Opsiphanes cassina* Felder & Felder (Lepidoptera, Nymphalidae) feeding on *Elaeis* oil palm trees (Arecaceae). ZooKeys 1061: 11–22. https://doi.org/10.3897/zookeys.1061.67458

Abstract

A new species of microgastrine wasp, *Cotesia cassina* Salgado-Neto, Vásquez & Whitfield, **sp. nov.**, is described from southwestern Colombia in Tumaco, Nariño. This species is a koinobiont gregarious larval endoparasitoid, and spins a common mass of cocoons underneath the host caterpillars of *Opsiphanes cassina* (Felder & Felder) (Lepidoptera, Nymphalidae), feeding on oil palm trees (interspecific hybrid *Elaeis oleifera* × *E. guineensis*) (Arecaceae). While superficially similar, both morphologically and biologically, to *C. invirae* Salgado-Neto & Whitfield from southern Brazil, the two species are distinct based on DNA barcodes, host species, geographical range and morphological characters.

Keywords

Butterfly, DNA barcode, integrative taxonomy, morphology, natural enemy, new species

Introduction

The nymphalid butterfly *Opsiphanes cassina* Felder & Felder occurs from Mexico to the Amazon Basin (Brazil, Bolivia, Colombia, Ecuador, French Guiana, Guyana, Peru, Suriname and Venezuela) (Lamas 2004). This species is widespread in Colombia but is most commonly found within the States of Nariño, Cauca and Putumayo (Benavides and Cárdenas 1970; Fuentes 1973; Pava et al. 1983; Posada 1989; Villegas 1993). *Opsiphanes cassina* is considered a pest of oil palm trees (interspecific hybrid *Elaeis oleifera* × *Elaeis guineensis*) (Arecaceae) in south-west Colombia (Genty 1978; Mexzón and Chinchilla 1996; Posada and Cárdenas 1996; Loría et al. 2000; González 2011). In southwestern Colombia, the occurrence of the subspecies *O. cassina numatius* Fruhstorfer was recorded by Martínez (1970). We also recorded the presence of three additional subspecies: *O. cassina chiriquensis* Stichel, *Opsiphanes cassina periphetes* Fruhstorfer, and *Opsiphanes cassina caliensis* Bristow.

Five species of Braconidae have been recorded as endoparasitoids of species of *Opsiphanes* (larval stage): *Cotesia biezankoi* (Blanchard), *Cotesia opsiphanis* (Schrottky), *Cotesia alia* (Muesebeck) (Mason 1981; Penteado-Dias 1987; De Santis 1989; Salgado-Neto 2013), *Cotesia invirae* Salgado-Neto & Whitfield (Salgado-Neto et al. 2019), and *Rhysipolis* sp. (Sauer 1946; Costa Lima 1950, 1962; Silva et al. 1968; Briceño-Vergara 1978; De Santis 1980; Mason 1981; Penteado-Dias 1987; Briceño-Vergara 1997; Mexzón 1997; Rodríguez et al. 2006). Here we describe a new species of *Cotesia* Cameron, reared from *O. cassina* feeding on oil palms in southwestern Colombia.

Cotesia is easily recognizable morphologically among microgastrine braconids, although the huge variety of species can be difficult to distinguish from each other (Whitfield et al. 2009), especially those without host data. The wasps have a koinobiont habit (Kankare and Shaw 2004) and both solitary and gregarious species are known. *Cotesia* (Braconidae, Microgastrinae) currently contains roughly 300–400 described species (Fernandez-Triana et al. 2020), but this number will certainly increase dramatically, as world estimates range from 1000–2000 species (Mason 1981; Michel-Salzat and Whitfield 2004; Whitfield et al. 2018; Fernandez-Triana et al. 2020), and a relatively small number of studies recording Neotropical species of *Cotesia* and their biology are available so far (Whitfield 1997; Whitfield et al. 2018), particularly in South America.

As *Cotesia* species appear to be highly host specialized (Kankare and Shaw 2004), with many cryptic species and geographically restricted distributions (Fiaboe et al. 2017), the use of an integrative taxonomic approach (combining morphological, molecular, biological and geographical data) is critical for recognizing and distinguishing these parasitoid wasps (Smith et al. 2008; Kaiser et al. 2017).

Using such an integrative taxonomic approach, this paper provides a description of a new species of *Cotesia*, whose brood was produced from caterpillars of *Opsiphanes cassina* (Felder & Felder) (Lepidoptera, Nymphalidae) (Fig. 1) feeding on palm trees (interspecific hybrid *Elaeis oleifera* × *E. guineensis*) (Arecaceae) in Tumaco, Nariño, south-west Colombia. We compare it with the other described species of *Opsiphanes* that have been formally recorded from the Neotropical region, two of which have been well characterized and two of which are of uncertain identity.

Materials and methods

Between April 2018 and March 2019; we collected 35 larvae of *Opsiphanes cassina* as part of a survey carried out on exotic palms in the Palmeiras plantation A.S., 58 km from San Andrés de Tumaco, Nariño, Colombia (1°47'28.0"N, 78°47'33.9"W, 28 m elev. – see Fig. 1A, B). The larvae of *O. cassina* were found on the interspecific hybrid *Elaeis oleifera* × *E. guineensis* (Arecaceae). Upon collecting, larvae were kept in the laboratory (25 ± 1 °C; 70% RH; photoperiod of 14 hours of light) and observed daily until the emergence of the butterflies or parasitoids, which were then preserved in 70% ethanol.

Photographs of the caterpillar and parasitoid cocoons (Fig. 1C, D) were taken in the field by CANV. Morphological photographs of the *Cotesia* (Fig. 2A–F) were taken by DSM at the University of Illinois, USA using a Leica M205 C stereo microscope (467 nm resolution) fitted with a 5 megapixel Leica DFC 425 digital microscope camera. Images were stacked using a motor drive on the microscope and Zerene Stacker software. Morphological terms and measurements of structures are mostly those used by Salgado-Neto et al. (2019).

To characterize and compare the new species at the molecular level, the mitochondrial (DNA barcode) gene cytochrome oxidase I (COI) was analyzed. For the amplification of a fragment of approximately 460 bp of this gene, we used the following primer pair: COI-F (5'-GATTTTTTGGKCAYCCMGAAG-3') and COI-R (5'CRAATACRGCTCCTATWGATAAWAC-3') (Gusmão et al. 2010). DNA extraction of one specimen was performed with the GenElute Mammalian Genomic DNA Miniprep Kit (Sigma-Aldrich) and followed the manufacturer's protocol. The product was amplified via Polymerase Chain Reaction (PCR) according to the following schedule: 94 °C for 2 minutes, 40 cycles of 94 °C for 30 seconds, 54 °C for 30 seconds, 72 °C for 40 seconds and 72 °C for 4 minutes. Then the PCR product was purified using polyethylene glycol precipitation (PEG; Schmitz and Riesner 2006). These samples were sequenced using the Big Dye 3.1 reagent (Life Technologies) and a 3500 XL automatic sequencer (Life Technologies).

Descriptive taxonomy

***Cotesia cassina* Salgado-Neto, Vásquez & Whitfield, sp. nov.**
http://zoobank.org/3C8E3CC9-C4D2-4221-BE00-6652F17F5BD4

Material examined. ***Holotype*** Female, Colombia: Nariño, San Andrés de Tumaco (1°47'28.0"N, 78°47'33.9"W, 28 m elev.), March 2019, coll. Consuelo Vásquez, ex larva *Opsiphanes cassina* Felder & Felder (Lepidoptera, Nymphalidae). Deposited in the collection of the National University of Colombia (UNC, Dr Fernando Fernandez, curator). ***Paratypes*** 2 males, deposited in UNC, same data as holotype. 1 female, also same data as holotype, deposited in the Illinois Natural History Survey (INHS). ***Non-types.*** 2 females, in poor condition, also deposited at INHS.

Table 1. Diagnostic morphological characters distinguishing *Cotesia cassina* sp. nov. from the Brazilian *C. invirae* Salgado-Neto & Whitfield.

Character	*C. invirae*	*C. cassina*
Color	Generally lighter. T3 and all tergites posterior to T3 mostly bright yellow orangish. Mesopleuron with some light yellow/brown on ventral side	Generally darker. T3 and all tergites posterior to T3 are more brown to black rather than orangish. Mesopleuron almost entirely black
T2 Sculpture	Mostly smooth. Sculpture is more uniform across width; less punctate laterally	More punctate laterally, smooth medially
T2 Shape	Posterior margin/groove straight	Posterior margin slightly convex apically, with length greatest medially

Diagnosis. As discussed above, *Cotesia* is a huge worldwide genus of hundreds of species, with many morphologically similar species. While useful world identification keys are not available, it is currently possible to successfully diagnose species regionally, especially combined with molecular and host data. The closest described species, morphologically, biologically and within the region, is *Cotesia invirae* from southern Brazil, which also parasitizes *Opsiphanes* on palms (different species). The table below provides a diagnostic comparison between the two species.

Cotesia alia (Muesebeck), also recorded from *Opsiphanes*, resembles these two species but has a relatively longer first metasomal tergite (see illustration in Muesebeck 1958). Like *C. cassina*, the second tergite has the medial part of the second tergite longer than the lateral portions, and the tergites tend to both be blackish (tending to be mostly orangish in *C. invirae*). The other two named *Cotesia* species recorded from *Opsiphanes*, *C. biezankoi* (Blanchard) and *C. opsiphanis* (Schrottky), are both very poorly characterized in their descriptions and their type locations are unknown (Fernandez-Triana et al. 2020), so they are not compared here. There is a possibility that *C. invirae* might prove to be a junior synonym of *C. biezankoi*, based on shared host and geographic region, if the holotype of the latter were to resurface and be examined. Our understanding of the correct nomenclature for the entire complex would benefit from a full review of the named and putative unnamed species across all of Central and South America, especially if all the types could eventually be located. In the meantime, it is possible to characterize the relationships among the species for which we can clearly establish the identity.

Description. Female. Body length 3.1–3.3 mm; fore wing length 2.9–3.1 mm. **Coloration** (Fig. 2A–F). General body coloration black except: scape shading from light to dark brown, palps pale yellow, tegulae brown, fore legs all yellowish, middle legs all yellowish, hind legs all yellowish except distal end of femur brown/black dorsally; distal end of tibia brown, coxae translucent yellowish, laterotergites yellowish ventrally, shading to brown dorsally; sternites and hypopygium translucent yellowish. ***Head*** (Fig. 2A, E). Facial sculpture weakly punctate; vertex sculpture smooth to very weakly punctate; distance between posterior ocellae nearly identical with distance from outer ocelli to compound eyes. ***Mesosoma*** (Fig. 2A, B, F). Pronotum with both dorsal and ventral grooves present, ventral groove crenulate. Mesoscutum fully and distinctly but shallowly punctate; scutoscutellar scrobe slightly sunken groove and formed by 8 pits.

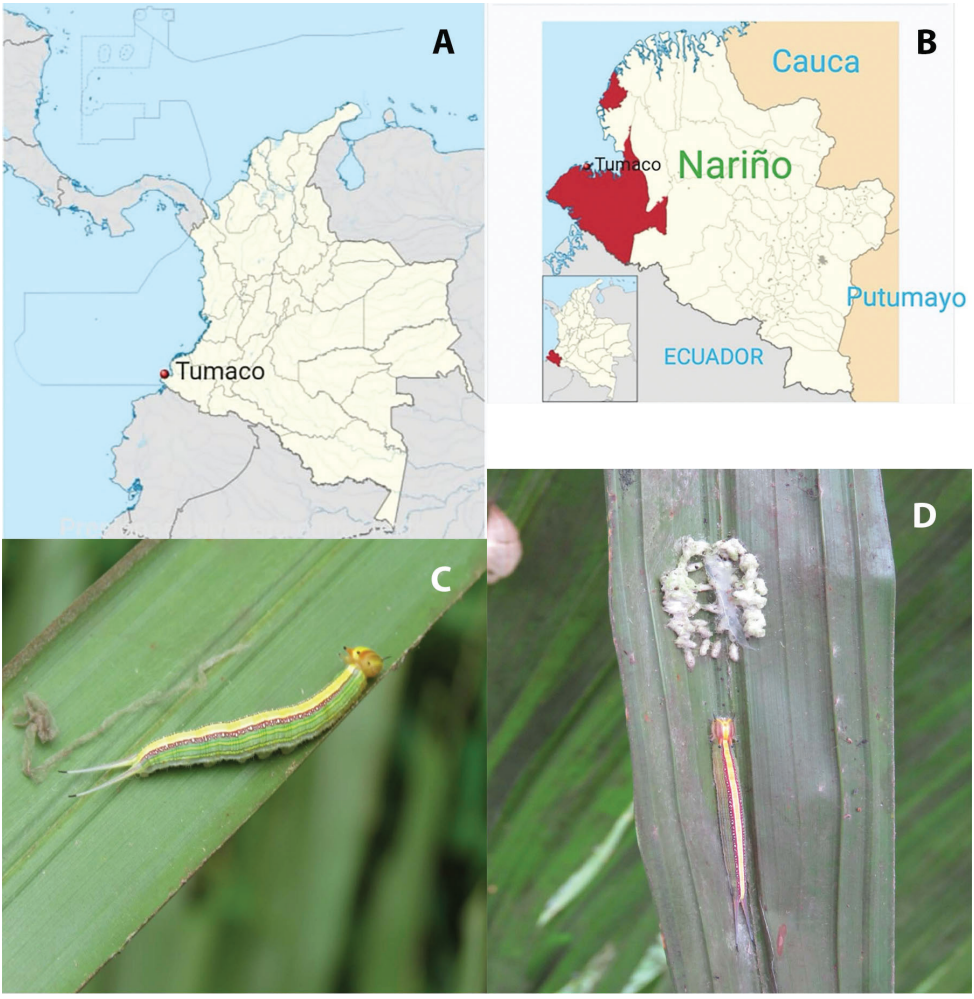

Figure 1. A simplified map of Colombia, showing rough location of Tumaco **B** close-up of southwestern Colombia, with location of Tumaco highlighted **C** caterpillar of *Opsiphanes cassina* on frond of the palm *Elaeis oleifera* × *E. guineensis* **D** same as **C** but with cocoons of emerged *Cotesia cassina* arranged below (normally underneath caterpillar).

Scutellum shield-shaped to subtriangular (anteriorly straight and posteriorly rounded) and weakly convex, weakly punctate. Mesopeuron smooth and polished throughout. Propodeum generally finely rugose/punctate with indistinct longitudinal medial carina. ***Legs*** (Fig. 2A–C). Hind coxa mostly smooth with faint sculpture on dorsal face; inner hind tibial spurs slightly longer than outer. ***Wings*** (Fig. 2B, C). Fore wing hyaline with dark brownish vein pigmentation; stigma more than 2× as long as broad, without obvious pale spot at proximal end. Metacarp extending 0.60–0.70 to end of 3Rs fold along wing edge; r approximately same length as 2RS vein and meeting it at a distinct shallow angle; vannal lobe edge roughly semicircular with distal end slightly flattened;

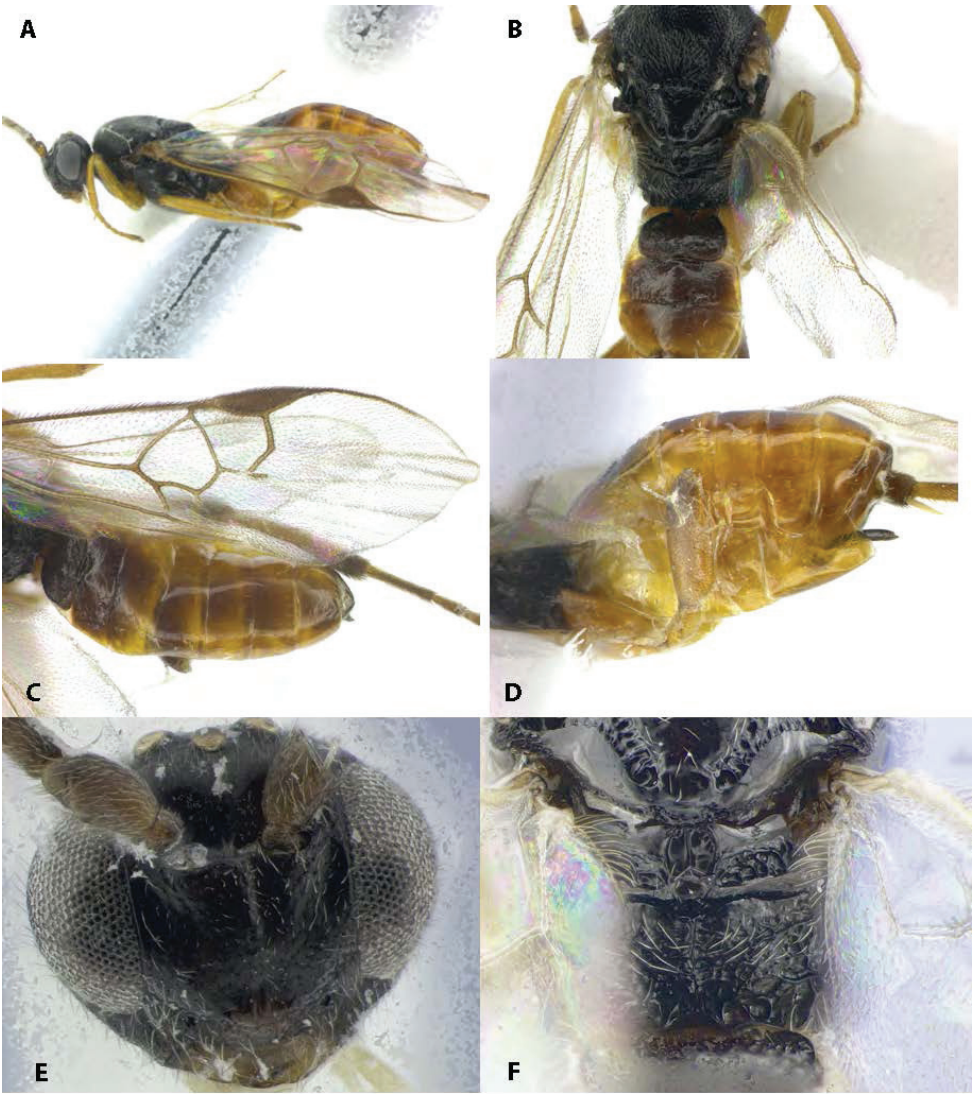

Figure 2. *Cotesia cassina*, sp. nov. **A** lateral habitus **B** dorsal view of mesosoma and anterior metasomal tergites **C** fore wing **D** lateral view of metasoma with hind leg removed, showing laterotergites, sternites, hypopygium and ovipositor sheaths **E** frontal view of head **F** dorsal view of posterior portions of mesosoma, especially propodeum.

vannal lobe fringe even and dense. **Metasoma** (Fig. 2B–D, F). Tergite 1 roughly as long as broad, evenly widening from anterior margin then rounding over posterior half, mostly rugulose; tergite 2 very weakly rugulose peripherally, mostly smooth and slightly raised centrally, roughly twice as broad as long, subrectangular with posterior margin slightly longer medially than laterally. Hypopygium with angled but blunt tip, not extending past dorsal end of metasoma; ovipositor with very sparse setae at tip.

Male. Similar to female except with slightly narrower metasoma.

Molecular data. COI barcode deposited in GenBank (MW405620). Using the identification tools in the Barcode of Life Database (Ratnasingham and Hebert 2007), *C. cassina* is closest to *C. salebrosa* (Marshall), a primarily Eurasian species attacking geometrid larvae, at a similarity level of 97.4%. Interestingly, *C. invirae* appears closest (97.02% similarity) to *Cotesia* Whitfield78 and *Cotesia* Whitfield20, two apparently conspecific sets of rearings of an undescribed species from the Lepidoptera Inventory of the Guanacaste Conservation Area (ACG) in northwest Costa Rica (Janzen et al. 2009); these rearings are from another species of *Opsiphanes*. It thus appears that there is a complex of at least four closely related species attacking different *Opsiphanes* species in a variety of geographically dispersed Neotropical habitats, as suggested by Salgado-Neto et al. (2019). BOLD and NCBI use slightly different criteria to make cutoffs in sequence comparisons, and to calculate % similarity. They also contain different sets of sequences. We checked the BOLD investigations of related species by using BLASTn (Altschul et al. 1990) to query the NCBI nucleotide database (NCBI 1988). The same most closely related species to *Cotesia cassina* and *C. invirae*, respectively, were recovered, with the exception that for *C. cassina*, *C. melitaearum* (Wilkinson) and *C. koebelei* (Riley), both attacking other genera of Nymphalidae but in the Holarctic region, joined *C. salebrosa* as closest, at roughly 94.6–95.6% similarity for all of them. In neither the BOLD nor the NCBI search did *C. cassina* come within 2.5% similarity of any other known *Cotesia* species.

Host. *Opsiphanes cassina* (Felder & Felder) (Lepidoptera, Nymphalidae) (Fig. 1C, D).

Biology/ecology. *Cotesia cassina* is a gregarious parasitoid wasp that occurs mainly in the wet season (March-May); however, their host, *O. cassina*, occurs throughout the year, mainly in the rainy season (March-July). *Cotesia cassina* larvae kill the host larva before the end of the last instar and form their cocoons in a regular mass of dirty whitish cocoons, regularly arranged disposed under the host (Fig. 1B). The larvae of this gregarious species all emerge from the host in a short time through many different holes in the host cuticle and spin a common woolly cocoon mass within which the individual cocoons can be distinguished.

Distribution. Known so far from San Andrés de Tumaco, Nariño, Colombia (Neotropical Region).

Etymology. The specific epithet *cassina*, is a reference to *Opsiphanes cassina* (Felder & Felder) (Lepidoptera, Nymphalidae), the host caterpillar name. The word cassina is the feminine of cassino which in Italian means playhouse.

Acknowledgements

We are grateful to Dr Ricardo Harakava of Instituto Biológico de São Paulo for analyses of the DNA barcode, and to Joshua C. Gibson at the University of Illinois for assistance with the wasp photography.

References

Altschul SF, Gish W, Miller W, Myers EW, Lipman DJ (1990) Basic Local Alignment Search Tool. Journal of Molecular Biology 215: 403–410. https://doi.org/10.1016/S0022-2836(05)80360-2

Benavides M, Cárdenas R (1970) Visita al corregimiento de Pueblo Tapado, Municipio de Montenegro, Quindío. Cabrito del plátano *Opsiphanes* sp. Informe. Programa de Entomología ICA. Regional 5, 4 pp.

Briceño-Vergara AJ (1997) Perspectivas de un manejo integrado del gusano verde del platano, *Opsiphanes tamarindi* Felder (Lepidoptera: Brassolidae). Revista de la Facultad de Agronomia 14(5): 475–590.

Briceño-Vergara AJ (1978) Algunos parasitos y depredadores de *Opsiphanes tamarindi* Felder (Lepidoptera: Brassolidae) en Venezuela. Revista de la Facultad de Agronomia 26: 117–128.

Bristow R (1991) A revision of the brassoline genus Opsiphanes (Lepidoptera: Rhopalocera). Zoological Journal of the Linnean Society 101: 203–293. https://doi.org/10.1111/j.1096-3642.1991.tb00282.x

Cameron P (1911) On a collection of parasitic Hymenoptera (chiefly bred) made by Mr. W.W. Froggatt, F.L.S., in New South Wales, with description of new genera and species. Part i. Proceedings of the Linnean Society of New South Wales 36: 333–346. https://doi.org/10.5962/bhl.part.21902

Costa Lima AM (1950) Insetos do Brasil, Lepidopteros. 6° tomo, 2ª parte, Série Didática da Escola Nacional de Agronomia, Universidade Rural, Rio de Janeiro, 420 pp.

Costa Lima AM (1962) Insetos do Brasil, Himenópteros**.** 12° tomo, 2° parte, Escola Nacional de Agronomia, Rio de Janeiro, 393 pp.

De Santis L (1980) Catalogo de los Himenópteros Brasilenos de la Serie Parasitica: Incluyendo Bethyloidea. Editora da Universidade Federal do Paraná, Curitiba, 395 pp.

De Santis L (1989) Catalogo de de los Himenopteros Calcidoides (Hymenoptera) al sur de los Estados Unidos, segundo suplemento. Acta Entomologica Chilena 15: 1–12.

Felder C, Felder R (1862) Specimen faunae lepidopterologicae riparum fluminis negro superioris in Brasilia septentrionali. Wiener entomologische Monatschrift 6: 175–192.

Fernandez-Triana JL, Shaw MR, Boudreault C, Beaudin M, Broad GR (2020) Annotated and illustrated world of Microgastrinae parasitoid wasps (Hymenoptera, Braconidae). Zootaxa 920: 1–1089. https://doi.org/10.3897/zookeys.920.39128.figure159

Fernandez-Triana JL, Whitfield JB, Rodriguez JJ, Smith MA, Janzen DH, Hallwachs W, Hajibabaei M, Burns JM, Solis MA, Brown J, Cardinal S, Goulet H, Hebert PDN (2014) Review of *Apanteles* (Hymenoptera, Braconidae, Microgastrinae) from Area de Conservacion Guanacaste, Costa Rica, with keys to all described species from Mesoamerica. ZooKeys 383: 15–65. https://doi.org/10.3897/zookeys.383.6418

Ferreira JMS, Lima MF, Santana DLQ, Moura JIL, Souza LA (1998) Pragas do coqueiro. In: Ferreira, JMS, Warwick DRN, Siqueira LA (Eds) A cultura do coqueiro no Brasil (2nd edn. rev. ampl.). Brasília, Embrapa-SPI/Aracaju, Embrapa CPATC, 189–267.

Fiaboe KKM, Fernandez-Triana JL, Nyamu FW, Agbodzavu KM (2017) *Cotesia icipe* sp. nov., a new Microgastrinae wasp (Hymenoptera, Braconidae) of importance in the biological

control of Lepidopteran pests in Africa. Journal of Hymenoptera Research 61: 49–64. https://doi.org/10.3897/jhr.61.21015

Fruhstorfer H (1912) Family: Brassolidae. In: Seitz A (Ed.) Die Gross-Schmetterlinge der Erde (Vol. 5). Alfred Kernen, Stuttgart, 285–332.

Fruhstorfer H (1912) Brassolidae, in Seitz-Macrolep. do Mundo 5: 285–332.

Fuentes R (1973) Dípteros parásitos de larvas de lepidópteros en algunos municipios del Valle del Cauca. Acta agronomica (Palmira) 23(1/2): 7–50. [+ 9 pls., 7 tabs]

Genty P et al. (1978) Las plagas de la palma aceitera en América Latina. Oléagineux 33: 324–594.

González GR et al. (2011)Metodología para muestrear las fases inmaduras del defoliador *Opsiphanes cassina* Felder (1862) (Lepidoptera: Nymphalidae) en palma aceitera. Revista Científica UDO Agrícola 11(1): 104–108.

Greeney HF, Whitfield JB, Stireman JO, Penz CM, Dyer LA (2011) Natural History of *Eryphanis greeneyi* (Lepidoptera: Nymphalidae) and Its Enemies, With a Description of a New Species of Braconid Parasitoid and Notes on Its Tachinid Parasitoid. Annals of the Entomological Society of America 104(6): 1078–1090. https://doi.org/10.1603/AN10064

Gusmão FA, Harakava R, Campos AEC (2010) Fire-ants of the *Solenopsis saevissima* species-group (Hymenoptera: Formicidae) nesting in parks in the city of São Paulo: identification based on mtDNA sequences and morphological characters. Sociobiology 56: 353–362.

Janzen DH, Hallwachs W, Blandin P, Burns JM, Cadiou J-M, Chacon I, Dapkey T, Deans AR, Epstein ME, Espinoza B, Franclemont JG, Haber WA, Hajibabaei M, Hall JPW, Hebert PDN, Gauld ID, Harvey DJ, Hausmann A, Kitching IJ, LaFontaine D, Landry J-F, Lemaire C, Miller JY, Miller JS, Miller L, Miller SE, Montero J, Munroe E, Rab Green S, Ratnasingham S, Rawlins JE, Robbins RK, Rodriguez JJ, Rougerie R, Sharkey MJ, Smith MA, Solis MA, Sullivan JB, Thiaucourt P, Wahl DB, Weller SJ, Whitfield JB, Willmott KR, Wood DM, Woodley NE, Wilson JJ (2009) Integration of DNA barcoding into an ongoing inventory of complex tropical diversity. Molecular Ecology Resources 9(suppl. 1): 1–26. https://doi.org/10.1111/j.1755-0998.2009.02628.x

Kaiser L, Fernandez-Triana J, Capdevielle-Dulac C, Chantre C, Bodet M, Kaoula F, Benoist R, Calatayud PA, Dupas S, Herniou EA, Jennette R, Obonyo J, Silvain JF, Ru BL (2017) Systematics and biology of *Cotesia typhae* sp. n. (*Hymenoptera*, *Braconidae*, *Microgastrinae*), a potential biological control agent against the noctuid Mediterranean corn borer, *Sesamia nonagrioides*. ZooKeys 682: 105–136. https://doi.org/10.3897/zookeys.682.13016

Kankare M, Shaw MR (2004) Molecular phylogeny of *Cotesia* Cameron, 1891 (Insecta: Hymenoptera: Braconidae: Microgastrinae) parasitoids associated with Melitaeini butterflies (Insecta: Lepidoptera: Nymphalidae: Melitaeini). Molecular Phylogenetics and Evolution 32: 207–220. https://doi.org/10.1016/j.ympev.2003.11.013

Lamas G (2004) Checklist: Part 4A, Hesperioidea-Papilionoidea. In: J. Heppner (Ed.) Atlas of Neotropical Lepidoptera, Association for Tropical Lepidoptera, Scientific Publishers, 439–439.

Link D, Alvarez Filho A (1979) Palmeiras atacadas por lagartas de Brassolidae (Lepidoptera) em Santa Maria, RS. Revista do Centro Ciências Rurais 9(2): 221–225.

Link D, Biezanko CM, Carvalho S, Tarragó MFS (1980) Lepidoptera de Santa Maria e Arredores. III. Morphidae e Brassolidae. Revista do Centro de Ciências Rurais 10(2): 191–195.

Loría R, Chinchilla CM, Domínguez J, Mexzón RG (2000) An effective trap to capture adults of *Opsiphanes cassina* F. (Lepidoptera, Nymphalidae) and observations on the behavior of the pest in oil palm. Una trampa efectiva para capturar adultos de *Opsiphanes cassina* F. (Lepidoptera; Nymphalidae) y observaciones sobre el comportamiento de la plaga en palma aceitera. ASD Oil Palm Papers 21: 1–12.

Martínez E (1970) Informe anual de progreso 1969. Programa Entomología. C.N.I.A. "Marconia". Informes anuales. Programa Entomología. ICA. Regional 3, 9 pp.

Mason WRM (1981) The polyphyletic nature of *Apanteles* Foerster (Hymenoptera: Braconidae): a phylogeny and reclassification of Microgastrinae. Memoirs of the Entomological Society of Canada 115: 1–147. https://doi.org/10.4039/entm113115fv

Mexzón RG (1997) Entomofauna prejudicial, enemigos naturales y malezas útiles en pal-. ma aceitera en América Central. Manejo Integrado de Plagas (C.R.) 20/21: 1–7.

Mexzón RG, Chinchilla CM (1996) Natural enemies of harmful arthropods in oil palm (*Elaeis guineensis* Jacq.) in Tropical America. Enemigos naturales de los artrópodos perjudiciales a la palma aceitera (*Elaeis guineensis* Jacq.) en América Tropical. ASD Oil Palm Papers 13: 9–33. [+ 9 figs., 6 tabs]

Michel-Salzat A, Whitfield JB (2004) Preliminary evolutionary relationships within the parasitoid wasp genus *Cotesia* (Hymenoptera: Braconidae: Microgastrinae): combined analysis of four genes. Systematic Entomology 29: 371–382. https://doi.org/10.1111/j.0307-6970.2004.00246.x

Muesebeck CFW (1958) New Neotropical wasps of the family Braconidae (Hymenoptera) in the U.S. National Museum. Proceedings of the United States National Museum 107: 405–461. https://doi.org/10.5479/si.00963801.108-3389.405

NCBI [National Center for Biotechnology Information] [Internet] (1988) Bethesda (MD): National Library of Medicine (US), National Center for Biotechnology Information; [1988]. [accessed 1 Apr 2021]

Pava J, Castillo E, González A, Patiño H (1983) Aspectos de interés fitosanitario de la palma de chontaduro *Bactris gasipae*s H.B.K. en algunas regiones del Valle y Chocó. Acta agronómica (Palmira) 33(1): 25–35.

Penteado-Dias AM (1987) Contribuição para o conhecimento da morfologia e biologia de *Cotesia alius* (Muesebeck, 1958) (Hymenoptera: Braconidae, Microgastrinae). Revista Brasileira de Entomologia 31(3): 439–443.

Penz CM (2008) Phylogenetic revision of *Eryphanis* Boisduval, with a description of a new species from Ecuador (Lepidoptera, Nymphalidae. Insecta Mundi 0035: 1–25.

Posada FJ (1989) Todos en palma. Notas y Noticias entomológicas (Bogotá) 1989(7/8): e63.

Posada FJ (1989) Enemigos eficientes. Notas y Noticias entomológicas (Bogotá)1989(7/8): e63.

Posada FJ, Cárdenas R (1996) Gusanos en otra palma. MIP – Notas y Noticias (Bogotá) 2(6): e15.

Ratnasingham S, Hebert PDN (2007) BOLD: The Barcode of Life Data System. Molecular Ecology Notes 7: 355–364. https://doi.org/10.1111/j.1471-8286.2007.01678.x

Rodríguez G, Fariñas J, Díaz A, Silva-Acuña R, Piña E (2006) Plantas atrayentes de enemigos naturales de insectos plaga en palma aceitera. Revista Digital CENIAP HOY Número 10, 2006. Maracay, Aragua, Venezuela. ISSN 1690-4117, Depósitolegal: 00302AR1449.

www.ceniap.gov.ve/ceniaphoy/articulos/n10/arti/rodriguez_g/arti/rodriguez_g.htm [Accessed: 05/11/2007]

Salgado-Neto G (2013) Aspects of biology of *Cotesia alius* (Muesebeck 1958) (Hymenoptera: Braconidae: Microgastrinae) on *Opsiphanes invirae amplificatus* Stichel (Lepidoptera: Nymphalidae) for Rio Grande do Sul, Brazil. Estudos de Biologia 35(84): 35–41. https://doi.org/10.7213/estud.biol.7854

Salgado-Neto G, Whitfield JB, Mello Garcia FR (2019) *Cotesia invirae*, sp. nov., from South Brazil: a new gregarious microgastrine wasp (Hymenoptera: Braconidae) reared from *Opsiphanes invirae* (Nymphalidae) feeding on palms. Revista Brasiliera Entomologia 63: 136–140. https://doi.org/10.1016/j.rbe.2019.02.003

Sauer HFG (1946) Constatação de himenópteros e dipteros Entomófagos no Estado de São Paulo. Boletim Fitossanitário 3(1): 7–23.

Schmitz A, Riesner D (2006) Purification of nucleic acids by selective precipitation with polyethylene glycol 6000. Analytical Biochemistry 354: 311–313. https://doi.org/10.1016/j.ab.2006.03.014

Shaw MR, Huddleston T (1991) Classification and biology of braconid wasps (Hymenoptera, Braconidae). Handbooks for the Identification of British Insects. Royal Entomological Society of London 7: 1–126.

Silva AG de, Gonçalves CR, Galvão DM, Gonçalves AJL, Gomes J, Silva MN, Simoni L (1968) Quarto catálogo dos insetos que vivem nas plantas do Brasil; seus parasitas e predadores. Rio de Janeiro, Ministério da Agricultura, tomo 1, part. 2, 622 pp.

Smith MA, Rodriguez JJ, Whitfield JB, Deans AR, Janzen DH, Hallwachs W, Hebert PDN (2008) Extreme diversity of tropical parasitoid wasps exposed by iterative integration of natural history, DNA barcoding, morphology, and collections. Proceedings of the National Academy of Sciences of the United States of America 105(35): 12359–12364. https://doi.org/10.1073/pnas.0805319105

Sousa-Lopes B, Bächtold A, Del-Claro K (2016) Biology, natural history and temporal fluctuation of the geometrid *Oospila pallidaria* associated with host plant phenology. Studies on Neotropical Fauna and Environment 51(2): 135–143.

Sousa-Lopes B, Whitfield JB, Salgado-Neto G, Del-Claro K (2018) *Cotesia itororensis*, sp. nov., from Brazilian savanna: a new reared microgastrinae wasp (Hymenoptera: Braconidae) described using an integrative taxonomic approach. Zootaxa 4544(3): 437–445. https://doi.org/10.11646/zootaxa.4544.3.9

Souza LA, Lemos WP (2007) Sistema de produção do açaí. Embrapa Amazônia Oriental. http://sistemasdeproducao.cnptia.embrapa.br/FontesHTML/Acai/SistemaProducaoAcai_2ed/paginas/pragas.htm [Access 03/11/2007]

Stichel H (1904) Lepidoptera, Rhopalocera, Fam. Nymphalidae, Subfam. Brassolinae. In: Wytsman P (Ed.) Genera Insectorum (Vol. 20), 48 pp.

Stichel H (1909) Brassolidae. Das Tierreich, 25, [xiv,] 244 pp.

Stichel H (1932) Lepidopterorum Catalogus (Vol. 51): Brassolidae. W. Junk, Berlin. https://doi.org/10.5962/bhl.title.124190

Villegas D (1993) Más benéficos. Notas y Noticias entomológicas (Bogotá) 1992(11/12): e75.

Whitfield JB (1997) Subfamily Microgastrinae. In: Wharton RA, Marsh PM, Sharkey MJ (Eds) Identification Manual to the New World Genera of the Family Braconidae (Hymenoptera). International Society of Hymenopterists Special Publication, 333–364.

Whitfield JB, Austin AD, Fernandez-Triana JL (2018) Systematics, biology and evolution of microgastrine parasitoid wasps. Annual Review of Entomology 63: 389–406. https://doi.org/10.1146/annurev-ento-020117-043405

Whitfield JB, Rodriguez JJ, Masonick PK (2009) Reared microgastrine wasps (Hymenoptera: Braconidae) from Yanayacu Biological Station and environs (Napo Province, Ecuador): diversity and host specialization. Journal of Insect Science 9(1): e31. https://doi.org/10.1673/031.009.3101

Yu DSK, Van Achterberg C, Horstmann K (2016) Taxapad, Ichneumonoidea 2015. Ottawa, Ontario. http://www.taxapad.com

ZooKeys 1061: 23–55 (2021)
doi: 10.3897/zookeys.1061.49999
https://zookeys.pensoft.net

RESEARCH ARTICLE

A peer-reviewed open-access journal
ZooKeys
Launched to accelerate biodiversity research

Tipula (*Vestiplex*) crane flies (Diptera, Tipulidae) of Korea

Pavel Starkevich[1], Sigitas Podėnas[1,2], Virginija Podėnienė[2], Sun-Jae Park[3], A-Young Kim[3]

1 *Nature Research Centre, Akademijos str. 2, LT-08412 Vilnius, Lithuania* **2** *Life Sciences Centre of Vilnius University, Sauletekio str. 7, LT-10257 Vilnius, Lithuania* **3** *Animal Resources Division, National Institute of Biological Resources, Incheon 22689, South Korea*

Corresponding author: Pavel Starkevich (pavel.starkevic@gmail.com)

Academic editor: C. Borkent | Received 9 January 2020 | Accepted 18 September 2020 | Published 30 September 2021

http://zoobank.org/ FFA31901-68EF-457D-A4BF-DC807033F6BF

Citation: Starkevich P, Podėnas S, Podėnienė V, Park S-J, Kim A-Y (2021) Tipula (Vestiplex) crane flies (Diptera, Tipulidae) of Korea. ZooKeys 1061: 23–55. https://doi.org/10.3897/zookeys.1061.49999

Abstract

The Korean species of *Tipula* (*Vestiplex*) Bezzi, 1924 crane flies are taxonomically revised. Five species are recognized. *Tipula* (*V.*) *coquillettiana* Alexander, 1924, *T.* (*V.*) *kuwayamai* Alexander, 1921, *T.* (*V.*) *tchukchi* Alexander, 1934, and *T.* (*V.*) *verecunda* Alexander, 1924 are newly recorded from the Korean Peninsula, and *T.* (*V.*) *serricauda* Alexander, 1914 was previously recorded. The larva of *T.* (*V.*) *serricauda* is described and illustrated, and the larvae of the subgenus *T.* (*Vestiplex)* are divided into four groups based on spiracular lobe morphology. An identification key, redescriptions, and illustrations of Korean *T.* (*Vestiplex*) adults and grouping of known larvae are presented.

Keywords

distribution, hypopygium, larva, new record, North Korea, ovipositor, South Korea, taxonomy

Introduction

Tipula Linnaeus, 1758 is the largest genus in the family Tipulidae with a worldwide distribution, and it is divided into 41 subgenera. The subgenus *T.* (*Vestiplex*) Bezzi, 1924 is a terrestrial group represented by 177 species and subspecies recorded from Holarctic and Oriental regions (Oosterbroek, 2019). The highest diversity of this

group is documented in the Eastern Palaearctic (76 species) and Oriental (74 species) regions (Oosterbroek 2019).

The first *T.* (*Vestiplex*) crane flies from the Korean Peninsula were collected by A.M. Yankovsky in 1938–1940. He lived and worked in the northern part of Korea. Only one species, *T.* (*V.*) *serricauda* Alexander, 1914, had been recorded from the Korean Peninsula (Starkevich et al. 2015).

The aim of this study was to document, redescribe, illustrate, and prepare keys for all Korean *T.* (*Vestiplex*) species.

Material and methods

The specimen material examined in this paper (Table 1) was obtained from: the United States National Museum (USNM), Smithsonian Institution, Washington, DC, USA; the Snow Entomological Museum, University of Kansas (SEM), Lawrence, KS, USA; the National Institute of Biological Resources (NIBR), Incheon, South Korea and the Korea University (KU), Seoul, South Korea; the Academy of Natural Sciences of Drexel University (ANSP), Philadelphia, PA, USA; Zoological Museum of the Zoological Institute of the Russian Academy of Sciences, St. Petersburg, Russia (ZIN), and the Nature Research Centre (NRC), Vilnius, Lithuania.

Adult crane flies were collected by insect net and at lights. Some specimens were preserved dry in envelopes in the field and later mounted in the laboratory on their side on a paper point with legs generally surrounding the insect pin. The specimens are pinned except when noted otherwise.

Adult specimens were studied with a Nikon SMZ800 stereomicroscope. Photographs were taken with an INFINITY-1 camera mounted on a Nikon Eclipse 200 stereomicroscope and with a Canon EOS 80D camera mounted on an Olympus SZX10 dissecting microscope. Genitalia were studied after heating them in 10 percent NaOH solution for 5–10 minutes and then preserved in microvials filled with glycerol attached to the pin. All redescriptions and illustrations are based only on Korean material, except when otherwise mentioned.

Two identical last instar larvae were collected by hand and one of them was left for rearing. A female of *T.* (*V.*) *serricauda* emerged after 36 days. The larva is preserved in 70% ethanol though the head capsule was slide-mounted in glycerin jelly with corresponding label. The larva was studied with an Olympus SZX10 dissecting microscope with photographs taken with a Canon EOS 80D digital camera fitted with a Canon MP-E 65 mm macro lens.

Collecting localities with approximate coordinates are summarized in Table 1, and this was used to generate the geographical distribution maps (Figs 86–90). The identification key is based on morphological characters primarily observed in Korean specimens, but in cases when females are unknown from Korea, characters were observed from other specimens collected in other Asian countries.

Descriptive terminology of adults generally follows that of Cumming and Wood (2017). The term appendage of ninth sternite is adopted from Mannheims (1963),

Table 1. Collecting sites in Korea.

Locality	Year	Method	Collector	Museum	N*	E*
North Korea, Ompo (now called Onbo, Hamgyeongbuk-do,Gyeongsung-gun)	1937, 1938	Net	A.M. Yankovsky	USNM	41°30'48.9"N	129°34'41.2"E
North Korea, Seren Mts.(Hamgyeongbuk-do, Gyeongsung-gun)	1938	Net	A.M. Yankovsky	USNM	41°41'14.3"N	129°18'33.1"E
North Korea, Kankyo Nando, Puksu Pyaksan (now, Yanggang-do, Pungseo-gun, Mt Buksubaeksan)	1939	Net	A.M. Yankovsky	USNM	40°41'59.5"N	127°42'57.6"E
North Korea, Chonsani (Yanggang-do, Daehongdan-gun)	1940	Net	A.M. Yankovsky	USNM	41°59'37.0"N	128°45'09.0"E
Suoth Korea, # 8, Central National Forest, 18 miles NE of Seul	1954	Net	G.W. Byers	SEM	37°45'16.0"N	127°09'57.4"E
South Korea, #14, Oho-ri, east coast	1954	Net	G.W. Byers	SEM	38°20'00.0"N	128°30'00.0"E
South Korea, Gyeongi-do, Pocheon-si, Soheul-eup, Gwangneung Forest	1961	Net	Gyeong-suk Jeon	KU	37°45'02.8"N	127°09'41.7"E
South Korea, Geongsanbuk-do, Chilgok-gun, Jicheon-myeon, Mt Hwanghaksan,	1978	Net	Seon-hui Lee	KU	36°02'06.5"N	128°29'54.3"E
South Korea, Chungcheonnam-do, Danyang-gun, Danyang-eup, Mt Sobaeksan	1981	Net	K-S Lee	KU	36°57'06.9"N	128°26'45.6"E
South Korea, Gyeonggi-do, Namyangju-si, Hwado-eup, Mt Cheonmasan	1984	Net	Yeong-cheol Heo	KU	37°40'50.4"N	127°16'21.9"E
South Korea, Gyeonggi-do, Seongnam-si, Sangjeok-dong, Mt Cheongyesan	1984	Net	In-suk Hyeon	KU	37°24'51.4"N	127°02'29.2"E
South Korea, Jeollanam-do, Suncheon-si, Songgwang-myeon, Mt Jogyesan	1988	Net	Dokgo	KU	35°00'09.0"N	127°18'49.3"E
South Korea, Hadong-gun, Okjong-myeon, Wolhoeng-ri	1990	Net	M.J. Gang	NIBR	35°12'08.9"N	127°50'56.1"E
South Korea, Chungcheongnam-do, Gongju-si, Gyeryong-myeon	1997	Net	Yeong Lee, Minjeong Kim	KU	36°22'11.3"N	127°09'31.3"E
South Korea, Hadong-gun, Geumseong-myeon, Gadoek-ri, Hwaryeokbonbu	1998, 2000	Net	J.S. Jeon, J.S. Park	NIBR	34°57'23.2"N	127°49'42.7"E
South Korea, Goseong-gun, Sangri-myeon, Osan-ri, Mt Odu	1999	Net	G.H. Gang, J.S. Jeon, J.S .Park, S.Y. Lee	NIBR	35°00'18.6"N	128°11'12.4"E
South Korea, Geochang-gun, Gajo-myeon, Suwol-ri, Mt Bigye, Gogyeonsa	2000	Net	J.S. Choi, S.B. Jeong, S.H. Baek	NIBR	35°43'47.8"N	128°02'16.1"E
South Korea, Gwangyang-si, Junggun-dong, Mt Gaya, Hanseokgwangwangnongwon	2000, 2001	Net	J.H. Son, J.S. Park, K.L. Han	NIBR	34°57'52.7"N	127°41'03.8"E
South Korea, Ulju-gun, Sangbuk-myeon, Doekhyeon-ri, Mt Gaji, Helkijang	2001	Net	Y.S. Kim	NIBR	35°37'43.8"N	129°00'58.6"E
South Korea, Gwangyang-si, Junggun-dong, Mt Gaya, Gunjangijae	2003	Net	T.H. An.	NIBR	34°58'17.8"N	127°41'18.1"E
South Korea, Jirisan Hamyang, Songjeon-li Munsu-sa (Starkevich et. all 2015)	2005	Net	Tripotin	CMNH	35°24'44.4"N	127°43'49.2"E
South Korea, Changpyeong-ri, Bongsung-myeon, Bonghwa-gun, Gyeongsangbuk-do	2014	Net	H.-W. Byun	NIBR	36°55'07.7"N	128°48'39.4"E
South Korea, Jeollanam-do, Gurye-gun, Toji-myeon, Naeseo-ri, Jirisan National Park, Piagol valley	2014, 2016	Light	S. Podenas	NIBR	35°15'57.2"N	127°34'51.5"E
South Korea, Jeollanam-do, Gurye-gun, Toji-myeon, Naeseo-ri, Jirisan National Park, Piagol valley	2015	Hand*	V. Podienene	NIBR	35°16'28.1"N	127°33'49.6"E
South Korea, Jeollanam-do, Gurye-gun, Toji-myeon, Naeseo-ri, Jirisan National Park, Piagol valley	2016	Light	S. Podenas	NIBR	35°15'57.1"N	127°34'51.2"E
South Korea, Jeollanam-do, Gurye-gun, Toji-myeon, Naeseo-ri, Jirisan National Park, Piagol valley	2016	Net	S. Podenas	NIBR	35°16'18.4"N	127°34'17.3"E
South Korea, Jeollanam-do, Gurye-gun, Toji-myeon, Naeseo-ri, Jirisan National Park, Piagol valley	2016	Net	S. Podenas	NIBR	35°16'24.0"N	127°34'09.3"E
South Korea, Jeju-do, Seogwipo, Sanghyo-dong	2017	Light	S. Podenas	NIBR	33°18'30.9"N	126°33'34.0"E
South Korea, Jeju-do, Cheju, Jochon-eup, Seonheul-ri	2017	Light	S. Podenas	NIBR	33°30'35.8"N	126°42'55.5"E
South Korea, Jeju-do, Jeju-si, Yonggang-dong	2017	Light	S. Podenas, V. Podeniene	NIBR	33°25'49.6"N	126°35'50.5"E
South Korea, Gyeonggi-do, Gunpo-si, Suri-dong	2017	Light	S. Podenas	NIBR	37°21'02.1"N	126°54'56.1"E
South Korea, Jeju-do, Seogwipo, Saekdal-dong	2019	Net	S. Podenas, H.-Y. Seo	NIBR	33°21'27.4"N	126°27'51.2"E
South Korea, Jeju-do, Seogwipo, Saekdal-dong	2019	Net	S. Podenas	NIBR	33°21'37.6"N	126°27'45.9"E

* Collecting site of larva.

the terms ventral lobe and dorsal lobe of appendage of ninth sternite are adopted from Gelhaus (2005), the term gonocoxal fragment (= sclerites *sp1* and *sp2* (Neumann, 1958), = genital bridge (Dobrotworsky 1968)) for inner structure covered by ninth tergite is adopted from Brodo (2017). Descriptive terminology of larva generally follows that of Gelhaus (1986) and Neugart et al. (2009).

The overall world distribution of species is given according to Oosterbroek (2019).

Taxonomy

Tipula (*Vestiplex*) Bezzi, 1924

Tipula (*Vestiplex*) Bezzi 1924: 230; Edwards 1931: 79; Alexander 1934: 396; 1935: 117; 1965: 355; Mannheims 1953: 116; Savchenko 1964: 132.

Type species. *Tipula cisalpina* Riedel, 1913.

Vestiplex was first proposed by Bezzi (1924) as a subgenus of the genus *Tipula* for the type species *T. cisalpina* Riedel, 1913, which was recorded from the Western Palaearctic (Italy and Switzerland). No fossil species of *T.* (*Vestiplex*) are described so far and only Matthews and Telka (1997) mentioned ovipositors of possibly *T.* (*Vestiplex*) females from Cape Deceit Formation in Western Alaska (1.8 MY old).

The world fauna of the subgenus *T.* (*Vestiplex*) includes 177 recent species and subspecies, which are distributed throughout the Nearctic, Palaearctic, and Oriental regions (Oosterbroek 2019). The majority of the species are associated with mountain systems (Pyrenees, Alps, Caucasus, and Himalayas) where adults are commonly found at altitudes ranging from 700 to 2500 m and rarely up to 4500 m (Savchenko 1960).

Females belonging to subgenus *T.* (*Vestiplex*) are characterized by the ovipositor having powerful cerci, which are heavily sclerotized, and serrated along outer margin (but smooth in several Asiatic species), and small to rudimentary hypovalva (Alexander 1935, 1965; Alexander and Byers 1981). The male genitalia are extremely polymorphic (Savchenko 1964), typically with the ninth tergite forming a shallowly concave and sclerotized saucer, with other species having their ninth tergite completely divided longitudinally by a pale membrane (Alexander 1935; Alexander and Byers 1981).

Just seven species have described larvae. Two are North American species, *T.* (*V.*) *arctica* Curtis, 1835 and *T.* (*V.*) *platymera* Walker, 1856 (Alexander 1920a, Gelhaus 1986), and five are European species, *T.* (*V.*) *excisa excisa* Schummel, 1833, *T.* (*V.*) *hortorum* Linnaeus, 1758, *T.* (*V.*) *nubeculosa* Meigen, 1804, *T.* (*V.*) *semivittata* Savchenko, 1960, and *T.* (*V.*) *scripta* Meigen, 1830 (Chiswell 1956; Theowald 1965; Savchenko 1986; Podeniene 2003; Lantsov 2003).

The immature stages develop in terrestrial habitats such as the uppermost layer of soil under leaf or needle litter, or under mosses (Chiswell 1956; Rogers 1942; Theowald 1967; Teale and Gelhaus 1984; Lantsov 2003; Podeniene 2003). Larvae of *T.* (*Vestiplex*) are easily recognized because of a brown band separating the anus from the anal papillae.

The lobes surrounding spiracular field are subconical with the lateral lobe situated dorsolaterally. The sclerotization of the dorsal lobe varies depending on species, with some species bearing a sclerite only on the basal part of the posterior surface, while in other species the entire anterior and posterior surfaces are sclerotized. In this case the apex of the dorsal lobe is sclerotized, pointed, and directed anteriorly. The lateral lobe may possess a narrow and vertical sclerite, but it may be entirely absent in some species. The ventral lobe is the smallest and trianglar. It varies from extensively sclerotized to possessing only a small sclerite. Larvae have two pairs of short, blunt anal papillae. The length and macrosetal arrangement is consistent on the dorsum and tergum among all known species. Short microscopic hairs are arranged in transverse rows and cover most of the abdomen.

List of Korean *Tipula* (*Vestiplex*) crane flies

Tipula (*Vestiplex*) *coquillettiana* Alexander, 1924
Tipula (*Vestiplex*) *kuwayamai* Alexander, 1921
Tipula (*Vestiplex*) *serricauda* Alexander, 1914
Tipula (*Vestiplex*) *tchukchi* Alexander, 1934
Tipula (*Vestiplex*) *verecunda* Alexander, 1924

Key to Korean *Tipula* (*Vestiplex*) crane flies

Males

1 Gonocoxite armed with a powerful black spine or bifurcate horn (Figs 3, 32) ...**2**
– Gonocoxite simple, unarmed (Figs 16, 71) **3**
2 Flagellum bicolored with inconspicuous basal enlargement. Gonocoxite with a strong black spine (Fig. 32). Ninth tergite divided by pale midline (Fig. 31)..... ***Tipula* (*Vestiplex*) *serricauda***
– Flagellum dark brown with weak basal enlargement. Gonocoxite horn-shaped with bifurcate margin (Fig. 3). Ninth tergite forming narrow sclerotised saucer (Fig. 2) ..... ***Tipula* (*Vestiplex*) *coquillettiana***
3 Eighth sternite with long setae (Figs 67, 70). Ninth sternite ventrally with median tubercle (Fig. 67). Appendage of ninth sternite present, finger-shaped (Figs 74, 75). Ninth tergite divided by pale midline (Fig. 68) .... ***Tipula* (*Vestiplex*) *verecunda***
– Eighth sternite without long setae (Fig. 16). Ninth sternite without ventral tubercle (Fig. 16). Appendage of ninth sternite absent. Ninth tergite forming a sclerotised saucer (Figs 17, 56) **4**
4 Size relatively small (body length 16.8 mm, wing length 17.1 mm). Wing pattern indistinct, only weak darkening along vein CuA. Abdomen with median stripe..... ***Tipula* (*Vestiplex*) *tchukchi***
– Size large (body length 17.8–19.7 mm, wing length 19.8–22.9 mm). Wing distinctly marbled. Abdomen without median stripe..... ..... ***Tipula* (*Vestiplex*) *kuwayamai***

Females

1 Wing well developed, extends beyond middle of abdomen **2**

– Wing reduced, not reaching middle of abdomen ..... ***Tipula* (*Vestiplex*) *coquillettiana***

2 Wing pattern indistinct, only weak darkening along vein CuA. Cercus apically with incision in addition to serrated border (Fig. 65) ..... ***Tipula* (*Vestiplex*) *tchukchi***

– Wing pattern distinctly marbled. Cercus without apical incision (Figs 11, 27, 38, 80) 3

3 Antennal flagellum brownish-black. Cercus with smooth ventral margin (Fig. 80). Hypovalva long, blade-shaped (Figs 81, 82)..... ***Tipula* (*Vestiplex*) *verecunda***

– Antennal flagellum yellow or bicolored. Cercus with serrate ventral margin (Fig. 27, 38). Hypovalva short, filamentous or plate-shaped (Figs 28, 39) ... **4**

4 Large species with wing length 24.5–26.1 mm. Antennal flagellum bicolored. Hypovalva filamentous (Fig. 28) ..... ***Tipula* (*Vestiplex*) *kuwayamai***

– Smaller species with wing length16.4–17.1 mm. Antennal flagellum varies from yellow to bicolored. Hypovalva in the shape of a dark brown plate (Fig. 39)..... ***Tipula* (*Vestiplex*) *serricauda***

Tipula (*Vestiplex*) *coquillettiana* Alexander, 1924

Figs 1–15, 86

Tipula coquillettiana Alexander 1924: 605; 1925: 91.

Tipula (*Vestiplex*) *coquillettiana*: Alexander 1934: 405; 1935: 118; Savchenko 1960: 172; 1964: 180; Oosterbroek and Theowald 1992: 154.

Type material examined. Holotype, male, **RUSSIA**, Odasam [Southern Sakhalin], 5 August 1922, Esaki; paratype, male (USNM).

Other examined material (Fig. 86). **NORTH KOREA**, 1 male, Seren Mts, alt. 3000 ft, 25 June 1938, Yankovsky (USNM); 2 males, alt. 3000 ft, 26 June 1938, Yankovsky (USNM); 2 males, alt. 3000–4000 ft, 29–30 June 1938, Yankovsky (USNM); 1 male, alt. 3500–5500 ft, 29–30 June 1938, Yankovsky (USNM); 3 males, alt. 4000–5000 ft, 29–30 June 1938, Yankovsky (USNM); 1 male, alt. 5000 ft, 29–30 June 1938, Yankovsky (USNM); 2 females, alt. 4000 ft, 30 June 1938, Yankovsky (USNM); 2 males, alt. 3500 ft, 5 July 1938, Yankovsky (USNM); 3 males, alt. 4500 ft, 5–6 July 1938, Yankovsky (USNM); 1 male, alt. 4000 ft, 10–11 July 1938, Yankovsky (USNM); 1 male, alt. 5500 ft, 18 July 1938, Yankovsky (USNM); 1 male, Kankyo Nando Puksu Pyaksan, alt. 6000 ft, 23 June 1939, Yankovsky (USNM); 1 male, alt. 6000 ft, 31 July 1939, Yankovsky (USNM); 1 male, alt. 5000 ft, 2 August 1939, Yankovsky (USNM); 2 males, Chonsani, alt. 4000 ft, 2 June 1940, Yankovsky (USNM); 1 male, alt. 3000 ft, 8 June 1940, Yankovsky (USNM); 4 males, alt. 4500 ft, 20 June 1940, Yankovsky (USNM); 1 male, alt. 4000 ft, 23 June 1940, Yankovsky (USNM).

Diagnosis. *Tipula* (*V.*) *coquillettiana* can be easily recognized by the ninth tergite, which forms a narrow, saucer-shaped plate, and the horn-shaped gonocoxite. The tip of the gonocoxite is bifurcate. The female of this species has a gray, elongated abdomen and greatly reduced wing. The cercus is straight with its tip narrowed and the ventral margin and apical part of the dorsal margin distinctly serrated. The hypovalva is in the shape of an elongated filament.

Male. Body length 17.1–21.3 mm, wing length 18.9–22.8 mm. General body coloration brownish yellow.

Head. Vertex and occiput gray with dark median line. Rostrum yellowish, thinly dusted with gray dorsally. Nasus distinct. Antenna 13-segmented, if bent backward extending beyond wing base. Scape and pedicel yellow; first flagellar segment basally yellow, distally brownish black; succeeding flagellar segments brownish black. Each flagellomere, except first, with basal enlargement and small incision. Apical flagellomere small, reduced. Verticils approximately as long as corresponding segments. Palpus with first segment yellowish, second brownish yellow, and other segment brownish black.

Thorax. Pronotum yellowish, thinly dusted with gray. Prescutum and presutural scutum gray; stripes bluish gray bordered by brown. Postsutural scutum, scutellum, and postnotum gray with bluish shade; all sclerites with dark, median line. Pleura brownish, dusted with gray. Coxa gray; trochanter yellowish; femur brownish yellow with tip broadly darkened; tibia brownish yellow; tarsal segments dark brown. Tarsal claw without tooth. Wing patterned with brown. Halter brownish yellow with brown knob.

Abdomen. Yellow. First abdominal segment dusted with gray. Abdominal segments 2 and 3 yellow, 4 and 5 brownish-yellow, and remaining segments dark brown. Lateral margin of tergites pale yellow. Dorsal median stripe pale, broadly interrupted.

Hypopygium. Brown (Fig. 1). Ninth tergite distally forming a narrow saucer-shaped plate (Figs 1, 2). Tergal saucer posteriorly with broad median notch; lateral comer with serrated and blackened margin, provided with setae. Anterior margin elevated into narrow, blackened rim reaching lateral part of tergal saucer and terminating into acute projection. Gonocoxite apically extended, with tip split into blackened beak pointed caudad and rounded projection (Figs 1, 3). Outer gonostylus slightly curved, finger-shaped with tip narrowed (Fig. 4). Inner gonostylus in the shape of a curved plate; beak blackened, triangular; dorsal margin claw-shaped; middorsal edge extended and serrated (Fig. 5). Gonocoxal fragment with flattened medial sclerites, fused into broad, nearly triangular base (Fig. 6). Lateral sclerite flattened and bilobed. Adminiculum boat-shaped, with tip and dorsal edge apically blackened (Fig. 7). Semen pump with flattened central vesicle (Figs 8, 9). Compressor apodeme with round median incision, forming a 30° angle with posterior immovable apodeme. Posterior immovable apodeme much longer than compressor apodeme, flattened, rounded apically. Anterior immovable apodeme flattened, rounded. Intromittent organ tube-shaped, about twice as long as semen pump, brownish-black. Distal part with preapical yellow membrane, apex with pale median incision, lateral parts split, filament-shaped (Fig. 10).

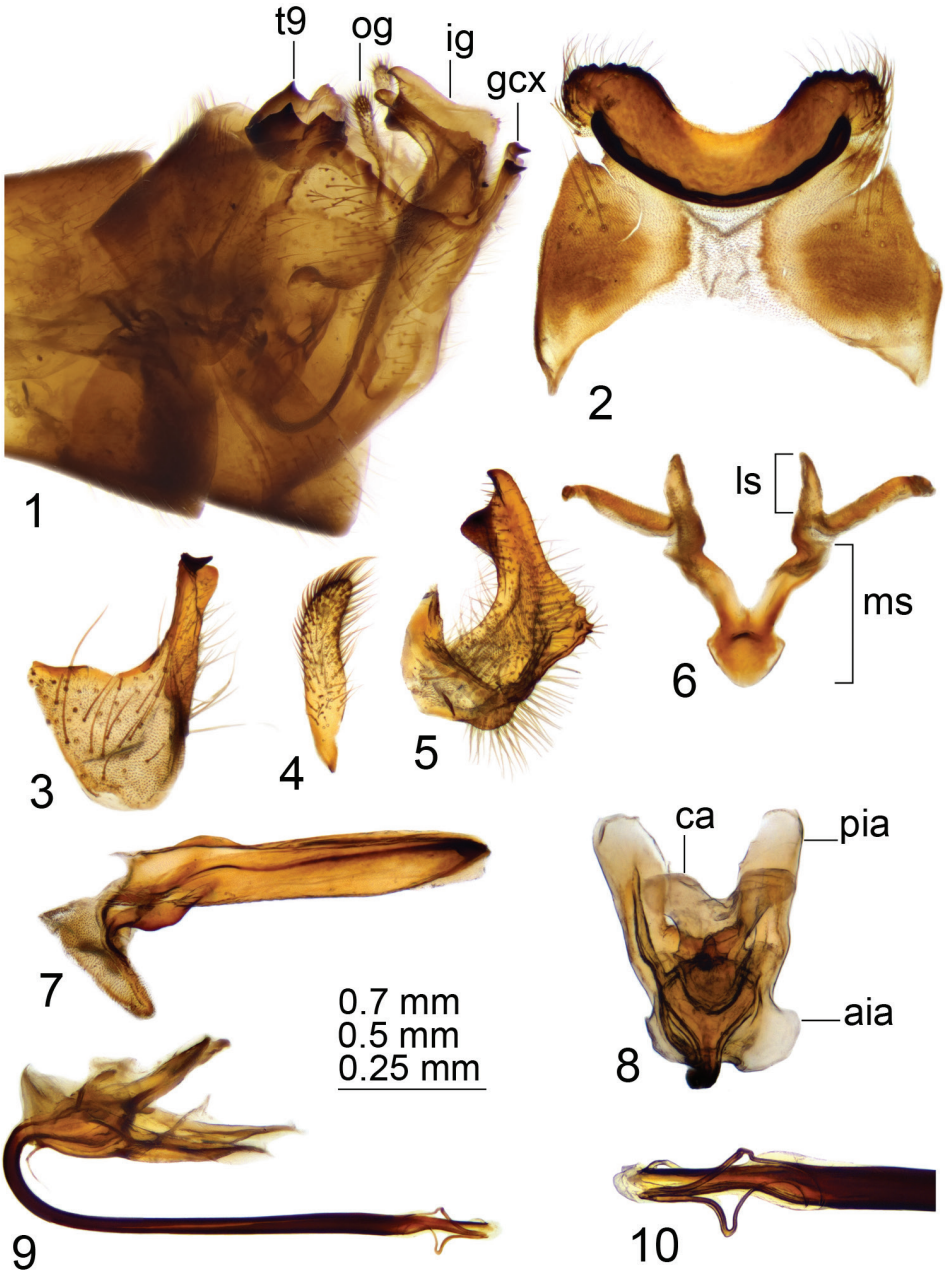

Figures 1–10. Male terminalia of *T.* (*Vestiplex*) *coquillettiana* **1** hypopygium, lateral view **2** ninth tergite, dorsal view **3** left gonocoxite, lateral view **4** left outer gonostylus **5** left inner gonostylus, lateral view **6** gonocoxal fragment, dorsal view **7** adminiculum, lateral view **8** semen pump, dorsal view **9** semen pump and intromittent organ, lateral view **10** distal part of intromittent organ, lateral view. Abbreviations: aia, anterior immovable apodeme; ca, compressor apodeme; gcx, gonocoxite; ig, inner gonostylus; ls, lateral sclerite of gonocoxal fragment; ms, medial sclerite of gonocoxal fragment; og, outer gonostylus; pia, posterior immovable apodeme; t9, ninth tergite. Scale bars: 0.7 mm (**1**); 0.5 mm (**2–9**); 0.25 mm (**10**).

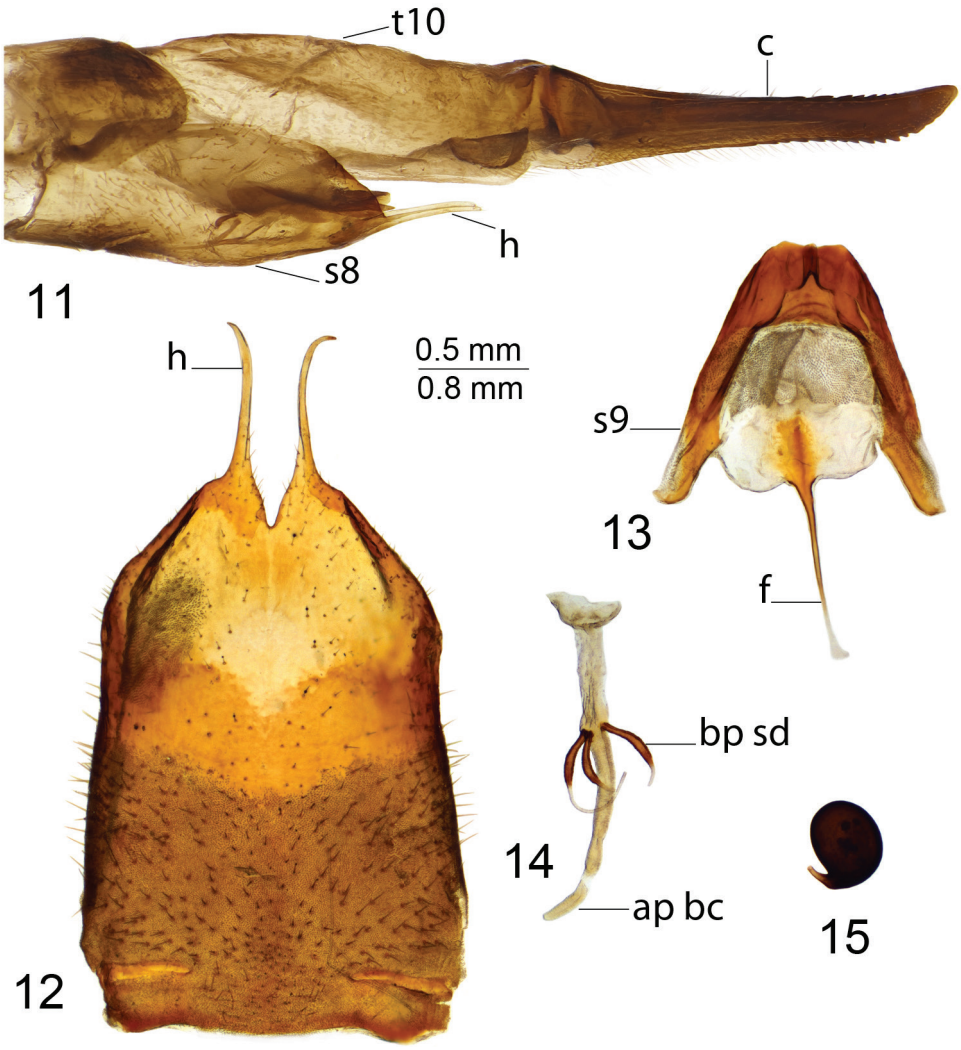

Figures 11–15. Female terminalia of *T.* (*Vestiplex*) *coquillettiana* **11** ovipositor, left lateral view **12** eighth sternite with hypovalvae, ventral view **13** ninth sternite with furca, dorsal view **14** *bursa copulatrix*, dorsal view **15** spermatheca, lateral view. Abbreviations: ap bc, anterior part of *bursa copulatrix*; bp sd, basal part of spermathecal duct; c, cerci; f, furca; h, hypovalvae; s8, eighth sternite; s9, ninth sternite; t10, tenth tergite. Scale bars: 0.8 mm (**11**), 0.5 mm (**12–14**).

Female. Body length 26.9–30.2 mm, wing length 4.7–5.7 mm. Generally similar to male, but with elongated and gray abdomen. Tergites and sternites with pale margins. Wing greatly reduced.

Female terminalia. Tenth tergite shining dark brown. Cercus brown, straight, as long as tenth tergite, with tip narrowed; ventral margin and apical part of dorsal margin distinctly serrated (Fig. 11). Hypovalva elongated and filamentous (Fig. 12). Median incision between hypovalvae deeper than posterior margin of eighth sternite. Lat-

eral angle of eighth sternite sloping. Ninth sternite with lateral parts straight (Fig. 13). Furca anteriorly narrowed, shaped posteriorly as broad membranous plate (Fig. 13). *Bursa copulatrix* with spermathecal duct sclerotized at base, in shape of thickened, curved stick (Fig. 14). Spermatheca broadened at base, pear-shaped (Fig. 15).

Known distribution. Russia, Kazakhstan, and Japan (Oosterbroek 2019). Recorded here for the first time from North Korea.

Tipula (*Vestiplex*) *kuwayamai* Alexander, 1921

Figs 16–29, 87

Tipula kuwayamai Alexander 1921: 130; 1925: 93.
Tipula (*Vestiplex*) *kuwayamai*: Alexander 1934: 405; 1935: 118; Savchenko 1964: 179; Oosterbroek and Theowald 1992: 156.

Type material examined. Holotype, male, **JAPAN**, Maruyama, Sapporo, 1 June 1919, Kuwayama (USNM).

Other examined material (Fig. 87). **NORTH KOREA**, 4 males, Ompo, 23 May 1937, Yankovsky (USNM); 1 female, alt. 500 ft, 2 May 1938, Yankovsky (USNM); 1 male, alt. 400 ft, 10 May 1938, Yankovsky (USNM); 1 male, Chonsani, alt. 4900 ft, 2 June 1940, Yankovsky (USNM); 1 female, alt. 3500 ft, 13 June 1940, Yankovsky (USNM). **SOUTH KOREA**, 1 male, #8, Central National Forest, 18 miles NE of Seoul, 28 May 1954, G.W. Byers (SEM); 1 male, Gyeongi-do, Pocheon-si, Soheul-eup, Gwangneung Forest, 30 May 1961, Gyeong-suk Jeon (KU); 1 female, Chungcheonnam-do, Danyang-gun, Danyang-eup, Mt Sobaeksan, 6 June 1981, K-S Lee (KU); 1 female, Gyeonggi-do, Seongnam-si, Sangjeok-dong, Mt Cheongyesan, 4 May1984, In-suk Hyeon (KU); 1 female, Gyeonggi-do, Namyangju-si, Hwado-eup, Mt Cheonmasan, 20 May 1984, Yeong-cheol Heo (KU); 1 male, 3 females, Geochang-gun, Gajo-myeon, Suwol-ri, Mt Bigye, Gogyeonsa, 6–7 May 2000, S.B. Jeong, IN0000297019, IN0000297023, IN0000296935, IN0000297021 (NIBR); 1 female, S.H. Baek, IN0000296936 (NIBR); 1 female, J.S. Choi, IN0000297020 (NIBR); 1 female, Ulju-gun, Sangbuk-myeon, Doekhyeon-ri, Mt Gaji, Helkijang, 18–19 May 2001, Y.S. Kim, IN0000226477 (NIBR). **CHINA**, 1 male, Heilongjiang Province, Hsiaoling, 20 May 1938, leg. Weymarn (USNM); 6 males, 2 females, Heilongjiang Province, Maoershan, 8 June 1941, [collector not designated] (USNM); 1 female, 11 June 1941 (USNM); 1 male, 13 June 1941 (USNM); 1 female, 14 June 1941 (USNM); 1 female, 16 June 1941 (USNM); 1 male, Jilin Province, Yablonia Station [Yabuli], 26 May 1939, [collector not designated] (USNM).

Diagnosis. *Tipula* (*V.*) *kuwaymai* can be recognized by the unarmed gonocoxite and by the ninth tergite forming a sclerotized, oval saucer which has an elevated edge anteriorly and is yellow posteriorly with the posterolateral angle blade-shaped. The wing is distinctly patterned with brown. The female has the cercus brownish yellow with the tip narrowed and upturned, and the ventral margin has distinct serration. The

hypovalva is filamentous. The median incision between hypovalvae is slightly deeper than posterior margin of eighth sternite.

Male. Body length 17.8–19.7 mm, wing length 19.8–22.9 mm. General body coloration brownish yellow.

Head. Vertex and occiput gray with brown median line. Rostrum dark brown, dorsally dusted with gray. Nasus small, almost lacking. Antenna 13-segmented, if bent backward extending beyond the wing base. Scape and pedicel reddish yellow, flagellum dark brown. Each flagellomere except first one with distinct basal enlargement and incision. Apical flagellomere small, reduced. Verticils longer than corresponding segments. Palpus dark brown.

Thorax. Pronotum gray with brown median line. Prescutum and presutural scutum gray. Median stripes anteriorly gray, posteriorly brown, bordered by darker brown, fused at base. Lateral stripes blackish gray, bordered by brown. Postsutural scutum blackish gray; each lobe with light brown spot bordered by brown. Scutellum and postnotum brownish, dusted with gray, each with brown median line. Pleura brownish, dusted with gray. Wing distinctly patterned with brown. Halter pale with brown knob. Coxa gray; trochanter yellow; femur brownish yellow with tip dark brown; tibia and tarsal segments brown. Tarsal claw with tooth.

Abdomen. Brownish yellow. First tergite laterally brown, dorsally yellow, tergites 2–5 yellow with pale and interrupted dorsal stripe. Tergites 6–9 brown, without median stripe. Lateral stripe distinct. First sternite yellow, sternites 2–6 yellow; remaining sternites dark brown.

Hypopygium. Dark brown (Fig. 16). Ninth tergite forming concave sclerotized saucer (Fig. 17). Central part of tergal saucer brownish, in the shape of an oval, concave, transverse plate, anteriorly with elevated edge, laterally and posteriorly with blackened, medially interrupted rim. Posterior part of tergal saucer yellow, posterolateral angle blade-shaped, with blackened ridge connecting with central part of tergal saucer. Gonocoxite narrow, unarmed (Fig. 18). Outer gonostylus club-shaped (Fig. 19). Inner gonostylus in the shape of a curved plate, bidentate at apex, dorsally with acute tooth, beak claw-shaped (Fig. 20). Gonocoxal fragment with medial sclerites slender, fused at base; lateral parts apically flattened (Fig. 46). Lateral sclerite relatively small, nearly V-shaped. Adminiculum semi-open, nearly triangular in lateral view (Fig. 22), flattened and broadened at base in ventral view (Fig. 23). Semen pump with swollen central vesicle (Figs 24, 25). Compressor apodeme with broad and round median incision, forming a 75° angle with posterior immovable apodeme. Posterior immovable apodeme much longer than compressor apodeme, flattened, with acute tip. Anterior immovable apodeme narrow, rounded. Intromittent organ tube-shaped, about five times as long as semen pump, basally and medially brown but passing into brownish yellow towards apex. Distal part yellow, funnel-shaped (Fig. 26).

Female. Body length 27.4–34.4 mm, wing length 24.5–26.1 mm. Generally similar to male. Antenna with four basal segments yellow; remaining flagellomeres bicolored.

Female terminalia. Tenth tergite shining-brownish. Cercus brownish yellow, as long as tenth tergite, with tip narrowed and upturned, ventral margin with distinct serra-

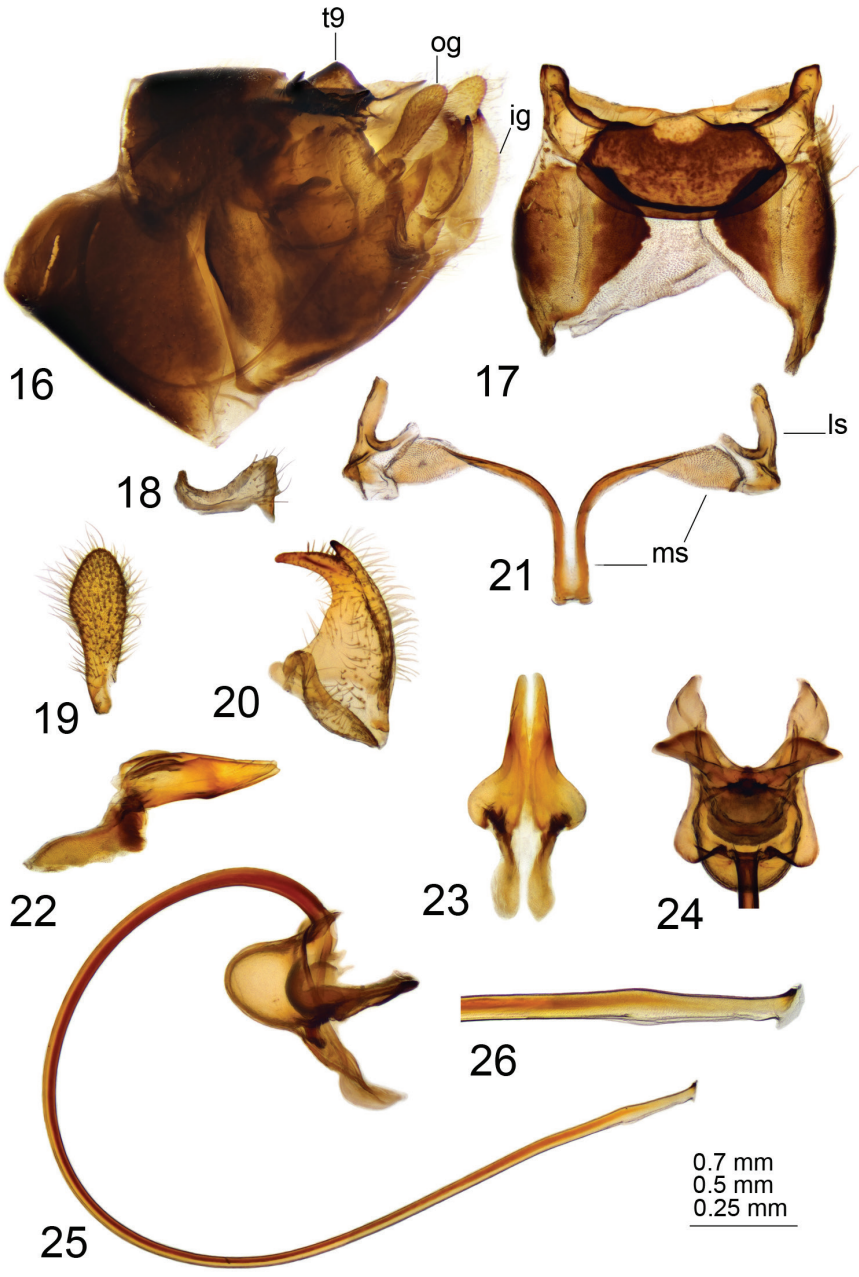

Figures 16–26. Male terminalia of *T.* (*Vestiplex*) *kuwayamai* **16** hypopygium, lateral view **17** ninth tergite, dorsal view **18** left gonocoxite, lateral view **19** left outer gonostylus **20** left inner gonostylus, lateral view **21** gonocoxal fragment, dorsal view **22** adminiculum, lateral view **23** adminiculum, ventral view **24** semen pump, dorsal view **25** semen pump and intromittent organ, lateral view **26** distal part of intromittent organ, lateral view. Abbreviations: ig, inner gonostylus; ls, lateral sclerite of gonocoxal fragment; ms, medial sclerite of gonocoxal fragment; og, outer gonostylus; t9, ninth tergite. Scale bars: 0.7 mm (**16**); 0.5 mm (**17–25**); 0.25 mm (**26**).

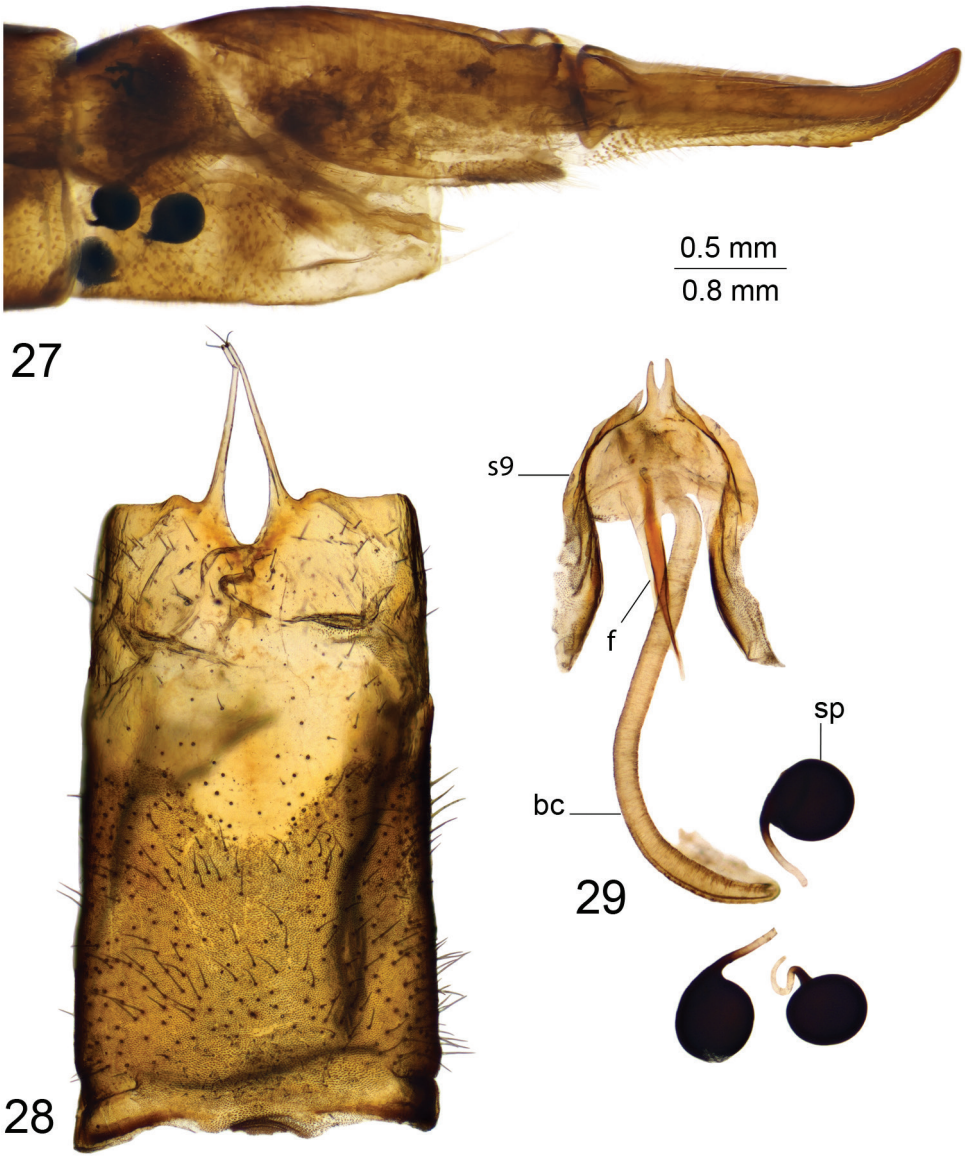

Figures 27–29. Female terminalia of *T.* (*Vestiplex*) *kuwayamai* **27** ovipositor, left lateral view **28** eighth sternite with hypovalvae, ventral view **29** ninth sternite with furca, *bursa copulatrix* and spermathecae, dorsal view**.** Abbreviations: bc, *bursa copulatrix*; f, furca; s9, ninth sternite; sp, spermatheca. Scale bars: 0.8 mm (**27**); 0.5 mm (**28–29**).

tion (Fig. 27). Hypovalva filamentous, distally pale, with short trichia at tip (Fig. 28). Median incision between hypovalvae slightly deeper than posterior margin of eighth sternite. Lateral incision scarcely outlined, posterior margin with fine additional projec-

tion. Lateral angle of eighth sternite rectangular. Ninth sternite posteriorly with split tip (Fig. 29). Furca in the shape of narrow stripe (Fig. 29). Spermatheca spherical (Fig. 29).

Known distribution. Russia, Japan China (Oosterbroek, 2019) and North and South Korea. Recorded here for the first time from the Korean Peninsula.

Tipula (*Vestiplex*) *serricauda* Alexander, 1914

Figs 30–55, 88

Tipula serricauda Alexander 1914: 237; 1920b: 18.
Tipula asio Alexander 1918: 68 (synonymy after Alexander 1953: 156).
Tipula (*Vestiplex*) *asio*: Alexander 1935: 118.
Tipula (*Vestiplex*) *serricauda*: Alexander 1935: 118; Oosterbroek and Theowald 1992: 159.

Type material examined. Holotype, female, **JAPAN**, Tokyo, August 1912 (USNM).

Other examined material (Fig. 88). **SOUTH KOREA**, 2 males, #14, Oho-ri, east coast, 10–50 ft, 128°30'E, 38°20'N, 11 June 1954, G.W. Byers (SEM); 1 female, Geongsanbuk-do, Chilgok-gun, Jicheon-myeon, Mt Hwanghaksan, 4 June 1978, Seon-hui Lee (KU); 1 male, 1 female, Jeollanam-do, Suncheon-si, Songgwang-myeon, Mt Jogyesan, 23 May 1988, Dokgo (KU); 1 male, Hadong-gun, Okjong-myeon, Wolhoeng-ri, 24 May 1990, M.J. Gang, IN0000296230 (NIBR); 1 male, Chungcheongnam-do, Gongju-si, Gyeryong-myeon, 5–7 June 1997, Yeong Lee (KU); 1 male, Minjeong Kim (KU); 1 male, Hadong-gun, Geumseong-myeon, Gadoek-ri, Hwaryeokbonbu, 19–20 September 1998, J.S. Jeon, IN0000298240 (NIBR); 3 males, 1 female, Goseong-gun, Sangri-myeon, Osan-ri, Mt Odu, 10–11 September 1999, J.S. Jeon, IN0000298933, IN0000298927, IN0000298197, IN0000297995 (NIBR); 3 females, J.S. Park, IN0000298194, IN00000298192, IN0000298188 (NIBR); 2 males, 1 female, S.Y. Lee, IN0000298932, IN0000298935, IN0000298193 (NIBR); 2 females, G.H.Gang, IN0000298196, IN0000298187(NIBR); 2 females, Hadong-gun, Geumseong-myeon, Gadoek-ri, Hwaryeokbonbu, 22–23 September 2000, J.S. Park, NIBR IN0000333964 (NIBR); 1 male, Gwangyang-si, Junggun-dong, Mt Gaya, Hanseokgwangwangnongwon, 22–23 September 2000, J.H. Son, IN0000333965; 2 females, K.L. Han, IN0000333962, IN0000333956 (NIBR); 1 male, Gwangyang-si, Junggun-dong, Mt Gaya, Hanseokgwangwangnongwon, 26–27 May 2001, J.S. Park, IN0000323569 (NIBR); 2 females, Gwangyang-si, Junggun-dong, Mt Gaya, Gun-jangijae, 31 May–1 June 2003, T.H. An, IN0000298937, IN0000299044 (NIBR); 1 male, Changpyeong-ri, Bongsung-myeon, Bonghwa-gun, Gyeongsangbuk-do, 36°55.12'N, 128°48.65'E, 2014.05.05, H.-W. Byun (NIBR); 1 male, Jeollanam-do, Gurye-gun, Toji-myeon, Naeseo-ri, Jirisan National Park, Piagol valley, 35°15.95'N, 127°34.85'E, alt. 450 m, 24 August 2014, S. Podenas (NIBR); 1 female, 1 larva, Piagol valley, 35°16.47'N, 127°33.82'E, alt. 600 m, 1 May 2015, female emerged 5 June 2015, V. Podeniene (NIBR); 1 male, 2 females, Piagol valley, 35°15.95'N, 127°34.85'E, alt. 450 m, 2 June 2016, S. Podenas (NIBR); 1 male, 6 females, Piagol valley, 35°15.95'N,

127°34. 85'E, alt. 450 m, 3 June 2016, S. Podenas (NIBR); 16 males, 4 females, Piagol valley, 35°15.95'N, 127°34.85'E, alt. 450 m, 3 June 2016, S. Podenas (NIBR); 1 male, 2 females, Piagol valley, 35°16.31'N, 127°33.29'E, alt. 500 m, 3 June 2016, S. Podenas (NIBR); 2 males, 3 females, Piagol valley, 35°16.4'N, 127°34.15'E, alt. 550 m, 3 June 2016, S. Podenas (NIBR); 8 males (in alcohol), Piagol valley, 35°15.95'N, 127°34.85'E, alt. 450 m, 24 June 2016 S. Podenas, at light (NIBR); 4 males (in alcohol), 26 June 2016, S. Podenas, at light (NIBR); 3 males (in alcohol), 2 males, 2 females, Jeju-do, Jeju Island, Seogwipo, Sanghyo-dong, 33°18.51'N, 126°33.57'E, alt. 500 m, 22 May 2017, S. Podenas (NIBR); 2 males, Jeju-do, Jeju Island, Cheju, Jochon-eup, Seonheul-ri, 33°30.59'N, 126°42.92'E, alt. 1500 m, 23 May 2017, at light, S. Podenas (NIBR); 1 male, Jeju-do, Jeju Island, Jeju-si, Yonggang-dong, 33°25.82'N, 126°35.84'E, alt. 600 m, 24 May 2017, at light, S. Podenas, V. Podeniene (NIBR); 1 male, Gyeonggi-do, Gunpo-si, Suri-dong, 37°21.03'N, 126°54.93'E, alt. 140 m, 27 May 2017, S. Podenas, at light, (NIBR); 1 male, 1 female (in alcohol), Jeju-do, Jeju Island, Seogwipo, Saekdal-dong, 33°21.45'N, 126°27.85'E, alt. 1100 m, 19 June 2019, S. Podenas (NIBR); 1 male, 18 June 2019, H.-Y. Seo (NIBR). Also material listed by Starkevich et al. (2015).

Diagnosis. *Tipula* (*V.*) *serricauda* can be recognized by the gonocoxite being armed with a black spine and the ninth tergite divided by pale membrane with ventral portion yellow and bearing a pair of blackened lobes. The body is yellowish, with short antenna reaching the pronotum if bent backward. Female can be recognized by the short, plate-shaped hypovalvae.

***Male*.** Body length 12.9–17.3 mm, wing length 15.6–20.2 mm. General body coloration yellowish.

Head. Yellowish dusted with gray, vertex and occiput yellowish, with dark brown median line. Rostrum yellowish with conspicuous nasus. Antenna 12-segmented, if bent backward reaching pronotum. Scape, pedicel, the first and second flagellar segments yellow; flagellar segments 3–10 darkened at base and yellow apically; remaining segments dark brown. Each flagellomere, except first one, with small, inconspicuous enlargement. Apical flagellomere very small, reduced, distinctly shorter than preceding segment. Verticils longer than corresponding segments. Palpus dark brown.

Thorax. Brownish yellow. Pronotum gray with brown median line. Prescutum and presutural scutum with four longitudinal, grayish-brown stripes bordered by darker brown. Intermediate pair brownish, fused anteriorly and posteriorly, separated in the first third. Lateral stripe grayish. Interspace between median and lateral stripes light brown. Postsutural scutum yellowish, dusted with light gray; scutal lobe with two yellowish spots. Scutellum yellowish; postnotum yellowish, lightly dusted with gray with brown median line. Pleura brownish yellow, lightly dusted with gray. Coxa yellowish; trochanter yellow; femur yellow, distally brown; tibia yellowish brown; tarsal segments dark brown; claw with tooth. Wing distinctly patterned with brown. Halter yellow, knob brown with distal part pale yellow.

Abdomen. Brownish yellow, tergites 1 and 2 with brown spots; tergites 3–5 with dorsal stripe which varies from pale to brown; tergites 6–9 with dorsal stripe distinct, dark brown. Lateral stripe distinct, dark brown. Posterior and lateral margins of ter-

gites pale. First sternite yellowish, sternites 2–4 reddish yellow, remaining sternites passing into brown.

Hypopygium. Brownish (Fig. 30). Ninth tergite divided by pale membrane; dorsal portion brown medially, provided with long setae; ventral portion yellow with a pair of blackened, microscopically roughened lobes on either side of midline (Fig. 31). Tip of lobe obliquely truncated; anal plate shaped as a brown, oblong sclerite. Gonocoxite apically produced into a strong, black spine; ventromesal portion a black point (Fig. 32). Outer gonostylus club-shaped (Fig. 33). Inner gonostylus yellow; beak slender and blackened; lower beak small, nearly triangular (Fig. 34). Dorsal margin with distinct incision; dorso-lateral crest rounded. Dorsal surface medially with blackened area. Adminiculum triangular in ventral view; apex acute and split (Figs 30, 35), fused medially forming a distinct sclerite with raised base. Ventral lobe of appendage of ninth sternite blackened, roughly rounded, and provided with setae; dorsal lobe reduced into small, rounded sclerite (Fig. 35). Semen pump with central vesicle swollen (Figs 36, 37). Compressor apodeme with median incision forming a 65° angle with posterior immovable apodeme. Posterior immovable apodeme longer than compressor apodeme, basally narrow, apically flattened. Anterior immovable rounded. Intromittent organ tube-shaped, about three times as long as semen pump, basally and medially brownish-yellow, passing into yellow towards acute apex.

Female. Body length 20.2–21.1 mm, wing length 16.4–17.1 mm. Generally similar to male. Antenna, if bent backward, reaching pronotum; scape, pedicel, and two basal flagellar segments yellow; remaining flagellomeres vary from yellow to bicolored. Abdomen trivittate, with broad dorsal stripe.

Female terminalia. Tenth tergite shining brown. Cercus reddish brown, nearly straight with tip narrowed and upturned; ventral margin with small, distinct serration; dorsal margin distally also with small serration (Fig. 38). Eighth sternite brown, apically darker brown (Fig. 39). Hypovalva short, dark brown, in the shape of an obliquely truncated plate. Lateral angle of eighth sternite obtuse, with small and distinct incision. Median incision between hypovalvae with serrated edge and provided with setae. Ninth sternite with lateral sclerites nearly straight, posteriorly with incision; surface covered by short setae (Fig. 40). Furca long and narrow (Fig. 40). Spermathecae nearly oval (Fig. 41).

Larva (N = 1). Length 29 mm, width 4 mm. Body light brown (Figs 42–44).

Head capsule. Length 2.3 mm, width 1.2 mm. Head capsule prognathous, hemicephalic, oval, slightly depressed dorsoventrally, and heavily sclerotized (Figs 45, 46). Internolateralia and externolateralia separated by incisions which reach almost middle of head capsule. Externolateralia widely separated ventrally (Fig. 46). Premaxillary suture separates side plate from rest of head capsule. Side plate wide, elongated, with two sensory pits and two long setae anteromedially; a short seta located posteromedially (Fig. 47). Hypostomium asymmetrical, basally fused with ventral margins of genae and side plates; bearing eight sharp teeth: four on left side, most prominent tooth in middle, and three on right side (Fig. 48). Prementum visible from below, bearing five large, sharp teeth on anterior margin; sides of prementum strongly sclerotized (Fig. 49). La-

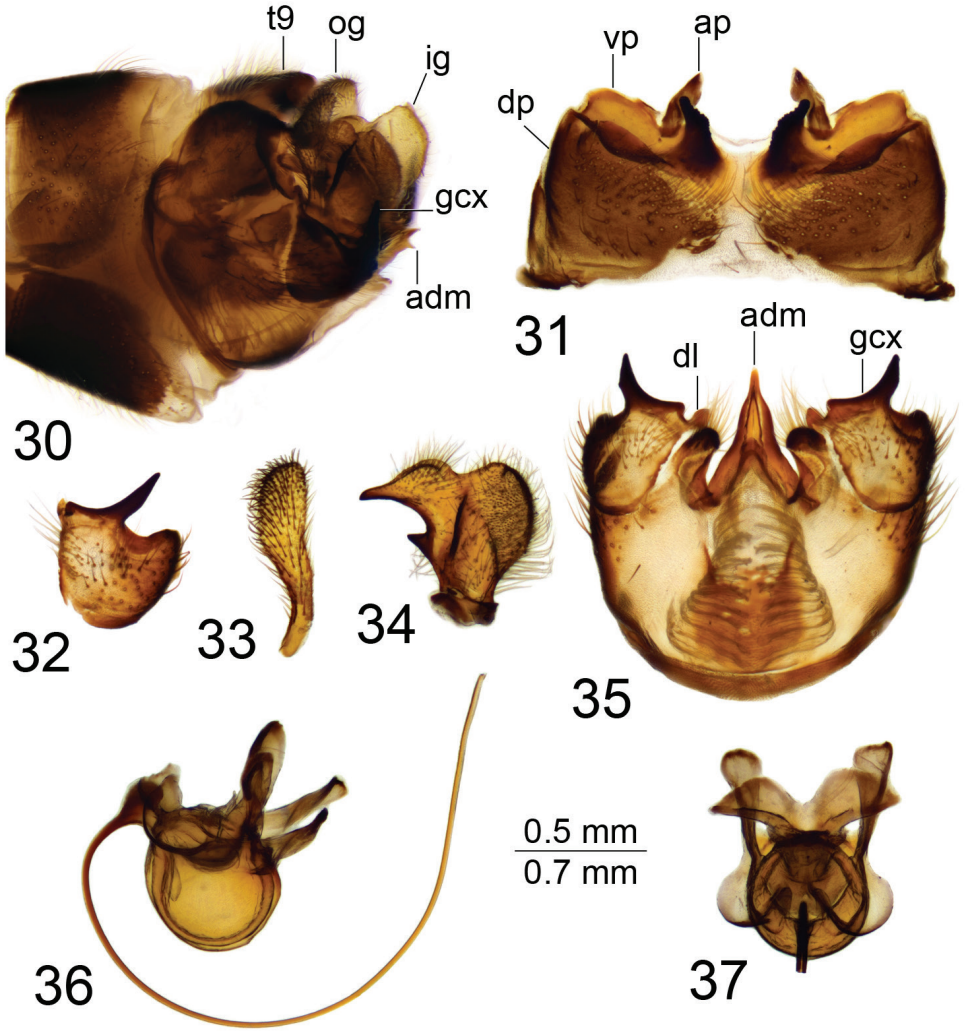

Figures 30–37. Male terminalia of *T.* (*Vestiplex*) *serricauda* **30** hypopygium, lateral view **31** ninth tergite, dorsal view **32** left gonocoxite, lateral view **33** left outer gonostylus **34** left inner gonostylus, lateral view **35** ninth sternite, ventral view (ninth tergite, outer and inner gonostyles removed) **36** semen pump and intromittent organ, lateral view **37** semen pump, dorsal view. Abbreviations: adm, adminiculum; ap, anal plate; dl, dorsal lobe of appendage of ninth sternite; dp, dorsal portion of ninth tergite; gcx, gonocoxite; ig, inner gonostylus; og, outer gonostylus; t9, ninth tergite; vp, ventral portion of ninth tergite. Scale bars: 0.7 mm (**30**); 0.5 mm (**31–37**).

bial area entirely covered with firm bristles and bearing a pair of cone-shaped palpes. Prementum dorsally fused with hemispherical and membranous hypopharynx which is covered with numerous short hairs. Lateral arm of hypopharynx curved and strongly sclerotized. Frontoclypeus fused with internolateralia. Clypeal part of frontoclypeus membranous, frontal part sclerotized. One long seta and three sensory pits on anterior

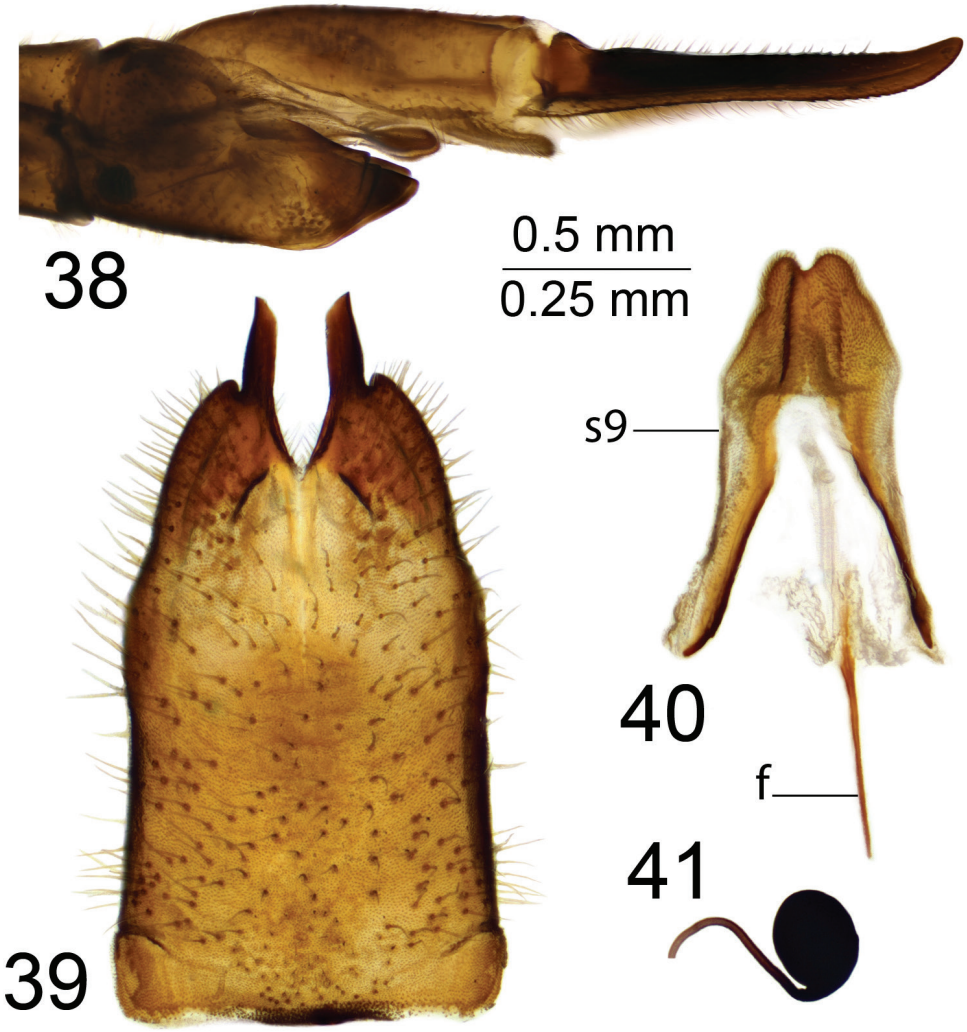

Figures 38–41. Female terminalia of *T.* (*Vestiplex*) *serricauda* **38** ovipositor, left lateral view **39** eighth sternite with hypovalvae, ventral view **40** ninth sternite with furca, dorsal view **41** spermatheca, dorsal view. Abbreviations: f, furca; s9, ninth sternite. Scale bars: 0.25 mm (**38**); 0.5 mm (**39–41**).

part of clypeus; three short setae near inner margin of antenna (Fig. 50). Clypeolabral suture obscure. Dorsal ecdysial sutures (frontal sutures) present, meeting each other posteriorly and forming a short median coronal suture. Ecdysial sutures enclose V-shaped frontoclypeus and extend anteriorly only to base of clypeus. Labrum trapezoidal and composed of two triangular plates separated by membranous area (Fig. 50). Apical part of labrum and epipharynx covered with numerous, short hairs. Membranous part of labrum with a pair of medium-long setae in middle. Labral plates sclerotized only posteriorly and bearing numerous long firm spines on outer margin. Each plate bears

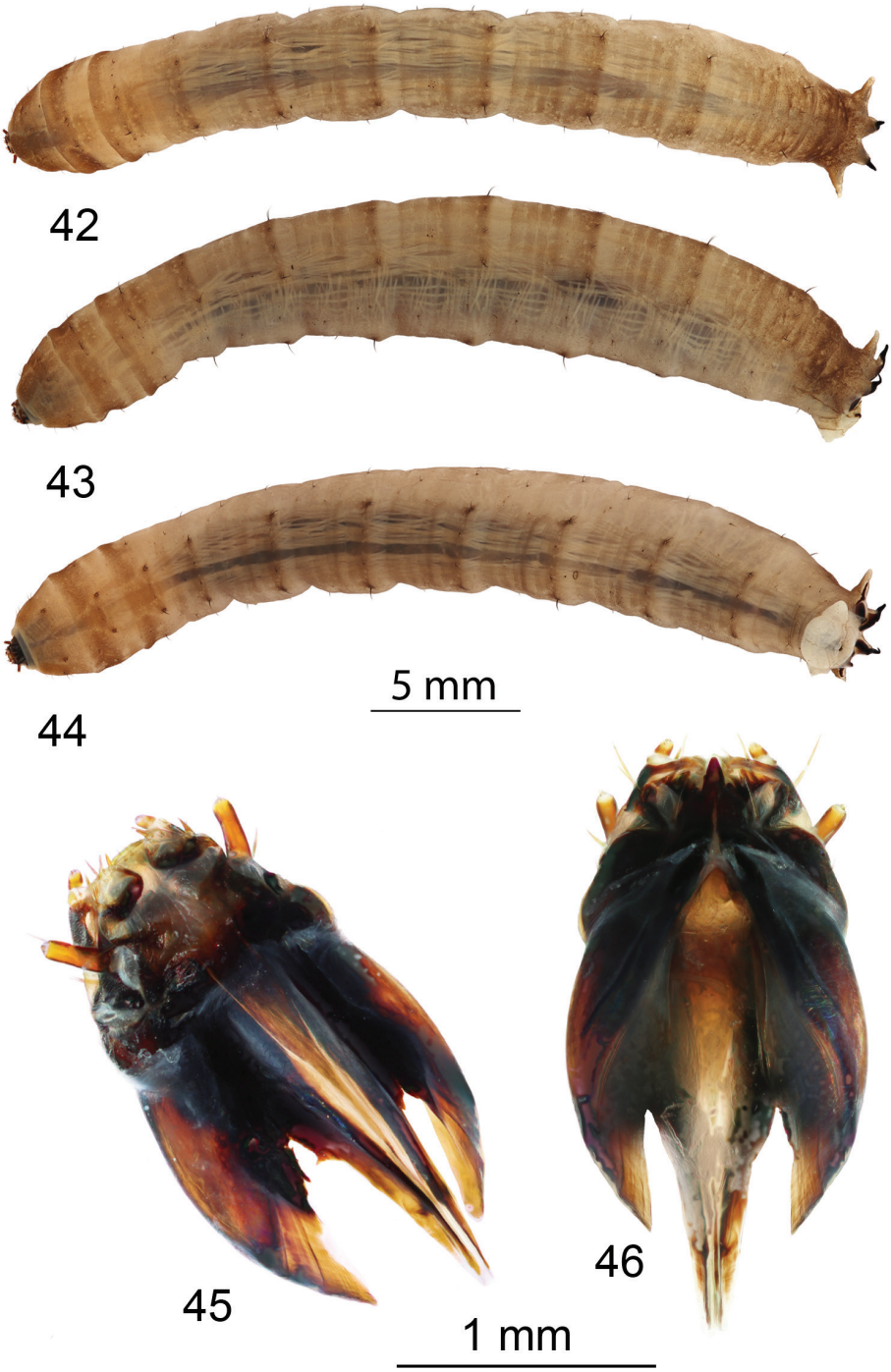

Figures 42–46. Larva of *T.* (*Vestiplex*) *serricauda* **42** general view, dorsal aspect **43** general view, lateral aspect **44** general view ventral aspect **45** general view of head capsule, dorsal aspect **46** general view of head capsule, ventral aspect. Scale bars: 5 mm (**42–44**); 1 mm (**45–46**).

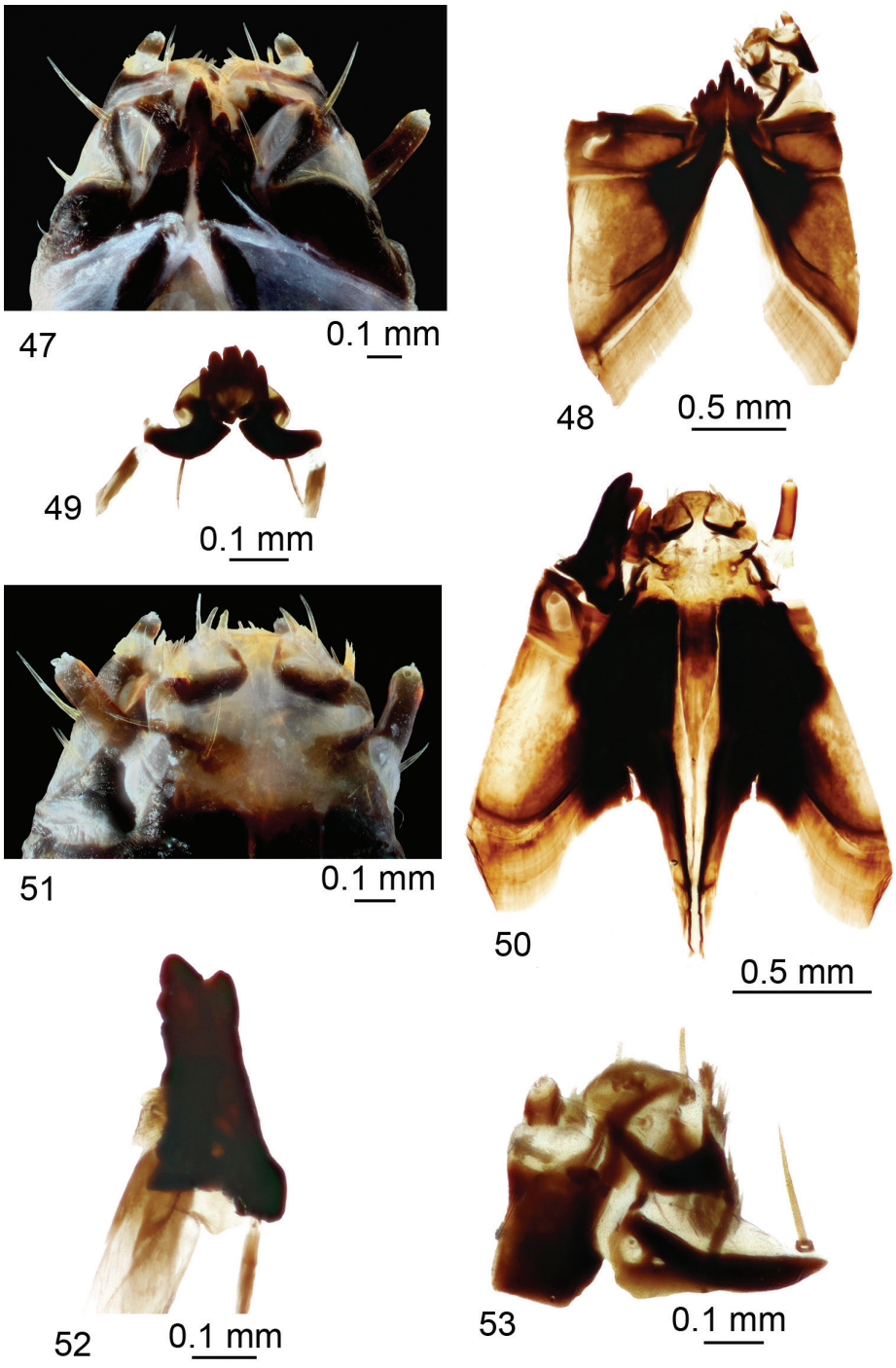

Figures 47–53. Larva of *T.* (*Vestiplex*) *serricauda* **47** side plates **48** hypostoma **49** hypopharynx and prementum **50** frontoclypeus **51** labrum and antennae **52** right mandible, dorsal view **53** left maxilla, ventral view. Scale bars: 0.1 mm (**47, 49, 51–53**); 0.5 mm (**48, 50**).

a long seta, one long and two very short papillae on anterior part, one long seta almost at middle, and a sensory pit on postero-lateral part (Fig. 51). Antenna elongated, cylindrical. It has just one cylindrical segment, which is three times as long as wide at base (Fig. 51). Apically it has one small cone-shaped and several (exact number difficult to establish) small, peg-like sensillae; dorsally it has a sensory pit near middle. Mandible 1-segmented and more sclerotized than rest of head capsule, armed with four teeth (Fig. 52). Apical tooth is the most prominent; first dorsal and ventral teeth smaller than apical; second dorsal tooth smallest. Prostheca or *lacinia mobilis* present on dorsal side of mesal mandibular base; prostheca sclerotized, distinctly widening distally, and set with numerous hairs. Lateral margin of mandible with two long setae near base; a sensory pit present at base of dorsal side of mandible. Mandibles operate in horizontal plane. Conspicuous larval eye spot present below base of mandible. Maxilla consists of cardo and outer and inner lobes. Cardo wedge-shaped, bearing two long setae near distal end and a long seta near its base (Fig. 53). Outer lobe (stipes) sclerotized, except apex, which bears prominent, cylindrical palpus with several sensory structures. Short sensory structure and several long, sclerotized spines (exact number difficult to establish) on inner margin of stipes. Inner lobe (galea fused with lacinia) ventrally bears elongated, narrow sclerite extending around inner margin onto its dorsal surface; diamond-shaped sclerite present dorsally at base (Fig. 53); apical part with numerous short hairs, three long setae, and prominent sensory structure. Lacinia armed with several stout bristles and bears a ridge with sclerotized spines on outer margin.

Thorax. All thoracic segments wider than long. Anterior part of second and third segments covered with much denser pubescence than posterior (Figs 42–44).

Abdomen. First abdominal segment almost twice as long as wide. Abdominal segments II–VII almost as long as wide. All abdominal segments except last one covered by short microscopic hairs arranged into transverse rows, which are interrupted by pubescence on ventral and dorsal sides. Most macrosetae dark brown except L2 and L3. Dorsal setae D2 and D3 longest; seta D1 only slightly shorter than D2 and D3; setae D4–D6 short and appressed, more than three times shorter than D2 and D3. Setae D2 + D3 and D5 + D6 close to each other and separate from others. Lateral setae L2 and L3 very short and pale; L1 and L4 long and almost equal in length; L2 dorsolateral to L1. Setae L1, L4 more than four times as long as L2 and L3. V2 almost equal to V3 and both the longest of ventral setae. Setae V4 and V5 slightly shorter than V2 and V3. Seta V1 very short, more than five times shorter than V2 and V3.

Anal division. Dorsal and lateral lobes of spiracular disc subconical, lateral lobes in dorsolateral position (closer to dorsal than to ventral lobes). Dorsal and lateral lobes similar in length, twice as long as wide at base (Fig. 54). Ventral lobe very small, triangular, its length almost equal to width at base. Ventral lobe almost five times as short as dorsal or lateral lobe. Dorsal lobe completely sclerotized, with apex extended into acute, anteriorly directed point (Fig. 55). Lateral lobe with long, narrow, curved, dark sclerite that starts near base of spiracle and extends to mid-length of lobe; a long seta present in middle of outer edge of lobe. Ventral lobe with three small, dark spots at base; outermost spot most prominent. Distal half of lobe sclerotized, with long apical

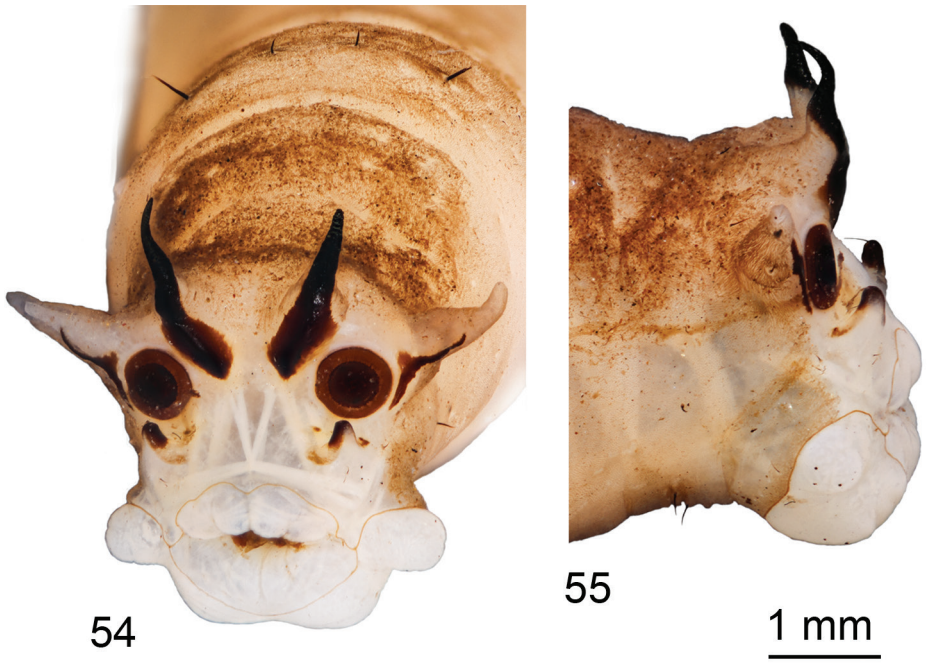

Figures 54–55. Larva of *T.* (*Vestiplex*) *serricauda* **54** spiracular field **55** anal division, lateral view. Scale bar: 1 mm.

seta. Spiracle subcircular, inner circle black, outer ring brown; distance between spiracles almost twice diameter of a spiracle. Remaining area around spiracles white and glabrous. Four white, fleshy anal papillae arranged into anterior and posterior pairs. Anterior papilla broadly rounded; posterior papilla more elongated (Fig. 54). A brown band separates anus and anal papillae; this band connected to marginal band.

Habitat. Larvae were found under leaf litter and woody debris accumulated on boulders. Two identical last instar larvae were collected and one of them was kept for rearing. A female emerged after 36 days and identified as *T.* (*V.*) *serricauda*.

Known distribution. China, Japan, and South Korea (Starkevich et al. 2015; Oosterbroek 2019).

Remarks. A single male belonging to *T.* (*V.*) *serricauda* was erroneously identified and published as *T.* (*Mediotipula*) *anatoliensis* Theowald, 1978 by Baek and Bae (2016) based on Korean material. The hypopygium, with broken apical part of gonocoxite (Baek and Bae 2016: fig. 2E), is identical to that of *T.* (*V.*) *serricauda* and can be easily recognized by the shape of inner gonostylus.

New data received from the larvae of *T.* (*V.*) *serricauda* once again confirm that the most important synapomorphy in the subgenus *T.* (*Vestiplex*) is a brown band separating the anus from the anal papillae, which is a unique character for this subgenus. According to the type of sclerotization of the spiracular field, larvae of the subgenus *T.* (*Vestiplex*) (based on *T.* (*V.*) *nubeculosa* Meigen, 1804, *T.* (*V.*) *hortorum* Linnaeus,

1758, *T*. (*V*.) *montana* Curtis, 1834, *T*. (*V*.) *excisa* Schummel, 1833, *T*. (*V*.) *scripta* Meigen, 1830, *T*. (*V*.) *platymera* Walker, 1856, *T*. (*V*.) *arctica* Curtis, 1835, *T*. (*V*.) *semivittata* Savchenko, 1960, and *T*. (*V*.) *serricauda*) can be divided into four groups. The first group includes larvae of such species as *T*. (*V*.) *scripta*, *T*. (*V*.) *platymera*, and *T*. (*V*.) *semivittata*. They possess sclerotized dorsal lobes with sclerotization encompassing the apices of the lobes and forming an acute, slightly anteriorly directed point. In addition, each lateral lobe has a thin, straight, and more or less vertical sclerite. The ventral lobes of this first group have sclerotized apices with several short setae and a narrow sclerotized band (with three dark spots inside) extending across the base. The second group includes *T*. (*V*.) *arctica*, *T*. (*V*.) *nubeculosa*, and *T*. (*V*.) *hortorum*. This group possesses sclerotized dorsal lobes but the sclerotization does not reach the apex of the lobe. Lateral and ventral lobes are very similar to that of the first group. The third group includes *T*. (*V*.) *excisa* and *T*. (*V*.) *montana*. This group of species possesses sclerotized dorsal lobes, with the sclerotization reaching the apex, but never forming anteriorly directed points. The lateral and ventral lobes are very similar to that of the first and second groups. The fourth group consists of only *T*. (*V*.) *serricauda*. Each dorsal lobe of this species is sclerotized both anteriorly and posteriorly, with each apex forming an acute, strongly anteriorly directed point. Each lateral lobe has a long, narrow, curved, dark sclerite, extending from near the base of a spiracle to the mid-length of each lobe. Each ventral lobe has a sclerotized distal part with a long apical seta, the base of each lobe with three small dark spots, with the narrow band missing. Sclerotization of the spiracular field of the fourth group most resembles that of larvae of *T*. (*Triplicitipula*) but not as seen in other groups of the subgenus *T.* (*Vestiplex*). The macrosetal arrangement on the dorsum and venter of the abdomen appears to be consistent in the subgenus, but the arrangement of the abdominal lateral setae is species-specific. Head capsules have never been comparatively studied in detail for the genus *Tipula* or the subgenus *T.* (*Vestiplex*); thus, comparison has been impossible among species and subgenera.

***Tipula* (*Vestiplex*) *tchukchi* Alexander, 1934**

Figs 56–66, 89

Tipula (*Vestiplex*) *tchukchi* Alexander 1934: 408.
Tipula (*Vestiplex*) *tchukchi obtusidens* Savchenko 1964: 205 (synonymy after Starkevich and Paramonov 2016).
Tipula (*Vestiplex*) *bo* Mannheims 1967: 148 (synonymy after Mannheims and Savchenko 1973).

Type material examined. Holotype, male, **RUSSIA**, Chukchi Peninsula, Chukotka Autonomous Okrug, Markovo township near Anadyr town, 6 July 1896, Gondatti (ZIN); paratype, female, topotypic (ZIN); paratype, male, Kamchatka Kray, mouth of Kichiga River, 27 June 1910, Skorikov (ZIN).

Other examined material (Fig. 89). **NORTH KOREA**, 1 male, Seren Mts, alt. 3500 ft, 25 June 25 1938, Yankovsky (USNM); 1 female, **MONGOLIA**, Tov Aimag, Erdene Soum, Gorkhi Terelj National Park, unnamed tributary of Tuul River on its west side, 1.6 km upstream from Daichin crossing, 48.21780°N, 107.90392°E, alt. 1600 m, 9 July 2003, SRP#03070902, coll. O. Yadamsuren (ANSP).

Diagnosis. *Tipula* (*V.*) *thukchi* can be recognized by the unarmed gonocoxite and the ninth tergite forming a concave, roughly rectangular, sclerotized saucer. The body coloration is blackish yellow, and the wing pattern is indistinct. The female has the cercus with an apical incision and outer margin rough and distinctly serrated. The eight sternite has a distinct lateral incision, and the hypovalvae are filamentous.

***Male*.** Body length 16.8 mm, wing length 17.1 mm. General body coloration blackish yellow.

Head. Gray, vertex and occiput gray with brown median line. Rostrum brown, dorsally dusted with gray. Nasus short. Antenna 13-segmented, if bent backward extending beyond the wing base. Scape and pedicel yellowish; first flagellar segment brownish; subsequent flagellar segments dark brown. Each flagellomere except first one with basal enlargement and moderately incised. Apical flagellomere small, reduced. Verticils shorter than corresponding segments. Palpus dark brown.

Thorax. Brown, dusted with grey. Pronotum blackish, gray dusted, with brown median line. Prescutum and presutural scutum brown, grey pruinose with four longitudinal stripes bordered by brown. Intermediate pair fused into brown median line. Interspace between median and lateral stripes light gray. Postsutural scutum blackish, gray pruinose with median line. Scutal lobe with two spots bordered by brown. Scutellum brown, postnotum brown, dusted with gray-brown; both sclerites with darker median line. Pleura brown, dusted with gray. Coxa brown, grey pruinose. Trochanter, femur, and tibia yellowish. Tarsal segments brown. Distal part of femur and tibia dark brown. Tarsal claws toothed. Wing pattern indistinct, only weak darkening along vein CuA. Halter yellowish, with brown knob.

Abdomen. Yellow. Abdominal segments 1–4 yellow, subsequent segments passing into dark brown. Tergites with lateral margins narrowly pale; dorsal stripe broad; lateral stripe pale.

Hypopygium. Brownish black. Ninth tergite forming a large, concave, roughly rectangular sclerotized saucer. Main body of tergal saucer brown and rim blackened (Fig. 56). Posterior margin of tergal saucer toothed with small denticles, broadly emarginated, with deep median U-shaped notch. Lateral angles of tergal saucer obtuse, broadly truncated. Anterior and lateral portions of tergal saucer raised into sclerotized border; border laterally produced into obtuse point directed caudad and situated under lateral angle of tergal saucer so that ninth tergite with two teeth in lateral view. Gonocoxite unarmed (Fig. 57). Outer gonostylus flattened, slightly curved, with apex rounded (Fig. 58). Inner gonostylus in the shape of a curved plate, terminating dorsally with obtuse tooth; beak claw-shaped (Fig. 59). Gonocoxal fragment large, with lateral and medial sclerites well developed (Fig. 60). Medial sclerites fused anteriorly

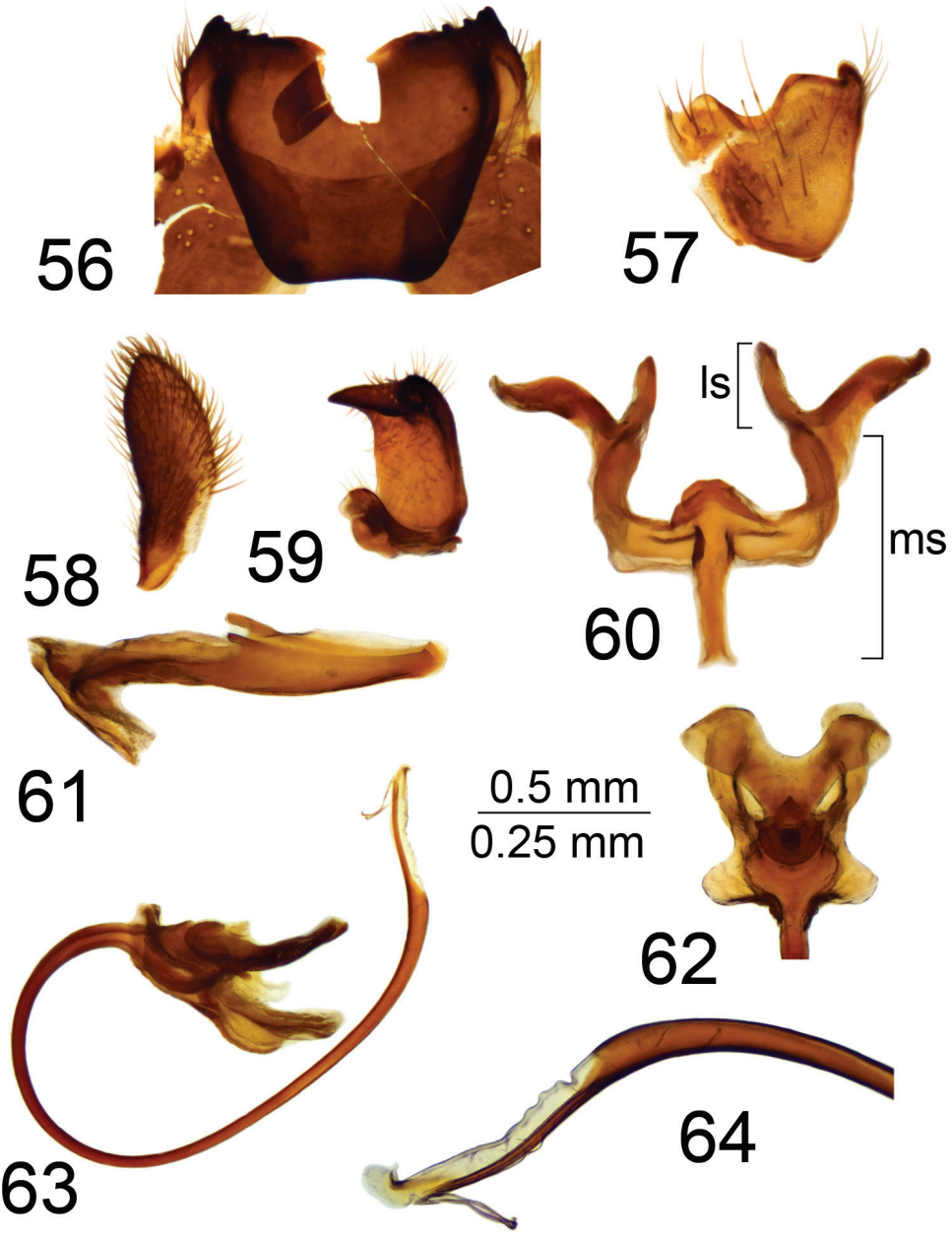

Figures 56–64. Male terminalia of *T.* (*Vestiplex*) *tchukchi* **56** ninth tergite, dorsal view **57** left gonocoxite, lateral view **58** left outer gonostylus **59** left inner gonostylus, lateral view **60** gonocoxal fragment, dorsal view **61** adminiculum, lateral view **62** semen pump, dorsal view **63** semen pump and intromittent organ, lateral view **64** distal part of intromittent organ, lateral view. Abbreviations: ls, lateral sclerite of gonocoxal fragment; ms, medial sclerite of gonocoxal fragment. Scale bars: 0.5 mm (**56–63**); 0.25 mm (**64**).

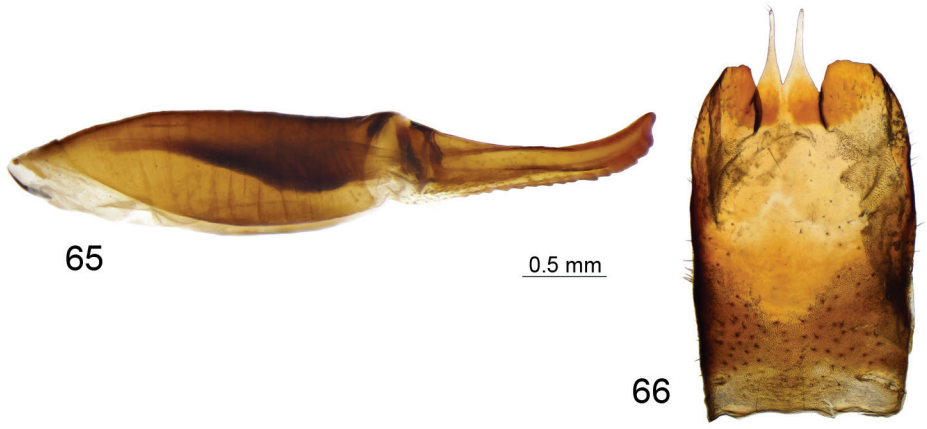

Figures 65–66. Female terminalia of *T.* (*Vestiplex*) *tchukchi* (Mongolia). **65** tenth tergite with cercus, left lateral view **66** eighth sternite with hypovalvae, ventral view. Scale bar: 0.5 mm.

into long, narrow apodeme; posteriorly with rounded apodeme; lateral parts broadened and arched. Lateral sclerite large and bilobed, expanded at base. Adminiculum canoe-shaped (Fig. 61). Semen pump with central vesicle relatively small and flattened (Figs 62, 63). Compressor apodeme with broad median incision, forming a 50° angle with posterior immovable apodeme. Posterior immovable apodeme approximately as long as compressor apodeme. Anterior immovable apodeme rounded. Intromittent organ tube-shaped, about four times as long as semen pump, basally and medially brown, passing into yellow towards apex. Distal part ventrally truncated, shovel-shaped, with rough edge and two stripped fragments (Fig. 65).

Female. Female not known from Korean Peninsula, but can be recognized by cercus having apical incision and rough and distinctly serrated outer margin (Fig. 65). Hypovalva filamentous, flattened, broadened at base, distally pale, with short trichia at tip (Fig. 66). Median incision between hypovalvae deeper than posterior margin of eighth sternite; lateral incisions distinct.

Known distribution. Finland, Sweden, Russia, and Mongolia (Oosterbroek 2019). Recorded here for the first time from the Korean Peninsula.

Tipula (*Vestiplex*) *verecunda* Alexander, 1924

Figs 67–85, 90

Tipula verecunda Alexander 1924: 606.
Tipula (*Vestiplex*) *verecunda*: Alexander 1935: 118; Savchenko 1964: 152; Oosterbroek and Theowald 1992: 160.

Type material examined. Holotype, male, **RUSSIA**, [Sakhalin Island] Toyohara [Yuzhno-Sakhalinsk], July16, 1922, Esaki (USNM); paratypes, 3 males, 1 female,

13–14 July 1922, Esaki, topotypic (USNM); paratype, female, Shimizu [Southern Sakhalin], 27 July 1922, Esaki (USNM); paratype, female, Odasam [Southern Sakhalin], 31 July 1922, Esaki (USNM).

Other examined material (Fig. 90). **SOUTH KOREA**, 5 males, 3 females, Jeju-do, Jeju Island, Seogwipo, Saekdal-dong, 33°21.45'N, 126°27.85'E, alt. 1100 m, 18 June 2019, H.-Y. Seo (NIBR); 6 males, Seogwipo, Saekdal-dong, 35°21.62'N, 126°27.76'E, alt. 1100 m, 18 June 2019, S. Podenas (NIBR). **CHINA**, 1 male, Shaanxi, Qinling Mts, Hauzherza vill., 33°52.42'N, 107°48.77'E, alt. 1600 m, 2–3 June 2009, leg. Saldaitis & Floriani (NRC).

Diagnosis. *Tipula* (*V.*) *verecunda* can be easily recognized by the eighth sternite laterally having long setae and the ninth sternite being ventrally produced into a small tubercle. The ninth tergite has a U-shaped notch posteriorly, and anterior to the notch, the tergite is divided by a pale membrane. The ventral portion of the ninth tergite is yellow, with a pair of blackened narrow plates, and the gonocoxite is unarmed. The thorax is grey, with four darker grey stripes narrowly bordered by brown, and the wing is distinctly patterned with dark brown. The female can be recognized by the cercus having a smooth margin and a long, blade-shaped hypovalvae.

***Male*.** Body length 17.4–21.6 mm, wing length 20.0–24.5 mm. General body coloration brownish yellow.

Head. Vertex and occiput ochraceous yellow, with dark median line. Rostrum dark brown, dorsally narrowly ochraceous yellow. Nasus distinct. Antenna 13-segmented, if bent backward extending beyond the wing base. Scape and pedicel yellow; flagellum brownish black. Each flagellomere, except for first one, with weak basal enlargement. Apical flagellomere small, reduced. Verticils longer than corresponding segments. Palpus dark brown.

Thorax. Pronotum ochraceous yellow, with dark median spot. Prescutum and presutural scutum grey, with four darker grey stripes, narrowly bordered by brown. Intermediate pair fused anteriorly. Interspace ochraceous light yellow. Postsutural scutal lobe with two ochraceous brownish yellow spots bordered by brown. Scutellum brown, with broad, dark brown median line. Postnotum brownish, with pale median line, and dusted with gray. Pleura yellowish. Wing distinctly patterned with dark brown. Halter pale, with brownish-black knob. Coxa yellowish; trochanter yellow; femur basally yellow, passing into brown towards dark brown tip. Tibia and tarsal segments brownish black. Tarsal claw with tooth.

Abdomen. Abdominal segments 1–4 yellow; segment 5 blackish, yellowish laterally; remaining segments black. Dorsal stripe on first tergite broad, on tergites 2–4 pale, on fifth tergite black. Lateral abdominal stripe distinct.

Hypopygium. Black (Fig. 67). Ninth tergite posteriorly with deep U-shaped notch, anteriorly to notch divided by pale membrane, dorsal portion dark brown, posterior margin provided with setae, additional short projection on either side of midline (Figs 68, 69). Ventral portion yellow with a pair of blackened and microscopically serrated narrow plates; tip of plate pointed outward. Anal plate shaped as a small brown sclerite (Fig. 68). Gonocoxite unarmed, irregular in outline (Fig. 71).

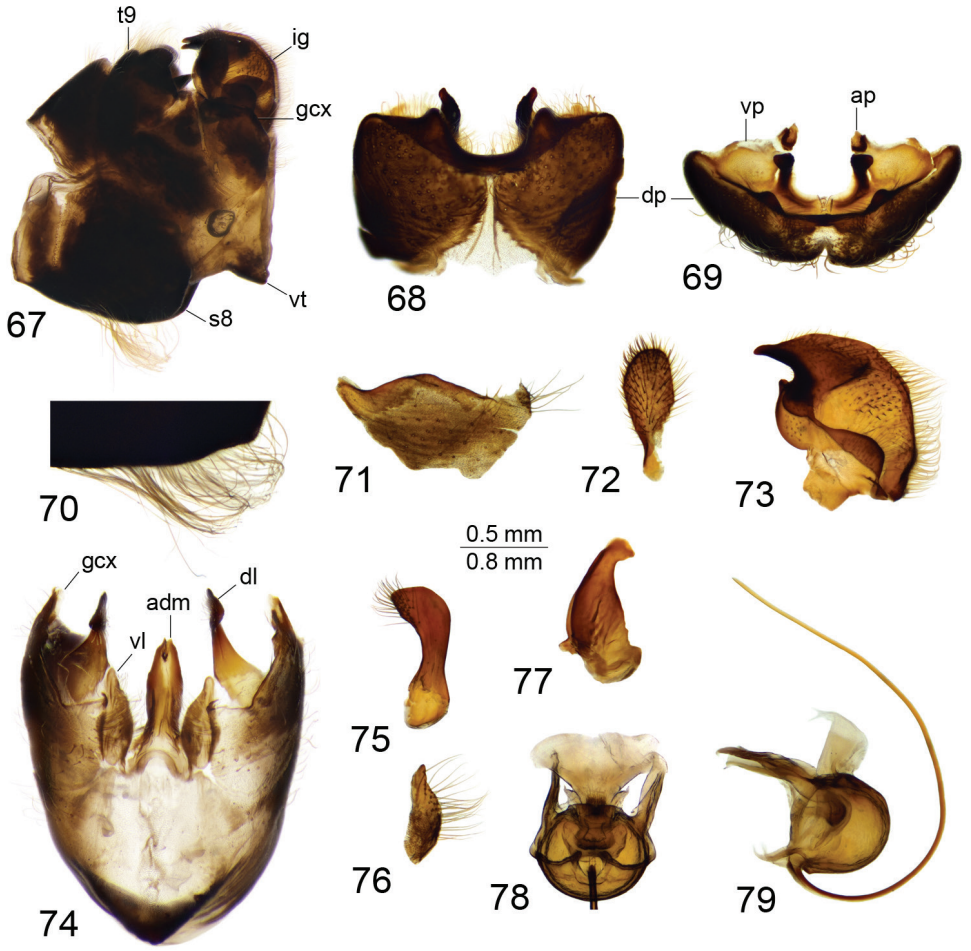

Figures 67–79. Male terminalia of *T.* (*Vestiplex*) *verecunda* **67** hypopygium, lateral view **68** ninth tergite, dorsal view **69** ninth tergite, caudal view **70** eighth sternite, lateral view **71** left gonocoxite, lateral view **72** left outer gonostylus **73** left inner gonostylus, lateral view **74** ninth sternite, ventral view (ninth tergite, outer and inner gonostyles removed) **75** right dorsal lobe of appendage of ninth sternite **76** right ventral lobe of appendage of ninth sternite **77** adminiculum, lateral view **78** semen pump, dorsal view **79** semen pump and intromittent organ, lateral view. Abbreviations: adm, adminiculum; ap, anal plate; dl, dorsal lobe of appendage of ninth sternite; dp, dorsal portion of ninth tergite; gcx, gonocoxite; gcx, gonocoxite; ig, inner gonostylus; og, outer gonostylus; s8, eighth sternite; vl, ventral lobe of appendage of ninth sternite; vp, ventral portion of ninth tergite; vt, ventral tubercle of ninth sternite. Scale bars: 0.8 mm (**67**); 0.5 mm (**68–79**).

Outer gonostylus nearly oval, with basal part narrowed (Fig. 72). Inner gonostylus in the shape of rounded sclerite, terminating into a short upper beak with a small lower beak; beaks separated by round incision (Fig. 73). Dorsal crest with yellow setae and short, black spines grouped on dorsal surface, edge basally bent outward. Adminiculum nearly parallel-sided in ventral view, fused medially forming a distinct sclerite

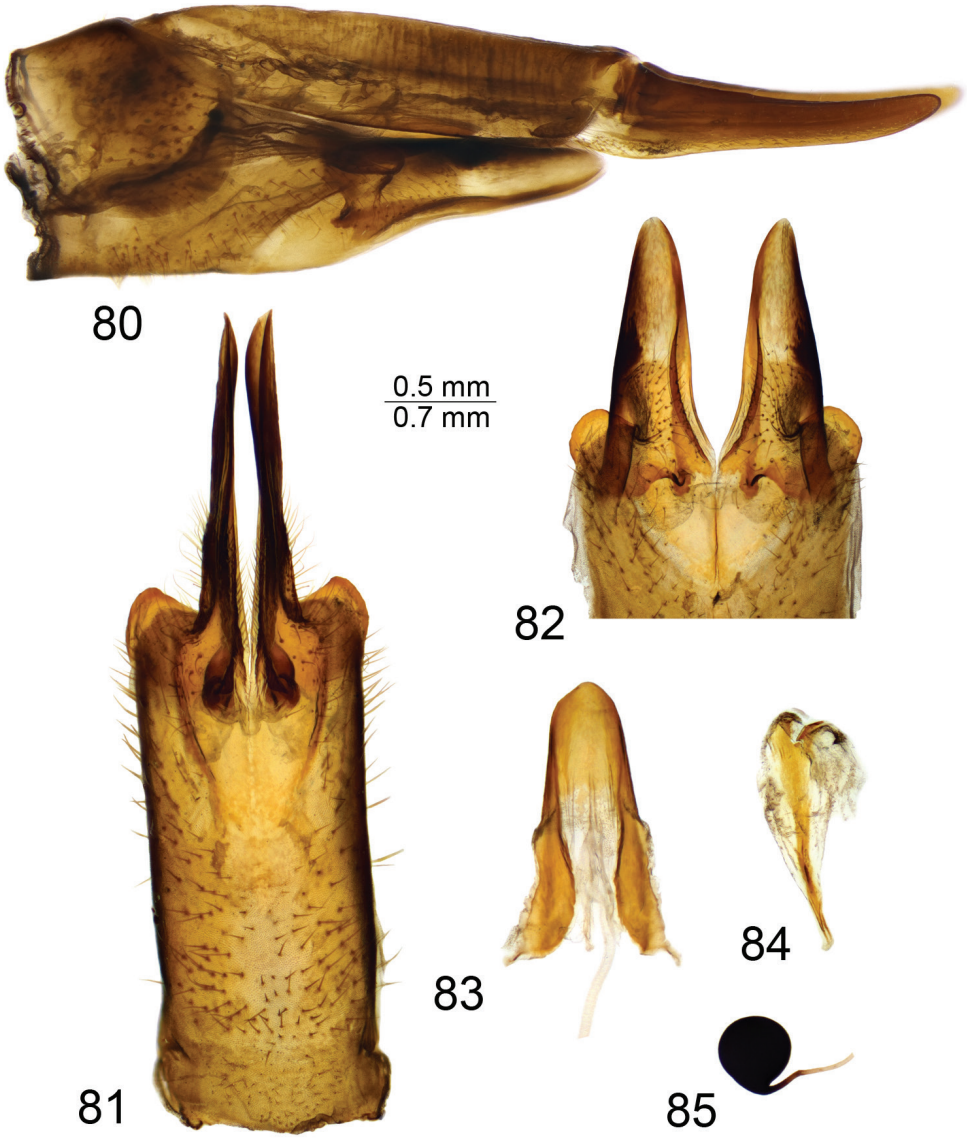

Figures 80–85. Female terminalia of *T.* (*Vestiplex*) *verecunda* **80** ovipositor, left lateral view **81** eighth sternite with hypovalvae, ventral view **82** distal part of eighth sternite with hypovalvae, ventral view **83** ninth sternite, dorsal view **84** furca, dorsal view **85** spermatheca, dorsal view**.** Scale bars: 0.7 mm (**80, 82**); 0.5 mm (**81, 83–85**).

(Fig. 74). Basal part of adminiculum broadened and raised; apex funnel-shaped, with preapical incision in ventro-lateral view (Fig 77). Ninth sternite ventrally produced into small tubercle (Figs 67, 74). Appendage of ninth sternite with ventral lobe oblong, tip narrowed, surface with setae (Figs 74, 76). Dorsal lobe in the shape of flattened, curved plate; tip on inner surface provided with setae (Figs 74, 75). Eighth

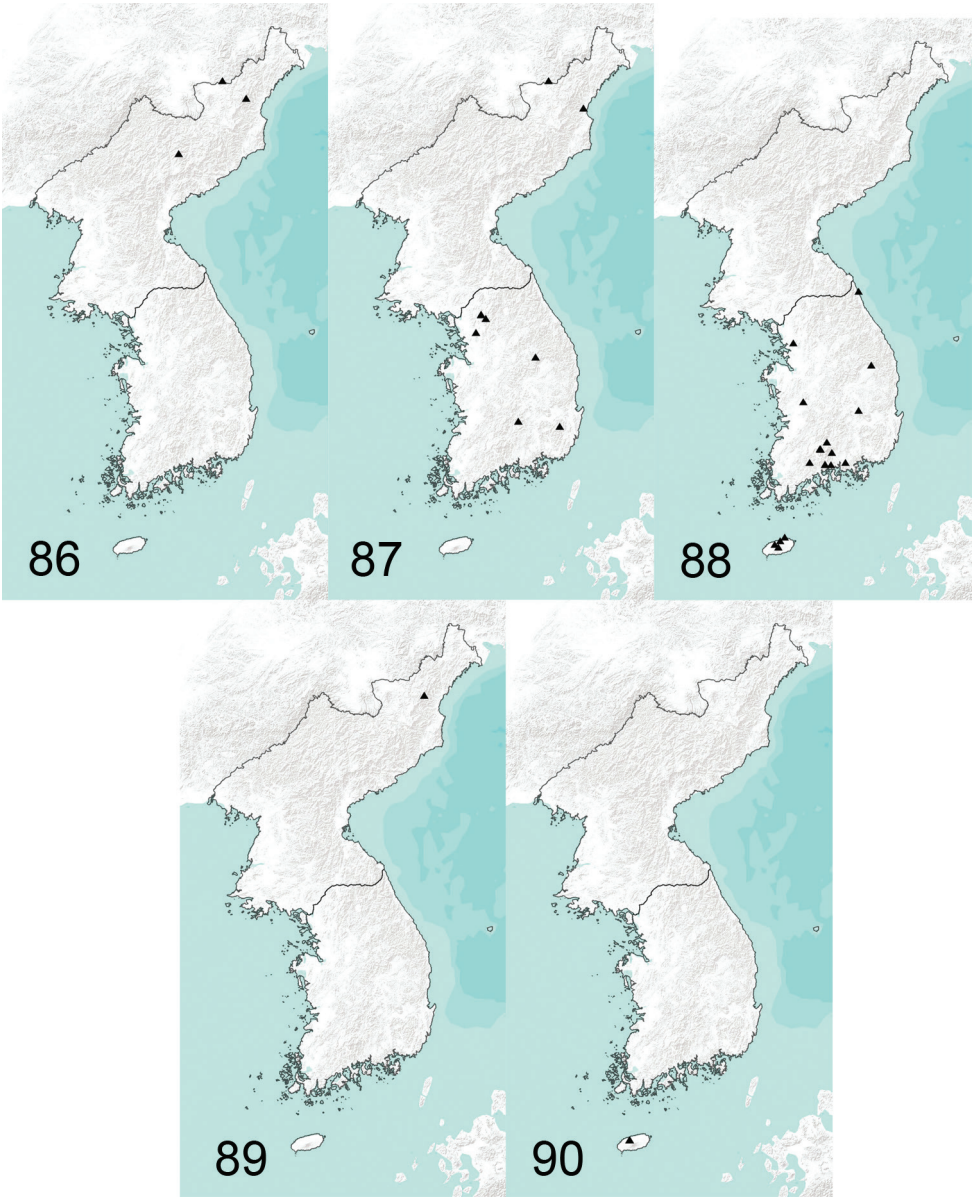

Figures 86–90. Collecting sites of *T.* (*Vestiplex*) in Korean Peninsula **86** *T.* (*V.*) *coquillettiana* **87** *T.* (*V.*) *kuwayamai* **88** *T.* (*V.*) *serricauda* **89** *T.* (*V.*) *tchukchi* **90** *T.* (*V.*) *verecunda*.

sternite posteriorly with pale median area; laterally provided with long setae reaching 1.1 mm long. Semen pump with central vesicle swollen (Figs 78, 79). Compressor apodeme flattened forming a 50° angle with posterior immovable apodeme. Posterior immovable apodeme shorter than compressor apodeme, narrowed. Anterior immovable apodeme narrow. Intromittent organ tube-shaped, about three times as long

as semen pump, basally and medially brownish yellow, passing into yellow towards acute apex.

***Female*.** Body length 27.3–28.7 mm, wing length 23.0–24.5 mm. Generally similar to male. Thorax brown. Abdomen with distinct median stripe. Tergites and sternites with lateral margin pale.

Female terminalia. Tenth tergite basally shining brown but on other two-thirds shining black. Cercus reddish brown, nearly straight, with tip narrowed; ventral margin smooth (Fig. 80). Eighth sternite with hypovalva long, blade-shaped, basally with setae (Figs 80–82). Lateral angle of eighth sternite flattened and slightly extended. Ninth sternite with posterior half funnel-shaped, rounded apically (Fig. 83). Furca in the shape of a pale stripe narrowed anteriorly (Fig. 84). Spermatheca spherical (Fig. 85).

Known distribution. Russia, Japan, and China (Oosterbroek 2019). Recorded here for the first time from South Korea.

Acknowledgements

We give our warmest thanks to all our Korean friends and colleagues who helped us during our visits to South Korea. We are very grateful for professor Y.J. Bae for the specimens from the Korea University, Seoul, Republic of Korea; J.C. Thomas (SEM) for the help with Korean specimens from the University of Kansas, USA.; Dr F. Shockley and Dr T. Dikow (USNM), Dr J.K. Gelhaus (ANSP) for use of the USNM specimens; Dr N. Paramonov (ZIN), St. Petersburg, Russia; and A. Saldaitis (NRC), Vilnius, Lithuania. We thank J. Kim (KU) for the help with Korean labels.

We are grateful to Dr F. Brodo (Canadian National Collection of Insects, Arachnids and Nematodes, Ottawa, Canada) and Dr J. Gelhaus (ANSP) for revising and improving the manuscript.

This work was supported by a grant from the National Institute of Biological Resources (NIBR), funded by the Ministry of Environment (MOE) of the Republic of Korea (NIBR201902108).

References

Alexander CP (1914) Report on a collection of Japanese crane-flies (Tipulidae, Diptera) [concl.]. Canadian Entomologist 46: 236–242. https://doi.org/10.4039/Ent46236-7

Alexander CP (1918) New species of tipuline crane-flies from eastern Asia (Tipulidae, Diptera). Journal of the New York Entomological Society 26: 66–75.

Alexander CP (1920a) The crane-flies of New York. Part II. Biology and phylogeny. Memoirs, Cornell University Agricultural Experiment Station 38: 691–1133. https://doi.org/10.5962/bhl.title.33641

Alexander CP (1920b) New or little-known crane-flies from Japan (Tipulidae, Diptera). Transactions of the American Entomological Society 46: 1–26.

Alexander CP (1921) Undescribed species of Japanese crane-flies (Tipulidae, Diptera). Part II. Annals of the Entomological Society of America 14: 111–134. https://doi.org/10.1093/aesa/14.2.111

Alexander CP (1924) New or little-known crane flies from northern Japan (Tipulidae, Diptera). Philippine Journal of Science 24: 531–611.

Alexander CP (1925) New or little-known crane-flies. Part I. Encyclopedie Entomologique, (B II), Diptera 2: 87–93.

Alexander CP (1934) New or little-known Tipulidae from eastern Asia (Diptera). XVII. Philippine Journal of Science 52: 395–442.

Alexander CP (1935) New or little-known Tipulidae from eastern Asia (Diptera). XXV. Philippine Journal of Science 57: 81–148.

Alexander CP (1953) Records and descriptions of Japanese Tipulidae (Diptera). Part II. The crane-flies of Shikoku. II. Philippine Journal of Science 82: 141–179.

Alexander CP (1965) New subgenera and species of crane-flies from California (Diptera: Tipulidae). Pacific Insects 7: 333–386.

Bezzi M (1924) Una nuova *Tipula* delle Alpi con ali ridotte anche nel maschio (Dipt.). Annali del Museo Civico di Storia naturale di Genova 51: 228–233.

Baek HM, Bae YJ (2016) New records of the genus *Tipula* (Diptera: Tipulidae: Tipulinae) in Korea. Entomological Research Bulletin 32: 161–164.

Brodo F (2017) Taxonomic review of *Angarotipula* Savchenko, 1961 (Diptera: Tipulidae) in North America. Canadian Entomologist 150: 12–34. https://doi.org/10.4039/tce.2017.43

Chiswell JR (1956) A taxonomic account of the last instar larvae of some British Tipulinae (Diptera: Tipulidae). Transactions of the Royal Entomological Society of London 108: 409–484. https://doi.org/10.1111/j.1365-2311.1956.tb01273.x

Cumming JM, Wood DM (2017) Adult morphology and terminology. In: Kirk-Spriggs AH, Sinclair BJ (Eds) Manual of Afrotropical Diptera, Volume 1: Introductory Chapters and Keys to Diptera Families. Suricata 4. South African National Biodiversity Institute, Pretoria, 89–133.

Dobrotworsky NV (1968) The Tipulidae (Diptera) of Australia. I. A review of the genera of the subfamily Tipulinae. Australian Journal of Zoology 16: 459–494. https://doi.org/10.1071/ZO9680459

Edwards FW (1931) Some suggestions on the classification of the genus *Tipula* (Diptera, Tipulidae). Annals and Magazine of Natural History 8(10): 73–82. https://doi.org/10.1080/00222933108673359

Gelhaus JK (1986) Larvae of the crane fly genus Tipula in North America (Diptera: Tipulidae). The University of Kansas Science Bulletin 53: 121–182.

Gelhaus JK (2005) Systematics and biogeography of the desert crane fly subgenus *Tipula* (*Eremotipula*) Alexander (Diptera: Tipulidae). Memoirs of the American Entomological Society 46: 1–235.

Lantsov VI (2003) Biology, ecology and preimaginal stages of the crane fly *Tipula semivittata semivittata* (Diptera, Tipulidae). Entomological Review 83: 906–913.

Mannheims B (1953) 15. Tipulidae. In: Lindner E (Ed.) Die Fliegen der palaearktischen Region, 3(5)1, Lief 173: 113–136.

Mannheims B (1963) 15. Tipulidae. In: Lindner E (Ed.) Die Fliegen der palaearktischen Region, 3(5)1, Lief 238: 137–176.

Mannheims B (1967) *Tipula* (*Vestiplex*) *bo* sp. n. und andere Tipuliden aus Fennoskandien (Diptera). Notulae Entomologicae 47: 147–156.

Mannheims B, Savchenko EN (1973) Ergebnisse der zoologischen Forschungen von Dr. Z. Kaszab in der Mongolei, 303. Tipulidae (Diptera), II. Folia Entomologica Hungarica, (N.S.), Supplement 26: 157–186.

Neugart C, Schneeberg K, Beutel RG (2009) The morphology of the larval head of Tipulidae (Diptera, Insecta), the dipteran groundplan and evolutionary trends. Zoologischer Anzeiger 248: 213–235. https://doi.org/10.1016/j.jcz.2009.10.001

Neumann H (1958) Der Bau und die Funktion der mannlichen Genitalapparate von *Trichocera annulata* Meig. und *Tipula paludosa* Meig. (Dipt. Nematocera). Deutsche Entomologische Zeitschrift (N.F.) 5: 235–298.

Oosterbroek P (2019) Catalogue of the Craneflies of the World (CCW), 12 Nov. 2019. http://nlbif.eti.uva.nl/ccw/index.php [Accessed on: 29 Nov. 2019]

Oosterbroek P, Theowald B. (1992) Family Tipulidae. In: Soós Á, Papp L (Eds) Catalogue of Palaearctic Diptera 1. Hungarian Natural History Museum, Budapest, 56–178.

Podeniene V (2003) Morphology and ecology of the last instar larvae of the crane flies (Diptera, Tipulomorpha) of Lithuania. Doctoral dissertation, Vilnius University, 1–295.

Rogers JS (1942) The crane flies (Tipulidae) of the George Reserve, Michigan. Miscellaneous Publications, Museum of Zoology, University of Michigan 53: 1–128.

Savchenko EN (1960) A contribution to the taxonomy of crane-flies (Diptera, Tipulidae) of the subgenus *Vestiplex* Bezzi of the genus *Tipula* L. Horae Societatis Entomologicae Rossicae Unionis Soveticae 47: 143–216. [In Russian]

Savchenko EN (1964) Crane-flies (Diptera, Tipulidae), Subfam. Tipulinae, Genus *Tipula* L., 2. Fauna USSR, N.S. 89, Nasekomye Dvukrylye [Insecta Diptera] 2(4): 1–503. [In Russian]

Starkevich P, Paramonov NM (2016) New records of *Tipula* (*Vestiplex*) crane flies from the Palaearctic [Diptera: Tipulidae] with a new synonym. Journal of the Kansas Entomological Society 89: 80–84. https://doi.org/10.2317/151024.1

Starkevich P, Podenas S, Young CW (2015) New distribution records for crane flies of *Tipula* (*Vestiplex*) Bezzi (Diptera, Tipulidae). Journal of the Kansas Entomological Society 88: 121–123. https://doi.org/10.2317/JKES1303.31.1

Teale SA, Gelhaus JK (1984) Natural history and synonymy of *Tipula* (*Vestiplex*) *platymera* Walker (Diptera: Tipulidae) with description of the larvae and pupae. Journal of the Kansas Entomological Society 57: 423–429.

Theowald B (1967) Familie Tipulidae (Diptera, Nematocera). Larven und Puppen. Bestimmungsbucher zur Bodenfauna Europas 7: 1–100.

ZooKeys 1061: 57–73 (2021)
doi: 10.3897/zookeys.1061.70176
https://zookeys.pensoft.net

RESEARCH ARTICLE

A peer-reviewed open-access journal
ZooKeys
Launched to accelerate biodiversity research

The complete mitochondrial genome of *Microphysogobio elongatus* (Teleostei, Cyprinidae) and its phylogenetic implications

Renyi Zhang[1*], Qian Tang[1*], Lei Deng[1]

1 *Key Laboratory of National Forestry and Grassland Administration on Biodiversity Conservation in Karst Mountainous Areas of Southwestern China, School of Life Sciences, Guizhou Normal University, 550001, Guiyang, Guizhou, China*

Corresponding author: Renyi Zhang (zhangrenyi@gznu.edu.cn)

Academic editor: Bruno F. Melo | Received 15 June 2021 | Accepted 1 September 2021 | Published 1 October 2021

http://zoobank.org/328C1B4B-B141-4FDB-A1B4-D54B368F457C

Citation: Zhang R, Tang Q, Deng L (2021) The complete mitochondrial genome of *Microphysogobio elongatus* (Teleostei, Cyprinidae) and its phylogenetic implications. ZooKeys 1061: 57–73. https://doi.org/10.3897/zookeys.1061.70176

Abstract

Mitochondria are important organelles with independent genetic material of eukaryotic organisms. In this study, we sequenced and analyzed the complete mitogenome of a small cyprinid fish, *Microphysogobio elongatus* (Yao & Yang, 1977). The mitogenome of *M. elongatus* is a typical circular molecule of 16,612 bp in length containing 13 protein-coding genes (PCGs), 22 transfer RNA genes, two ribosomal RNA genes, and a 930 bp control region. The base composition of the *M. elongatus* mitogenome is 30.8% A, 26.1% T, 16.7% G, and 26.4% C. All PCGs used the standard ATG start codon with the exception of *COI*. Six PCGs terminate with complete stop codons, whereas seven PCGs (*ND2*, *COII*, *ATPase 6*, *COIII*, *ND3*, *ND4*, and *Cyt b*) terminate with incomplete (T or TA) stop codons. All tRNA genes exhibited typical cloverleaf secondary structures with the exception of $tRNA^{Ser(AGY)}$, for which the dihydrouridine arm forms a simple loop. The phylogenetic analysis divided the subfamily Gobioninae in three clades with relatively robust support, and that *Microphysogobio* is not a monophyletic group. The complete mitogenome of *M. elongatus* provides a valuable resource for future studies about molecular phylogeny and/or population genetics of *Microphysogobio*.

Keywords

Gobioninae, mitogenome, paraphyly

* These authors contributed equally to this work.

Introduction

The genus *Microphysogobio* Mori, 1934, small gudgeons of the subfamily Gobioninae, was originally established by Mori (1934) for *M. hsinglungshanensis* Mori, 1934 (Sun et al. 2021). Currently, this genus comprises approximately 30 species that are widely distributed in East Asia, including China, Vietnam, Mongolia, Laos, and the Korean Peninsula (Jiang et al. 2012; Huang et al. 2016; Huang et al. 2017). The prominent feature of the lip papillae was considered a diagnostic character for defining the genus *Microphysogobio* and distinguishing it from other genera in the subfamily Gobioninae (Yue 1998). Molecular phylogenetic studies of the subfamily Gobioninae has confirmed the monophyletic nature of the Gobioninae (Tang et al. 2011; Zhao et al. 2016). However, the phylogenetic relationships of *Microphysogobio* and related genera have not been fully resolved, and it is a long-standing issue in the classification of Gobioninae.

The typical vertebrate mitogenome is approximately 15–18 kb in length, consisting of 13 protein-coding genes (PCGs), 22 transfer RNA (tRNA) genes, two ribosomal RNA (rRNA) genes, and one non-coding control (*D-loop*) region (Wolstenholme 1992; Boore 1999). Mitochondrial genomic DNA has the following characteristics: small size, multiple copies, maternal inheritance, conservative gene products, no introns, fast evolutionary rate, and rare recombination (Boore 1999; Xiao and Zhang 2000). Therefore, it is widely used in species identification, molecular evolution, and phylogenetic studies (Imoto et al. 2013; Sharma et al. 2020). Historically, several genes on the mitochondrial genome, such as *Cyt b* gene and *D-loop* (Wang et al. 2002; He and Chen 2006) were used to study the evolutionary relationships. More recently, with advances in sequencing technology and data analysis methods, information on fish mitogenomes has been accumulating in public databases (Miya and Nishida 2000; Miya et al. 2003; Saitoh et al. 2006; Yamanoue et al. 2007; Kim et al. 2009).

Microphysogobio elongatus (Yao & Yang, 1977) is a small, benthic, freshwater fish which is widely distributed in China (Yue 1998; Wang 2019). However, little is known regarding *M. elongatus*, with previous studies focusing on resources investigation and taxonomy (Li et al. 2012; Liu et al. 2013; Zhang et al. 2018). In this study, we sequenced, annotated, and characterized the complete mitochondrial genome of *M. elongatus*. Additionally, we reconstructed the mitogenomic phylogeny of Gobioninae, involving 103 species and subspecies based on 13 PCGs to confirm the taxonomic status of *M. elongatus* and its relationships within Gobioninae.

Materials and methods

Ethics statements

For field collection, no specific permissions are required for the collection of gobionine fishes from public areas. The field collections did not involve endangered or protected species, and the collection site is not a protected area.

Sample collection and DNA extraction

Individuals of *M. elongatus* were collected from Jiangkou County, Guizhou Province, China (27°46'12"N, 108°46'56"E), in August 2019. The specimens were preserved in 95% ethanol and stored at –20 °C until DNA extraction. Genomic DNA was extracted using a standard high-salt method (Sambrook et al. 1989). The integrity of the genomic DNA was measured by 1% agarose gel electrophoresis, and the concentration and purity of DNA were determined using an Epoch 2 Microplate Spectrophotometer (Bio Tek Instruments, Inc., Vermont, USA).

PCR amplification and sequencing

The entire mitogenome of *M. elongatus* was amplified in overlapping PCR fragments by 14 primer pairs designed from the mitogenome of *M. kiatingensis* (GenBank accession number NC_037402) by Primer Premier v. 5.0 software (Lalitha 2000). The primers used in this study are provided in Suppl. material 1: Table S1. Each PCR reaction was carried out in 35 μL total volume, containing 17.5 μL of 2×Taq Plus Master-Mix (CoWin Biosciences, Beijing, China), 1 μL of each primer (10 μM) and 1.0 μL of template DNA (100 ng). The PCR reactions were performed under the following conditions: an initial pre-denaturation at 95 °C for 5 min, 35 cycles of 95 °C for 30 s, 42–55 °C for 30 s, 72 °C for 1–2 min, and a final extension at 72 °C for 10 min. Amplification products were fractionated by electrophoresis through 1% agarose gels. The lengths of fragments were determined by comparison with the DL2000 DNA marker (TaKaRa, Japan). The PCR products were sequenced by ABI PRISM 3730 (Sangon Biotech. Co., Ltd, China).

Mitogenome annotation and sequence analysis

The mitogenome was initially assembled by the SeqMan software of DNAStar (DNASTAR Inc., Madison, WI, USA), then manually proofread based on sequencing peak figures. The assembled mitogenome sequence was subsequently annotated using MitoAnnotator on the MitoFish homepage (Iwasaki et al. 2013). All tRNA genes were identified with tRNAscan-SE search server (Lowe and Chan 2016) and MITOS WebServer (Bernt et al. 2013). The base composition, codon usage, and relative synonymous codon usage (RSCU) of all PCGs were calculated using MEGA v. 6.0 (Tamura et al. 2013). Strand asymmetry was calculated using the following formulae: AT-skew = (A – T) / (A + T) and GC-skew = (G – C) / (G + C) (Perna and Kocher 1995).

Phylogenetic analysis

For phylogenetic analysis, 103 gobionine fishes were downloaded from GenBank. Additionally, *Acheilognathus omeiensis* (NC_037404.1), *Rhodeus ocellatus* (NC_011211.1), and *R. sinensis* (NC_022721.1) were used as outgroups. Species

used in the analysis are listed in Suppl. material 2: Table S2. The shared 13 concatenated protein-coding genes (PCGs) were extracted and recombined to construct a matrix using PhyloSuite v. 1.1.16 (Zhang et al. 2020). The 13 PCGs were aligned separately using MAFFT v. 7.313 (Katoh and Standley 2013) and concatenated. The optimal partition strategy and nucleotide sequence substitution model of each partition were estimated by PartitionFinder v. 2.1.1 (Lanfear et al. 2017) with the Corrected Akaike information criterion (AICc) algorithm under a greedy search. A Bayesian inference (BI) analysis was performed using MrBayes v. 3.2.6 (Ronquist et al. 2012) with the models determined by PartitionFinder. Two independent runs of four Markov Chain Monte Carlo (MCMC) chains (one cold chain and three heated chains) were performed for two million generations sampling every 100 generations. The first 25% of the generations were discarded as burn-in and a 50% majority rule consensus tree was constructed. A maximum likelihood (ML) analysis was performed using IQ-TREE v. 1.6.8 (Nguyen et al. 2015) with 10,000 bootstrap replicates using the ultrafast bootstrapping algorithm (Minh et al. 2013). All software were integrated into PhyloSuite v. 1.1.16 (Zhang et al. 2020). The phylogenetic trees were visualized using FigTree v. 1.4.2 (http://tree.bio.ed.ac.uk/software/figtree/).

Results and discussion

Genome organization and nucleotide composition

The complete mitochondrial genome of *M. elongatus* was first reported and analyzed in this study. The full length of the *M. elongatus* mitochondrial genome sequence had 16,612 bp. The complete mitochondrial genome of *M. elongatus* was annotated and submitted to GenBank (GenBank accession number MN832777). It consisted of 13 PCGs, 22 tRNA genes, two rRNA genes, and one control region (Fig. 1; Table 1). All mitochondrial genes were encoded on the heavy strand (H strand), except the *ND6* gene and eight tRNAs (Table 1). The arrangement and content of these genes were conserved and typical of *Microphysogobio* mitochondrial genomes (Hwang et al. 2014; Lin et al. 2014; Cheng et al. 2015). The *M. elongatus* mitogenome contained a total of 21 bp overlapping regions which were in six pairs of neighboring genes, ranging from 1 to 7 bp in length. The longest overlapping region (7 bp) was located between *ATP8* and *ATP6*, *ND4L* and *ND4*. A total of 65 bp intergenic nucleotides (IGN) were dispersed in 13 locations, ranging from 1 to 31 bp in length (Table 1). The longest intergenic spacer was located between $tRNA^{Asn}$ and RNA^{Cys}. These overlapping and intergenic regions are very common in fish mitochondrial genomes (Zhang and Wang 2018; Wang et al. 2020).

The nucleotide composition of the *M. elongatus* mitogenome was as follows: 30.8% A, 26.1% T, 16.7% G, and 26.4% C, and were slightly (56.9%) A+T rich (Table 2). In addition, the A+T contents of PCGs, rRNAs, and tRNAs were also slightly A+T rich (Table 2). Compared to the entire mitogenome, the control region, known as an A+T

Table 1. Mitochondrial genome organization of *Microphysogobio elongatus*.

Gene	Strand	Position		Length	Intergenic nucleotide	Anticodon	Codon	
		From	To	(bp)			Start	Stop
tRNA-Phe	H	1	69	69	0	GAA		
12S rRNA	H	70	1029	960	0			
tRNA-Val	H	1030	1101	72	0	TAC		
16S rRNA	H	1102	2793	1692	0			
tRNA-Leu (UUR)	H	2794	2869	76	1	TAA		
ND1	H	2871	3845	975	4		ATG	TAG
tRNA-Ile	H	3850	3921	72	-2	GAT		
tRNA-Gln	L	3920	3990	71	1	TTG		
tRNA-Met	H	3992	4060	69	0	CAT		
ND2	H	4061	5106	1046	0		ATG	TA-
tRNA-Trp	H	5107	5177	71	2	TCA		
tRNA-Ala	L	5180	5248	69	1	TGC		
tRNA-Asn	L	5250	5322	73	31	GTT		
tRNA-Cys	L	5354	5421	68	2	GCA		
tRNA-Tyr	L	5424	5493	70	1	GTA		
COI	H	5495	7045	1551	0		GTG	TAA
tRNA-Ser (UCN)	L	7046	7116	71	3	TGA		
tRNA-Asp	H	7120	7191	72	13	GTC		
COII	H	7205	7895	691	0		ATG	T—
tRNA-Lys	H	7896	7971	76	1	TTT		
ATPase 8	H	7973	8137	165	-7		ATG	TAA
ATPase 6	H	8131	8813	683	0		ATG	TA-
COIII	H	8814	9597	784	0		ATG	T—
tRNA-Gly	H	9598	9669	72	0	TCC		
ND3	H	9670	10019	350	0		ATG	TA-
tRNA-Arg	H	10020	10088	69	0	TCG		
ND4L	H	10089	10385	297	-7		ATG	TAA
ND4	H	10379	11760	1381	0		ATG	TA-
tRNA-His	H	11761	11829	69	0	GTG		
tRNA-Ser (AGY)	H	11830	11898	69	1	GCT		
tRNA-Leu (CUN)	H	11900	11972	73	0	TAG		
ND5	H	11973	13808	1836	-4		ATG	TAG
ND6	L	13805	14326	522	0		ATG	TAG
tRNA-Glu	L	14327	14395	69	5	TTC		
Cyt b	H	14401	15541	1141	0		ATG	T—
tRNA-Thr	H	15542	15613	72	-1	TGT		
tRNA-Pro	L	15613	15682	70	0	TGG		
D-loop	H	15683	16612	930	0			

rich region, contained the highest A+T content (68.1%) (Table 2). The skew statistics revealed a positive AT-skew and a negative GC-skew across the whole mitogenome (Table 2), indicating a bias toward As and Cs.

Protein-coding genes and codon usage

The 13 PCGs were 11,423 bp in total length. The longest PCG was 1836 bp (*ND5*), and the shortest was 165 bp (*ATP8*) (Table 1). The average base composition of the 13 PCGs were as follows: 28.7% A, 28.2% T, 16.2% G, and 26.9% C (Table 2). All PCGs were initiated with the typical ATG codon except *COI* with GTG as its initiator codon. Six PCGs (*ND1*, *COI*, *ATPase 8*, *ND4L*, *ND5*, and *ND6*) terminated with a

Table 2. Nucleotide composition of the *Microphysogobio elongatus* mitochondrial genome.

	Length(bp)	A%	T%	G%	C%	A+T%	AT-skew	GC-skew
Genome	16612	30.8	26.1	16.7	26.4	56.9	0.081	–0.226
PCGs	11423	28.7	28.2	16.2	26.9	56.9	0.009	–0.249
1st codon position	3808	27.7	29.6	16.0	26.7	57.3	–0.032	–0.251
2nd codon position	3808	30.1	27.5	14.5	27.9	57.6	0.045	–0.318
3rd codon position	3807	28.3	27.4	18.2	26.1	55.7	0.016	–0.179
rRNA	2652	34.2	20.0	21.2	24.6	54.2	0.261	–0.073
tRNA	1562	28.4	26.9	23.5	21.2	55.3	0.028	0.052
D-loop region	930	34.2	33.9	13.3	18.6	68.1	0.005	-0.165

complete stop codon. The others terminated with an incomplete stop codon TA- or T—, which would be completed as TAA by post-transcriptional polyadenylation at the 3' end of the mRNA (Ojala et al. 1981).

The relative synonymous codon usage (RSCU) values of the 13 PCGs were analyzed and shown in Suppl. material 5: Fig. S5 and Suppl. material 3: Table S3. The total number of codons, excluding termination codons, in the 13 PCGs was 3808 (Suppl. material 3: Table S3). Among them, CUA, AUU, and UUA were most frequent. Seven codons (AAG, UCG, AGG, AGA, CGC, CGU, and GCG) were rarely represented. Furthermore, the three most frequent amino acids were Leu, Ser, and Ile (Suppl. material 6: Fig. S6).

Transfer and ribosomal RNAs

The mitogenome of *M. elongatus* contains 22 tRNAs, which were interspersed across the circular genome, ranging from 68 bp ($tRNA^{Cys}$) to 76 bp ($tRNA^{Leu\ (UUR)}$ and $tRNA^{Lys}$) in length (Table 1). The secondary structure of all tRNA sequences were predicted and the results showed they are capable of folding into typical cloverleaf secondary structures except for $tRNA^{Ser(AGY)}$, in which the dihydrouridine (DHU) arm did not form a stable structure (Suppl. material 7: Fig. S7). This unique secondary structure has been commonly witnessed in many other fishes (Zhang and Wang 2018; Zhong et al. 2018). The average base composition of the tRNAs was 28.4% A, 26.9% T, 23.5% G, and 21.2% C (Table 2).

The 12S rRNA and 16S rRNA were the only two ribosomal genes in the mitogenome of *M. elongatus*. They were 960 bp and 1692 bp in length, respectively (Table 1). Similar to other fishes (Broughton et al. 2001; Zhang and Wang 2018), the 12S rRNA and 16S rRNA were located between $tRNA^{Phe}$ and $tRNA^{Val}$, and between $tRNA^{Val}$ and $tRNA^{Leu\ (UUR)}$, respectively (Table 1). Their average base composition was as follows: 34.2% A, 20.0% T, 21.2% G, and 24.6% C. The average A + T content of both rRNAs was 54.2% (Table 2). The lengths and A + T content of these two rRNAs were well within the ranges observed in other *Microphysogobio* mitogenomes (Lin et al. 2014; Hwang et al. 2014; Cheng et al. 2015).

Mitochondrial control region

The mitochondrial control region (CR), or *D-loop*, is responsible for replication and transcription of the mitogenome (Boore 1999). The CR of *M. elongatus* was 930 bp

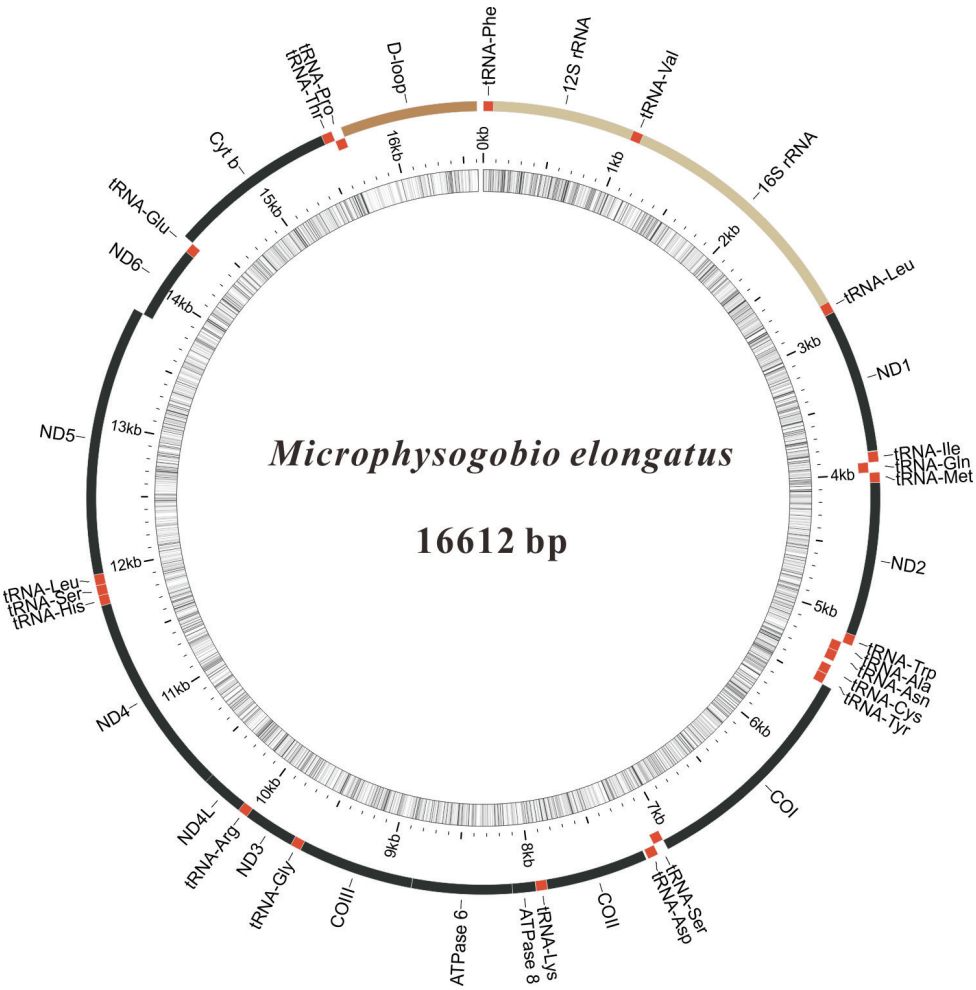

Figure 1. Circular map of the M. elongatus mitogenome.

in length and located between $tRNA^{Phe}$ and $tRNA^{Pro}$. Multiple homologous sequence alignment revealed three conserved structures (termination-associated sequence (TAS), central conserved sequence blocks (CSB-F, CSB-E, and CSB-D) and conserved sequence blocks (CSB-1, CSB-2, and CSB-3)) within the CR (Suppl. material 8: Fig. S8), as seen in most fish mitogenomes (Broughton et al. 2001; Zhang and Wang 2018).

Mitochondrial phylogeny within Gobioninae

We reconstructed the phylogenetic tree of gobionine fishes based on the 13 concatenated protein-coding genes. The optimal partitioning scheme for the dataset and the best-fitting substitution model for each partition were provided in Suppl. material 4: Table S4. The trees resulting from the BI and ML analyses showed a consensus topology, and

the only differences were the Bayesian posterior probabilities and ML bootstrap values (Fig. 2, Suppl. material 9: Fig. S9). The phylogenetic analysis revealed that Gobioninae could be separated into three clades (Tribe Sarcocheilichthyini, Tribe Gobionini and *Hemibarbus-Squalidus* group) with *Squalidus gracilis majimae* excluded (Fig. 2), which was consistent with previous phylogenetic studies (Tang et al. 2011; Zhao et al. 2016).

The *Hemibarbus-Squalidus* group includes *Belligobio*, *Hemibarbus*, and *Squalidus* (BS = 99%, PP = 100%). The *Hemibarbus-Squalidus* group was located at the basal position Gobioninae in the phylogenetic tree. This confirmed morphology-based hypothesis that *Hemibarbus* and *Belligobio* might represent the primitive group of Gobioninae (Bănărescu 1992). *Hemibarbus* and *Belligobio* were similar in morphological, and therefore, Bănărescu and Nalbant (1973) assigned *Belligobio* as a subgenus of *Hemibarbus*. The phylogenetic tree of Gobioninae subfamily based on single gene confirmed the close relationship of *Squalidus* to *Hemibarbus* (Yang et al. 2006; Liu et al. 2010; Tang et al. 2011). Nonetheless, the phylogenetic tree suggests that the classification of *S. g. majimae* should be further revised.

The tribe Gobioninae includes *Gobiobotia*, *Xenophysogobio Saurogobio*, *Pseudogobio*, *Platysmacheilus*, *Biwia*, *Microphysogobio*, *Romanogobio*, *Abbottina*, *Acanthogobio*, *Gobio*, and *Ladislavia* (BS = 85%, PP = 97%). Within the group, *Ladislavia taczanowskii* was at the basal position. The phylogenetic tree from mtDNA supported *Ladislavia* should be included in the Gobioninae group (Tang et al. 2011). Bănărescu and Nalbant (1973) highlighted that *Acanthogobio* seemed to be a morphologically derived species of *Gobio*, as confirmed in our study. *Microphysogobio* is not monophyletic because of the placement of *Biwia*, *Romanogobio*, and *Platysmacheilus* which are found nested within *Microphysogobio*; this is in accordance with previous studies based on mitochondrial and nuclear genes (Yang et al. 2006; Tang et al. 2011). In morphology, *P. exiguous* and *Microphysogobio* showed similar characteristics that were a single row of dentition, with indicated that the evolutionary process was the decreasing number of teeth rows (Yu and Liu 2011). The taxonomic status of *Microphysogobio* remains uncertain because its putative member species were found to be broadly polyphyletic.

The tribe Sarcocheilichthyini includes *Coreius*, *Coreoleuciscus*, *Gnathopogon*, *Paracanthobrama*, *Gobiocypris*, *Pungtungia*, *Pseudopungtungia*, *Pseudorasbora*, *Rhinogobio*, and *Sarcocheilichthys* (BS = 86%, PP = 100%). Based on our trees, *Pungtungia herzi* was assigned to *Pseudopungtungia*, and a grouping like this has been proposed in an earlier study (Kim et al. 2013). Our results and a previous study by Kim et al. (2013) suggested an unstable taxonomic status of the *Pseudopunungtungia* genus, which is polyphyletic. The placement of *Gobiocypris* within the *Gnathopogon* gives support to *Gobiocypris* as a subgenus of *Gnathopogon* (Tang et al. 2011). Moreover, we found that *Paraleucogobio* was also included in *Gnathopogon*, so we speculated that *Paraleucogobio* might also be a subgenus of *Gnathopogon*. Surprisingly, the phylogenetic tree showed that *Sarcocheilichthys biwaensis* and *S. variegatus microoculus* had almost non-existent branch lengths. Komiya (2014) et al. suggested multiple colonization events of Lake Biwa by *S. biwaensis* and *S. v. microoculus* and confirmed the rapid speciation of *S. biwaensis* from an ancestral *S. v. microoculus* form. Therefore, we surmise that *S. biwaensis*

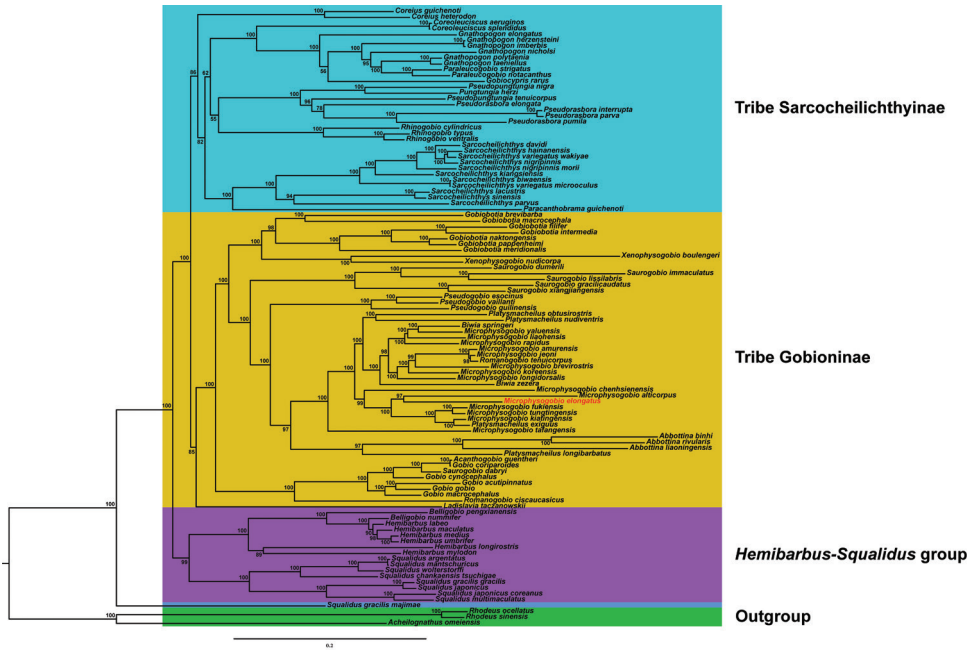

Figure 2. Phylogenetic relationships of Gobioninae based on complete mitochondrial genomes using maximum likelihood (ML) analyses. ML bootstrap values are shown at the nodes.

and *S. v. microoculus* probably have mitochondrial introgression. Introgressive hybridization was not rare between closely related species (Yang et al. 2006).

Several monophyletic clades of *Coreius*, *Coreoleuciscus*, *Pseudorasbora*, *Rhinogobio*, *Sarcocheilichthys*, *Gobiobotia*, *Xenophysogobio*, *Saurogobio*, *Pseudogobio*, *Abbottina*, and *Squalidus* were supported (Fig. 2). The monophyletic of *Sarcocheilichthys*, *Rhinogobio*, *Coreius*, *Gobiobotia*, *Saurogobio*, *Pseudogobio*, and *Squalidus* are consistent with the phylogenetic results of Yang et al. (2006) on 44 species of Gobioninae using the mitochondrial *Cyt b*. Our results showed that phylogenetic analyses utilizing mitogenome sequences partially resolved genus- and species-level relationships within Gobioninae. However, extensive taxon sampling is required to completely resolve the relationships within the subfamily Gobioninae.

Conclusions

In the present study, we sequenced and described the complete *M. elongatus* mitogenome (16,612 bp) that contains 37 genes and one control region as typical for vertebrate mitogenomes. The characteristics of the newly sequenced mitogenome are mostly consistent with those reported in other *Microphysogobio* mitogenomes. The subfamily Gobioninae was composed of three major lineages, and the phylogenetic trees strongly supported the non-monophyly of *Microphysogobio*. The results of the present study will be useful for further investigation of the evolutionary relationships within Gobioninae.

Acknowledgements

This work was supported by the Joint Fund of the National Natural Science Foundation of China and the Karst Science Research Center of Guizhou Province (grant no. U1812401), Guizhou Provincial Science and Technology Foundation (Qiankehejichu[2018]1113), Natural Science Foundation of Guizhou Educational Committee (QianjiaoheKY[2021]306) and Doctoral Foundation of Guizhou Normal University (2016). The authors declare that they have no conflicts of interest.

References

Bănărescu P, Nalbant TT (1973) Pisces, Teleostei, Cyprinidae (Gobioninae). Das Tierreich, Lieferung 93. Walter de Guryter, Berlin.

Bănărescu P (1992) A critical updated checklist of Gobioninae (Pisces, Cyprinidae). Travaux du Muséum d'Histoire Naturelle "Grigore Antipa" 32: 303–330.

Bernt M, Donath A, Jühling F, Externbrink F, Florentz C, Fritzsch G, Pütz J, Middendorf M, Stadler PF (2013) MITOS: improved *de novo* metazoan mitochondrial genome annotation. Molecular Phylogenetics and Evolution 69: 313–319. http://doi.org/10.1016/j.ympev.2012.08.023

Boore JL (1999) Animal mitochondrial genomes. Nucleic Acids Research 27: 1767–1780. http://doi.org/10.1093/nar/27.8.1767

Broughton RE, Milam JE, Roe BA (2001) The complete sequence of the zebrafish (*Danio rerio)* mitochondrial genome and evolutionary patterns in vertebrate mitochondrial DNA. Genome Research 11: 1958–1967. http://doi.org/10.1101/gr.156801

Cheng CY, Wang JP, Ho CW, Cheng JW, Ueng YT (2015) Complete mitochondrial DNA genome of *Microphysogobio brevirostris* (Cypriniformes: Cyprinidae). Mitochondrial DNA 26: 293–294. https://doi.org/10.3109/19401736.2013.825781

He D, Chen Y (2006) Biogeography and molecular phylogeny of the genus *Schizothorax* (Teleostei: Cyprinidae) in China inferred from cytochrome b sequences. Journal of Biogeography 33: 1448–1460. https://doi.org/10.1111/j.1365-2699.2006.01510.x

Huang SP, Chen IS, Shao KT (2016) A new species of *Microphysogobio* (Cypriniformes: Cyprinidae) from Fujian Province, China, and a molecular phylogenetic analysis of *Microphysogobio* species from southeastern China and Taiwan. Proceedings of the Biological Society of Washington 129: 195–211. https://doi.org/10.2988/0006-324X-129.Q3.195

Huang SP, Zhao Y, Chen IS, Shao KT (2017) A new species of *Microphysogobio* (Cypriniformes: Cyprinidae) from Guangxi province, southern China. Zoological Studies 56: e8. http://doi.org/10.6620/ZS.2017.56-08

Hwang DS, Song HB, Lee JS (2014) Complete mitochondrial genome of the freshwater gudgeon, *Microphysogobio koreensis* (Cypriniformes, Cyprinidae). Mitochondrial DNA 25: 15–16. http://doi.org/10.3109/19401736.2013.775267

Imoto JM, Saitoh K, Sasaki T, Yonezawa T, Adachi J, Kartavtsev YP, Miya M, Nishida M, Hanzawa N (2013) Phylogeny and biogeography of highly diverged freshwater fish species

(Leuciscinae, Cyprinidae, Teleostei) inferred from mitochondrial genome analysis. Gene 514: 112–124. https://doi.org/10.1016/j.gene.2012.10.019

Iwasaki W, Fukunaga T, Isagozawa R, Yamada K, Maeda Y, Satoh TP, Sado T, Mabuchi K, Takeshima H, Miya M, Nishida M (2013) MitoFish and MitoAnnotator: a mitochondrial genome database of fish with an accurate and automatic annotation pipeline. Molecular Biology and Evolution 30: 2531–2540. http://doi.org/10.1093/molbev/mst141

Jiang ZG, Gao EH, Zhang E (2012) *Microphysogobio nudiventris*, a new species of gudgeon (Teleostei: Cyprinidae) from the middle Chang-Jiang (Yangtze River) basin, Hubei Province, South China. Zootaxa 3586: 211–221. https://doi.org/10.11646/zootaxa.3586.1.19

Katoh K, Standley DM (2013) MAFFT multiple sequence alignment software version 7: improvements in performance and usability. Molecular Biology and Evolution 30: 772–780. http://doi.org/10.1093/molbev/mst010

Kim KY, Lim YH, Bang IC, Nam YK (2009) Phylogenetic relationships among three new *Hemibarbus* mitogenome sequences belonging to the subfamily Gobioninae (Teleostei, Cypriniformes, and Cyprinidae). Mitochondrial DNA 20: 119–125. http://doi.org/10.3109/19401730903176896

Kim KY, Ko MH, Liu HZ, Tang QY, Chen XL, Miyazaki JI, Bang IC (2013) Phylogenetic relationships of *Pseudorasbora*, *Pseudopungtungia*, and *Pungtungia* (Teleostei; Cypriniformes; Gobioninae) inferred from multiple nuclear gene sequences. BioMed Research International 2013: 347242. http://doi.org/10.1155/2013/347242

Komiya T, Yanagibayashi SF, Watanabe K (2014) Multiple colonizations of Lake Biwa by *Sarcocheilichthys* fishes and their population history. Environmental Biology of Fishes 97(7): 741–755. http://doi.org/10.1007/s10641-013-0176-9

Lalitha S (2000) Primer Premier 5. Biotech Software & Internet Report 1: 270–272. http://doi.org/10.1089/152791600459894

Lanfear R, Frandsen PB, Wright AM, Senfeld T, Calcott B (2017) PartitionFinder 2: new methods for selecting partitioned models of evolution for molecular and morphological phylogenetic analyses. Molecular Biology and Evolution 34: 772–773. http://doi.org/10.1093/molbev/msw260

Li J, Li XH, Jia XP, Tan XC, Wang C, Li YF, Shao XF (2012) Relationship between fish community diversity and environmental factors in the Lianjiang River, Guangdong, China. Acta Ecologica Sinica 32: 5795–5805. http://doi.org/10.5846/stxb201108041142

Lin DY, Lin HD, Tzeng SJ, Chiang TY (2014) Complete mitochondrial genome of *Microphysogobio alticorpus* (Cypriniformes, Cyprinidae). Mitochondrial DNA 25: 173–174. http://doi.org/10.3109/19401736.2013.792062

Liu H, Yang J, Tang Q (2010) Estimated evolutionary tempo of East Asian gobionid fishes (Teleostei: Cyprinidae) from mitochondrial DNA sequence data. Chinese Science Bulletin 55: 1501–1510. http://doi.org/10.1007/s11434-010-3159-7

Liu Y, Hou XF, Zhou J (2013) Fish species composition in Shibing of Guizhou, Southwest China, a candidate World Heritage Site. Chinese Journal of Applied Ecology 32: 1850–1856. http://doi.org/10.13292/j.1000-4890.2013.0394

Lowe TM, Chan PP (2016) tRNAscan-SE On-line: integrating search and context for analysis of transfer RNA genes. Nucleic Acids Research 44: W54–W57. http://doi.org/10.1093/nar/gkw413

Minh BQ, Nguyen MAT, von Haeseler A (2013) Ultrafast approximation for phylogenetic bootstrap. Molecular Biology and Evolution 30: 1188–1195. https://doi.org/10.1093/molbev/mst024

Miya M, Nishida M (2000) Use of mitogenomic information in teleostean molecular phylogenetics: a tree-based exploration under the maximum-parsimony optimality criterion. Molecular Phylogenetics and Evolution 17: 437–455. http://doi.org/10.1006/mpev.2000.0839

Miya M, Takeshima H, Endo H, Ishiguro NB, Inoue JG, Mukai T, Satoh TP, Yamaguchi M, Kawaguchi A, Mabuchi K (2003) Major patterns of higher teleostean phylogenies: a new perspective based on 100 complete mitochondrial DNA sequences. Molecular Phylogenetics and Evolution 26: 121–138. http://doi.org/10.3897/10.1016/S1055-7903(02)00332-9

Nguyen LT, Schmidt HA, Haeseler AV, Minh BQ (2015) IQ-TREE: a fast and effective stochastic algorithm for estimating maximum-likelihood phylogenies. Molecular Biology and Evolution 32: 268–274. http://doi.org/10.1093/molbev/msu300

Ojala D, Montoya J, Attardi G (1981) tRNA punctuation model of RNA processing in human mitochondria. Nature 290: 470–474. http://doi.org/10.1038/290470a0

Perna NT, Kocher TD (1995) Patterns of nucleotide composition at fourfold degenerate sites of animal mitochondrial genomes. Journal of Molecular Evolution 41: 353–358. http://doi.org/10.1007/BF00186547

Ronquist F, Teslenko M, van der Mark P, Ayres Daniel L, Darling A, Höhna S, Larget B, Liu L, Suchard MA, Huelsenbeck JP (2012) MrBayes 3.2: efficient Bayesian phylogenetic inference and model choice across a large model space. Systematic Biology 61: 539–542. http://doi.org/10.1093/sysbio/sys029

Sambrook J, Fritsch EF, Maniatis T (1989) Molecular Cloning: a Laboratory Manual. 2nd edn. Cold Spring Harbor Press, New York, 1695 pp.

Saitoh K, Sado T, Mayden RL, Hanzawa N, Nakamura K, Nishida M, Miya M (2006) Mitogenomic evolution and interrelationships of the Cypriniformes (Actinopterygii: Ostariophysi): the first evidence toward resolution of higher-level relationships of the world's largest freshwater fish clade based on 59 whole mitogenome sequences. Journal of Molecular Evolution 63: 826–884. http://doi.org/10.1007/s00239-005-0293-y

Sharma A, Siva C, Ali S, Sahoo PK, Nath R, Laskar MA, Sarma D (2020) The complete mitochondrial genome of the medicinal fish, *Cyprinion semiplotum*: Insight into its structural features and phylogenetic implications. International Journal of Biological Macromolecules 164: 939–948. http://doi.org/10.1016/j.ijbiomac.2020.07.142

Sun ZX, Kawase S, Zhang R, Zhao YH (2021) Taxonomic revision and redescription of *Microphysogobio hsinglungshanensis*, the type species of *Microphysogobio* Mori, 1934 (Cypriniformes: Cyprinidae). Journal of Fish Biology 2021: 1–11. http://doi.org/10.1111/jfb.14725

Tamura K, Stecher G, Peterson D, Filipski A, Kumar S (2013) MEGA6: molecular evolutionary genetics analysis version 6.0. Molecular Phylogenetics and Evolution 30: 2725–2729. http://doi.org/10.1093/molbev/mst197

Tang KL, Agnew MK, Chen WJ, Hirt MV, Raley ME, Sado T, Schneider LM, Yang L, Bart HL, He S, Liu H, Miya M, Saitoh K, Simons AM, Wood RM, Mayden RL (2011) Phylogeny of the gudgeons (Teleostei: Cyprinidae: Gobioninae). Molecular Phylogenetics and Evolution 61: 103–124. http://doi.org/10.1016/j.ympev.2011.05.022

Wang IC, Lin HD, Liang CM, Huang CC, Wang RD, Yang JQ, Wang WK (2020) Complete mitochondrial genome of the freshwater fish *Onychostoma lepturum* (Teleostei, Cyprinidae): genome characterization and phylogenetic analysis. ZooKeys 1005: 57–72. http://doi.org/10.3897/zookeys.1005.57592

Wang X (2019) Construction of fish DNA barcode database and excavation of cryptical species in Henan Province. Master thesis, Henan Normal University, Xinxiang.

Wang W, He S, Chen Y (2002) Mitochondrial d-loop sequence variation and phylogeny of gobiobotine fishes. Progress in Natural Science 12: 866–868.

Wolstenholme DR (1992) Animal mitochondrial DNA: structure and evolution. International Review of Cytology 141: 173–216. http://doi.org/10.1016/S0074-7696(08)62066-5

Xiao WH, Zhang YP (2000) Genetics and evolution of mitochondrial DNA in fish. Acta Hydrobiologica Sinica 24: 384–391. http://doi.org/10.3321/j.issn:1000-3207.2000.04.014

Yamanoue Y, Miya M, Matsuura K, Yagishita N, Mabuchi K, Sakai H, Katoh M, Nishida M (2007) Phylogenetic position of tetraodontiform fishes within the higher teleosts: Bayesian inferences based on 44 whole mitochondrial genome sequences. Molecular Phylogenetics and Evolution 45: 89–101. http://doi.org/10.1016/j.ympev.2007.03.008

Yang J, He S, Freyhof J, Witte K, Liu H (2006) The phylogenetic relationships of the Gobioninae (Teleostei: Cyprinidae) inferred from mitochondrial cytochrome b gene sequences. Hydrobiologia 553: 255–266. http://doi.org/10.1007/s10750-005-1301-3

Yu Z, Liu H (2011) The evolution of pharyngeal bones and teeth in Gobioninae fishes (Teleostei: Cyprinidae) analyzed with phylogenetic comparative methods. Hydrobiologia 664: 183–197. http://doi.org/10.1007/s10750-010-0598-8

Yue PQ (1998) Gobioninae. In: Chen YY (Ed.) Fauna Sinica, Osteichthyes, Cypriniformes (II). Science Press, Beijing, 232–378.

Zhang D, Gao F, Jakovlić I, Zou H, Zhang J, Li WX, Wang GT (2020) PhyloSuite: an integrated and scalable desktop platform for streamlined molecular sequence data management and evolutionary phylogenetics studies. Molecular Ecology Resources 20: 348–355. http://doi.org/10.1111/1755-0998.13096

Zhang F, Wu HH, Yang CX, Li CL, Wang YF, Gao YN, Gu QH, Zhou CJ, Meng XL, Nie GX (2018) Length-weight relationships of 5 Gobioninae species from the Yellow River basin and Huaihe River basin in Henan Province, China. Journal of Applied Ichthyology 34: 1320–1323. http://doi.org/10.1111/jai.13793

Zhang R, Wang X (2018) Characterization and phylogenetic analysis of the complete mitogenome of a rare cavefish, *Sinocyclocheilus multipunctatus* (Cypriniformes: Cyprinidae). Genes & Genomics 40: 1033–1040. http://doi.org/10.1007/s13258-018-0711-3

Zhao J, Xu D, Zhao K, Diogo R, Yang J, Peng Z (2016) The origin and divergence of Gobioninae fishes (Teleostei: Cyprinidae) based on complete mitochondrial genome sequences. Journal of Applied Ichthyology 32: 32–39. http://doi.org/10.1111/jai.12920

Zhong L, Wang M, Li D, Tang S, Zhang T, Bian W, Chen X (2018) Complete mitochondrial genome of *Odontobutis haifengensis* (Perciformes, Odontobutiae): a unique rearrangement of tRNAs and additional non-coding regions identified in the genus *Odontobutis*. Genomics 110: 382–388. http://doi.org/10.1016/j.ygeno.2017.12.008

Supplementary material 1

Table S1. Primers used for PCR

Authors: Renyi Zhang, Qian Tang, Lei Deng

Data type: molecula data

Link: https://doi.org/10.3897/zookeys.1061.70176.suppl1

Supplementary material 2

Table S2. List of species used to construct the phylogenetic tree in the present study

Authors: Renyi Zhang, Qian Tang, Lei Deng

Data type: molecula data

Link: https://doi.org/10.3897/zookeys.1061.70176.suppl2

Supplementary material 3

Table S3. Codon usage in the PCGs of the *Microphysogobio elongatus* mitogenome

Authors: Renyi Zhang, Qian Tang, Lei Deng

Data type: molecula data

Link: https://doi.org/10.3897/zookeys.1061.70176.suppl3

Supplementary material 4

Table S4. PartitionFinder results

Authors: Renyi Zhang, Qian Tang, Lei Deng

Data type: molecula data

Link: https://doi.org/10.3897/zookeys.1061.70176.suppl4

Supplementary material 5

Figure S1. Relative synonymous codon usage (RSCU) in the *M. elongatus* mitogenome

Authors: Renyi Zhang, Qian Tang, Lei Deng

Data type: molecula data

Explanation note: Codon families are provided on the X-axis and the RSCU values on the Y-axis.

Link: https://doi.org/10.3897/zookeys.1061.70176.suppl5

Supplementary material 6

Figure S2. Codon distribution in the *M. elongatus* mitogenome

Authors: Renyi Zhang, Qian Tang, Lei Deng

Data type: molecula data

Explanation note: CDspT, codons per thousand codons. Codon families are provided on the X-axis.

Link: https://doi.org/10.3897/zookeys.1061.70176.suppl6

Supplementary material 7

Figure S3. Putative secondary structures of the 22 tRNA genes identified in the mitochondrial genome of *M. elongatus*

Authors: Renyi Zhang, Qian Tang, Lei Deng

Data type: molecula data

Explanation note: All tRNA genes are shown in the order of occurrence in the mitochondrial genome starting from $tRNA^{Phe}$. The tRNAs are labelled with abbreviations of their corresponding amino acid. Dashed lines (-) indicate Watson-Crick base pairings.

Link: https://doi.org/10.3897/zookeys.1061.70176.suppl7

Supplementary material 8

Figure S4. Control region of the *M. elongatus* mitochondrial genome

Authors: Renyi Zhang, Qian Tang, Lei Deng

Data type: molecula data

Explanation note: The termination associated sequence domain (TAS), the central conserved domains (CSB-F, CSB-E, CSB-D) and the conserved sequence block domains (CSB-1, CSB-2, CSB-3) are shown in red font, and the conserved sequences are marked by black font and underlined.

Link: https://doi.org/10.3897/zookeys.1061.70176.suppl8

Supplementary material 9

Figure S5. Phylogenetic relationships of Gobioninae based on complete mitochondrial genomes using Bayesian analyses

Authors: Renyi Zhang, Qian Tang, Lei Deng

Data type: phylogenetic data

Explanation note: Bayesian posterior probabilities are shown at the nodes.

Link: https://doi.org/10.3897/zookeys.1061.70176.suppl9

ZooKeys 1061: 75–86 (2021)
doi: 10.3897/zookeys.1061.70130
https://zookeys.pensoft.net

RESEARCH ARTICLE

A peer-reviewed open-access journal
ZooKeys
Launched to accelerate biodiversity research

Extinct before discovered? *Epactoides giganteus* sp. nov. (Coleoptera, Scarabaeidae, Scarabaeinae), the first native dung beetle to Réunion island

Michele Rossini[1], Fernando Z. Vaz-de-Mello[2], Olivier Montreuil[3], Nicholas Porch[4], Sergei Tarasov[1]

1 *Finnish Museum of Natural History (LUOMUS), University of Helsinki, Pohjoinen Rautatiekatu 13, Helsinki, 00014, Finland* **2** *Departamento de Biologia e Zoologia, Instituto de Biociências, Universidade Federal de Mato Grosso, Av. Fernando Correa da Costa, n 2367, Boa Esperança, 78060-900, Cuiabá, Mato Grosso, Brazil* **3** *UMR 7179 MNHN/CNRS, MECADEV, Muséum National d'Histoire Naturelle, Entomologie, CP 50, 45 rue Buffon, 75231 Paris cedex 05, France* **4** *School of Life and Environmental Sciences, Faculty of Science Engineering & Built Environment, Deakin University, Melbourne Burwood Campus, 221 Burwood Highway, Burwood, VIC 3125, Australia*

Corresponding author: Michele Rossini (micros.naturae@gmail.com)

Academic editor: Andrey Frolov | Received 14 June 2021 | Accepted 31 August 2021 | Published 1 October 2021

http://zoobank.org/7B8C086B-59FA-48F6-B87E-C2825B0FABBC

Citation: Rossini M, Vaz-de-Mello FZ, Montreuil O, Porch N, Tarasov S (2021) Extinct before discovered? *Epactoides giganteus* sp. nov. (Coleoptera, Scarabaeidae, Scarabaeinae), the first native dung beetle to Réunion island. ZooKeys 1061: 75–86. https://doi.org/10.3897/zookeys.1061.70130

Abstract

We describe a new species of dung beetle, *Epactoides giganteus* **sp. nov.**, from a single female specimen allegedly collected in the 19th century on Réunion island and recently found at the Muséum national d'Histoire naturelle, Paris. This species differs from other species of *Epactoides* by larger size and a set of other distinctive morphological characters. *Epactoides giganteus* **sp. nov.** is the first native dung beetle (Scarabaeinae) of Réunion, and its discovery expands the known area of distribution of the genus *Epactoides*, which was hitherto believed to be endemic to Madagascar. Like other taxa from Madagascar and peripheral islands (e.g., Comoro, Seychelles, Mascarenes), *E. giganteus* **sp. nov.** may have reached Réunion by over-water dispersal. Given the rapid loss of biodiversity on Réunion island and the fact that no additional specimens were re-collected over the last two centuries, it is very likely that *E. giganteus* **sp. nov.** has gone extinct. However, we have unconfirmed evidence that the holotype of *E. giganteus* **sp. nov.** might be a mislabeled specimen from Madagascar, which would refute the presence of native dung beetles on Réunion. We discuss both hypotheses about the specimen origin and assess the systematic position of *E. giganteus* **sp. nov.** by examining most of the described species of Madagascan *Epactoides*. Additionally, we provide a brief overview of the dung beetle fauna of Mascarene Archipelago.

Keywords
Dung beetles, extinction, Madagascar, Malagasy region, Mascarene Archipelago, Nicolas Bréon, overwater dispersal

Introduction

The Mascarene archipelago is located in the southwestern Indian Ocean and comprises three main volcanic isles, namely Réunion, Mauritius, and Rodrigues. At about 2,510 km^2, Réunion is the largest of the Mascarene islands and the closest to Madagascar (ca 550 km), followed by Mauritius (ca 1865 km^2) and Rodriguez (ca 110 km^2), which are situated at an increasing distance from Madagascar, about 900 km and 1,500 km, respectively.

The three Mascarene islands are globally renowned as iconic examples of recent and rapid loss of a great part of their biotas. According to early reports and ecological inferences based on current vegetation, at the time of their discovery, the Mascarene islands were completely covered with dense, high forests (Cheke and Hume 2008). Uncontrolled logging, over-hunting, and accidental and voluntary introduction of alien animals, along with a long list of invasive plants had a devastating effect on local Mascarene biotas. Nowadays, agricultural practices primarily linked to the large production of sugarcane have extensively modified native ecosystems. However, fortunately, the rugged topography of Mauritius and Réunion would seem to have played a crucial role for the survival of small fragments of native and very fragile ecosystems. For example, in Mauritius, many of these areas are today officially protected by conservation actions (e.g., Conservation Management Areas; Griffiths and Florens 2006; Cheke and Hume 2008).

Mauritius was colonized in 1598 and since then 98% of its primary forests and about 40% of native endemic terrestrial fauna disappeared (Florens 2013). Likewise, since the arrival of Europeans in 1665, about 70% of native terrestrial vertebrate fauna of Réunion went extinct, and its flora is nowadays dominated by an extremely high number of invasive plants (Lagabrielle et al. 2011). Rodrigues was the last of the Mascarene islands to have been reached by humans, yet its historical epilogue was not that different from the other two islands. Leguat (1708) provided the first descriptive framework of the natural environments of Rodriguez at the time of its discovery, bearing witness to the drastic environmental changes suffered by the island over the last three centuries (see Strahm 1989).

Emblematic examples of lost vertebrate in the Mascarene islands are the dodo (*Raphus cucullatus* (Linnaeus, 1758)), the Rodrigues solitaire (*Pezophaps solitaria* (Gmelin, 1789)), day-geckos (genus *Phelsuma* Gray, 1828), giant tortoises (genus *Cylindraspis* Fitzinger, 1835) and fruit bats (genus *Pteropus* Brisson, 1762) (see Griffiths and Florens 2006; Cheke and Hume 2008; Florens 2013). However, very little is known about the invertebrate fauna, and especially insects. As many other oceanic islands (e.g., Antilles, New Caledonia, New Zealand, Madagascar), the Mascarene islands still hold their own endemic taxa and scarabaeine dung beetles are not the exception. Mauritius today

harbors two endemic dung beetle genera (i.e., the monotypic *Nesovinsonia* Martínez & Pereira, 1958 and *Nesosisyphus* Vinson, 1946) and a total of five described species; no dung beetles are mentioned from Rodrigues. However, about 12 new subfossil species of scarabaeines have been recently found (Nicholas Porch unpubl. data), which proves that in the past local ecosystems sustained an impressively rich dung beetles fauna. Finally, Réunion seems to host only a few introduced Indian and African *Onthophagus* Latreille, 1802 and some Aphodiinae (Lacroix and Poussereau 2019). Nevertheless, one of us (Fernando Vaz-de-Mello), during a recent visit at the Coleoptera collection of the Muséum national d'Histoire naturelle, Paris, found a gigantic female specimen of *Epactoides* Olsoufieff, 1947 that had two labels: the older label bears the handwritten accession number "4112.33", which recalls one of the several lots of insects collected and sent by Nicolas Bréon from Réunion; the second, more recent and printed label reads "La Réunion", including also the collector name and the same accession number (Fig. 1B).

With about 40 species (Fairmaire 1898; Paulian 1935, 1975, 1976, 1991, 1992; Lebis 1953; Montreuil 2003, 2005, 2017; Wirta and Montreuil 2008), the genus *Epactoides* is nowadays considered to be endemic to Madagascar. Most of the described species were formerly included in *Epactoides* and its subgenus *Aleiantus* (Lebis 1953). Later, new genera were erected to accommodate one or two species each, such as *Sikorantus* Paulian, 1976, *Phacomosoides* Martínez & Pereira, 1958, and *Madaphacosoma* Paulian, 1975. Recently, the phylogenetic analyses by Wirta and Montreuil (2008) has proved the inconsistency of such classification and all these taxon names, including *Aleiantus*, were eventually synonymized under *Epactoides*.

Epactoides dung beetles are very small, with body length ranging from 2–5 mm. However, the external phenotype is quite variable: body evenly dark colored or with large and symmetrical yellow spots; dorsal surface of the body polished, shining and punctation very superficial and weak, or body opaque, with deeper and coarse punctation, tubercles, granules, cavities and wrinkles; when present, sexual dimorphisms manifested in the shape of the procoxal cavities (distinctly wider in male), modification of pro- (with medial tooth anteriorly) and metafemora (widened posteriorly), and sometimes in the shape of protibiae (slender and strongly curved apically).

In this study, we describe a new *Epactoides* species from Réunion. The description of the external phenotype is based on a fairly well-preserved female, which is to date the only specimen available to us. The morphological study of a large sample of Madagascan *Epactoides*, the consultation of relevant literature along with historical accession catalogues stored at the Muséum national d'Histoire naturelle, Paris (MNHN), allow us to speculate about the provenance of this gigantic *Epactoides* and to discuss the systematic value and uniqueness of its phenotypic characters.

Material and methods

The morphological examination of the holotype of the new species was carried out under a Leica S9D stereomicroscope. Photographs of the dorsal habitus and disarticulated

body parts were taken with a Canon EOS 5D camera and a Canon MP-E 65 mm, f/2.8, 1–5× macro lens, using the Cognisys Stackshot automated system. Images were subsequently enhanced and edited in Adobe Photoshop and Illustrator CC. Morphological analyses were carried out on specimens deposited in the following institutes:

MNHN Muséum national d'Histoire naturelle, Paris (O. Montreuil);
MZHF Finnish Zoology Museum of Natural History (LUOMUS), Helsinki (S. Tarasov, J. Mattila).

Original label data are provided *verbatim*; data of different labels are separated by slashes ("/"), while data contained in single label are separated by commas (",").

Results and discussion

***Epactoides giganteus* Rossini, Vaz-de-Mello & Montreuil, sp. nov.**
http://zoobank.org/CD8ECE33-60B4-4FCA-BE78-CAD7DC56207C
Figure 1A–K

Type material. ***Holotype***, female: "MUSEUM PARIS, LA RÉUNION, BRÉON, 4112·33 / 4112, 33 / HOLOTYPE, *Epactoides giganteus* Rossini, Vaz-de-Mello, Montreuil, 2021", (MNHN).

Diagnosis. *Epactoides giganteus* sp. nov. is easily distinguished from congeneric species by the uniquely large size (body length 9 mm, while Madagascan *Epactoides* includes only small-sized species, with body length ranging from 2–5 mm); from above, dorsal portion of eyes wide (0.2 mm, while very narrow in Madagascan *Epactoides*); presence of a shallow groove close to the external and internal edges of the eye; elytral stria 7 pseudocarinated, stria 8 entirely carinated (elytral stria 7 entirely carinated in most Madagascan *Epactoides*); presence of a prosternal medial spur (absent in Madagascan *Epactoides*). Also, *E. giganteus* sp. nov. is endemic to and the only known native scarabaeine of Réunion island (but see discussion below). Currently, it is the only species of the genus recorded outside Madagascar.

Description. Body length. 9 mm.

Color. Dorsal habitus completely black, lateral sides of head and pronotum, and ventral side of body mahogany brown; hairs yellow; mouthparts, tarsi, and antennal articles brownish (antennal club lacking).

***Head*.** Semicircular and barely emarginated in clypeogenal junction; genae finely margined, clypeal edge without margin; clypeus with two median, blunt teeth separated by a wide depression; external side of each clypeal tooth with a deep, V-shaped emargination; dorsal portion of eyes wide (0.2 mm) (Fig. 1A, F); internal and external edges of eyes flanked by a superficial groove that disappears anteriorly; internal groove more distinct and runs from postoccipital margin (Fig. 1F); head largely smooth, with coarse and very shallow punctures in proximity of clypeal teeth.

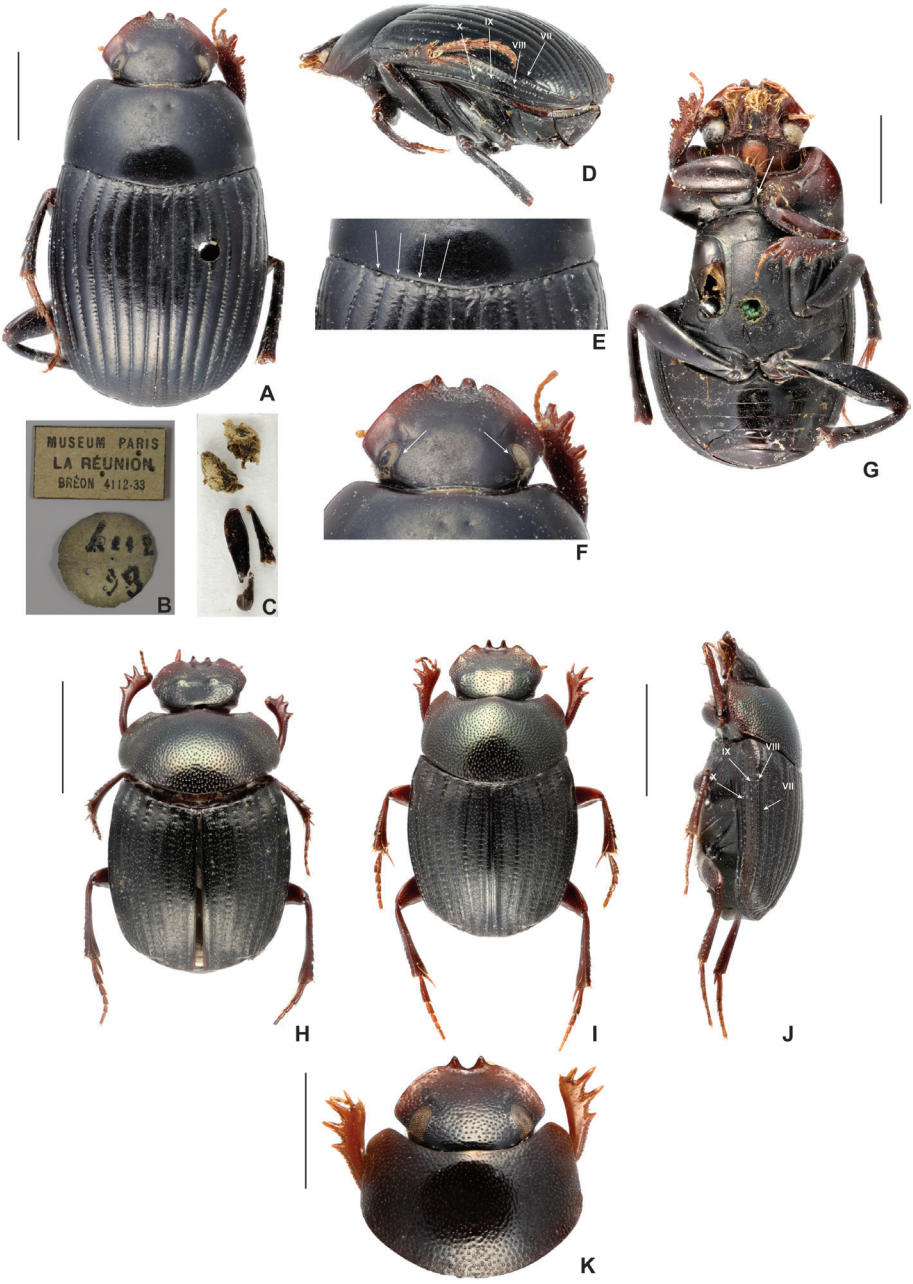

Figure 1. *Epactoides giganteus* sp. nov. **A** dorsal habitus of the holotype **B** original labels **C** disarticulated body parts pinned with the holotype **D** detail of the entire carina of the elytral stria 8 and pseudocarina on the apical part of the stria 7; arrows indicate striae 7–10 **E** detail of the base of elytral interstriae; arrows indicate basal tubercles on interstriae 2–5 **F** detail of the dorsal portion of eyes; arrows indicate the internal groove **G** ventral habitus of the holotype; arrow indicates the prosternal spur. *Epactoides frontalis* (Montreuil) **H, I** dorsal habitus of male and female **J** lateral habitus of the female; arrows indicate elytral stria 7–10; stria 7 completely carinated. *Ochicanthon ceylonicus* Cuccodoro, **K** detail of the wide eyes in dorsal view.

Thorax. Pronotum feebly convex, lateral and anterior edges finely margined, posterior edge without margin; lateral edges nearly straight and parallel, slightly curved distally; anterior angles rounded; anteromedial region of pronotum with two small, symmetrical pits (Fig. 1A, F); pronotal surface without punctation. Propleuron with a strong and rather thick ridge that runs from lateral margin of procoxae to external margin of pronotum; anterior side of propleuron very slightly excavated. Prosternum smooth, with an anteromedial, blunt spur (Fig. 1G). Meso- and metasternum simple; meso- metasternal junction indicated by a transverse bead, slightly swollen medially. Elytra with 10 striae (two striae on epipleuron); 7th stria pseudocarinated (swollen) from middle to subapical region of elytra; 8th stria completely carinated (Fig. 1D); strial punctures coarse and close; interstriae unpunctated, basomedial margin of interstriae 2–5 with small, rounded tubercles (Fig. 1E).

Abdomen. Sternites well visible ventrally, without punctures and setae; pygidial edges completely margined, basal edge with prominent border; pygidium swollen at middle, highest point of hump connected by two blunt ridges to basal angles of pygidium; abdominal tergite 8th medially interrupted by a deep longitudinal groove.

Legs. Protarsi simple, with 2–3 setae in ventroapical side; mesotarsi long, with a series of aligned setae in ventral and dorsal sides; metatarsi are lacking; protibiae with three big external teeth, externobasal edge serrated; meso- and metatibiae long, straight and distally feebly wider; pro-, meso- and metafemurs unmodified.

Distribution. Réunion island, Mascarene Archipelago (no additional collecting data available).

Taxonomically informative characters of *Epactoides giganteus* sp. nov.

The external morphology of *E. giganteus* sp. nov. unequivocally indicates its belonging to the genus *Epactoides*: body oval, rather flat dorsoventrally; genae finely margined; clypeus with anteromedial teeth; elytral striae well indicated. This new species is only known from one female specimen, which makes it difficult to suggest any hypothesis of relationships with other *Epactoides*. At the moment, we consider it to be tentatively related to *E. frontalis* (Montreuil, 2003) (Fig. 1H–J) and *E. spinicollis* (Montreuil, 2003). Additional specimens may help to clarify its systematic position.

Epactoides giganteus sp. nov. exhibits a series of unique phenotypic characters within the genus:

(i) Clypeus with four teeth: this character does not occur in any other *Epactoides* species. Among the Madagascan *Epactoides* examined in this study, *E. frontalis*, *E. spinicollis*, *E. semiaeneus* (Paulian, 1976), and *E. mesoalae* (Paulian, 1976) are the only Madagascan species whose clypeal shape may recall that of *E. giganteus* sp. nov., albeit the lateral clypeal teeth are not as distinctly shaped as in *E. giganteus* sp. nov. (Fig. 1A, F).

(ii) Dorsal portion of eyes wide: this phenotypic trait is unique within *Epactoides*, as the eyes of all described species are narrow. Recent phylogenetic reconstructions

(Wirta et al. 2010; Mlambo et al. 2014) consider *Epactoides* to be a close relative to the Oriental genus *Ochicanthon* Vaz-de-Mello, 2003, which includes several species with wide eyes (see for example *Ochicanthon ceylonicus* Cuccodoro, 2011; Fig. 1K).

(iii) Distinct furrow in the inner side of the eyes connected with the postoccipital margin of the head (Fig. 1F): none of the analyzed *Epactoides* species exhibits this character. Similar furrow is common in the Madagascan dung beetle genus *Apotolamprus* Olsoufieff, 1947, where, however, the groove is deeper and never connected with the postoccipital margin of the head.

(iv) Elytra with 10 distinct striae; elytral stria 7 pesudocarinated from the middle to the subapical region of the elytra; stria 8 entirely carinated (Fig. 1D). All described *Epactoides* have nine distinct elytral striae, however, some species show an additional stria on the top of the carina of the 7th stria (see for example *E. frontalis*; Fig. 1J).

(v) Base of elytral interstriae 2–5 tuberculated (Fig. 1E): this trait is quite rare in *Epactoides*, but common in the allied genus *Ochicanthon*. *Epactoides helenae* (Montreuil, 2005) shows tiny and pointed tubercles on the basal margin of the interstriae 3–6.

(vi) Prosternal spur (Fig. 1G): usually, the prosternum of *Epactoides* is simple and rather flat, without central spurs or tubercles, but the prosternum of *E. giganteus* sp. nov. has a well-developed spur in its medial region.

Finally, the holotype of *E. giganteus* sp. nov. has two anteromedial pronotal pits (Fig. 1A, F). Our examination has confirmed that this character is not sexually dimorphic and intraspecifically variable within *Epactoides* (found in *E. frontalis* and *E. lissus* Lebis, 1953) and other Madagascan genera (e.g., *Apotolamprus* and *Arachnodes* Westwood, 1842). We examined if these pits serve as sites of muscle attachment by bleaching the body of some Madagascan *Epactoides*, *Apotolamprus*, and *Arachnodes* in hydrogen peroxide. However, no traces of muscular connections were found. Thus, so far, the anatomical function and systematic informativeness of the pronotal pits remains unknown.

Historical notes and hypotheses on the origin of the holotype of *Epactoides giganteus*

The holotype of *E. giganteus* sp. nov. was apparently collected by Jean Nicolas Bréon, botanist and then director of the current Jardin de l'État in Saint-Denis (Réunion). Bréon arrived in Réunion in 1817, but health problems forced him to leave the island in 1833 (Bouchard-Huzard 1865). During this period, he undertook numerous expeditions to the southeastern of Madagascar (Anôsy) and Île de Sainte-Marie (northeastern Madagascar). Also, it is known that in Réunion, Bréon occasionally collected insects and sent lots of entomological material to the MNHN. However, mislabeling seems to be common with his specimens. Macquart (1843) was the first author to point out that some of the flies supposedly collected by Bréon in Réunion and sent to the MNHN (accession number 4112.33) were actually mislabeled, as they belonged to common European species [e.g., *Spilogaster quadrivittata*, but see taxonomic corrections by Pont (2012)]. According to Pont (2012), the historical accession catalogue of

the MNHN of Paris indicates that the specimens under the accession number 4112.33 belong to a set of insects collected and sent by Bréon from Île Bourbon (ancient name of Réunion island). Beneath this information, in the same catalogue, A.C. Pont found a note from the coleopterist E.J.B. Fleutiaux (1858–1951) saying that "three Elateridae (Coleoptera) labelled as collected on La Réunion by Bréon are in fact European species". Nonetheless, within the same bunch of insects, there was also the holotype of the melolonthid *Gymnogaster buphthalma* Blanchard, 1850, which was originally described from a single female. The provenance of this specimen was questioned for more than 130 years, when eventually new specimens were recollected in the north of the island (Lacroix 1988), indicating that *G. buphthalma* is endemic to Réunion.

Given the aforementioned facts, we cannot rule out the possibility that *E. giganteus* sp. nov. has been collected in Madagascar and mislabeled afterwards. On one hand, it is noteworthy to consider that during the last 20 years Madagascan dung beetles have been intensively surveyed (e.g., Hanski et al. 2007; Rahagalala et al. 2009; Viljanen et al. 2010; Knopp et al. 2011) and no other specimens of *E. giganteus* sp. nov. were collected. On the other hand, however, it is important to remark that since 1950, Madagascar lost about 44% of native rainforests (Morelli et al. 2020), which may have caused the disappearance of many forest-dwelling species, including dung beetles (Hanski et al. 2007). Indeed, likewise its congeneric species, *E. giganteus* sp. nov. is suggested to be a putative forest dweller, which may have gone extinct long before the beginning of the intensive dung beetle surveys.

Thus, the limited data we have do not allow to confirm the correct provenance of *E. giganteus* sp. nov. At the same time, we are lacking any direct evidence that could suggest the mislabeling of the holotype of *E. giganteus* sp. nov. Réunion is the island of the Mascarene Archipelago that still preserves the largest amount of forest habitats, with about one-third of its surface covered by native vegetation (Strasberg et al. 2005; Lagabrielle et al. 2011). It is logical to believe that Réunion could (or still can) harbor native dung beetles, likewise other islands of the Mascarene Archipelago (Mauritius: five extant species, Paulian 1939; Vinson 1939, 1946, 1958; Rodrigues: ca 12 undescribed subfossil species, Nicholas Porch unpubl. data). Therefore, based on the aforementioned facts and unique morphological features of the holotype, we consider *E. giganteus* sp. nov. to be the first native dung beetle discovered in Réunion.

Over the last decades, different coleopteran groups from Réunion have been surveyed (e.g., Poussereau et al. 2011; Poussereau 2014; Wanat and Poussereau 2019), but no systematic and geographically extensive monitoring of dung beetles have been carried out so far. To date, only occasional collecting events by hand and without standardized methods (i.e., pitfall baited with excrement) have recorded a few introduced *Onthophagus* dung beetles (Lacroix and Poussereau 2019; Jacques Poussereau pers. comm. to Olivier Montreuil). Hence, there is an urgent need to increase efforts to study scarabaeine dung beetles in Réunion island to confirm or contradict the possibility that today's still surviving pristine habitats can preserve any endemic species, including *E. giganteus* sp. nov., or even unveil their unknown diversity.

The volcanic Mascarene islands (ca 3–10 Myr) have never been connected to other landmasses, and over-water dispersal is the predominant scenario to explain the origin

of animals and plants inhabiting the Mascarene Archipelago (Vences et al. 2003; Yoder and Nowak 2006; Harmon et al. 2008; Buerki et al. 2013; Bukontaite et al. 2015). Importantly, over the last 65 Myr a series of now submerged continental fragments located in the northern part of the Mascarene Plateau fostered the Madagascar-to-Mauritius dispersal route (Bradler et al. 2015; Kehlmaier et al. 2019; Przybyłowicz et al. 2021). As a consequence, Mauritius played as critical source of biota for the geologically younger Réunion (Agnarsson and Kuntner 2012). Cases of direct colonization of Réunion from Madagascar are rare in the literature.

Thus, assuming that *E. giganteus* sp. nov. is native to Réunion and considering the nowadays consolidated hypothesis of Madagascan origin of the genus *Epactoides* (ca. 30–19 Myr) from African ancestors (Wirta et al. 2010), the most likely scenario is that *E. giganteus* sp. nov. colonized Réunion by over-water dispersal from Madagascar.

Acknowledgements

This study was supported by the Pentti Tuomikoski Fund and the Academy of Finland Grant (#331631), awarded to ST. We thank M. Lacroix and J. Poussereau for having provided additional information on Bréon's material deposited at the MNHN of Paris, as well as the current knowledge on dung beetles from Réunion island.

References

Agnarsson I, Kuntner M (2012) The generation of a biodiversity hotspot: biogeography and phylogeography of the western Indian Ocean islands. In: Anamthawat-Jónsson K (Ed.) Current Topics in Phylogenetics and Phylogeography of Terrestrial and Aquatic Systems. InTech, London, 33–82. https://doi.org/10.5772/38958

Bouchard-Huzard L (1865) Note biographique sur J.-N. Bréon, ancien jardinier botaniste en chef du jardin botanique de Saint-Denis, Île Bourbon. Bulletin de la Société Botanique de France 12: e60.

Bradler S, Cliquennois N, Buckley TR (2015) Single origin of the Mascarene stick insects: ancient radiation on sunken islands? BMC Evolutionary Biology 15: 1–10. https://doi.org/10.1186/s12862-015-0478-y

Buerki S, Devey DS, Callmander MW, Phillipson PB, Forest F (2013) Spatio-temporal history of the endemic genera of Madagascar. Botanical Journal of the Linnean Society 171: 304–329. https://doi.org/10.1111/boj.12008

Bukontaite R, Ranarilalatiana T, Randriamihaja JH, Bergsten J (2015) In or out-of-Madagascar? Colonization patterns for large-bodied diving beetles (Coleoptera: Dytiscidae). PLoS ONE 10: e0120777. https://doi.org/10.1371/journal.pone.0120777

Cheke A, Hume J (2008) Lost Land of the Dodo: An Ecological History of Mauritius, Réunion & Rodrigues. Yale University Press, New Haven and London, 464 pp. https://doi.org/10.5040/9781472597656

Fairmaire L (1898) Matériaux pour la faune coléoptérique de la région malgache (7e note). Annales de la Société Entomologique de Belgique 42: 463–477.

Florens VFB (2013) Conservation in Mauritius and Rodrigues: challenges and achievements from two ecologically devastated oceanic islands. In: Sodhi N, Gibson L, Raven P (Eds) Conservation Biology: Voices from the Tropics. Wiley-Blackwell, Chichester, 40–50. https://doi.org/10.1002/9781118679838.ch6

Griffiths OL, Florens VFB (2006) A Field Guide to the Non-marine Molluscs of the Mascarene Islands (Mauritius, Rodrigues and Réunion) and the Northern Dependencies of Mauritius. Bioculture Press, Mauritius, 185 pp.

Hanski I, Koivulehto H, Cameron A, Rahagalala P (2007) Deforestation and apparent extinctions of endemic forest beetles in Madagascar. Biology Letters 3: 344–347. https://doi.org/10.1098/rsbl.2007.0043

Harmon LJ, Melville J, Larson A, Losos JB (2008) The role of geography and ecological opportunity in the diversification of day geckos (*Phelsuma*). Systematic Biology 57: 562–573. https://doi.org/10.1080/10635150802304779

Kehlmaier C, Graciá E, Campbell PD, Hofmeyr MD, Schweiger S, Martínez-Silvestre A, Joyce W, Fritz U (2019) Ancient mitogenomics clarifies radiation of extinct Mascarene giant tortoises (*Cylindraspis* spp.). Scientific Reports 9: e17487. https://doi.org/10.1038/s41598-019-54019-y

Knopp T, Rahagalala P, Miinala M, Hanski I (2011) Current geographical ranges of Malagasy dung beetles are not delimited by large rivers. Journal of Biogeography 38: 1098–1108. https://doi.org/10.1111/j.1365-2699.2010.02463.x

Lacroix M (1988) *Gymnogaster buphthalma* Blanchard, espèce énigmatique de l'Île de Réunion (Coleoptera Melolonthidae). Revue Française d'Entomologie (1979)10: 25–29.

Lacroix M, Poussereau J (2019) Les Scarabéides de Réunion. Orphie, Réunion, 383 pp.

Lagabrielle E, Rouget M, Le Bourgeois T, Payet K, Durieux L, Baret S, Dupont J, Strasberg D (2011) Integrating conservation, restoration and land-use planning in islands – an illustrative case study in Réunion Island (Western Indian Ocean). Landscape and Urban Planning 101: 120–130. https://doi.org/10.1016/j.landurbplan.2011.02.004

Lebis E (1953) Révision des Canthoninae de Madagascar. Mémoires de l'Institut scientifique de Madagascar 3: 107–252.

Leguat de la FF (1708) Voyage et aventures de François Leguat et des ses compagnons en deux isles desertes des Indes Orientales. Jean Louis de Lorme, Amsterdam, 2 vol., 344 pp.

Macquart PJM (1843) Diptères exotiques nouveaux ou peu connus. Tome deuxième - 3e partie. Roret, Paris, 304 pp. https://doi.org/10.5962/bhl.title.15792

Mlambo S, Sole CL, Scholtz CH (2014) Affinities of the Canthonini dung beetles of the Eastern Arc Mountains. Organisms Diversity and Evolution 14: 115–120. https://doi.org/10.1007/s13127-013-0158-y

Montreuil O (2003) Contribution à l'étude des Canthonini Malgaches deuxième note: description de deux nouveaux *Aleiantus*. Revue Française d'Entomologie 25: 143–146.

Montreuil O (2005) Contribution à l'étude des Canthonini de Madagascar (5e note): description de nouveaux *Aleiantus* Olsoufieff, 1947. Revue Française d'Entomologie (Nouvelle Serie) 27: 153–160.

Montreuil O (2017) Un nouvel *Epactoides* Olsoufieff de Madagascar. Bulletin de la Société Entomologique de France 122: 476–470. https://doi.org/10.32475/bsef_1972

Morelli TL, Smith AB, Mancini AN, Balko EA, Borgerson C, Dolch R, Farris Z, Federman S, Golden CD, Holmes SM, Irwin M, Jacobs RL, Johnson S, King T, Lehman SM, Louis EE, Murphy A, Randriahaingo HNT, Randrianarimanana HLL, Ratsimbazafy J, Razafindratsima OH, Baden AL (2020) The fate of Madagascar's rainforest habitat. Nature Climate Change 10: 89–96. https://doi.org/10.1038/s41558-019-0647-x

Paulian R (1935) Faune entomologique de Madagascar. Coleoptera Lamellicornia, Scarabaeidae, Scarabaeini et Aphodiini. Bulletin de l'Academie Malgache 18: 121–144.

Paulian R (1939) Quelques nouvelles espèces de coléoptères lamellicornes coprophages. Bulletin de la Société Entomologique de France 44: 68–74.

Paulian R (1975) Sur quelques Canthonina (Coléoptères, Scarabéides) montagnards de Madagascar. Annales de la Société Entomologique de France 11: 221–252.

Paulian R (1976) Révision des *Canthonina* Longitarses de Madagascar. Annales de la Société Entomologique de France 12: 453–479.

Paulian R (1991) Les Scarabaeoidea obtenus d'excréments de *Propithecus diadema* à Madagascar. Bulletin de la Société Entomologique de France 96: 355–359.

Paulian R (1992) Un nouvel *Aleiantus* Olsoufieff. Bulletin de la Société Entomologique de France 97: 15–16.

Pont AC (2012) Muscoidea (Fanniidae, Anthomyiidae, Muscidae) described by P. J. M. Macquart (Insecta, Diptera). Zoosystema 34: 39–111. https://doi.org/10.5252/z2012n1a3

Poussereau J (2014) Mise à jour du catalogue des Anthribidae de l'Île de Réunion (Coleoptera, Curculionoidea). Bulletin de la Société Entomologique de France 119: 109–112.

Poussereau J, Jelínek J, Audisio P (2011) A new species of *Amystrops* Reitter, 1875, and an updated checklist of the Nitidulidae from Réunion Island (Coleoptera). Bulletin de la Société Entomologique de France 116: 421–428.

Przybyłowicz Ł, Wiorek M, Przystałkowska A, Wahlberg N (2021) Alone on an island: the reassessment of an enigmatic species of Handmaiden Moth (Lepidoptera, Erebidae) endemic to Mauritius. Zoologica Scripta 50: 1–17. https://doi.org/10.1111/zsc.12508

Rahagalala P, Viljanen H, Hottola J, Hanski I (2009) Assemblages of dung beetles using cattle dung in Madagascar. African Entomology 17: 71–89. https://doi.org/10.4001/003.017.0109

Strahm W (1989) Plant Red Data Book for Rodrigues. Koeltz Scientific Book, Konigstein, Germany, 241 pp.

Strasberg D, Rouget M, Richardson DM, Baret S, Dupont J, Cowling RM (2005) An assessment of habitat diversity and transformation on Réunion Island (Mascarene Islands, Indian Ocean) as a basis for identifying broad-scale conservation priorities. Biodiversity & Conservation 14: 3015–3032. https://doi.org/10.1007/s10531-004-0258-2

Vences M, Vieites DR, Glaw F, Brinkmann H, Kosuch J, Veith M, Meyer A (2003) Multiple overseas dispersal in amphibians. Proceedings of the Royal Society of London – Series B: Biological Sciences 270: 2435–2442. https://doi.org/10.1098/rspb.2003.2516

Viljanen H, Escobar F, Hanski I (2010) Low local but high beta diversity of tropical forest dung beetles in Madagascar. Global Ecology and Biogeography 19: 886–894. https://doi.org/10.1111/j.1466-8238.2010.00552.x

Vinson JFRES (1939) On the occurence of two species of *Sisyphus* in Mauritius with description of a new species and the description of a new *Adoretus* from Reunion (Coleoptera: Scarabaeidae). Proceedings of the Royal Entomological Society of London B8: 33–38. https://doi.org/10.1111/j.1365-3113.1939.tb01276.x

Vinson JFRES (1946) On *Nesosysiphus*, a new genus of coprine beetles from Mauritius. Proceedings of the Royal Entomological Society of London B15: 89–96. https://doi.org/10.1111/j.1365-3113.1946.tb00830.x

Vinson JFRES (1958) Catalogue of the Coleoptera of Mauritius and Rodriguez. Part 2. The Mauritius Institute Bulletin 4: 1–73.

Wanat M, Poussereau J (2019) *Mascarapion*, a new genus of the Apioninae (Coleoptera, Curculionoidea) from the Mascarene Islands. Zootaxa 4615: 343–350. https://doi.org/10.11646/zootaxa.4615.2.6

Wirta H, Montreuil O (2008) Evolution of the Canthonini Longitarsi (Scarabaeidae) in Madagascar. Zoologica Scripta 37: 651–663. https://doi.org/10.1111/j.1463-6409.2008.00352.x

Wirta H, Viljanen H, Orsini L, Montreuil O, Hanski I (2010) Three parallel radiations of Canthonini dung beetles in Madagascar. Molecular Phylogenetics and Evolution 57: 710–727. https://doi.org/10.1016/j.ympev.2010.08.013

Yoder AD, Nowak MD (2006) Has vicariance or dispersal been the predominant biogeographic force in Madagascar? Only time will tell. Annual Review of Ecology, Evolution, and Systematics 37: 405–431. https://doi.org/10.1146/annurev.ecolsys.37.091305.110239

ZooKeys 1061: 87–108 (2021)
doi: 10.3897/zookeys.1061.70420
https://zookeys.pensoft.net

RESEARCH ARTICLE

A peer-reviewed open-access journal
ZooKeys
Launched to accelerate biodiversity research

Molecular phylogenetic analysis of the genus *Gloydius* (Squamata, Viperidae, Crotalinae), with description of two new alpine species from Qinghai-Tibet Plateau, China

Jing-Song Shi[1,2], Jin-Cheng Liu[2], Rohit Giri[3], John Benjamin Owens[4,5], Vishal Santra[5,6], Sourish Kuttalam[5,6], Melvin Selvan[7], Ke-Ji Guo[8], Anita Malhotra[4]

1 *Key Laboratory of Vertebrate Evolution and Human Origins of Chinese Academy of Sciences, Institute of Vertebrate Paleontology and Paleoanthropology, Chinese Academy of Sciences, Beijing 100044, China* **2** *Institute of Herpetology, Shenyang Normal University, Shenyang 110034, China* **3** *Department of Zoology, Prithvi Narayan Campus, Bhimkalipatan-1, Pokhara 33700, Nepal* **4** *Molecular Ecology and Evolution at Bangor, School of Natural Sciences, Bangor University, Bangor, Gwynedd LL57 2UW, UK* **5** *Captive and Field Herpetology, Wales, UK* **6** *Society for Nature Conservation, Research and Community Engagement (CONCERN), Nalikul, Hooghly, West Bengal, India* **7** *Endangered Wildlife Trust, Dindigull, Tamil Nadu, India* **8** *Central South Inventory and Planning Institute of National Forestry and Grassland Administration, College of Life Sciences and Technology, Central South University of Forestry and Technology, Changsha, Hunan 410004, China*

Corresponding authors: Jing-Song Shi (shijingsong@ivpp.ac.cn), Anita Malhotra (a.malhotra@bangor.ac.uk)

Academic editor: Robert Jadin | Received 21 June 2021 | Accepted 20 August 2021 | Published 4 October 2021

http://zoobank.org/F2701BAC-D2E1-4F97-A0BD-DC8B09966247

Citation: Shi J-S, Liu J-C, Giri R, Owens JB, Santra V, Kuttalam S, Selvan M, Guo K-J, Malhotra A (2021) Molecular phylogenetic analysis of the genus *Gloydius* (Squamata, Viperidae, Crotalinae), with description of two new alpine species from Qinghai-Tibet Plateau, China. ZooKeys 1061: 87–108. https://doi.org/10.3897/zookeys.1061.70420

Abstract

We provide a molecular phylogeny of Asian pit vipers (the genus *Gloydius*) based on four mitochondrial genes (12S, 16S, ND4, and cytb). Sequences of *Gloydius himalayanus*, the only member of the genus that occurs south of the Himalayan range, are included for the first time. In addition, two new species of the genus *Gloydius* are described based on specimens collected from Zayu, Tibet, west of the Nujiang River and Heishui, Sichuan, east of the Qinghai-Tibet Plateau. The new species, *Gloydius lipipengi* sp. nov., can be differentiated from its congeners by the combination of the following characters: the third supralabial not reaching the orbit (separated from it by a suborbital scale); wide, black-bordered greyish postorbital stripe extending from the posterior margin of the orbit (not separated by the postoculars, covering most of the anterior temporal scale) to the ventral surface of the neck; irregular black annular crossbands on the mid-body; 23-21-15 dorsal scales; 165 ventral scales, and 46 subcaudal scales. *Gloydius swild* **sp. nov.** can be differentiated from its congeners by the narrower postorbital stripe (only half the width of the anterior

temporal scale, the lower edge is approximately straight and bordered with white); a pair of arched stripes on the occiput; lateral body lakes black spots; a pair of round spots on the parietal scales; 21 rows of mid-body dorsal scales; zigzag dark brown stripes on the dorsum; 168–170 ventral scales, and 43–46 subcaudal scales. The molecular phylogeny in this study supports the sister relationship between *G. lipipengi* **sp. nov.** and *G. rubromaculatus*, another recently described species from the Qinghai-Tibet Plateau, more than 500 km away, and indicate the basal position of *G. himalayanus* within the genus and relatively distant relationship to its congeners.

Keywords
Asian pit viper, *Gloydius himalayanus*, Heishui, molecular phylogeny, osteology, Qinghai-Tibet plateau, Zayu

Introduction

Asian pit vipers of the genus *Gloydius* Hoge & Romano Hoge, 1978 are small-bodied venomous snakes distributed mainly in northern Asia, but extending into southern Europe in the case of *G. halys*. They are quite common and have radiated into various habitats. At present, more than 20 species mainly belonging to three species groups (i.e., the *G. blomhoffii* complex, *G. intermedius–halys* complex, and *G. strauchi* complex) are recognized (Orlov and Barabanov 1999; Zhao 2006; Shi et al. 2017, 2018). Within *Gloydius*, most species having 21 rows of mid-body dorsal scales and three palatine teeth have been attributed to many subspecies of *G. strauchi* (Bedriaga, 1912). Recently, several former subspecies have been elevated to full species (e.g., *G. qinlingensis* (Song & Chen, 1985)), *G. liupanensis* (Liu, Song & Luo, 1989), and *G. monticola* (Werner, 1922)) and several new species have been described from across the range of the complex (e.g., *G. rubromaculatus*, *G. angusticeps*, and *G. huangi*; Xu et al. 2012; Shi et al. 2017; Shi et al. 2018; Wang et al. 2019).

Given that the *Gloydius strauchi* complex is widely distributed in western China (Zhao et al.1998; Zhao 1999, 2006), some of the specimens from previous studies are now attributable to the recently elevated species described above. The distribution of *G. strauchi* sensu stricto has been restricted to western Sichuan by recent molecular and morphological studies (Orlov and Barabanov 1999, 2000; Shi et al. 2017, 2018). With respect to Tibet, older records of the *G. strauchi* complex refer to at least two different species, *G. rubromaculatus* from Jiangda (Shi et al. 2017, 2018) and *G. huangi* from Chamdo (Wang et al. 2019). However, given this wide-ranging complex spans several biogeographic barriers and distinct environments in a poorly investigated region, we hypothesize that there still might be hidden species within the *G. strauchi* complex.

Additionally, *Gloydius himalayanus* (Günther, 1864) has long been regarded as a full species within the *G. strauchi* complex based on its unique morphological characters (e.g., the conspicuous rostralis and the triangular head in dorsal view; Gloyd and Conant 1990). In spite of numerous recent studies focused on the molecular phylogeny of the genus *Gloydius* (Xu et al. 2012; Eskandar et al. 2018; Shi et al. 2016, 2018; Asadi et al. 2019; Wang et al. 2019), the systematic and taxonomic position of

G. himalayanus in relation to the *G. strauchi* complex is still unclear due to lack of the sequence data for this species.

In this study, we use a molecular phylogeny of *Gloydius*, including data of *G. himalayanus* for the first time, and provide a description of two new species from the *Gloydius strauchi* complex from Zayu, Tibet, and Heishui, Sichuan, China.

Materials and methods

Specimen collection

We examined preserved specimens from the Chengdu Institute of Biology (**CIB**), Kunming Institute of Zoology (**KIZ**), Institute of Zoology (**IOZ**), and Shenyang Normal University (**SYNU**). Newly obtained specimens were deposited in the Institute of Vertebrate Paleontology and Paleoanthropology (**IVPP**), Beijing.

Morphology

Snout–vent length (SVL), tail length (TL), and total length (TTL; i.e., SVL + TL) were measured with a flexible ruler to the nearest 1 mm. Other morphological measurements were taken with 0–200 mm vernier calipers to the nearest 0.1 mm: head length (HL, from the tip of snout to the posterior margin of mandible), head width (HW, the widest part of the head in dorsal view), head depth (HD, the deepest part of the head in lateral view), snout length (SL, from the tip of snout to the anterior margin of the eye), eye diameter (ED, measured as a horizontal distance), interorbital space (IOS, the distance between the top margin of eyes), and internasal space (INS, the distance between nostrils). Numbers of supralabials (SPL), infralabials (IFL), dorsal scales (DS), ventral scales (V, excluding four preventral scales), and subcaudal scales (SC) were counted.

X-ray scanning and three-dimensional reconstructions

The scanning was carried out with 225-kV micro-computerized tomography, developed by the Institute of High Energy Physics (IHEP), CAS. A total of 720 transmission images were reconstructed into the 2048 × 2048 matrix of 1536 slices using two-dimensional reconstruction software developed by the IHEP, CAS. The final CT reconstructed skull model was exported with a minimum resolution of 26.7 μm.

DNA extraction, polymerase chain reaction (PCR) and sequencing

Tissue samples for molecular analyses were taken separately and preserved in 95% ethanol at –40 °C. Genomic DNA was extracted with Qiaprep Spin Miniprep kit (QiaGen). Four mitochondrial genome fragments were specifically amplified for this study:

a 859 bp fragment of 12S ribosomal RNA (12S), using primers 12SFPhe and 12SRVal, described by Knight and Mindell (1993); a 465 bp fragment of 16S ribosomal RNA (16S) using primers 16sFL and 16sRH described by Palumbi et al. (1991); a 1065 bp fragment of cytochrome *b* (cytb) using primers L14919 and H16064 described by Burbrink et al. (2000), and a 666 bp fragment of NADH dehydrogenase subunit 4 (ND4), using the primers ND4 and Leu, described by Arevalo et al. (1994). The standard PCR protocol was performed in a 20 μl reaction with at least 20 ng of template DNA and 10 pmol of primers. PCR conditions consisted of an initial denaturation for 3 min at 94 °C, followed by 35 cycles of denaturation at 94 °C for 30 sec, 30 sec of annealing at primer-specific temperatures (56 °C for ND4, 54 °C for 16S, 48 °C for cytb), and extension at 72 °C for 60 sec, finalized with an extension step of 10 min at 72 °C. Sequencing was conducted by Beijing Tianyi Huiyuan Bio-tech Co., Ltd.

Phylogenetic analyses

We use 46 individuals of the 22 recognized *Gloydius* species, except for unavailable sequence data of *G. halys boehmei* (Nilson, 1983), in a phylogenetic. In order to establish the monophyly of *Gloydius*, 12 additional species of outgroups from the family Viperidae (i.e., *Calloselasma*, *Deinagkistrodon*, *Ovophis*, *Protobothrops*, *Sinovipera*, *Trimeresurus*, *Viridovipera*, and *Vipera*) were also included.

Sequence data obtained from GenBank and from this study are listed in Table 2. Sequences were aligned in MEGA6 (Tamura et al. 2013). With respect to the different evolutionary characters of each molecular marker, the dataset was initially split into eight partitions by gene and codon positions, and then combined into five partitions taking advantage of PartitionFinder 2.1.1 (Lanfear et al. 2012) to find similarly evolving partitions.

Bayesian phylogenetic analysis was performed using MrBayes 3.1.2 (Ronquist et al. 2011). All searches consist of three heated chains and a single cold chain. Three independent iterations each comprising two runs of 100,000,000 generations were performed, sampling every 10,000 generations, and parameter estimates were plotted against generation. The first 25% of the samples were discarded as burn-in, resulting in a potential scale reduction factor (PSRF) of <0.005. Maximum likelihood analysis was run with the IQtree tool in the web server CIPRES (https://www.phylo.org/index.php), with 1,000 fast bootstrap repeats.

General time reversible (GTR) model, the most probable substitution model for the corrected ND4 *p*-distance matrix was calculated in PAUP 4.0.

Results

Morphology

Comparative data of specimens examined are listed in Table 1 and the holotypes are illustrated in Figures 1–4.

Table 1. Comparison of specimens of the *Gloydius strauchi* complex.

Taxa	Museum vouchers	Preserve	Localities	Sex	SVL	TTL	TL	HL	HW	HH	SL	ED	IOS	INS	V	Sc	DS	SPL (L/R)	IFL (L/R)	Reference
Gloydius lipipengi sp. nov.	IVPP OV 2720**	IVPP	Zawalong, Zayu, Tibet	M	540.6	628.2	87.6	25.2	13.2	8.2	7.4	2.9	9.6	5.4	165	46	23-21-15	7/7	10/11	This study
G. swild sp. nov.	IVPP OV 2725**	IVPP	Heishui, Aba, Sichuan	F	462.0	529.5	67.5	20.8	12.2	6.6	5.8	2.4	7.6	4.1	170	46	21-21-15	7/7	10/10	This study
	IVPP OV 2726*	IVPP	Heishui, Aba, Sichuan	F	552.0	629.1	77.1	23.8	15.7	8.4	6.2	3.2	9.6	5.0	168	43	21-21-17	7/7	10/10	This study
G. angusticeps	IVPP OV 2634**	IVPP	Xiaman, Sichuan	M	373.2	439.7	66.5	21.2	12.4	6.6	6.7	2.2	9.1	4.1	148	39	19-19-15	7/7	10/10	Shi et al. (2018)
	JS1507G5A*	SYNU	Xiaman	M	283.4	331.6	42.2	16.9	9.8	6.3	4.5	2.0	7.5	3.3	151	39	19-20-15	6/6	9/10	Shi et al. (2018)
	JS1306G1A*	SYNU	Golog, Qinghai	F	443.1	502.3	59.2	23.6	13.2	7.0	5.3	2.8	8.3	4.3	162	31	21-21-15	7/6	8/9	Shi et al. (2018)
	IOZ002317*	IOZ	Golog, Qinghai	F	457.2	459.4	72.2	22.1	11.8	7.1	—	—	8.0	4.5	157	35	19-21-15	6/6	10/10	Shi et al. (2018)
G. huangi	KIZ 027654**	KIZ	Chaya, Chamdo, Tibet,	F	532.0	455.0	67.0	23.2	14.6	—	—	3.1	8.4	4.3	174	43	21-21-15	7/7	10/10	Wang et al. (2019)
G. monticola	CIB72553	CIB	Zhongdian, Yunnan	F	274.0	308.0	34.0	18.1	9.5	6.4	—	1.5	6.9	4.7	145	30	21-21-15	6/6	9/10	Shi et al. (2017)
G. rubromaculatus	IOZ 032317**	IOZ	Yushu, Qinghai	M	473.0	554.0	81.0	24.6	15.8	7.4	7.8	3.1	8.2	4.6	158	43	21-21-15	7/8	10/11	Shi et al. (2017)
G. strauchi	SUNU1410G3△	SYNU	Kangding, Sichuan	M	407.3	482.7	75.4	21.5	13.4	7.8	—	2.8	9.3	4.4	144	45	21-21-15	7/7	10/10	Shi et al. (2017)
	CIB14356△	CIB	Kangding	M	338.5	405.0	66.3	19.4	11.8	6.2	—	2.1	7.7	4.2	151	38	21-21-16	7/7	—	Shi et al. (2017)
	CIB14357△	CIB	Kangding	M	347.2	412.4	65.2	19.9	12.1	8.7	—	2.2	7.8	3.7	146	41	21-21-15	7/7	—	Shi et al. (2017)
	SYNU1508G4	SYNU	Litang, Sichuan	M	372.3	436.4	64.1	20.3	12.7	6.5	5.9	2.1	8	4.3	148	42	21-21-15	7/7	10/10	Shi et al. (2017)
	CIB78588	CIB	Litang, Sichuan	M	427.3	504.6	77.3	24.6	15.6	8.2	—	2.7	9.9	5.3	151	40	21-21-16	7/7	10/10	Shi et al. (2017)
	CIB14358△	CIB	Kangding, Sichuan	F	384.1	438.3	54.2	22.4	12.4	7.9	—	2.4	8.4	5.6	158	35	21-21-15	7/7	—	Shi et al. (2017)
	CIB14359△	CIB	Kangding, Sichuan	F	450.3	505.5	55.2	20.9	12.4	7.2	—	1.9	7.8	6	160	33	21-21-15	7/7	—	Shi et al. (2017)

Note: **, holotype; *, paratype; △, topotype. Dimensions are measured to the nearest 0.1 mm.

Table 2. Details of the molecular samples used in this study.

Taxa	Museum voucher	Code	Locality	locus				Reference
				12s	*16s*	cytb	ND4	
Gloydius lipipengi sp. nov.	IVPP OV 2720**	G2	Zawalong, Zayu, Tibet	KY040542	KY040574	KY040628	KY040649	This study
G. swild sp. nov.	IVPP OV 2725**	GR1	Heishui, Aba, Sichuan	OK210582	OK184551	OK239647	OK239652	This study
	IVPP OV 2726*	GR2	Heishui, Aba, Sichuan	OK210583	OK184552	OK239648	OK239653	This study
G. angusticeps	JS1306G1A*	G1A	Golog, Qinghai	KY040541	KY040572	KY040627	KY040647	Shi et al. (2018)
	IVPP OV 2634**	G5C	Zoige, Sichuan	KY040545	KY040577	KY040631	KY040652	Shi et al. (2018)
G. blomhoffii	B524	B524	Japan	AY352719	AY352719	AY352751	AY352814	Malhotra (2003)
G. brevicaudus	CIB-DL70	B1	Liaoning	KY040552	KY040584	HQ528467	HQ528303	Shi et al. (2017)
G. caraganus	CR1	CR1	Kazakhstan	—	—	MF490455	MF490453	Shi et al. (2017)
	RIZ20426.1	426	Kyzylorda, Kazakhstan	MZ958021	MZ957012	MZ959165	MZ959158	This study
	RIZ29913	913	Mazandaran, Iran	MZ958022	MZ957013	MZ959166	MZ959159	This study
	NEZMUT_61	NE61	Alborz, Iran	—	—	MH378692	MH378729	Asadi et al. (2019)
G. changdaoensis	SYNUSHF01△	C1	Changdao, Shandong	KY040522	KY040554	KX063823	KX063796	Shi et al. (2017)
G. cognatus	CIB-QY224	QY224	Zoige, Sichuan	KY040529	KY040561	KY040619	KY040640	Shi et al. (2017)
	SYNU13109I3	I3	Saihan, Inner Mongolia	KY040531	KY040563	KY040621	KY040642	Shi et al. (2017)
G. shedaoensis	SYNU110D2△	D2	Lvshun, Liaoning	KY040523	KY040555	KX063819	KX063792	Shi et al. (2017)
G. halys halys	SYNU 1510151	H9	Greater Xing'an, Heilongjiang	KY040528	KY040560	KY040618	KY040639	Shi et al. (2017)
G. himalayanus	—	19.30	Himachal Pradesh, India	MZ958982	MZ958980	MZ959172	MZ959173	This study
G. huangi	R84	R84	Mangkang, Tibet	—	MZ957017	MW732035	MZ355578	This study
	KIZ 027654*	027654	Chaya, Chamdo, Tibet	MK227409	MK227412	MK227415	MK227418	Wang et al. (2019)
G. intermedius	SYNU150622**	22	Zhuanghe, Liaoning	KY040524	KY040556	KY040617	KY040638	Shi et al. (2017)
G. liupanensis	S083	S083	Ningxia	—	MK193903	MK201255	JQ687472	Xu et al. (2012)
	LP1	LP1	Guyuan, Gansu	MZ958024	MZ957015	MZ959168	MZ959161	This study
	LP4	LP4	Guyuan, Gansu	MZ958025	MZ957016	MZ959169	MZ959162	This study
	TC1	TC1	Tanchang, Gansu	MZ958023	MZ9570124	MZ959167	MZ959160	This study
G. monticola	SYNU1607DL1	DL1	Dali, Yunnan	KY040549	KY040581	KY040635	MG025935	Shi et al. (2017)
G. qinlingensis	SYNUQL1△	QLS	Xunyangba, Shanxi	KY040534	KY040566	KY040623	KY040644	Shi et al. (2017)
G. rickmersi	MHNG 2752.69	R1	Kyrgyzstan	—	—	—	KM078592	Wagner et al. (2015)
G. rubromaculatus	IOZ032317**	Y2	Qumarleb, Qinghai	KY040546	KY040578	KY040632	KY040653	Shi et al. (2017)
G. stejnegeri	SYNU1508S4△	S4	Linfen, Shanxi	KY040537	KY040569	KX063818	KX063791	Shi et al. (2017)
G. strauchi	SYNU1501G3△	G3	Kangting, Sichuan	KY040543	KY040575	KY040629	KY040650	Shi et al. (2017)
G. strauchi	SYNU1508G4	G4	Litang, Sichuan	KY040544	KY040576	KY040630	KY040651	Shi et al. (2017)
G. tsushimaensis	—	Ts1	Japan	JN870203	JN870196	JN870203	JN870211	Fenwick (2011)
G. ussuriensis	U1	U1	Heilongjiang	KP262412	KP262412	KP262412	KP262412	Xu et al. (2012)
Calloselasma rhodostoma			unknown	AY352779	AY352718	AY352813	—	Directly submitted
Deinagkistrodon acutus	—	A	Fujian	DQ343647	DQ343647	DQ343647	DQ343647	Yan et al. (2008)
Ovophis monticola	CAS_224424	—	Yunnan, China	HQ325303	HQ325117	HQ325238	HQ325176	Malhotra et al. 2011
O. zayuensis	CAS_233203	—	Tibet, China	HQ325304	HQ325118	HQ325239	HQ325177	Directly submitted
Ovophis okinavensis	—	—	Japan	AB175670	AB175670	AB175670	AB175670	Directly submitted
Protobothrops jerdonii	—	—	Guangdong, China	NC021402	NC021402	NC021402	NC021402	Directly submitted
P. mangshanensis	—	—	Hunan, China	NC026052	NC026052	NC026052	NC026052	Directly submitted
P. mucrosquamatus	—	—	Guangdong, China	NC021412	NC021412	NC021412	NC021412	Directly submitted

Taxa	Museum voucher	Code	Locality	locus				Reference
				12s	*16s*	cytb	ND4	
S. sichuanensis	SCKT2668	SCKT2668	Sichuan	KT2668	KT2668	KT2668	KT2668	Zhu et al. (2015)
Trimeresurus albolabris	—	—	Guangdong, China	NC022820	NC022820	NC022820	NC022820	Directly submitted
T. gracilis	—	A86	Taiwan, China	AY352789	AY352728	AY352823	—	Directly submitted
Viridovipera stejenegri	—	—	Taiwan, China	FJ752492	FJ752492	FJ752492	FJ752492	Directly submitted
Vipera berus	—	—	—	NC036956	NC036956	NC036956	NC036956	Directly submitted

Note: **, holotype; *, paratype; △, topotype. The data that not obtained are marked as "—".

Table 3. Partitions and their evolutionary models selected by PartitionFinder 2.1.1.

Partitions	Locus	Length (bp)	Models
Partition 1	12S	1,435	GTR+I+G
Partition 2	16S	475	GTR+I+G
Partition 3	cytb pos1, ND4 pos1	577	TVM+I+G
Partition 4	cytb pos2 and ND4 pos2	577	TVM+I+G
Partition 5	ND4 pos3 and cytb pos3	577	TIM+G

GTR: General Time-Reversible model; TVM: transversional substitution model; TIM: transitional substitution model.

Molecular phylogeny

Novel sequences were uploaded to GenBank and are available under accession numbers shown in Table 2, along with accession numbers for data obtained from GenBank. The final molecular dataset consisted of 3,065 bases containing 46 specimens. The evolutionary models assigned to each of the five partitions by PartitionFinder are shown in Table 3. The phylogeny from the Bayesian analysis (BI, Fig. 5) matches those given in earlier studies of the genus (Xu et al. 2012; Shi et al. 2017, 2018; Wang et al. 2019), except for the systematic position of the *G. qinlingensis-liupanensis* group, which do not form a monophyletic group with other members of the *G. strauchi* complex.

In this study, the topological structures of the maximum likelihood (ML) and Bayesian inference (BI) trees are generally consistent. The lineage of the new specimen from Zayu, Tibet (G2), constitutes a sister group to the clade of *G. rubromaculatus* from Sanjiangyuan, Qinghai (Y2), but is separated from it by significant branch lengths. The clade including *G. lipipengi* sp. nov. and *G. rubromaculatus* (Clade A) is sister to the clade formed by *G. huangi* and *G. monticola* (Clade B), forming a monophyletic lineage (Clade C). Clade C is sister to the monophyletic clade constituted by *G. strauchi* and *G. angusticeps* (Clade D), forming another monophyletic clade (Clade E).

The two new specimens from Heishui, Sichuan (GR1 and GR2), forming a strongly supported monophyletic group (Clade F). The clade of *G. qinlingensis* is sister to the clades of *G. liupanensis*, forming Clade G. The samples of the nine species of *G. halys-intermedius* group constitute another monophyletic group, Clade H. Clade G is sister to Clade F, forming a monophyletic Clade (Clade I) sister to the clade constituted by the new specimens from Heishui (Clade F), forming Clade J.

The phylogenetic position of *Gloydius himalayanus*, the only species of the genus to be found on the southern slopes of the Himalayan ranges, is basal to, and considerably distant from other species of *Gloydius* (13–16.1% *p*-distance for ND4, Table 4), although the genus as a whole is well supported as a monophyletic group in this analysis.

The corrected *p*-distance between the new specimen from Zayu, Tibet and *G. rubromaculatus* sequences is greater than those between other recognised species (4.4% for ND4, Table 4); the corrected *p*-distances between the new specimens from Heishui and one of its closest related congeners, *G. rubromaculatus*, are greater than those between other recognised species (8.5% for ND4, Table 4). Thus, the molecular phylogeny supports these new specimens from both Zayu and Heishui as phylogenetically independent species.

Taxonomic account

Viperidae Gray, 1825
***Gloydius* Hoge & Romano-Hoge, 1981**

***Gloydius lipipengi* Shi, Liu & Malhotra, sp. nov.**
http://zoobank.org/6DF30D06-937B-470B-AFE4-D4CABEAF7DAB

Etymology. The specific epithet of the new species from Tibet is dedicated to the senior author's Master's supervisor, Professor Pi-Peng Li (Institute of Herpetology, Shen-

Figure 1. *Gloydius lipipengi* sp. nov. (**A, B** IVPP OV 2720, holotype) and *Gloydius swild* sp. nov. (**C** IVPP OV 2725, holotype, **D** IVPP OV, 2726, paratype) in life, not to scale.

Figure 2. Holotype of *Gloydius lipipengi* sp. nov. (IVPP OV 2720) in preservative **A** dorsal view **B** ventral view.

yang Normal University) on Li's sixtieth birthday. Prof. Li has devoted himself to the study of the herpetological diversity of the Qinghai-Tibet Plateau. The senior author became an Asian pit viper enthusiast and professional herpetological researcher under his instruction. The common name of *Gloydius lipipengi* sp. nov. is suggested as "Nujiang pit viper" in English, and "Nù Jiāng Fù (怒江蝮)" in Chinese.

Type specimen. *Gloydius lipipengi* sp. nov., holotype. IVPP OV2720 (G2, Figs 1–4), adult male, collected from Muza Village, Zayu, Nyingchi Prefecture, Tibet (28.54°N, 98.23°E, 2883 m), by Jin-Cheng Liu, on 8 September 2014.

Diagnosis. The specimens of the new species, IVPP OV 2720, IVPP OV 2725 and IVPP OV 2726 were identified as the member of the genus *Gloydius* based on the small body size, bilateral pits, and divided subcaudal scales (Hoge and Romano-Hoge 1981).

Gloydius lipipengi sp. nov. differs from other congeneric species in the following characteristics: i) third supralabial scale not touching the orbit; ii) a pair of prominent black markings on the occiput; iii) black-bordered greyish cheek stripe extending from the posterior margin of orbit (not separated by the postoculars) to the ventral surface of the neck; iv) black irregular annular crossbands on the mid-body; iv) two rows of black blotches on the ventral side ; v) 23-21-15 circum-body scales; vi) 165 ventral scales; and vii) 46 subcaudal scales.

Table 5 provides a brief summary of the differences between *G. lipipengi* sp. nov., *G. swild* sp. nov. and other congeneric species.

Table 4. Corrected distance among *Gloydius* species (ND4, based on the general time-reversible [GTR] model). Values between *Gloydius lipipengi* sp. nov., *G. swild* sp. nov. and their congeners are highlighted in bold type.

		1	2	3	4	5	6	7	8	9	10	11	12	13	14	15	16	17	18	19	20	21	22
1	*G. intermedius* (22)	-																					
2	*G. shedaoensis* (D2)	0.011	-																				
3	*G. halys* (H9)	0.041	0.042	-																			
4	*G. cognatus* (I3)	0.033	0.033	0.033	-																		
5	*G. stejnegeri* (S4)	0.045	0.050	0.047	0.041	-																	
6	*G. rickmersi* (R1)	0.052	0.051	0.054	0.049	0.065	-																
7	*G. caraganus* (CR1)	0.038	0.046	0.049	0.042	0.059	0.050	-															
8	*G. changdaoensis* (C1)	0.054	0.049	0.050	0.042	0.069	0.066	0.054	-														
9	*G. qinlingensis* (QL1)	0.110	0.122	0.106	0.104	0.113	0.113	0.114	0.113	-													
10	*G. liupanensis* (LP1)	0.090	0.099	0.088	0.086	0.097	0.102	0.097	0.095	0.039	-												
11	*G. strauchi* (G3A)	0.098	0.110	0.102	0.097	0.111	0.116	0.107	0.105	0.074	0.059	-											
12	*G. angusticeps* (G5C)	0.101	0.112	0.097	0.099	0.112	0.104	0.102	0.104	0.063	0.068	0.067	-										
13	*G. monticola* (DL1)	0.120	0.130	0.122	0.112	0.137	0.134	0.135	0.120	0.076	0.078	0.079	0.076	-									
14	*G. huangi* (R86)	0.111	0.123	0.117	0.112	0.122	0.122	0.119	0.124	0.081	0.080	0.086	0.080	0.078	-								
15	*G. rubromaculatus* (Y2)	0.106	0.115	0.100	0.109	0.118	0.109	0.113	0.112	0.086	0.085	0.090	0.079	0.089	0.085	-							
16	*G. lipipengi* sp. nov. (G2)	**0.112**	**0.125**	**0.114**	**0.127**	**0.124**	**0.121**	**0.119**	**0.132**	**0.078**	**0.081**	**0.092**	**0.081**	**0.088**	**0.089**	**0.044**	-						
17	*G. swild* sp. nov. (GR1)	**0.116**	**0.125**	**0.110**	**0.108**	**0.102**	**0.123**	**0.114**	**0.119**	**0.099**	**0.085**	**0.089**	**0.086**	**0.089**	**0.103**	**0.085**	**0.097**	-					
18	*G. swild* sp. nov. (GR2)	0.116	0.125	0.110	0.108	0.102	0.123	0.114	0.119	0.099	0.085	0.089	0.086	0.089	0.103	0.085	**0.097**	**0.000**	-				
19	*G. brevicaudus* (B1)	0.143	0.152	0.135	0.145	0.155	0.150	0.145	0.156	0.117	0.113	0.124	0.121	0.122	0.138	0.124	**0.126**	**0.138**	0.138	-			
20	*G. ussuriensis* (U1)	0.106	0.116	0.131	0.115	0.133	0.133	0.119	0.123	0.119	0.109	0.110	0.102	0.122	0.105	0.110	**0.128**	**0.118**	0.118	0.107	-		
21	*G. blomhoffii* (B524)	0.132	0.144	0.148	0.142	0.157	0.147	0.135	0.144	0.119	0.110	0.117	0.110	0.112	0.119	0.116	**0.125**	**0.125**	0.125	0.117	0.068	-	
22	*G. tsushimaensis* (Ts1)	0.121	0.135	0.145	0.133	0.152	0.142	0.139	0.146	0.126	0.113	0.118	0.108	0.110	0.121	0.130	**0.138**	**0.133**	0.133	0.122	0.054	0.053	-
23	*G. himalayanus* (19.30)	0.141	0.149	0.149	0.135	0.159	0.153	0.161	0.134	0.130	0.134	0.142	0.154	0.152	0.139	0.142	**0.146**	**0.146**	0.148	0.148	0.156	0.160	0.135

Table 5. Brief morphological comparisons between *Gloydius lipipengi* sp. nov., *G. swild* sp. nov. and other congeneric species.

Species	Dorsal head	Spots on supralabials	Canthus rostralis	Background coloration	Dorsal color patterns
G. lipipengi sp. nov.	triangular	greyish brown discrete spots	inconspicuous	greyish brown	irregular large black interlaced patches
G. swild sp. nov.	triangular	greyish brown discrete spots	inconspicuous	greyish brown or blueish-grey	irregular zigzag dark brown markings
G. angusticeps	triangular	greyish brown, vaporous spots	inconspicuous	greyish brown or yellowish brown	dark brown small blotches, large patcher or stripes
G. himalayanus	triangular	one triangular spot between the third and fourth supralabial	very conspicuous	reddish brown or light grey	brown, reddish brown or dark grey small blotches or large black bordered patches
G. huangi	rounded	yellowish brown small spots	inconspicuous	light or pale greyish yellow	regular large greyish brown patches
G. liupanensis	triangular	none	conspicuous	light reddish brown or yellowish brown	similar with qinlingensis, with white stripe on the body side
G. monticola	rounded	whitish borders of the labials along the mouth line	inconspicuous	greyish brown, greenish brown or reddish brown	dark grey or dark brown blotches or zigzag stripes
G. qinlingensis	triangular	none	conspicuous	light reddish brown or yellowish brown	two columns of irregular yellowish brown or dark brown
G. rubromaculatus	rounded	irregular small black spots	inconspicuous	khaki or yellowish brown	regular large (or discrete small) scarlet or brownish yellow patches or stripes
G. strauchi	rounded	large brown between the second, third and fourth or none	inconspicuous	greenish brown, yellowish brown or nut-brown	patches, transverse crossbands or four longitudinal zigzag strips

Gloydius lipipengi sp. nov. and *G. swild* sp. nov. can be differentiated from the species in the *G. blomhoffii* complex by having three palatine teeth (versus four palatine teeth), from the *G. halys* complex by having 21 rows of mid-body dorsal scales (versus 22 or 23 rows). *Gloydius lipipengi* sp. nov. differs from other species in *G. strauchi* complex by the third supralabial scale not touching the orbit, from *G. strauchi*, *G. huangi*, and *G. rubromaculatus* by having large irregular black markings on the back (versus four irregular longitudinal stripes or discrete blotches in *G. strauchi*, complete dark brown patches in *G. huangi*, and large red crossbands in *G. rubromaculatus* (Wang et al. 2019), from *G. monticola* by having seven supralabials (versus always six supralabials) and more subcaudal scales (46 pairs versus always fewer than 30 pairs), from *G. qinlingensis* and *G. liupanensis* by its greyish brown body colour (versus yellowish-brown body colour) and lacking a lateral white line on each lateral side (versus possessing a lateral white line on each side). *Gloydius lipipengi* sp. nov. can be differentiated from *G. himalayanus* by possessing an indistinct canthus rostralis (versus very distinct canthus rostralis; Gloyd and Conant 1990).

Description of the holotype. IVPP OV 2720, adult male, a slender pit viper with a total length of 628.2 mm (SVL 540.6 mm and TL 87.6 mm), preserved in 75% ethanol with its left hemipenes partially extruded (Figs 1, 2).

The head is slender and triangular shaped in dorsal view, distinct from the neck. Canthus rostralis are not distinct. The head is 25.2 mm in length, 13.2 mm in width and 8.2 mm in depth.

Scalation. Rostral scale slightly up-turned, visible from dorsal view; nasal divided, anterior part larger; seven supralabials on both sides: second smallest, not reaching the

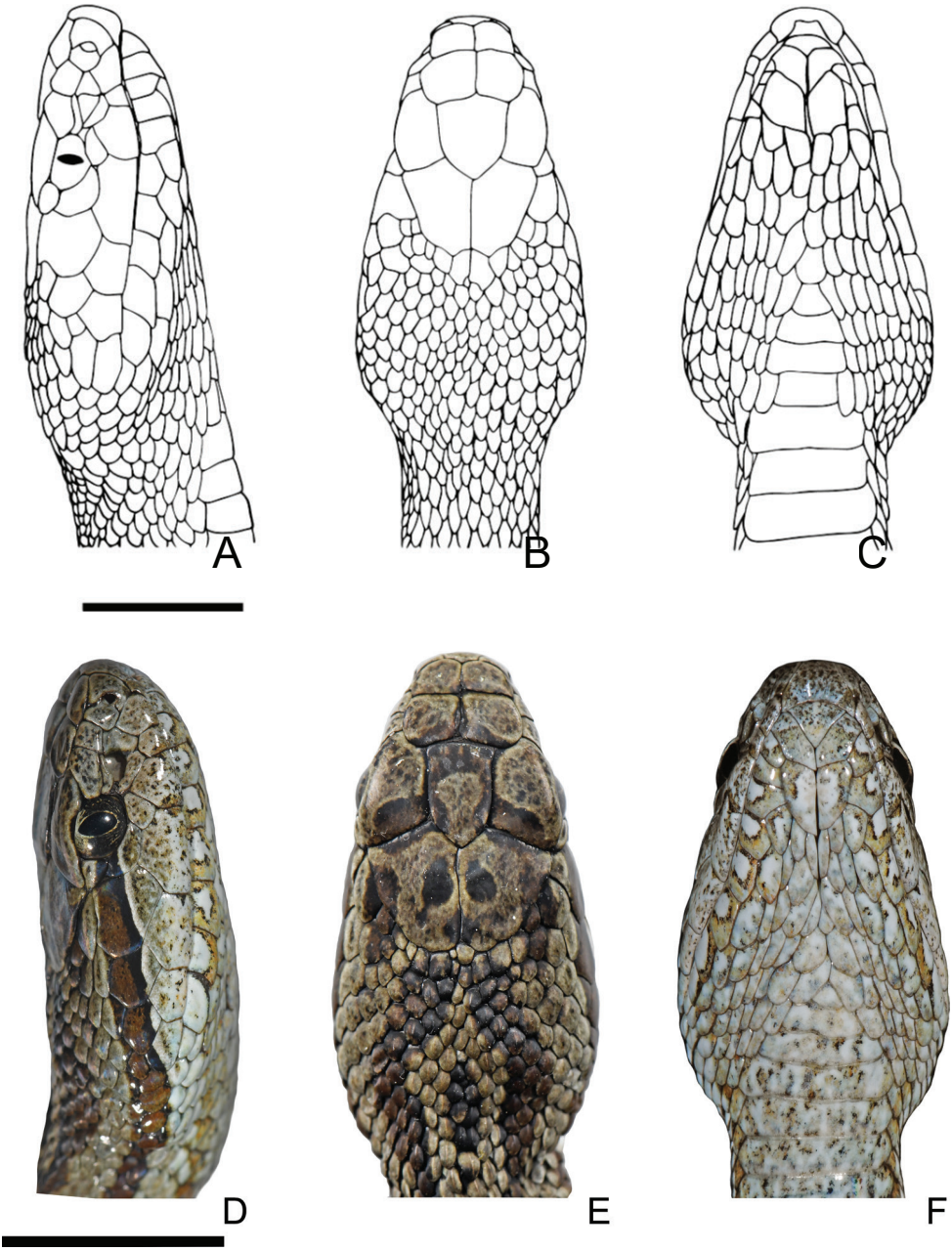

Figure 3. Head squamation of *Gloydius lipipengi* sp. nov. (Holotype, IVPP OV 2720: **A** lateral view **B** dorsal view **C** ventral view) and *G. swild* sp. nov. (Holotype, IVPP OV 2725: **D** lateral view **E** dorsal view **F** ventral view). Scale bar: 10 mm.

pit; third highest, not touching the bottom of orbit (separated by one small subocular); fourth longest, not touching the orbit; three preoculars, two postoculars, inferior one touching the top of the third supralabials, forming the bottom margin of the

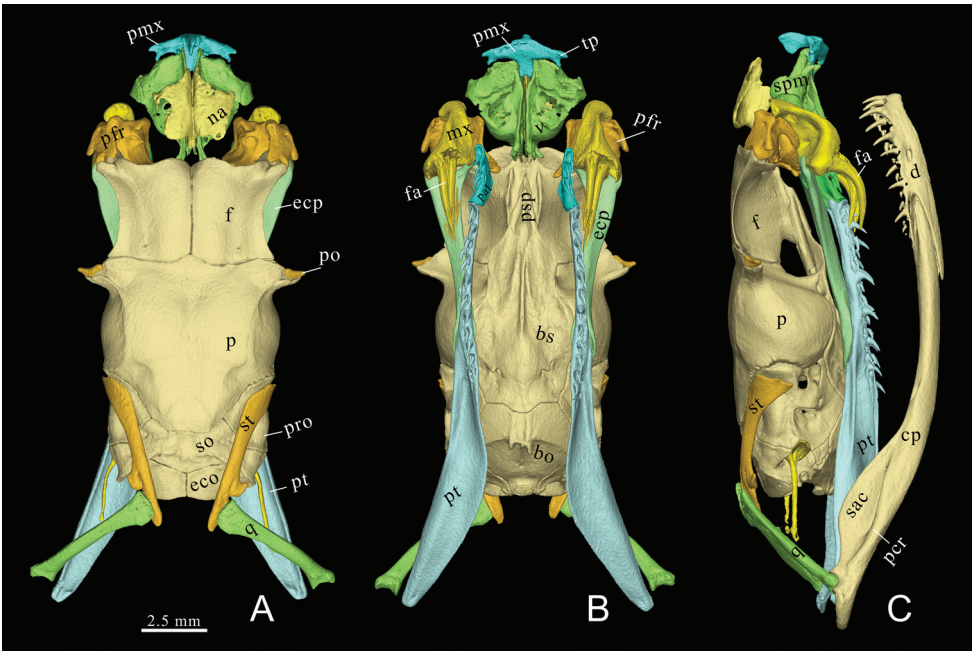

Figure 4. Color rendered three-dimensional model of *Gloydius lipipengi* sp. nov. (holotype, IVPP OV 2720) **A** dorsal view **B** palatal view, mandibles not shown **C** lateral view. Abbreviations: bo, basioccipital; bs, basisphenoid; col, columella; cp, compound bone; d, dentary; ecp, ectopterygoid; exo, exoccipital; f, frontal; na, nasal; ma, maxilla; p, parietal; pcr, prearticular crest of compound bone; pfr, prefrontal; pmx, premaxilla; po, postorbital; pp, palatine process of maxilla; pro, prootic; psp, parasphenoid rostrum; pt, pterygoid; sac, surangular crest of compound bone; spm; septomaxilla; so, supraoccipital; sp, splenial; st, supratemporal; v, vomer. Conducted by Ye-Mao Hou and Jingsong Shi.

orbit; two rows of temporals (2+4); infralabials 10 on left side while 11 on right, first pair in contact behind the mental; second, third and fourth pairs meet on the chin shield; chin shield is rhomboidal in shape, the posterior chin shield comprises two pairs of scales, forming the mental groove (Fig. 3A–C).

Dorsal scales in 23-21-15 rows (reducing from 19 to 18 posteriorly at ventral 94–96), keeled except for the first scale row bordering the ventral scales; ventral scales 165 (excluding four preventral scales); anal plate single; subcaudals 46, in pairs

Coloration. Eye dark brown on the upper half while black on the bottom half, pupil black, vertical with light yellow margins; postorbital stripe wide, greyish brown and black bordered on the lower edge, extending from the posterior orbit to the ventral surface of the neck; supralabials and infralabials greyish brown, scattered with very small irregularly sized black blotches. One black triangular mark on the anterodorsal head, covering the caudomedial part of prefrontals. One bold black M-shaped mark on the dorsomedial head, covering the caudal part of lateral frontals, the lateral part of parietals, merged with the postorbital stripe at the largest temporal scale (but not covering the upper postorbital). The upper postorbital white while the top part of the bottom postorbital is black (covered by the postorbital stripe).

The body coloration is dark greyish brown, with two rows of irregular black annular crossbands on the mid-body, each covering 20 or more scales, separated by a gap of two row scale vertically, extending laterally to one or two dorsal scales from the ventrals. Ventral scales light grey, with two large black blotches on each side, clustered into two ventral stripes. The tip of tail is similar to the main body in coloration (Figs 1, 2).

Skull. The description of the skull of *G. lipipengi* sp. nov. is based on the 3D-reconstructed model of the holotype.

Snout. The premaxilla has bifurcated transverse process on each side. The anterior margin of the premaxilla is blunt. The dorsal tip of the ascending process of premaxilla is triangular in lateral view, not reaching the anterior tip of nasals. The horizontal laminae of the nasals are scutiform in dorsal view. The septomaxillae have prominent dorsolateral processes, nearly meeting the horizontal laminae of the nasals.

Braincase. The parietal is roughly T-shaped in dorsal view. The anterolateral part of the parietal bulges prominently laterally while the dorsoposterior part tapers medially. The postorbital processes of the parietal are prominent. The frontals are squared. The lateral margin of frontals concaved obviously on each side, forming the dorsal edge of orbit. The prefrontal has an elongate blunt lateral process, posterolaterally pointed. The lacrimal foramen perforates the medial lamina of the prefrontal. The prefrontal-frontal join surface is waved in dorsal view.

The postorbital is relatively small and cashew-shaped, the top of the postorbital does not reach the posterolateral end of frontal. The basisphenoid is spearhead in shape, narrow anteriorly and expanded laterally. The supraoccipital is longitudinally compressed, occupies almost two thirds the total width of the otic region.

Palatomaxillary apparatus. The fang is relatively short and curved, roughly the same length of the maxilla, one third the length of ectopterygoid, attached with seven or eight replacement fangs on each side. The palatine bears three teeth. The ectopterygoid is flat and widened at the anterior part. The pterygoid is slender, the dentigerous process of pterygoid is straight, bearing 12/11 teeth (left/right), occupies almost half the total width of the pterygoid, the posterior portion of pterygoid is medially expanded.

Suspensorium and mandible. The supratemporal is slender, has a lateral process, anterolaterally pointed, lies in front of the supratemporal-quadrate articulation. The quadrate is straight, slender, and enlarged on both ends. The mandible is slender and moderately curved. The prearticular crest of the compound bone is prominent while the surangular crest is slightly concaved. The dental bone bears 11/12 teeth (left/right); the dentary teeth are perpendicular to the dentary bone, decreasing in size at the third tooth. The posterior tip of ventral process of dentary extends farther posteriorly than the dorsal process.

Dentition. Palatine: 3/3, pterygoid: 12/11, dentary: 11/12.

Hemipenes. The hemipenes of *G. lipipengi* sp. nov. are generally similar to those of *G. rubromaculatus* and *G. huangi* but differ by the possession of longer and stronger spines, seven or eight subcaudals in length, and forked for two subcaudals. Small and stubby spines range from the basal to the distal side of the organ, without any conspicuously enlarged spines (versus 3–5 enlarged spines on the base in the *G. halys* complex; Gloyd 1990). The spines gradually increase in length distally.

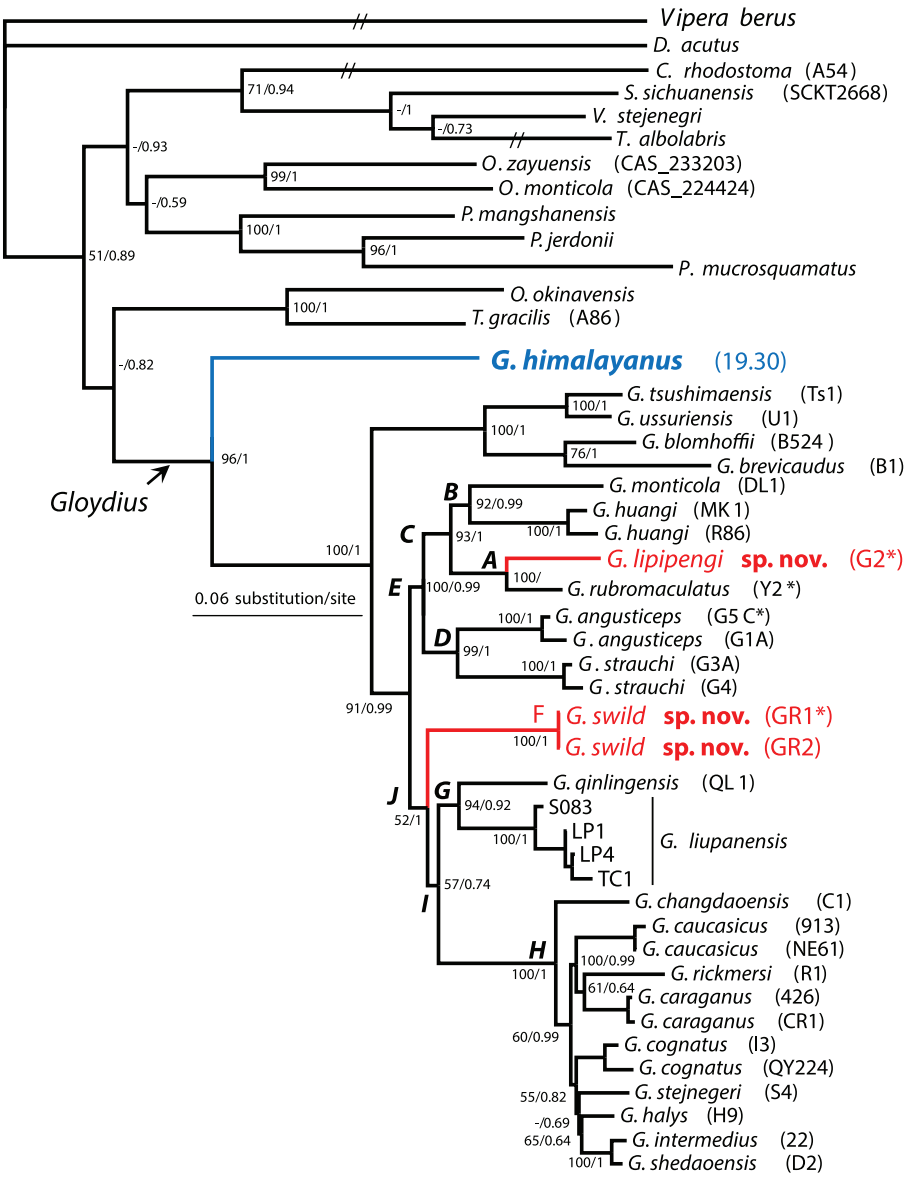

Figure 5. Bayesian inferenced tree of the genus *Gloydius*, along with some relative genus of the family Viperidae, based on 12S, 16S, ND4, and cytb sequences, with the maximum likelihood bootstrap supports (left, regular) and Bayesian posterior probabilities (right, italic) displayed on the nodes (those <50% are displayed as "-"). Holotypes are marked with asterisks.

Distribution and ecology. At present, *Gloydius lipipengi* sp. nov. has only been reported from the type locality, Muza village, Zayu, Tibet, China (Fig. 6). The specimen was collected at 09:00 h on leaf litter in forest near the hot, dry valley on the lower reaches of the Nujiang River (Fig. 7). *Gloydius lipipengi* sp. nov. accepted pink mice in captivity.

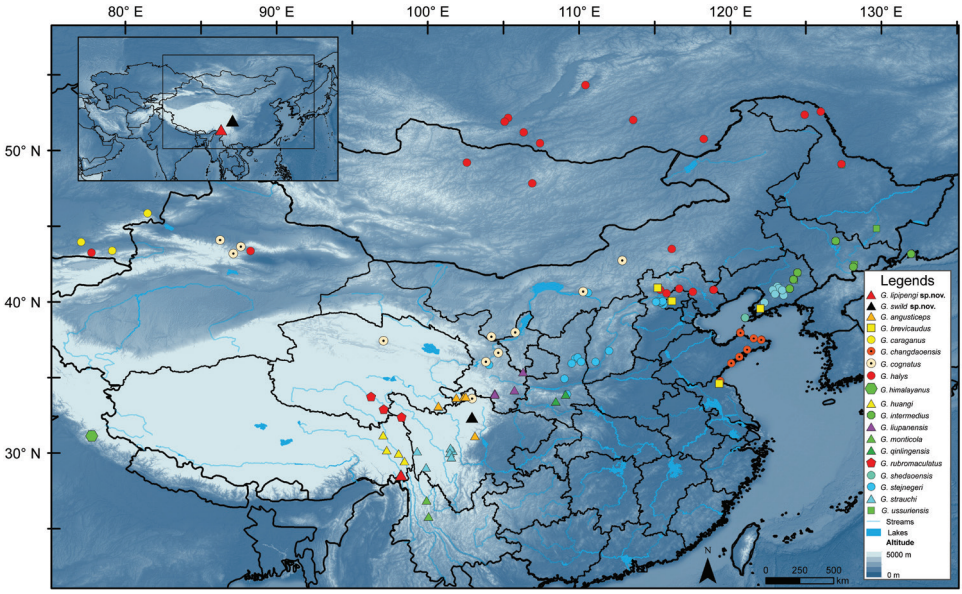

Figure 6. Type localities of *Gloydius lipipengi* sp. nov. (red triangles) and *G. swild* sp. nov. (black triangles), with the collection localities of some other congeneric species.

Gloydius swild Shi & Malhotra, sp. nov.

http://zoobank.org/77260121-7761-4D37-AC87-3FE77EEA378C

Etymology. The new species from Heishui, Sichuan is named after the SWILD Group (Southwest Wild, http://www.swild.cn/), who discovered the new species and collected the first species during an expedition to the Dagu Holy-glacier, Heishui, Sichuan. The common name of *G. swild* sp. nov. is suggested as "Glacier pit viper" in English, and "Bīng Chuān Fù (冰川蝮)" in Chinese.

Type series. *Gloydius swild* sp. nov, ***holotype***, IVPP OV2725 (G2, Figs 1, 3), adult female, collected from Heishui, Aba, Sichuan (32.23°N, 102.80°E, 2940 m), on 23 July, 2017, by the senior author; ***paratype***, IVPP OV 2726, adult female, the same locality as the holotype, collected by Jia-Wei Wu (chief executive officer of SWILD Group).

Diagnosis. *Gloydius swild* sp. nov. differs from other congeneric species in the following characteristics: i) the narrower postorbital stripe, ii) a pair of round spots on the parietal scales; iii) the absence of the black spots on the lateral body; iv) 21 rows of mid-body dorsal scales; v) a pair of arched stripes on the occiput; vi) 168–170 ventral scales, and vii) 43–46 subcaudal scales.

Morphologically, *Gloydius swild* sp. nov. is quite similar to *G. angusticeps*, but differs by the narrower, straight bordered brown postorbital stripe (versus wider postorbital stripe with dentate lower border in *G. angusticeps*). *G. swild* sp. nov. differs from *G. strauchi*, *G. huangi*, and *G. rubromaculatus* by the narrow triangular head from dorsal view (versus spoon-shaped head in above-mentioned species), from *G. monticola* by having seven supralabials (versus always six supralabials) and more subcaudal scales

Figure 7. The habitat of *Gloydius lipipengi* sp. nov. (**A** Muza Village, Zaty, Tibet, type locality of *G. lipipengi* sp. nov. **B** the landscape of the Nujiang River, 15 km from the type locality) and *Gloydius swild* sp. nov. (**C** Heishui, Sichuan) **A** and **B** Photographs by Jin-Cheng Liu.

(43–46 pairs versus always fewer than 30 pairs of subcaudal scales), from *G. qinlingensis* and *G. liupanensis* by its dark greyish brown background dorsal color (versus yellowish-brown body colour) and lacking a lateral white line on each side (versus possessing a lateral white line on each side), from *G. himalayanus* by possessing an indistinct canthus rostralis (versus very distinct canthus rostralis; Gloyd and Conant 1990).

Description of the holotype. *Gloydius swild* sp. nov., IVPP OV 2725, adult female, a slender pit viper with a total length of 529.5 mm (SVL 462 mm and TL 67.5 mm), preserved in 75% ethanol (Fig. 1).

The head is slender and narrow triangular shaped in dorsal view, distinct from the neck. Canthus rostralis not distinct. The head is 20.8 mm in length, 12.2 mm in width and 6.6 mm in depth.

Scalation. Rostral scale slightly up-turned, visible from dorsal view; nasal divided, anterior part larger; seven supralabials on both sides: second smallest, not reaching the pit; third highest, not touching the bottom of orbit on the left (separated by one small subocular) while touching the bottom of the orbit on the right; fourth longest, not touching the orbit; three preoculars, two postoculars, inferior one touching the top of the third supralabials, forming the bottom margin of the orbit; two rows of temporals: 3+5/2+4 (L/R); infralabials 10, first pair in contact behind the mental; second, third and fourth pairs meet on the chin shield; chin shield is rhomboidal in shape, the posterior chin shield comprises two pairs of scales, forming the mental groove (Fig. 3D–F). Dorsal scales in 21-21-15 rows, keeled except for the first scale row bordering the ventral scales; ventral scales 170 (excluding four preventral scales); anal plate single; subcaudals 46, in pairs.

Coloration. *Gloydius swild* sp. nov., eye light greyish brown on the upper half while black on the bottom half, pupil black, vertical with light yellow margins; postorbital stripe relatively narrow, only half the width of the anterior temporals, greyish brown and white bordered on the lower edge, extending from the posterior orbit to the lateral surface of the neck; supralabials and infralabials greyish white, scattered with large irregularly sized, black blotches, rendering the lateral head granitoid. One black Ω-shaped mark on the anterodorsal head, covering the posteromedial part of prefrontals, the anterior and lateral part of the frontals and the anterior part of the parietals. The infralabials are bordered with yellow on the lower edge.

The body coloration is dark blueish-grey, with two rows of irregular black X-shaped or C-shaped crossbands on the mid-body, each covering about 10 dorsal scales (or more), separated by a gap of one or two dorsal scales vertically, sometimes in contact with the adjacent ones forming zigzag stripes, but hardly merged on the medial dorsal line, extending laterally to one or two dorsal scales from the ventrals. Ventral scales light grey, scattered with dense irregular black blotches, rendering the ventral scales granitoid. The tip of tail is bony, similar to the main body in coloration on both ventral and dorsal sides (Figs 1C, D, 3D–F).

Infraspecific morphological variation. Despite the inconspicuous variation in the coloration among the type series of *G. swild* sp. nov., the scalations vary considerably between the two specimens. The range of the temporal scales of the holotype (IVPP OV 2725) is 3+5 on the left side but 2+4 on the right side, while in the paratype (IVPP OV 2726), the temporal scales are displayed as 2+4 on both sides. Ventrals range from 168–170 in females (n = 2), while range from 43–46 in females (n = 3, including one shed skin from the wild). Total length ranges from 529.5–629.1 in adult females. The infralabials of the paratype lack the greyish-yellow margins seen in the holotype.

Distribution and ecology. *Gloydius swild* sp. nov. has been found in east part of Qinghai-Tibet plateau and Hengduanshan mountains, Heishui country, north Sichuan, about 15 km away from Dagu Holy-glacier National Geological Park, from along the route of Red Army's long march (from June to August, 1935). They were found on or under the rocks (especially near the vegetations) on sunny slopes (Figs 6, 7C).

Viviparous reproduction. One adult female (Holotype) was collected when pregnant, gave birth to eight neonates (including a couple of conjoined twins) on September 20th, 2017 in captivity. The weight of the normal neonates ranged between 3.00–3.45 g (3.01, 3.22, 3.22, 3.23, 3.28, 3.45, average = 3.235, n = 6). The weight of the conjoined twins was 2.86 g (weighed after the first shedding).

Discussion

This study reveals the phylogenetic position of *G. himalayanus* within *Gloydius* for the first time. This study also reports two new *Gloydius* species, increasing the number of the recognized species in *Gloydius* to 23. The discovery of the new species has further verified the hypothesis that the Himalayan-Tibetan Plateau and Southwest Mountain Ranges should be considered as differentiation centres of Asian pit vipers. Furthermore, the discovery of *G. swild* sp. nov. suggests that the glaciers might be considered as key factors to the isolation and speciation of the alpine pit vipers in the southwest China.

Lastly, the systematic and taxonomic relationship of *G. qinlingensis* and *G. liupanensis* is still controversial. Despite their morphological similarities, these clades have not consistently formed a monophyletic group in earlier studies (Xu et al. 2012; Shi et al. 2017; Wang et al. 2019). In a subsequent study, which included more mitochondrial genes (specifically 16s rRNA) in the analysis (Li et al. 2020), *G. qinlingensis* and *G. liupanensis* formed a separate monophyletic lineage (Clade G) that is sister to the *G. halys* complex. The systematic position of the *G. qinlingensis-liupanensis* group that have been reconstructed in this study is consistent with Li et al. (2020).

In our analysis, the enigmatic clade formed by *Ovophis okinavensis* and *Trimeresurus gracilis* (Clade F) is basal to the genus *Gloydius*. As highlighted by Malhotra and Thorpe (2000), Tu et al. (2000), and numerous analyses since (Castoe and Parkinson 2006; Pyron et al. 2013; Alencar et al. 2016), the systematic status of these two species requires resolution.

As the squamation and body coloration variation is quite conservative within pit vipers (Gloyd and Conant 1990; Shi et al. 2017, 2018), it is necessary to obtain more specimens of the new species to investigate intraspecific variation in the new species. These data will be very helpful in verifying the stability of the diagnostic morphological characteristics of *G. lipipengi* sp. nov. Further fieldwork and molecular phylogenetics, particularly using nuclear genes, are still needed to investigate the origin, evolution, and migration of Asian pit vipers on the Qinghai-Tibet Plateau.

Acknowledgements

The Forest Department of Himachal Pradesh, India supplied permission to sample (permit no. FFE-FB-F (10)-3/2017). We are sincerely grateful to Li Ding, Ke Jiang, Shengchao Shi, Shuo Qi, Zhong-Yi Yao, Sheng-Bo Zhou, Zi-Long Liu, Shen-Mao Li, Xian-Chun Qiu and Fu Shu for providing tissue samples and photographs for this study. JSS thanks Pi-Peng Li for the professional advice. We would also like to extend our thanks to Wolfgang Wüster, Stuart Graham, Anatoli Togridou, Molla Talhauddin Ahmed, Nilanjan Mukherjee, Richard Southworth, Jasmine Torrez, Sankha Suvra Nandy, Shyamal Kumar Ghosh, Anweshan Patra, Jia-Wei Wu, Zoimador, Yong Lan Xu-yu Yang and Jiang-hong Ran for volunteering their help during fieldwork in Himachal Pradesh.

We thank the reviewers, Eskandar Rastegar Pouyani and Jesse Grismer, and subject editor Robert Jadin for their contributions, which have improved the manuscript.

This study was supported by the Second Tibetan Plateau Scientific Expedition and Research Program (grant no. 2019QZKK0705 to Tao Deng), the second National Survey of Terrestrial Wildlife Resources in Tibet of China and Independent Research and Development Project of National Forestry and Grassland Administration (grant no. 2020LC-3-04 to Ke-Ji Guo), the European Union Seventh Framework Programme (grant no. PIRSES-GA-2013-612131 to the BITES consortium led by AM) and the Rufford Foundation (grant no. 25313-1 to VS).

References

Alencar LRV, Quental TB, Grazziotin FG, Alfaro ML, Martins M, Venzon M, Zaher H (2016) Diversification in vipers: phylogenetic relationships, time of divergence and shifts in speciation rates. Molecular Phylogenetics & Evolution 105: 50–62. https://doi.org/10.1016/j.ympev.2016.07.029

Arevalo E, Davis SK, Sites JW (1994) Mitochondrial DNA sequence divergence and phylogenetic relationships among eight chromosome races of the *Sceloporus grammicus* complex (Phrynosomatidae) in central Mexico. Systematic Biology 43: 387–418. https://doi.org/10.1093/sysbio/43.3.387

Asadi A, Montgelard C, Nazarizadeh M, Moghaddasi A, Fatemizadeh F, Simonov E, Kami HG, Kaboli M (2019) Evolutionary history and postglacial colonization of an Asian pit viper (*Gloydius halys caucasicus*) into Transcaucasia revealed by phylogenetic and phylogeographic analyses. Scientific reports 9(1): 1–16. https://doi.org/10.1038/s41598-018-37558-8

Burbrink FT, Lawson R, Slowinski JB (2000) Mitochondrial DNA phylogeography of the polytypic North American rat snake (*Elaphe obsoleta*): a critique of the subspecies concept. Evolution 54: 2107–2118. https://doi.org/10.1111/j.0014-3820.2000.tb01253.x

Castoe TA, Parkinson CL (2006) Bayesian mixed models and the phylogeny of pitvipers (Viperidae: Serpentes). Molecular Phylogenetics & Evolution 39: 91–110. https://doi.org/10.1016/j.ympev.2005.12.014

Eskandar R, Pouyani H, Oraie A, Khosravani A, Akbari A (2018) Phylogenetic position of Iranian pitvipers (Viperidae, Crotalinae, *Gloydius*) inferred from mitochondrial cytochrome b sequences. Tropical Zoology 31: 55–67. https://doi.org/10.1080/03946975.2018.1442288

Gloyd HK (1990) Snakes of the Agkistrodon Complex: A Monographic Review. Society for the Study of Amphibians and Reptiles, USA, 614 pp. https://doi.org/10.5358/hsj1972.14.1_23

Knight A, Mindell DP (1993) Substitution bias, weighting of DNA sequence evolution, and the phylogenetic position of Fea's viper. Systematic Biology 42: 18–31. https://doi.org/10.1093/sysbio/42.1.18

Lanfear R, Calcott B, Ho SY, Guindon S (2012) PartitionFinder: combined selection of partitioning schemes and substitution models for phylogenetic analyses. Molecular Biology and Evolution 29: 1695–1701. https://doi.org/10.1093/molbev/mss020

Malhotra A, Dawson K, Guo P, Thorpe RS (2011) Phylogenetic structure and species boundaries in the mountain pitviper *Ovophis monticola* (Serpentes: Viperidae: Crotalinae) in Asia. Molecular Phylogenetics & Evolution 59(2): 444–457. https://doi.org/10.1016/j.ympev.2011.02.010

Malhotra A, Thorpe RS (2000) A phylogeny of the Trimeresurus group of pit-vipers: new evidence from a mitochondrial gene tree. Molecular Phylogenetics & Evolution 16: 199–211. https://doi.org/10.1006/mpev.2000.0779

Orlov NL, Barabanov AV (1999) Analysis of nomenclature, classification, and distribution of the Agkistrodon halys–Agkistrodon intermedius complexes: a critical review. Russian Journal of Herpetology 6: 167–192.

Orlov NL, Barabanov AV (1999) About type localities for some species of the genus Gloydius Hoge et Romano-Hoge, 1981 (Crotalinae: Viperidae: Serpentes). Russian Journal of Herpetology 7: 159–160.

Palumbi S, Martin A, Romano S, McMillan W, Stice L, Grabowski G (1991) The simple fool's guide to PCR, version 2.0. University of Hawaii, Honolulu, 45 pp.

Pyron RA, Burbrink FT, Wiens JJ (2013) A phylogeny and revised classification of Squamata, including 4161 species of lizards and snakes. BMC Evolutional Biology 13: e93. https://doi.org/10.1186/1471-2148-13-93

Shi J, Yang D, Zhang W, Qi S, Ding L, Li P (2016) Distribution and intraspecies taxonomy of *Gloydius halys-Gloydius intermedius* Complex in China (Serpentes: Crotalinae). Chinese Journal of Zoology 51(5): 777–798. https://doi.org/10.13859/j.cjz.201605008

Shi J, Wang G, Chen X, Fang Y, Ding L, Hou M, Liu J, Li P (2017) A new moth-preying alpine pit viper species from Qinghai-Tibetan Plateau (Viperidae, Crotalinae). Amphibia-Reptilia 38: 517–532. https://doi.org/10.1163/15685381-00003134

Shi J, Yang D, Zhang W, Peng L, Orlov NL, Jiang F, Ding L, Hou M, Huang X, Huang S (2018) A new species of the Gloydius strauchi complex (Crotalinae: Viperidae: Serpentes) from Qinghai, Sichuan, and Gansu, China. Russian Journal of Herpetology 25: 126–138. https://doi.org/10.30906/1026-2296-2019-25-2-126-138

Swofford DL (2001) PAUP: Phylogenetic Analysis Using Parsimony (and other methods) 4.0 b8. Sinauer, Sunderland.

Tamura K, Stecher G, Peterson D, Filipski A, Kumar S (2013) MEGA6: molecular evolutionary genetics analysis version 6.0. Molecular Biology and Evolution 30: 2725–2729. https://doi.org/10.1093/molbev/mst197

Tu CM, Wang HY, Tsai MP, Toda M, Lee WJ, Zhang FJ, Ota H (2000) Phylogeny, taxonomy, and biogeography of the Oriental Pitvipers of the Genus *Trimeresurus* (Reptilia: Viperidae: Crotalinae): A molecular perspective. Zoological Science 17(8): 1147–1157. https://doi.org/10.2108/zsj.17.1147

Wang K, Ren J, Dong W, Jiang K, Shi J, Siler CD, Che J (2019) A New Species of Plateau Pit Viper (Reptilia: Serpentes: *Gloydius*) from the Upper Lancang (= Mekong) Valley in the Hengduan Mountain Region, Tibet, China. Journal of Herpetology 53(3): 224–236. https://doi.org/10.1670/18-126

Xu Y, Liu Q, Myers EA, Wang L, Huang S, He Y, Peng P, Guo P (2012) Molecular phylogeny of the genus *Gloydius* (Serpentes: Crotalinae). Asian Herpetological Research 3: 127–132. https://doi.org/10.3724/SP.J.1245.2012.00127

Zhao E (2006) Snakes of China. Anhui: Hefei: Anhui Science and Technology Publishing House.

Zhao E, Zhong Y, Huang M (1998) Fauna sinica. Reptilia. Science Press, Beijing.

ZooKeys 1061: 109–130 (2021)
doi: 10.3897/zookeys.1061.71212
https://zookeys.pensoft.net

RESEARCH ARTICLE

A peer-reviewed open-access journal
ZooKeys
Launched to accelerate biodiversity research

Feather mites (Acariformes, Astigmata) from marine birds of the Barton Peninsula (King George Island, Antarctica), with descriptions of two new species

Yeong-Deok Han[1,2], Sergey V. Mironov[3], Jeong-Hoon Kim[4], Gi-Sik Min[1]

1 *Department of Biological Sciences, Inha University, Incheon 22212, Republic of Korea* **2** *Restoration Assessment Team, Research Center for Endangered Species, National Institute of Ecology, Gowol-gil 23, Yeongyang-gun, 36531, Republic of Korea* **3** *Zoological Institute, Russian Academy of Sciences, Universitetskaya embankment 1, Saint-Petersburg, 199034, Russia* **4** *Korea Polar Research Institute, Yeonsu-gu, Incheon 21990, Republic of Korea*

Corresponding authors: Jeong-Hoon Kim (jhkim94@kopri.re.kr), Gi-Sik Min (mingisik@inha.ac.kr)

Academic editor: Vladimir Pesic | Received 7 July 2021 | Accepted 18 August 2021 | Published 4 October 2021

http://zoobank.org/5239C960-59FE-4C04-B8BF-1D8FC33B4C75

Citation: Han Y-D, Mironov SV, Kim J-H, Min G-S (2021) Feather mites (Acariformes, Astigmata) from marine birds of the Barton Peninsula (King George Island, Antarctica), with descriptions of two new species. ZooKeys 1061: 109–130. https://doi.org/10.3897/zookeys.1061.71212

Abstract

We report on the first investigation of feather mites associated with birds living on the Barton Peninsula (King George Island, Antarctica). We found seven feather mite species of the superfamily Analgoidea from four host species. Two new species are described from two charadriiform hosts: *Alloptes* (*Sternalloptes*) *antarcticus* **sp. nov.** (Alloptidae) from *Stercorarius maccormicki* Saunders (Stercorariidae), and *Ingrassia chionis* **sp. nov.** (Xolalgidae) from *Chionis albus* (Gmelin) (Chionidae). Additionally, we provide partial sequences of the mitochondrial cytochrome c oxidase subunit I (COI), which was utilized as a DNA barcode, for all seven feather mite species.

Keywords

Alloptes, Analgoidea, Antarctica, feather mites, *Ingrassia*, systematics

Introduction

Feather mites (Astigmata, Analgoidea and Pterolichoidea) are a vast group of highly specialized parasites or mutualistic ectosymbionts that spend their entire life cycle on their bird hosts (Gaud and Atyeo 1996; Dabert and Mironov 1999; Proctor 2003). Most of

these mites occupy various microhabitats in the plumage of birds; however, representatives of a few families are parasites located on the skin and in the respiratory tract of their avian hosts. Owing to their specialization to particular microhabitats on birds and dispersal mainly by a direct contact of host individuals, feather mites usually show a high level of host-specificity (Mironov and Dabert 1999; Proctor and Owens 2000; Dabert 2005).

Antarctica is the fifth largest and most isolated continent on our planet (Peck 2018; Sancho et al. 2019). On this 14 million km^2 continent, less than 0.35% of the territory remains seasonally free of ice and snow (Bockheim 2015). Many endemic species inhabit these ice-free terrestrial areas, where birds and marine mammals breed in the coastal zones (Chown and Convey 2007; Hughes 2010). Approximately 400 species of birds have been recorded from the Antarctic continent and oceanic waters north to approximately 40°S (Shirihai 2007). Vanstreels et al. (2020) recently summarized data on the biodiversity of ectoparasites associated with Antarctic and Subantarctic birds and reported 30 feather mite species from 28 bird species in this region.

King George Island is the largest of the South Shetland Islands at the northwest tip of the Antarctic Peninsula (Potapowicz et al. 2020). This island has six areas designated as the Antarctic Specially Protected Areas (ASPA), one of which is ASPA No. 171, located on the southeast coast of the Barton Peninsula. Approximately 5,000 pairs of two penguin species, *Pygoscelis antarcticus* (Forster) and *P. papua* (Forster), breed in ASPA No. 171, and 14 other bird species have been observed on the Barton Peninsula: *Chionis albus* (Gmelin), *Larus dominicanus* Lichtenstein, *Stercorarius antarcticus* (Lesson), *S. maccormicki* Saunders, *Sterna paradisaea* Pontoppidan, and *St. vittata* Gmelin (Charadriiformes), *Leucocarbo bransfieldensis* (Murphy) (Pelecaniformes), *Daption capense* (Linnaeus), *Fregetta tropica* (Gould), *Fulmarus glacialoides* (Smith), *Macronectes giganteus* (Gmelin), *Oceanites oceanicus* (Kuhl) (Procellariiformes), *Eudyptes chrysolophus* (Brandt), *Pygoscelis adeliae* (Hombron & Jacquinot) (Sphenisciformes) (Kim et al. 2005, 2014).

To date, no studies have been conducted on feather mites associated with birds living on the Barton Peninsula. In the present work, we report seven analgoid feather mites, including descriptions of two new species from the genera *Alloptes* and *Ingrassia*, found on four bird species on the Barton Peninsula of King George Island. Additionally, we provide DNA barcodes for the mitochondrial cytochrome c oxidase subunit I (COI) from these seven analgoid feather mite species.

Materials and methods

Material sampling

Mite samples were obtained from the Antarctic Shag (*L. bransfieldensis*), South Polar Skua (*S. maccormicki*), Wilson's Storm Petrel (*O. oceanicus*), and three Snowy Sheatbills (*Ch. albus*) in the Barton Peninsula. The birds were captured using a hand net or loop according to 'SKUAS Manual for Fieldworkers' (PBEG 2003), and all birds were re-

leased after collecting the mites. Feather mites were collected using 3M ScotchMagicTape (3M, St. Paul, Minnesota, USA) from the wing, down, and tail feathers, and then immediately preserved in 70% ethanol for 3 h. The preserved samples were separated from Scotch tape under a dissecting microscope with a dissecting needle and then preserved in 95% ethanol. The collected mite specimens were cleared in 10% lactic acid for 24 h at room temperature and then mounted on microscope slides using PVA mounting medium (BioQuip, Rancho Dominguez, California, USA).

Descriptions of two new species are given according to standard formats used for the corresponding feather mite taxa (Mironov and Palma 2006; Mironov and Proctor 2008; Stefan et al. 2013; Hernandes et al. 2017). Terminology, idiosomal, and leg chaetotaxy follow Gaud and Atyeo (1996), with minor corrections for the coxal chaetotaxy by Norton (1998). All measurements are in micrometers (μm). All examined specimens are deposited at the National Institute of Biological Resources (NIBR), Korea. The classification and scientific names of birds follow Gill et al. (2021).

DNA sequencing

Before preparing the microscopic slides, genomic DNA was extracted from one leg of each specimen using a Tissue DNA Purification Kit (Cosmogenetech Inc., Seoul, Korea) according to the manufacturer's instructions. The COI barcode fragment was amplified using two universal primers: bcdF05 (5'-TTTTCTACHAAYCATAAAGATATTGC-3') and bcdR04 (5'- TATAAACYTCDGGATGNCCAAAAAA-3') under the following conditions: 2 min at 94 °C; 40 cycles at 98 °C for 15 s, 50 °C for 30 s, and 68 °C for 60 s; and a final extension at 68 °C for 5 min (Dabert et al. 2008). The amplified products were sequenced using an ABI3100 automated sequencer (Perkin Elmer, Foster City, California, USA). Sequence assembly, alignment, and trimming were performed using Geneious 8.1.9 software (Kearse et al. 2012). We obtained a 654 bp fragment sequence of the COI gene from two individuals per mite species.

Systematic account

Superfamily Analgoidea Trouessart & Mégnin, 1884
Family Alloptidae Gaud, 1957

Genus *Alloptes* Canestrini, 1879

Notes. *Alloptes* is one of the most specious genera of the family Alloptidae and currently includes about 50 described species (Gaud 1972; Vasyukova and Mironov 1991; Kivganov and Mironov 1992; Mironov and Palma 2006). All representatives of this genus are associated with birds of the order Charadriiformes, with exception of a questionable host association of *Alloptes tubinarii* Dubinin, 1949 reported from several procellariiform hosts (Dubinin 1949). Gaud (1972) subdivided the genus into

the three subgenera, *Alloptes* s. str., *Apodalloptes* Gaud, 1972, and *Conuralloptes* Gaud, 1972. Further, nearly a half of species of the subgenus *Conuralloptes* was arranged into a fourth subgenus, *Sternalloptes* Mironov, 1992 (in Kivganov and Mironov 1992). Three *Alloptes* species found on marine birds of the Barton Peninsular belong to three different dubgenera. Below we provide descimination features for these subgenera.

Subgenus *Alloptes* Canestrini, 1879

Notes. The subgenus *Alloptes* s. str. currently includes three species and is characterized by the following features (Gaud 1952, 1972; Mironov 1996): in both sexes, seta *mG* of genu II is spiculiform; in males, the opisthosoma is roughly shaped as an equilateral triangle with terminal part strongly enlarged, setae *h3* are present, setae *ps2* are well developed (half as long as *f2*); in females, the opisthosoma is rounded, the opisthosomal lobes are not developed, idiosomal setae *ps1* and *f2* are present. Representatives of the subgenus are known from birds of the families Scolopacidae and Chionidae (Gaud 1952, 1957, 1972; Vasyukova and Mironov 1991). Five *Alloptes* species described by Dubinin (1952) from auks (Alcidae) could also belong to this subgenus, because these mites have filiform genual setae *mG*II and females have the opisthosoma rounded or with strongly abbreviated lobes, but all these species need re-investigation.

Alloptes (*Alloptes*) *aschizurus* Gaud, 1952

Alloptes aschizurus Gaud, 1952: 163–164, fig. 2; Atyeo and Peterson 1967: 98; 1970: 129.
Alloptes (*Alloptes*) *aschizurus*: Gaud 1972: 59.

Material examined. 3 males and 3 females (NIBR No. NIBRIV0000887146–NIBRIV0000887151) from *Chionis albus* (Gmelin) (Charadriiformes, Chionidae), Antarctica, King George Island, Barton Peninsula, 62°14'16"S, 58°46'13"W, 8 January 2016, coll. Han Y.-D.

Remarks. *Alloptes* (*Alloptes*) *aschizurus* was initially described from specimens collected from the Black-faced Sheathbill, *Chionis minor* (Hartlaub) on Kerguelen Island (Gaud 1952). Later, this mite species was found on the same host on Heard Island and on the Snowy Sheathbill, *Ch. albus*, on Greenwich Island and Gaston Islands (Atyeo and Peterson 1967). As for all members of the subgenus *Alloptes* s. str., this mite species is characterized by the following features: in both sexes, genual setae *mG*II are spiculiform; in males, the opisthosoma is shaped as an equilateral triangle with a strongly enlarged posterior end; in females, the posterior end of the opisthosoma is rounded, and the opisthosomal lobes are not developed (Gaud 1972; Vasyukova and Mironov 1991; Mironov and Hernandes 2020). *Alloptes* (*A.*) *aschizurus* is distinguished from the closest species of the subgenus, *A.* (*A.*) *tringae* (Grube, 1859) [widely known under the

junior synonym *A.* (*A.*) *crassipes* (Canestrini, 1878)] in having the following features. In both sexes, the length of the idiosoma is approximately 500 long (vs approximately 450 in *A. tringae*), and trochanteral setae *sR*III are equal to or slightly longer than the trochanters III (vs distinctly shorter than the trochanters) (Gaud 1952; Atyeo and Peterson 1967; Vasyukova and Mironov 1991; Mironov and Hernandes 2020).

Molecular data. The COI sequences were obtained from two individuals and deposited in GenBank with accession numbers MZ489637 and MZ489638.

Subgenus *Conuralloptes* Gaud, 1972

Notes. The subgenus *Conurlloptes* currently includes 23 species and is characterized by the following features (Gaud 1972; Vasyukova and Mironov 1991): in both sexes, seta *mG* of genu II is short spine-like with widely rounded apex; in males, the opisthosoma is triangular, gradually narrowed posteriorly and without posterior enlargement, idiosomal setae *h3* are absent, setae *ps2* are strongly reduced (barely distinct); in females, opisthosoma with well-developed opisthosomal lobes, setae *ps1* and *f2* are present. This subgenus is known from birds of the families Chionidae, Pedionomidae, Recurvirostridae, and Scolopacidae in the order Charadriiformes (Gaud 1972; Vasyukova and Mironov 1991; Mironov and Palma 2006).

Alloptes (*Conuralloptes*) *chionis* Atyeo & Peterson, 1967

Alloptes chionis Atyeo & Person, 1967: 98, figs 1–4; 1970: 129–130, figs 15–17.
Alloptes (*Conuralloptes*) *chionis*: Mironov 2007: 619.

Material examined. 3 males and 3 females (NIBR No. NIBRIV0000887152–NIBRIV0000887157) from *Chionis albus* (Gmelin) (Charadriiformes, Chionidae), Antarctica, King George Island, Barton Peninsula, 62°14'3"S, 58°46'56"W, 13 January 2016, coll. Han Y.-D.

Remarks. *Alloptes* (*Conuralloptes*) *chionis* was described from specimens collected from *Ch. minor* (type host) on Heard Island and was also found on *Ch. albus* from the Gaston Islands (Atyeo and Person 1967). When this mite was described, the genus *Alloptes* had not yet been subdivided into subgenera. Gaud (1972) established three subgenera in this genus but did not consider the taxonomic position of this species. Mironov (2007) placed this mite in the subgenus *Conuralloptes* based on the following characters: in both sexes, genual setae *mG*II are shaped as short and thick spines with bluntly rounded apices; in males, the opisthosoma is not enlarged apically, and idiosomal setae *h3* are absent; in females, the idiosomal setae *ps1* and *f2* are present. The males of *A.* (*C.*) *chionis* can be distinguished from other species of the subgenus *Conuralloptes* by the following combination of features: the anterior margin of the hysteronotal shield is slightly convex, the pregenital sclerites are free from each other and

almost parallel, the adanal shields are C-shaped, and macrosetae *h2* are flattened and slightly widened in the medial part (Atyeo and Peterson 1967, 1970).

Molecular data. The COI sequences were obtained from two individuals and deposited in GenBank with accession numbers MZ489639 and MZ489640.

Subgenus *Sternalloptes* Mironov, 1992

Notes. The subgenus *Sternalloptes* includes about 20 species and is characterized by the following features (Kivganov and Mironov 1992; Mironov 1996): in both sexes, seta *mG* of genu II is shortspine-like with widely rounded apex; in males, the opisthosoma is triangular, gradually narrowed posteriorly and with noticeable terminal enlargement, idiosomal setae *h3* are present or absent, setae *ps2* are strongly reduced; in females, the opisthosoma with well-developed opisthosomal lobes, idiosomal setae *ps1* and *f2* are absent. Common hosts of the subgenus *Sternalloptes* are birds of the families Laridae and Stercorariidae in the order Charadriiformes (Gaud 1976; Vasyukova and Mironov 1991; Kivganov and Mironov 1992; Mironov and Kivganov 1993).

Alloptes (*Sternalloptes*) *antarcticus* sp. nov.

http://zoobank.org/5C7680DD-1773-4EE8-B7C5-D99285367323

Type material. Male holotype (NIBR No. NIBRIV0000887158), 3 males and 4 females paratypes (NIBR No. NIBRIV0000887159–NIBRIV0000887164) from *Stercorarius maccormicki* Saunders (Charadriiformes, Stercorariidae), Antarctica, King George Island, Barton Peninsula, 62°14'2"S, 58°46'20"W, 2 January 2016, coll. Han Y.-D.

Description. Male (Figs 1, 3A–E, 4A, B; holotype, range for 3 paratypes in parentheses): idiosoma, length × width, 370 (340–365) × 200 (175–205). Length of hysterosoma 228 (213–243). Prodorsal shield (Figs 1A, 4A): length 80 (78–80), width at posterior margin 114 (102–118), posterolateral corners truncate, posterior margin slightly concave. External scapular setae *se* situated on posterolateral extensions of prodorsal shield near their anterior margins. Hysteronotal shield: greatest length 255 (235–258), width at anterior margin 100 (98–108), anterior margin slightly concave, lateral margins without incisions at bases of setae *d2* and fused ventrally with bases of epimerites IV. Length between prodorsal and hysteronotal shields along midline 31 (18–22). Dorsal setae *c2* 32 (33–36) long, shorter than trochanters III (Fig. 4C). Subhumeral setae *c3* narrowly lanceolate, 23 (19–23) × 2 (3). Posterior part of opisthosoma gradually expanded at posterior end, width at level of setae *h2* 50 (46–53). Length of interlobar septum 82 (80–86). Terminal lamella with three pairs of festoons; incision between inner pair narrow slit-like or inner festoons slightly overlapping. Setae *h3* present, setae *ps2* distinct. Setae *h2* cylindrical, not expanded in medial part. Dorsal measurements: *se*:*se* 118 (96–106), *c2*:*d2* 55 (50–57), *d2*:*ps1* 165 (158–168). Bases of trochanters I, II flanked by narrow sclerotized bands connecting bases of correspond-

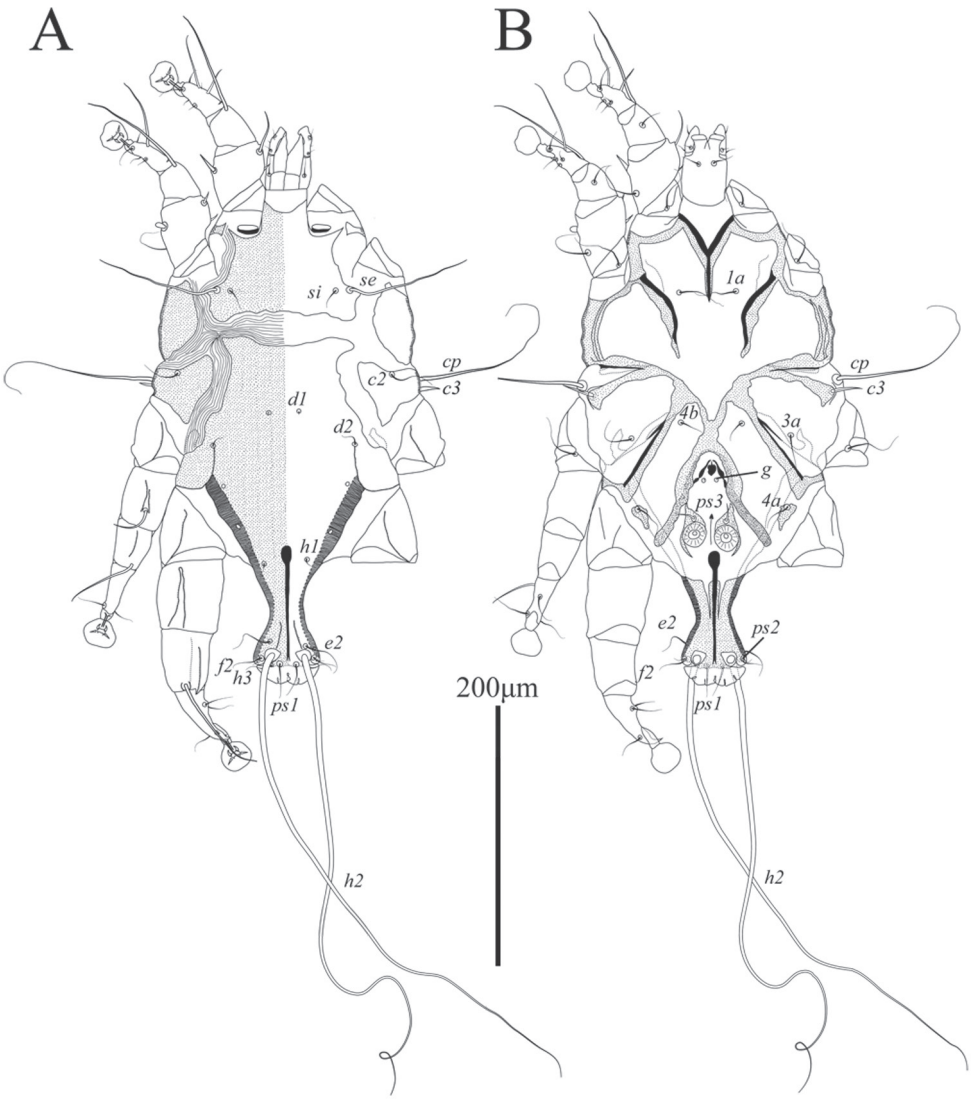

Figure 1. *Alloptes* (*Sternalloptes*) *antarcticus* sp. nov., male **A** dorsal view **B** ventral view.

ing epimerites (Fig. 1B). Pregenital sclerites fused as a Y, their anterior ends connected to inner ends of epimerites IIIa, posterior end fused with paragenital arch. Coxal fields III and IV closed. Length of genital-anal field 163 (158–168). Genital arch: 17 (15–17) × 20 (19–20). Coxal setae *4b* situated anterior to level of setae *3a*. Setae *4a* surrounded by sclerites of irregular form. Ventral measurements: *3a*:*4b* 10 (9–13), *4b*:*g* 45 (43–43), *4b*:*4a* 63 (60–65), *g*:*ps3* 30 (31–35), *ps3*:*ps1* 110 (109–117), *4a*:*4a* 120 (110–112). Setae *mG* of genua I thin spine-like with acute apex, setae *mG*II shaped as thick spine with bluntly rounded apex. Legs IV 203 (193–203) long. Distal margin of

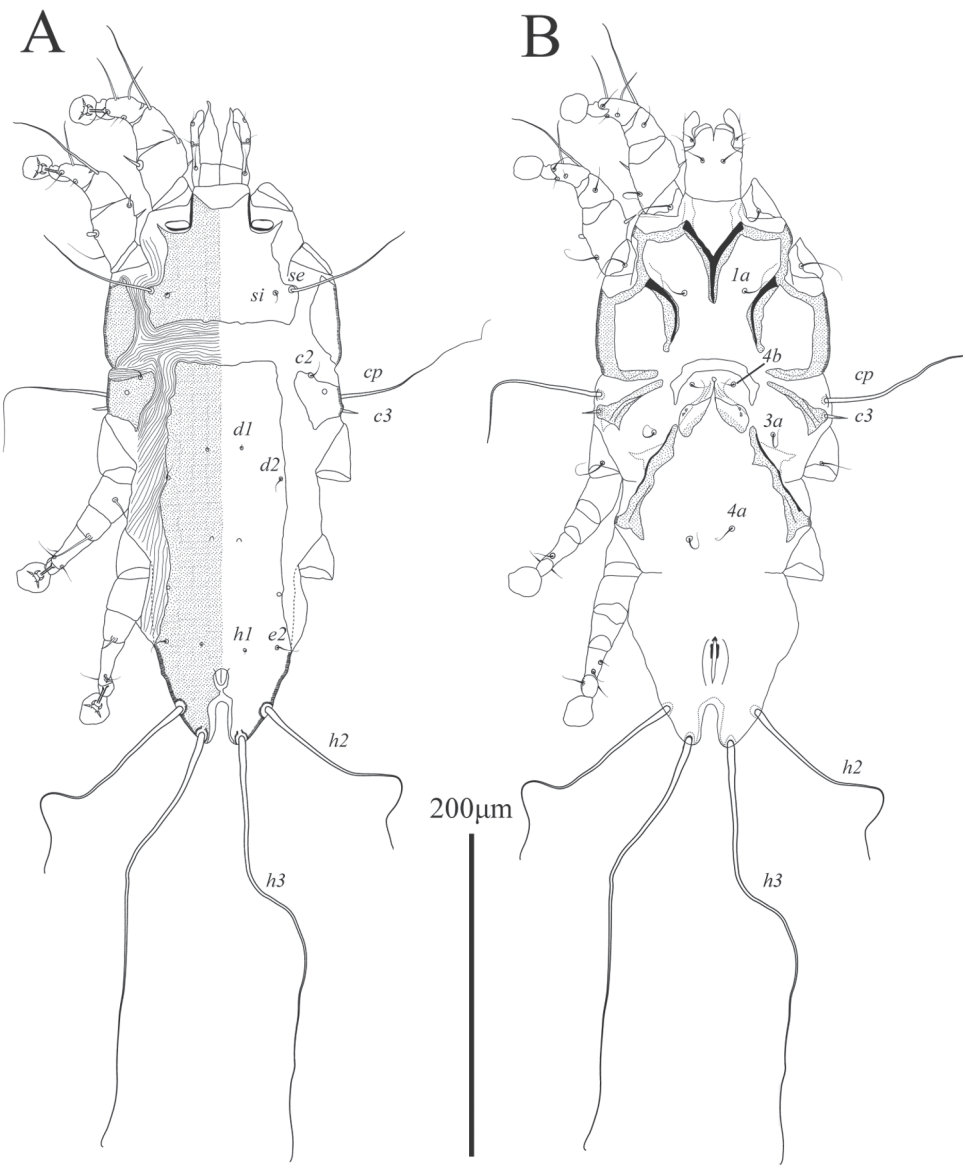

Figure 2. *Alloptes* (*Sternalloptes*) *antarcticus* sp. nov., female **A** dorsal view **B** ventral view.

tibia IV with small spine. Tarsus IV 54 (49–55) long, with claw-like apex; setae *d* and *e* small spine-like, seta *e* situated near tarsal apex, seta *d* at level of seta *f*, setae *r* and *w* in basal one-third of the segment (Fig. 3A–C).

Female (Figs 2, 4F, G, 4C; range for 4 paratypes): idiosoma, length × width, 350–360 × 148–153 (Fig. 2A). Hysterosoma 238–250 long. Prodorsal shield: shaped as in male, 80–83 × 85–90. Setae *c2* 10–14 long, shorter than trochanters III. Setae *c3* lan-

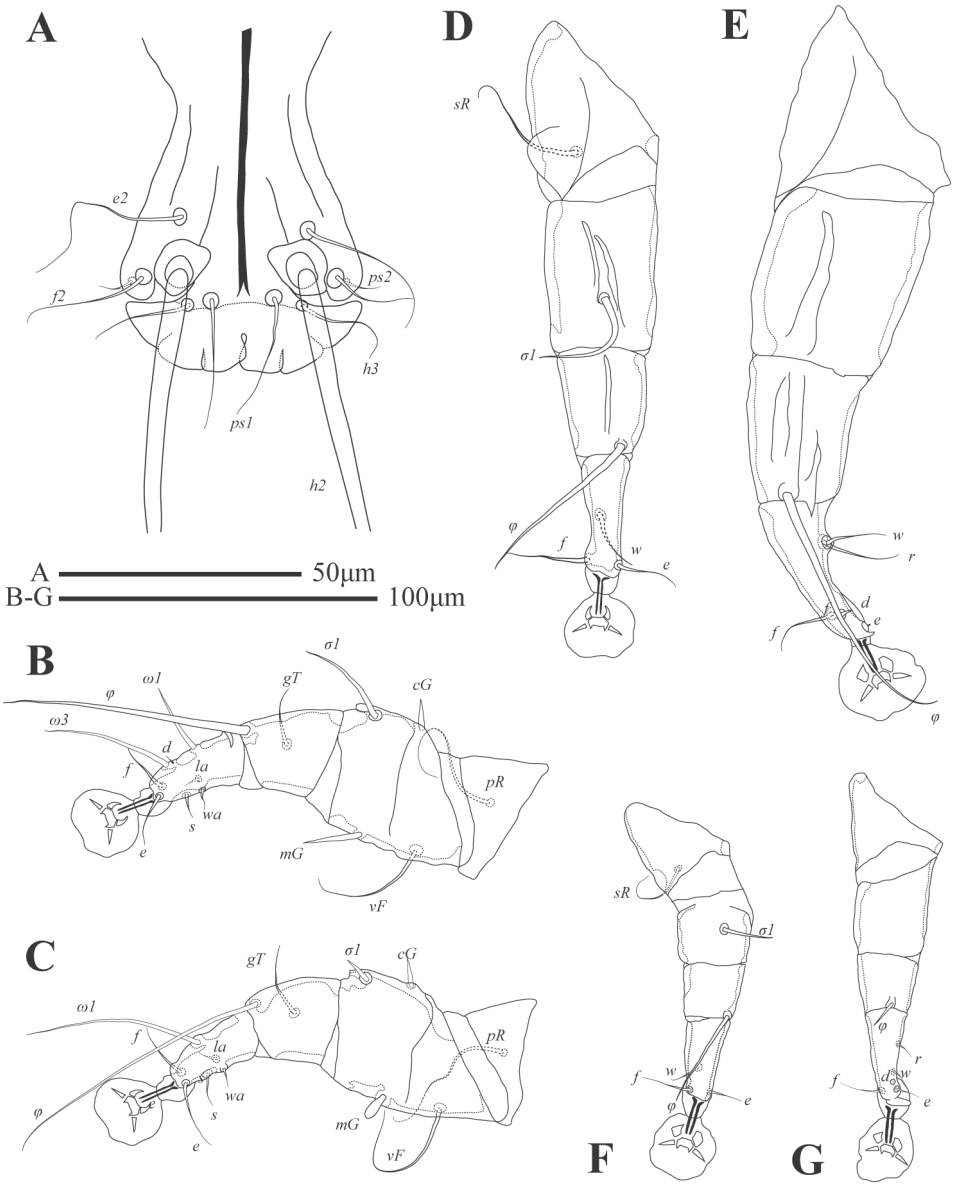

Figure 3. *Alloptes* (*Sternalloptes*) *antarcticus* sp. nov., details **A** opisthosoma of male, dorsal view **B** leg I of male **C** leg II of male **D** leg III of male **E** leg IV of male **F** leg III of female **G** leg IV of female.

ceolate, 13–15 × 2–3. Hysteronotal shield: 233–238 × 60–62, anterior margin straight or slightly concave, surface without ornamentation. Setae *h1* and *e2* situated at same transverse level. Setae *f2* and *ps1* absent. Distance between prodorsal and hysteronotal shields along midline 23–33. Supranal concavity ovate, opened posteriorly, delimited from terminal cleft by short extensions. Opisthosomal lobes well developed, approxi-

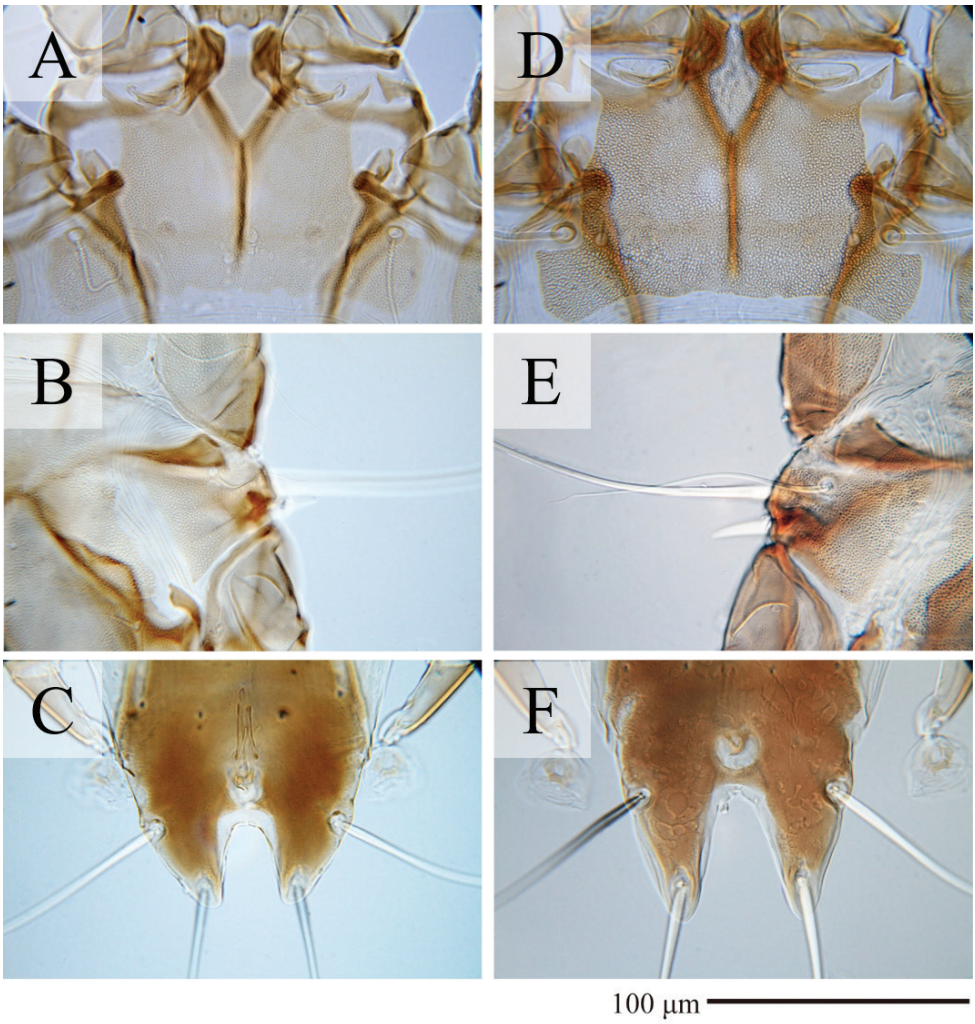

Figure 4. *Alloptes* species **A–C** *Alloptes* (*Sternalloptes*) *antarcticus* sp. nov. **D–F** *A.* (*S.*) *catharacti* **A, D** prodorsal shield of males **B, E** humeral shield of males **C, F** opisthosomal lobes of females.

mately as long as wide at base, terminal cleft as an inverted U, 24–30 long, 12–20 wide (Fig. 4C). Anterior end of supranal concavity extending slightly beyond level of setae *h2*. Dorsal measurements: *se*:*se* 83–89, *c2*:*d2* 64–67, *d2*:*e2* 104–106, *e2*:*h2* 39–43, *h2*:*h3* 19–20, *h2*:*h2* 55–60, *h3*:*h3* 25–31. Bases of trochanters I, II flanked by narrow sclerotized bands connecting bases of corresponding epimerites (Fig. 2B). Epimerites IVa barely distinct. Epigynum bow-shaped, 24–27 × 55–59. Legs IV with ambulacral discs reaching level of insertions of setae *h2* (Figs 2, 3F, G).

Differential diagnosis. Among 18 previously known species in the subgenus *Sternalloptes* (Kivganov and Mironov 1992; Mironov and Kivganov 1993; Kivganov 1996; Hernandes et al. 2017), the new species *Alloptes* (*S.*) *antarcticus* sp. nov. is

most similar to *A.* (*S.*) *catharacti* Mironov, 1991 found on the same host, *S. maccormicki* from Mirny station (Queen Mary Land, Antarctica), in having setae *c3* lanceolate and short (shorter that trochanters III), the pregenital sclerite fused into a Y connecting the tips of epimerites IIIa and the apex of the paragenital arch, and setae *h2* not expanded (Mironov 1991). *Alloptes* (*S.*) *antarcticus* sp. nov. differs from *A.* (*S.*) *catharacti* in having the following characteristics: in both sexes, the external scapular setae *se* are situated on the posterolateral extensions of the prodorsal shield; in males, the dorsal setae *c2* (32–36) are approximately 1.5 times longer than setae *c3* (19–23) and shorter than trochanters III (Fig. 4A, B); in females, the terminal cleft is shorter (24–30 long), and the supranal concavity is open posteriorly into the terminal cleft (Fig. 4C). In both sexes of *A.* (*S.*) *catharacti*, setae *se* are situated on the soft tegument near the anterior margin of the posterolateral extensions of the prodorsal shield; in males, the dorsal setae *c2* (63–93) are 2–3 times longer than setae *c3* (24–29) and exceed the length of trochanters III (Fig. 4D, E); in females, the terminal cleft is longer (38–48), and the supranal concavity is separated from the terminal cleft (Mironov 1991) (Fig. 4F).

Remark. The comparative material of *A.* (*S.*) *catharacti* used here to illustrate morphological differences was collected from the same host species, *S. maccormicki*, at Jangbogo station, Terra Nova Bay, Antarctica, in 2016, by Ji-Yong Lee.

Molecular data. The COI sequences were obtained from two individuals and deposited in GenBank with accession numbers MZ489641 and MZ489642.

Etymology. The specific name refers to the geographical range of the type host.

Family Avenzoariidae Oudemans, 1905
Subfamily Bonnetellinae Atyeo & Gaud, 1981
Genus *Scutomegninia* Dubinin, 1951
Subgenus *Scutomegninia* Dubinin, 1951

***Scutomegninia* (*Scutomegninia*) *subantarctica* Mironov, 2000**

Scutomegninia phalacrocoracis: Atyeo & Peterson 1967: 100, figs 5–8; 1970: 150, figs 68–70.
Scutomegninia subantarctica Mironov, 1990: 53, nom. nudum.
Scutomegninia (*Scutomegninia*) *subantarctica*: Mironov 2000: 14–18, fig. 5.

Material examined. 1 male and 3 females (NIBR No. NIBRIV0000887165–NIBRIV0000887168) from *Leucocarbo bransfieldensis* (Murphy) (Suliformes, Phalacrocoracidae), Antarctica, King George Island, Barton Peninsula, 62°14'4"S, 58°46'52"W), 8 January 2016, coll. Han Y.-D.

Remarks. Mites of the genus *Scutomegninia*, collected from the Imperial Shag, *Leucocarbo atriceps* (King) (= *Phalacrocorax atriceps*) in Maipo Island (Buls Bay on Brabant Island, Palmer Archipelago, Antarctica) by Atyeo and Peterson (1967), were originally identified as *S. phalacrocoracis* (Dubinin and Dubinina, 1940). Furthermore,

Atyeo and Peterson (1970) reported *S.* (*S.*) *phalacrocoracis* from *Leucocarbo georgianus* (Lönnberg) (= *P. atriceps georgianus*) from Bird Island, South Georgia. Later, Mironov (1990, 2000) described specimens from the Palmer Archipelago as a separate species, *S.* (*S.*) *subantarctica*. According to the present taxonomic view, *Phalacrocorax atriceps* belongs to the genus *Leucocarbo* and is split into several separate species restricted to particular areas of the Antarctic and subantarctic regions (Gill et al. 2021). Taking into consideration this concept, *S.* (*S.*) *subantarctica* reported by previous researchers (Atyeo and Peterson 1967, 1970) were collected from the Antarctic Shag, *L. bransfieldensis* (Antarctic Peninsula and Palmer Archipelago), and the South Georgia Shag, *L. georgianus* (South Georgia).

Scutomegninia (*S.*) *subantarctic*a belongs to the *phalacrocoracis* group (species associated with Phalacrocoracidae and Anhingidae), and it is most similar to *S.* (*S.*) *pygmaea* Mironov, 1990. It differs from *S.* (*S.*) *pygmaea* and other species of the *phalacrocoracis* group by the following combination of characters in males: the terminal ends of the interlobar membrane have a small spine-like process; the lateral adanal shields have acute posterior ends, while the medial adanal shields have the posterior ends bluntly rounded; the anteromedial ends of adanal apodemes are rounded; setae *s* of tarsus III are spine-like, strongly attenuate apically, and bear two small denticles; the terminal cleft is 1.8–2 times longer than wide; and the incision in the interlobar membrane extends to the level of setae *h2* (Mironov 1990, 2000).

Molecular data. The COI sequences were obtained from two individuals and deposited in GenBank with accession numbers MZ489643 and MZ489644.

Genus *Zachvatkinia* Dubinin, 1949

Zachvatkinia hydrobatidii Dubinin, 1949

Zachvatkinia hydrobatidii Dubinin, 1949: 219, figs 9b, 10b; 1952, 256; Atyeo and Peterson 1967: 101, figs 9–12; 1970: 146, figs 61–63; Mironov 1989: 110–115, figs 5, 7, 8.

Material examined. 3 males and 3 females (NIBR No. NIBRIV0000887169–NIBRIV0000887174) from *Oceanites oceanicus* (Kuhl) (Procellariiformes, Oceanitidae), Antarctica, King George Island, Barton Peninsula, 62°14'15'S, 58°46'28"W, 9 January 2016, coll. Han Y.-D.

Remarks. *Zachvatkinia hydrobatidii* was described by Dubinin (1949) based on specimens collected from the Wilson's Storm Petrel, *O. oceanicus* in Massachusetts (USA), and also from 10 other storm petrels of the genera *Fregetta*, *Garrodia*, *Pelagodroma* (Oceanitidae), and *Oceanodroma* (Hydrobatidae) from various parts of the world. Mironov (1989) re-examined most of this material and referred to this mite species only the specimens from the oceanitids *O. oceanicus* and *F. tropica*. In Antarctica, *Z. hydrobatidii* was previously reported from *O. oceanicus*, *F. tropica*, and *Pagodroma nivea* (Forster) (Procellariidae) (Atyeo and Peterson 1967, 1970). The record

from the procellariid host seems to be questionable. *Zachvatkinia hydrobatidii* is very close to *Z. oceanodromae* Mironov, 1989 associated with storm petrels of the genus *Oceanodroma,* and differs in having the following features: in males, the genital arch is shaped as a completely closed ring, and the distance between setae *ps1* and *h3* is less than 40; in females, the posterior margin of the opisthosoma between the terminal extensions is not sclerotized, and setae *e1* are situated on the inner margins of the lateral hysteronotal shields (Mironov 1989).

Molecular data. The COI sequences were obtained from two individuals and deposited in GenBank with accession numbers MZ489645 and MZ489646.

Zachvatkinia stercorarii Dubinin, 1952

Zachvatkinia stercorarii Dubinin, 1949: 227, fig. 12, nom. nudum, 1952: 255, figs 1, 2; Atyeo and Peterson 1967: 103, 1970: 147; Mironov 1989: 100–111, figs 3, 7, 8.

Material examined. 3 males and 3 females (NIBR No. NIBRIV0000887175–NIBRIV0000887180) from *Stercorarius maccormicki* Saunders (Charadriiformes, Stercorariidae), Antarctica, King George Island, King Sejong station, Barton Peninsula, 62°14'2"S, 58°46'20"W, 21 January 2016, coll. Han Y.-D.

Remarks. *Zachvatkinia stercorarii* was described by Dubinin (1952) based on specimens collected from three species of skuas or jaegers, *Stercorarius pomarinus* (Temminck) (type host), *S. parasiticus* (Linnaeus), and *S. longicaudus* Vieillot, from Wrangel Island, Russia. Furthermore, it was shown that mites from *S. parasiticus* and *S. longicaudus* belong to a separate species, *Z. isolata* Mironov, 1989 (Mironov 1989; Dabert et al. 2015). In Antarctica, *Z. stercorarii* was previously reported from *S. antarcticus* (Lesson) from Adelaide Island and the Palmer Archipelago and from *S. maccormicki* from Cape Hallett, Haswell Islands, Ross Island, and Victoria Land (Atyeo and Peterson 1967, 1970).

Although *Z. stercorarii* and *Z. isolata* are associated with birds in the order Charadriiformes, these mite species belong to the *puffini* species group, which is characterized by a single dorsobasal spine on tarsus IV in males and setae *d1* situated off the lateral hysteronotal shields in females (Mironov 1989). All remaining species of the *puffini* group are associated with Procellariiformes, while other representatives of the genus *Zachvatkinia* associated with Charadriiformes belong to the *sternae* species group. It was hypothesized that the common ancestors of *Z. stercorarii* and *Z. isolata* were probably transferred from some procellariiform hosts to the ancestor of the family Stercorariidae (Dabert and Mironov 1999).

Zachvatkinia stercorarii can be clearly distinguished from *Z. isolata* in having the following features: in males, the bases of genital setae *g* are adjacent (vs distant from each other); in females, the posterior margin of the prodorsal shield is just slightly convex (vs strongly convex), and the lateral margins of this shield have small incisions posterior to the bases of setae *se* (vs smooth and without incisions) (Mironov 1989).

Molecular data. The COI sequences were obtained from two individuals and deposited in GenBank with accession numbers MZ489647 and MZ489648.

Family Xolalgidae Dubinin, 1953
Subfamily Ingrassiinae Gaud & Atyeo, 1981

Genus *Ingrassia* Oudemans, 1905

Notes. The genus *Ingrassia* is the most specious genus within the subfamily Ingrassiinae, including 28 species up to now (Gaud 1972; Vasyukova and Mironov 1991; Mironov and Proctor 2008; Stefan et al. 2013). Representatives of the genus have been recorded on hosts from six orders of aquatic birds: Anseriformes, Charadriiformes, Pelecaniformes, Podicipediformes, Procellariiformes, and Sphenisciformes. Identification keys to species of *Ingrassia* are available only for those associated with birds in the order Charadriiformes in Africa (Gaud 1972) and northern Eurasia (Vasyukova and Mironov 1991). To date, only six species of the genus *Ingrassia* have been recorded from procellariiform birds (Stefan et al. 2013).

***Ingrassia chionis* sp. nov.**
http://zoobank.org/D6242043-BF80-4B66-B6AB-41CB5B073134

Type material. Male holotype (NIBR No. NIBRIV0000887181), 2 males and 3 females paratypes (NIBR No. NIBRIV0000887182–NIBRIV0000887186) from *Chionis albus* (Gmelin) (Charadriiformes, Chionidae), Antarctica, King George Island, Barton Peninsula, 62°14'13"S, 58°46'33"W, 11 January 2016, coll. by Han Y.-D.

Description. Male (Figs 5, 7A–D; holotype, range for 2 paratypes in parentheses): length of idiosoma from anterior end to bases of setae *h3* 350 (350–355), greatest width 220 (230–240), length of hysterosoma 175 (173–175). Prodorsal shield: narrow longitudinal plate with almost parallel lateral margins and acute posterior end extending beyond level of scapular setae *se*; length along midline 113 (118), greatest width 28 (27–29); anterior end with short longitudinal ridge about 1/8th the length of shield (Fig. 5A). Setae *se* and *si* at same transverse level, bases of setae *se* situated on teardrop-shaped sclerites and separated by 69 (73–77). Scapular shields wide, inner margins slightly convex, without suprategumental extensions. Hysteronotal shield: anterior margin convex, length of shield from anterior end to bases of setae *h3* 213 (205–210). Setae *c2* and *d2* represented by macrosetae, 150 (150–150) and 110 (95–110) long, respectively; both pairs approximately 1.5 time shorter than humeral macrosetae *cp*. Opisthosomal lobes slightly longer than wide at base. Supranal concavity ovate, poorly outlined, separated from terminal cleft. Terminal cleft semi-ovate in shape, slightly narrowed anteriorly; length of terminal cleft from anterior end to bases of setae *h3* 63 (58–62), greatest width 40 (41–42). Terminal membranous extensions on lobar apices short and widely rounded, length from bases of setae *h3* to apices of terminal exten-

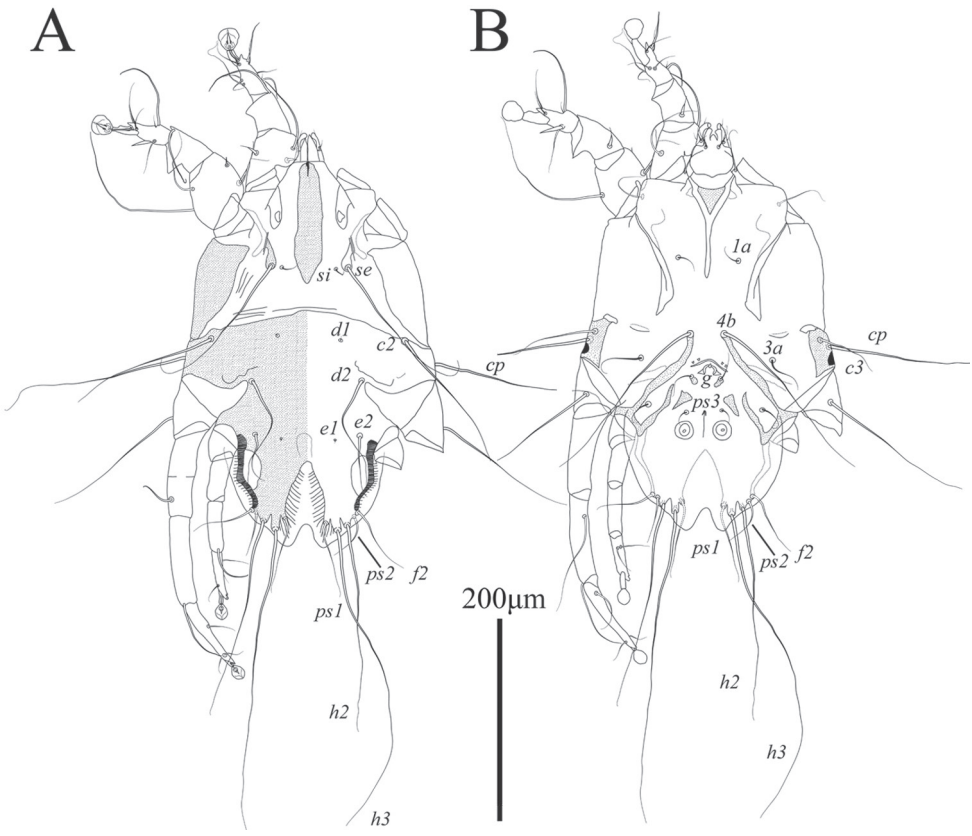

Figure 5. *Ingrassia chionis* sp. nov., male **A** dorsal view **B** ventral view.

sions 20 (18–19), width of extensions at base 32 (27–28), length of incision between extensions 22 (19–20). Setae *ps1* situated approximately at level of setae *h2*. Distance between dorsal setae: *c2*:*c2* 183 (180–188), *c2*:*d2* 33 (37–38), *d2*:*e2* 52 (50–53), *e2*:*h3* 88 (83–84), *h3*:*h3* 59 (55–57), *ps1*:*ps1* 39 (36–37).

Sternum about half as long as total length of epimerites I (Fig. 5B). Anterior ends of epimerites IIIa free, widely separated from each other. Setae *4b* situated on anterior ends of epimerites IIIa and almost extending to mid-length of opisthosomal lobes. Pregenital apodeme (epiandrum) small bow-shaped, 10 (7–9) long, 35 (32–38) wide. Genital apparatus 13 (10–12) long and 27 (27–28) wide. Setae *g* situated on small genital shields. Adanal shields triangular, situated anterolateral to setae *ps3*. Epimerites IVa long, almost completely enclosing coxal fields IV. Central part of coxal fields IV not sclerotized. Diameter of adanal suckers 19 (19–20). Distance between ventral setae: *4b*:*4b* 33 (35–36), *4b*:*3a* 24 (27–29), *4b*:*g* 41 (42–43), *g*:*ps3* 29 (32–33), *ps3*:*h3* 97 (93–95).

Tarsi I, II each with short apicodorsal extension. Tibiae I, II with well-developed ventral spine-like processes (Fig. 7A, B). Seta *s* of tibia II spiculiform. Femorogenu II with thick spine-like retrograde apophysis. Tibia III with small angular apical extension bearing base of solenidion *φ*. Length of tarsus III 81 (78–79). Tarsus IV with finger-like

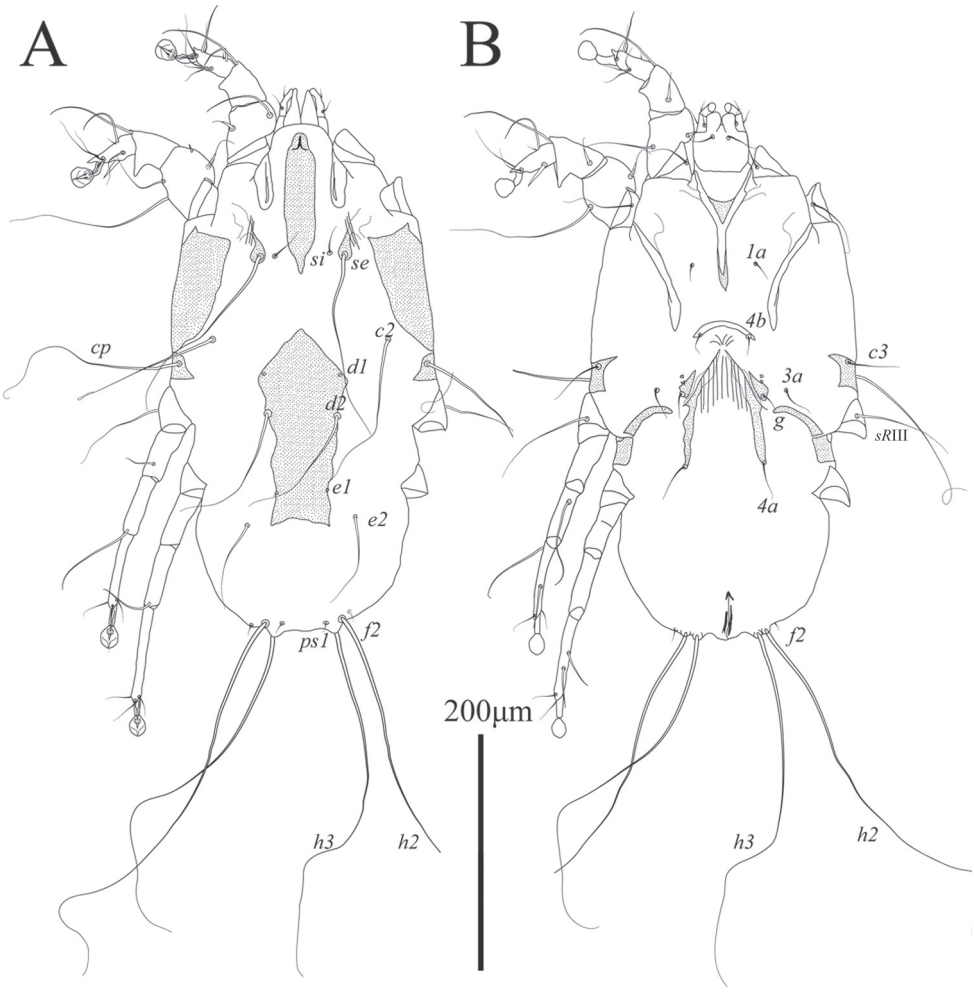

Figure 6. *Ingrassia chionis* sp. nov., female **A** dorsal view **B** ventral view.

apical extension; modified setae *d*, *e* short spiculiform, seta *e* situated on tarsal apex, seta *d* subapical (Fig. 7C). Legs IV excluding pretarsus 55 (51–58) long, with tarsus and distal half of genu extending beyond level of lobar apices (bases of setae *h3*) (Figs 5, 7D).

Female (Figs 6, 7E, F; range for 3 paratypes): length of idiosoma 400–435, greatest width 225–250, length of hysterosoma 220–238. Prodorsal shield: shaped approximately as in male, length 118–123, greatest width 30–33, anterior end with short longitudinal ridge about 1/8th the length of shield (Fig. 6A). Setae *se* and *si* at same transverse level; bases of setae *se* situated on teardrop-shaped sclerites and separated by 75–82. Scapular shields wide, with smooth inner margin. Humeral shields well developed, without anteromesal extensions. Setae *c3* short, slightly longer than trochanters III. Hysteronotal shield: large longitudinal plate occupying median part of hysterosoma; anterior part slightly widened; anterior margin right-angular, extending to or beyond level of setae *c2*;

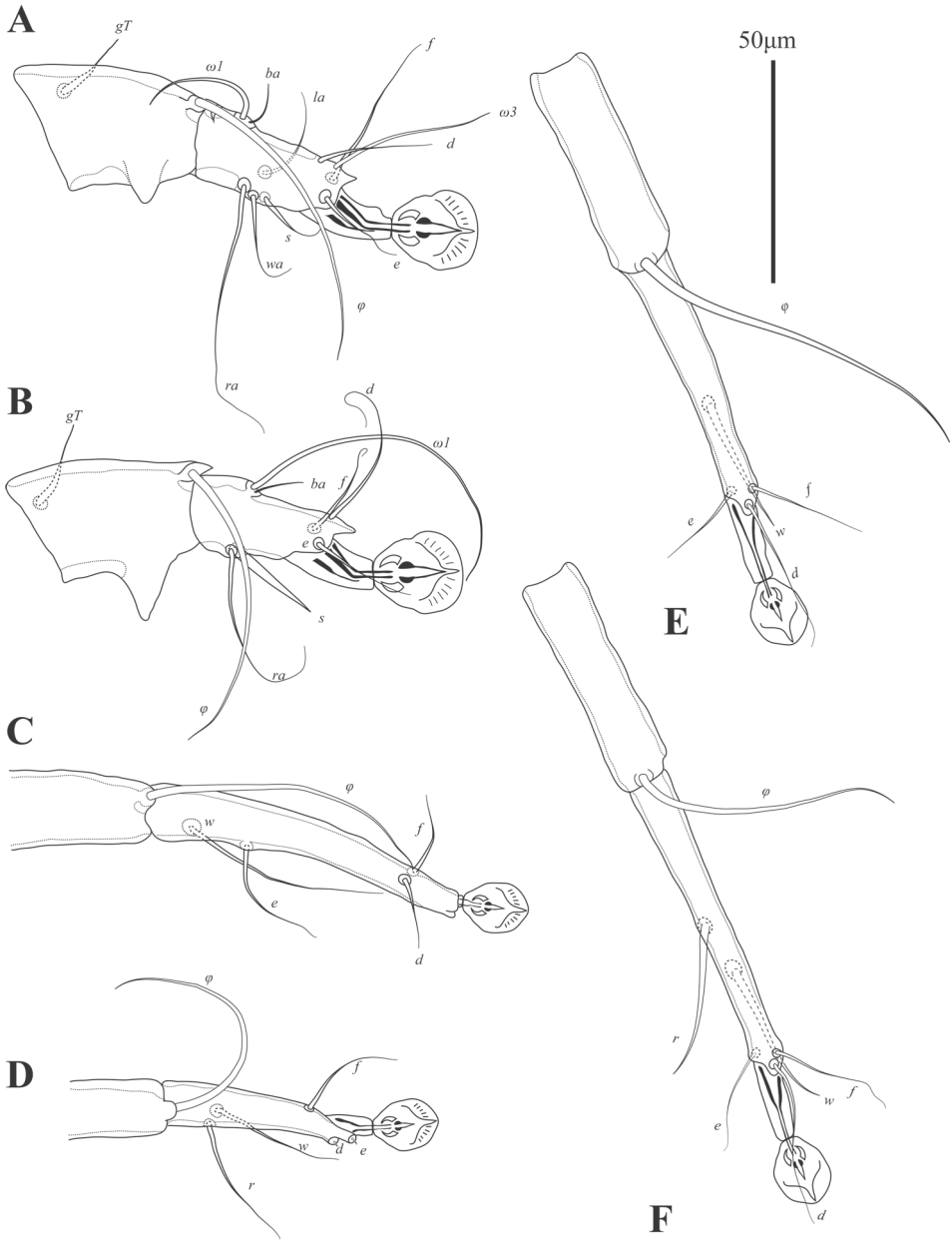

Figure 7. *Ingrassia chionis* sp. nov., legs **A** tibia and tarsus I of male **B** tibia and tarsus II of male **C** tibia and tarsus III of male **D** tibia and tarsus IV of male **E** tibia and tarsus III of female **F** tibia and tarsus IV of female.

lateral margins unevenly sinuous; posterior margin truncate or slightly concave, extending to level of setae *e2*; greatest length 158–168, greatest width 85–93. Setae *c2*, *d2*, and *e2* represented by macrosetae, 139–151, 112–131 and 81–93 long, respectively. Setae

d1, *d2*, and *e1* situated on hysteronotal shield, setae *c2*, *e2* situated on striated tegument. Distance between dorsal setae: *c2*:*d2* 63–73, *d2*:*e2* 84–87, *e2*:*h3* 82 87, *h3*:*h3* 52–70.

Sternum about half as long as epimerites I. Epigynum thick and is bow-shaped, 13–22 long, 58–64 wide, with tips bearing bases of setae *4b*. Apodemes of oviporus long, their posterior ends long and narrow, encompassing bases of setae *4a* (Fig. 6B). Setae *4b*, *g*, *3a*, and *4a* short, not exceeding length of femorogenua III, IV. Setae *h3* approximately two-thirds the length of setae *h2*.

Legs I, II as in the male. Legs IV with tarsus extending beyond posterior end of opisthosoma. Tarsi III, IV without apical spines, length of tarsi III, IV 60–61 and 72–74, respectively. Setae *sR*III subequal to combined length of corresponding femur, genu, and tibia. Seta *w* of tarsus III and setae *r*, *w* of tarsus IV spiculiform (Figs 6, 7).

Differential diagnosis. The new species *Ingrassia chionis* sp. nov. belongs to a group of species associated with the Charadriiformes and is characterized by a retrograde spine-like apophysis on femorogenu II in both sexes (Gaud 1972; Vasyukova and Mironov 1991). Among this species grouping, the new species is most similar to *I. tringae* Vitzthum, 1922 (= *I. minuta* Gaud, 1972) described from *Calidris minuta* (Leisler) (Scolopacidae) in having the following features: in males of both species, the opisthosomal lobes are relatively short, equal to or slightly longer than wide at the bases, and the supranal concavity is completely separated from the terminal cleft; in females, the hysteronotal shield is shaped as a large longitudinal plate occupying the median area of the hysterosoma. *Ingrassia chionis* is distinguished from *I. tringae* by the following features: in both sexes, the prodorsal shield is narrow, parallel-sided, with the width about one-third the distance between setae *se*, and the posterior end of this shield is tapering; in males, the terminal cleft is semi-ovate, narrowed only in the anterior end, and tibia III bears a small apical spine of rectangular shape; in females, the anterior margin of the hysteronotal shield is right-angled and extends to the level of setae *c2*, and the posterior margin of this shield is truncate and extends to the level of setae *e2*. In both sexes of *I. tringae*, the prodorsal shield is a longitudinal plate widened posteriorly, with its greatest width equal to or larger than the halfway between setae *se*, and the posterior margin is widely rounded; in males, the anterior half of the terminal cleft is strongly narrowed, and tibia III bears a pointed apical spine; in females, the anterior margin of the hysteronotal shield is semi-ovate and does not extend to the level of setae *c2*, and the posterior margin of this shield is concave and extends beyond the level of setae *e2*.

Molecular data. The COI sequences were obtained from two individuals and deposited in GenBank with accession numbers MZ489649 and MZ489650.

Etymology. The specific name is taken from the generic name of the type host and is a noun in apposition.

Acknowledgements

This study was supported by Korea Polar Research Institute's projects on the "Ecophysiology of Antarctic terrestrial organisms to reveal mechanisms of adaptation to changing environment" (PE21130). The authors wish to thank Ji-Young Lee (Chonnam

National University, Korea) for sample collection. The permit for catching birds was officially approved the Korean Ministry of Foreign Affairs and Trade through the Korea Polar Research Institute.

References

Atyeo WT, Peterson PC (1967) Astigmata (Sarcoptiformes): Proctophyllodidae, Avenzoariidae (feather mites). Antarctic Research Series 10: 97–103. https://doi.org/10.1029/AR010p0097

Atyeo WT, Peterson PC (1970) Acarina: Astigmata: Analgoidea: feather mites of South Georgia and Heard Islands. Pacific Insects Monographs 23: 121–151.

Bockheim JG (2015) Soil-forming factors in Antarctica. In: the soils of Antarctica. Springer, Cham, 5–20. https://doi.org/10.1007/978-3-319-05497-1_2

Chown SL, Convey P (2007) Spatial and temporal variability across life's hierarchies in the terrestrial Antarctic. Philosophical Transactions of the Royal Society B: Biological Sciences 362(1488): 2307–2331. https://doi.org/10.1098/rstb.2006.1949

Dabert J [2004] (2005) Feather mites (Astigmata; Pterolichoidea, Analgoidea) and birds as models for cophylogenetic studies. In: Weigmann G, Alberti G, Woltman A, Ragusa S (Eds) Acarina Biodiversity in the Natural and Human Sphere, Proceedings of the V Symposium of the EURAAC. Phytophaga 14: 409–424.

Dabert J, Ehrnsberger R, Dabert M (2008) *Glaucalges tytonis* sp. nov. (Analgoidea, Xolalgidae) from the barn owl *Tyto alba* (Strigiformes, Tytonidae): compiling morphology with DNA barcode data for taxon descriptions in mites (Acari). Zootaxa 1719: 41–52. https://doi.org/10.11646/zootaxa.1719.1.2

Dabert J, Mironov SV (1999) Origin and evolution of feather mites (Astigmata). Exerimental and Applied Acarology 23: 437–454. https://doi.org/10.1023/A:1006180705101

Dabert M, Coulson SJ, Gwiazdowicz DJ, Moe B, Hanssen SA, Biersma EM, Pilskog HE, Dabert J (2015) Differences in speciation progress in feather mites (Analgoidea) inhabiting the same host: the case of *Zachvatkinia* and *Alloptes* living on arctic and long-tailed skuas. Experimental and Applied Acarology 65: 163–179. https://doi.org/10.1007/s10493-014-9856-1

Dubinin VB (1949) Feather mites of the Procellariiformes and their particulars. Parazitologicheskiy sbornik 11: 201–228. [In Russian]

Dubinin VB (1952) Feather mites of birds of Wrangel Island. Trudy Zoologicheskogo Instituta AN SSSR 12: 251–268. [In Russian]

Dubinin VB, Dubinina MN (1940) Parasite fauna of colonial birds of the Astrakhan Preserve. Trudy Astrakhanskogo Gosudarstvennogo Zapovednika 2: 190–298. [In Russian]

Gaud J (1952) Acariens plumicoles (Analgesidae) de quelques oiseaux des Iles Kerguelen (Récolte P. Paulian). Mémoires de l'Institut scientifique de Madagascar, Séries A7: 161–166.

Gaud J (1957) Acariens plumicoles (Analgesoidea) parasites des oiseaux du Maroc. I. Proctophyllodidae. Bulletin de la Société des Sciences naturelles et physiques du Maroc 37: 105–136.

Gaud J (1972) Acariens sarcoptiformes plumicoles (Analgoidea): parasites sur les oiseaux charadriiformes d'Afrique. Annales du Musée royale de l'Afrique centrale, Série in-8o, Sciences zoologiques 193: 1–116.

Gaud J (1976) Acariens sarcoptiformes plumicoles parasites sur les oiseaux: Lariformes et Columbiformes d'Afrique. Annales du Musée royal de l'Afrique centrale, Série in-8o, Sciences zoologiques 214: 1–101.

Gaud J, Atyeo WT (1996) Feather mites of the world (Acarina, Astigmata): the supraspecific taxa. Annales du Musée Royal de l'Afrique Centrale, Sciences Zoologiques 277, Pt. 1: 193 pp. [text], Pt. 2: 436 pp. [illustrations]

Gill F, Donsker D, Rasmussen P [Eds] (2021) IOC World Bird List (v. 11.2). http://www.worldbirdnames.org/

Hernandes FA, Bauchan GR, Ochoa R (2017) New and little known feather mites (Acariformes: Astigmata) analysed with low-temperature scanning electron microscopy. International Journal of Acarology 43(7): 499–517. https://doi.org/10.1080/01647954.2017.1367032

Hughes KA (2010) How committed are we to monitoring human impacts in Antarctica?. Environmental Research Letters 5(4): e041001. https://doi.org/10.1088/1748-9326/5/4/041001

Kearse M, Moir R, Wilson A, Stones-Havas S, Cheung M, Sturrock S, Buxton S, Cooper A, Markowitz S, Duran C, Thierer T, Ashton B, Meintjes P, Drummond A (2012) Geneious Basic: an integrated and extendable desktop software platform for the organization and analysis of sequence data. Bioinformatics 28: 1647–1649. https://doi.org/10.1093/bioinformatics/bts199

Kim JH, Chung H, Kim JH, Yoo JC, Ahn IY (2005) Nest distribution of skuas on Barton and Weaver Peninsulas of the King George Island, the Antarctic. Ocean and Polar Research 27(4): 443–450. https://doi.org/10.4217/OPR.2005.27.4.443

Kim JH, Joung JW, Lee WY, Chung H (2014) Antarctic Animal Handbook: Birds and Mammals of Antarctic Specially Protected Area No.171 Narębski Point. Geobok, Seoul, 77 pp.

Kivganov DA (1996) A review of feather mites associated with terns (Charadriiformes: Laridae) living in the Black Sea north-western coastal region and a description of a new species of the genus *Alloptes* (Analgoidea: Alloptidae). Parazitologiya 30(4): 302–306. [In Russian with English summary]

Kivganov DA, Mironov SV (1992) A new subgenus and three new species of the feather mite genus *Alloptes* (Analgoidea: Alloptidae) from terns of the Black Sea. Parazitologiya 26(3): 198–208. [In Russian with English summary]

Mironov SV (1989) A brief review of the feather mites of the genus *Zachvatkinia* in the USSR (Analgoidea, Avenzoariidae). Parazitologicheskii Sbornik 36: 91–115. [In Russian with English summary]

Mironov SV (1990) A review of species of feather mites in the genus *Scutomegninia* (Analgoidea, Avenzoariidae) from cormorants. Parazitologiya 24: 43–55. [In Russian with English summary]

Mironov SV (1991) Two new feather mite species of superfamily Analgoidea from Antarctic birds. Informatsionnyi Byulleten Sovetskoi Antarkticheskoi Ekspeditsii. Saint Petersburg, Gidrometeoizdat 116: 69–75. [In Russian]

Mironov SV (1996) On a validity of the genus *Plicatalloptes* (Acarina: Analgoidea: Alloptidae). Parazitologiya 30: 216–222. [In Russian with English summary]

Mironov SV (2000) A review of the feather mite genus *Scutomegninia* Dubinin, 1951 (Acarina: Analgoidea: Avenzoariidae). Acarina 8: 9–58.

Mironov SV (2007) Phylogeny of the feather mite family Alloptidae and coevolutionary trends with aquatic birds. In: Morales-Malacara JB, Behan-Pelletier V, Ueckermann E, Perez TM, Estrada-Venegas E, Badii M (Eds) Acarology XI: Proceedings of the International Congress (Merida, Yucatan, Mexico, 8–13 September 2002). Instituto de Biololgía and Facultad de Ciencias, Universidad Nacional Autónoma de México; Sociedad Latinoamericana de Acarología. México, 617–634.

Mironov SV, Dabert J (1999). Phylogeny and coevolutionary trends in feather mites of the subfamily Avenzoariinae (Analgoidea: Avenzoariidae). Experimental and Applied Acarology 23: 525–549. https://doi.org/10.1023/A:1006132806010

Mironov SV, Hernandes FA (2020) Taxonomic notes on feather mite species (Acariformes: Analgoidea) described by Adolf Eduard Grube. Acarina 28(2): 213–220. https://doi.org/10.21684/0132-8077-2020-28-2-213-220

Mironov SV, Kivganov DA (1993) New species of feather mites of the superfamily Analgoidea from charadriiformes of Black Sea. Parazitologiya 27(2): 161–167. [In Russian with English summary]

Mironov SV, Palma RL (2006) Two new feather mite species (Acari: Analgoidea) from the Tuamotu sandpiper *Aechmorhynchus parvirostris* (Charadriiformes: Scolopacidae). Tuhinga – Records of the Museum of New Zealand Te Papa Tongarewa 17: 49–59.

Mironov SV, Proctor HC (2008) The probable association of feather mites of the genus *Ingrassia* (Analgoidea: Xolalgidae) with the blue penguin *Eudyptula minor* (Aves: Sphenisciformes) in Australia. Journal of Parasitology 94(6): 1243–1248. https://doi.org/10.1645/GE-1579.1

Norton AR (1998) Morphological evidence for the evolutionary origin of Astigmata (Acari: Acariformes). Experimental and Applied Acarology 22: 559–594. https://doi.org/10.1023/A:1006135509248

PBEG [Polar and Bird Ecology Group] (2003) SKUA Manual for Fieldworkers. Polar and Bird Ecology Group, Jena, 11 pp.

Peck LS (2018) Antarctic marine biodiversity: adaptations, environments and responses to change. In: Hawkins SJ, Evans AJ, Dale AC, Firth LB, Smith IP (Eds) Oceanography and Marine Biology: an Annual Review 56: 105–236. https://doi.org/10.1201/9780429454455-3

Potapowicz J, Szumińska D, Szopińska M, Bialik RJ, Machowiak K, Chmiel S, Polkowska Ż (2020) Seashore sediment and water chemistry at the Admiralty Bay (King George Island, Maritime Antarctica) – geochemical analysis and correlations between the concentrations of chemical species. Marine Pollution Bulletin 152: 110888. https://doi.org/10.1016/j.marpolbul.2020.110888

Proctor HC (2003) Feather mites (Acari: Astigmata): ecology, behavior and evolution. Annual Review of Entomology 48: 185–209. https://doi.org/10.1146/annurev.ento.48.091801.112725

Proctor HC, Owens I (2000) Mites and birds: diversity, parasitism and coevolution. Trends in Ecology and Evolution 15: 358–364. https://doi.org/10.1016/S0169-5347(00)01924-8

Sancho LG, Pintado A, Green TG (2019) Antarctic studies show lichens to be excellent biomonitors of climate change. Diversity 11(3): 42. https://doi.org/10.3390/d11030042

Shirihai H (2007) A complete guide to Antarctic wildlife: the Birds and Marine Mammals of the Antarctic Continent and the Southern Ocean. A&C Black, London, 544 pp.

Stefan LM, Gomez-Diaz E, Mironov SV (2013) Three new species of the feather mite subfamily Ingrassiinae (Acariformes: Xolalgidae) from shearwaters and petrels (Procellariiformes: Procellariidae). Zootaxa 3682(1): 105–120. https://doi.org/10.11646/zootaxa.3682.1.4

Vanstreels RET, Palma RL, Mironov SV (2020) Arthropod parasites of Antarctic and Subantarctic birds and pinnipeds: a review of host-parasite associations. International Journal for Parasitology: Parasites and Wildlife 12: 275–290. https://doi.org/10.1016/j.ijppaw.2020.03.007

Vasyukova TT, Mironov SV (1991) Feather mites of Anseriformes and Charadriiformes of Yakutia. Systematics. Publisher: Nauka, Siberian Dept, Novosibirsk, 200 pp. [In Russian]

ZooKeys 1061: 131–163 (2021)
doi: 10.3897/zookeys.1061.70929
https://zookeys.pensoft.net

RESEARCH ARTICLE

A peer-reviewed open-access journal
ZooKeys
Launched to accelerate biodiversity research

A new species of *Micrurapteryx* (Lepidoptera, Gracillariidae) feeding on *Thermopsis lanceolata* (Fabaceae) in southern Siberia and its hymenopterous parasitoids

Natalia I. Kirichenko[1,2], Evgeny N. Akulov[3], Paolo Triberti[4], Sergey A. Belokobylskij[5,6]

1 *Sukachev Institute of Forest, Siberian Branch of the Russian Academy of Sciences, Federal Research Center "Krasnoyarsk Science Center SB RAS", Akademgorodok 50/28, 660036, Krasnoyarsk, Russia* **2** *Siberian Federal University, Svobodny pr. 79, 660041, Krasnoyarsk, Russia* **3** *All-Russian Plant Quarantine Center, Krasnoyarsk branch, Zhelyabova str. 6/6, 660020, Krasnoyarsk, Russia* **4** *Museo Civico di Storia Naturale, Lungadige Porta Vittoria 9, I37129, Verona, Italy* **5** *Zoological Institute of the Russian Academy of Sciences, Universitetskaya nab. 1, 199034, Saint Petersburg, Russia* **6** *Museum and Institute of Zoology, Polish Academy of Sciences, 64 Wilcza, Warszawa, 00–679, Poland*

Corresponding author: Natalia Kirichenko (nkirichenko@yahoo.com)

Academic editor: E. J. van Nieukerken | Received 1 July 2021 | Accepted 6 September 2021 | Published 8 October 2021

http://zoobank.org/1780D3A8-550B-44F6-9F1C-B4934C877EA9

Citation: Kirichenko NI, Akulov EN, Triberti P, Belokobylskij SA (2021) A new species of *Micrurapteryx* (Lepidoptera, Gracillariidae) feeding on *Thermopsis lanceolata* (Fabaceae) in southern Siberia and its hymenopterous parasitoids. ZooKeys 1061: 131–163. https://doi.org/10.3897/zookeys.1061.70929

Abstract

A new species of leaf-mining moth described here as *Micrurapteryx baranchikovi* Kirichenko, Akulov & Triberti, **sp. nov.** was detected in large numbers feeding on *Thermopsis lanceolata* (Fabaceae) in the Republic of Khakassia (Russia) in 2020. A morphological diagnosis of adults, bionomics and DNA barcoding data of the new species are provided. The developmental stages (larva, pupa, adult), male and female genitalia, as well as the leaf mines and the infestation plot in Khakassia are illustrated; the pest status of the new species in the studied region is discussed. Additionally, parasitism rate was estimated, the parasitoid wasps reared from pupae of the new species were identified (morphologically and genetically) and illustrated . Among them, one ichneumonid, *Campoplex* sp. aff. *borealis* (Zetterstedt) and two braconids, *Agathis fuscipennis* (Zetterstedt) and *Illidops subversor* (Tobias et Kotenko), are novel records for the Republic of Khakassia. Furthermore, they are all documented as parasitoids of Gracillariidae for the first time. The DNA barcode of *A. fuscipennis* is newly obtained and can be used as a reference sequence for species identification.

Keywords
Biology, DNA barcoding, leaf-mining moth, morphology, new species, parasitoid wasps, pest, the Republic of Khakassia

Introduction

The genus *Micrurapteryx* Spuler, 1910 (subfam. Ornixolinae Kuznetzov & Baryshnikova, 2001) is a group of leaf-mining micromoths accounting 14 species (Vieira and Karsholt 2010; De Prins and De Prins 2021). The majority are known from some parts of Eurasia: *M. bidentata* Noreika, 1992, *M. bistrigella* (Rebel, 1940), *M. caraganella* (Hering, 1957), *M. fumosella* Kuznetzov & Tristan, 1985, *M. gerasimovi* Ermolaev, 1982, *M. gradatella* (Herrich-Schäffer, 1855), *M. kollariella* (Zeller, 1839), *M. parvula* Amsel, 1935, *M. sophorella* Kuznetzov, 1979, *M. sophorivora* Kuznetzov & Tristan, 1985, *M. tibetiensis* Bai & Li, 2013, and *M. tortuosella* Kuznetzov & Tristan, 1985. The other two species, *M. occulta* Braun, 1922 and *M. salicifoliella* (Chambers, 1872), occur exclusively in North America. No *Micrurapteryx* species has a Holarctic distribution (De Prins and De Prins 2021). All these species were described in 19th and 20th centuries, except *M. tibetiensis* that was described from China in 2013 (Bai 2013) and *M. caraganella* that was redescribed from Siberia (Russia) in 2016 (Kirichenko et al. 2016).

The moths of *Micrurapteryx* are commonly specialised on legumes (Fabaceae), i.e., on *Astragalus*, *Cytisus*, *Genista*, *Laburnum*, *Lathyrus*, *Lupinus*, *Melilotus*, *Sophora*, *Trifolium*, *Vicia* etc. (De Prins and De Prins 2021). As an exception, *M. salicifoliella* feeds on willows *Salix* spp. (Salicaceae) and *M. bistrigella* on *Morella faya* (Aiton) Wilbur (Myricaceae). For two species, *M. bidentata* described from Kazakhstan and *M. tibetiensis* from China, host plants remain unknown (Noreika and Puplesis 1992; Bai 2013).

To date, no species of *Micrurapteryx* has been documented to feed on *Thermopsis* (Fabaceae) in Eurasia. In 1875, *Gracilaria* [sic] *thermopsella* was described by Chambers from Colorado (USA) (Chambers 1875). A few decades later, the species was transferred to the genus *Parectopa* (Braun 1925; McDunnough 1939; Davis 1983). Further examinations suggested that *Parectopa thermopsella* could belong to the genus *Micrurapteryx* (Eiseman 2019). According to Eiseman (2019), Don Davis examined two males reared from *Thermopsis* in the USA, and their genitalia were similar to *M. occulta*. As such, the historic records of *P. thermopsella* could be attributed to *M. occulta* known to feed on several legume genera in North America (Kirichenko et al. 2016). Unfortunately, no type or other specimens of the species are available (according to D. Davis, pers. comm. to J.-F. Landry, Kirichenko et al. 2016) and thus, comparative studies can be done only based on the description given in Chambers (1875).

DNA barcoding of a larva occasionally found in the mine on *Thermopsis lanceolata* R. Brown (Fabaceae) in the Republic of Khakassia near the Black Lake field station of Sukachev Institute of Forest SB RAS (Siberia, Russia) in 2019 pointed at the presence of a genetically divergent lineage of *Micrurapteryx.* Therefore, in 2020 intensive sampling was done in this location in order to collect leaf mines and rear moths for species identification.

Using the integrative taxonomy, we describe a new species, *Micrurapteryx baranchikovi* Kirichenko, Akulov & Triberti, sp. nov., reared from *Thermopsis lanceolata* R.Br. (Fabaceae) in the Republic of Khakassia, Russia. We provide morphological data with bionomic notes of the species, highlight diagnostic characteristics to distinguish between *M. baranchikovi* and the North American "*Parectopa*" *thermopsella*, and analyse DNA barcoding data to define the closest relatives and assess the DNA barcoding gap. Furthermore, we estimate the parasitism rate in the dense moth population in Khakassia and identify parasitoid species associated with *M. baranchikovi.* The different developmental stages (larva, pupa, adult), male and female genitalia of *M. baranchikovi*, as well as the adults of parasitoids, are illustrated, and the pest status of the new moth species in the studied region is discussed.

Materials and methods

Sampling

Thermopsis lanceolata plants with leaf mines of *Micrurapteryx baranchikovi* sp. nov. were collected in the Republic of Khakassia in two localities in July 2020 (Fig. 1A). A few plants were sampled on the bank of the Belyo Lake (Beljo Ozero) at the beach "Majorca" (Fig. 1B, D) on 6 July 2020, whereas the majority of plants with mines (99% of all plants with mines) were collected between 28–30 July 2020 on the bank of the Black Lake (Chyornoe Ozero), 5 km away from the Black Lake field station of Sukachev Institute of Forest SB RAS (SIF SB RAS) (Fig. 1C, E).

Leaves with young mines sampled in early July were placed in a herbarium; three tiny larvae dissected from the mines were preserved in 95% ethanol. In late July, ca. 50 plants (without roots) were collected and transferred to the insectarium of the Forest zoology laboratory at SIF SB RAS (Krasnoyarsk). Five larvae were dissected from older mines for the ethanol-preserved collection. Plants were placed in bouquets in 5-liter containers filled with water. They were kept in stable conditions (temperature 25 °C, humidity 65%) for one month (until the end of August) to allow larvae to complete their development and pupate. In the containers, water was changed every third day for one month, and the plants were inspected every second day to sample pupating individuals. The cocoons with pupae were cut with a small segment of leaflet and placed by 20 pupae in Petri dishes (90 mm in diameter, 15 dishes in total) lined with filter paper. Overall, 305 pupae were involved in the study, of which five pupae were preserved in 95% ethanol for morphological study.

Pupae were kept under laboratory conditions until September 1st, 2020. As no adult emerged from several-week-old pupae, we suspected that the pupae entered diapause and allowed them to overwinter. For that, the dishes with pupae were placed in the fridge (temperature +3 °C): half of the dishes (7 out of 15) on September 1st and the remaining 8 dishes on September 20th; the latter dishes were kept under room conditions longer in case some moths would emerge in the first half of September. The dishes were returned to

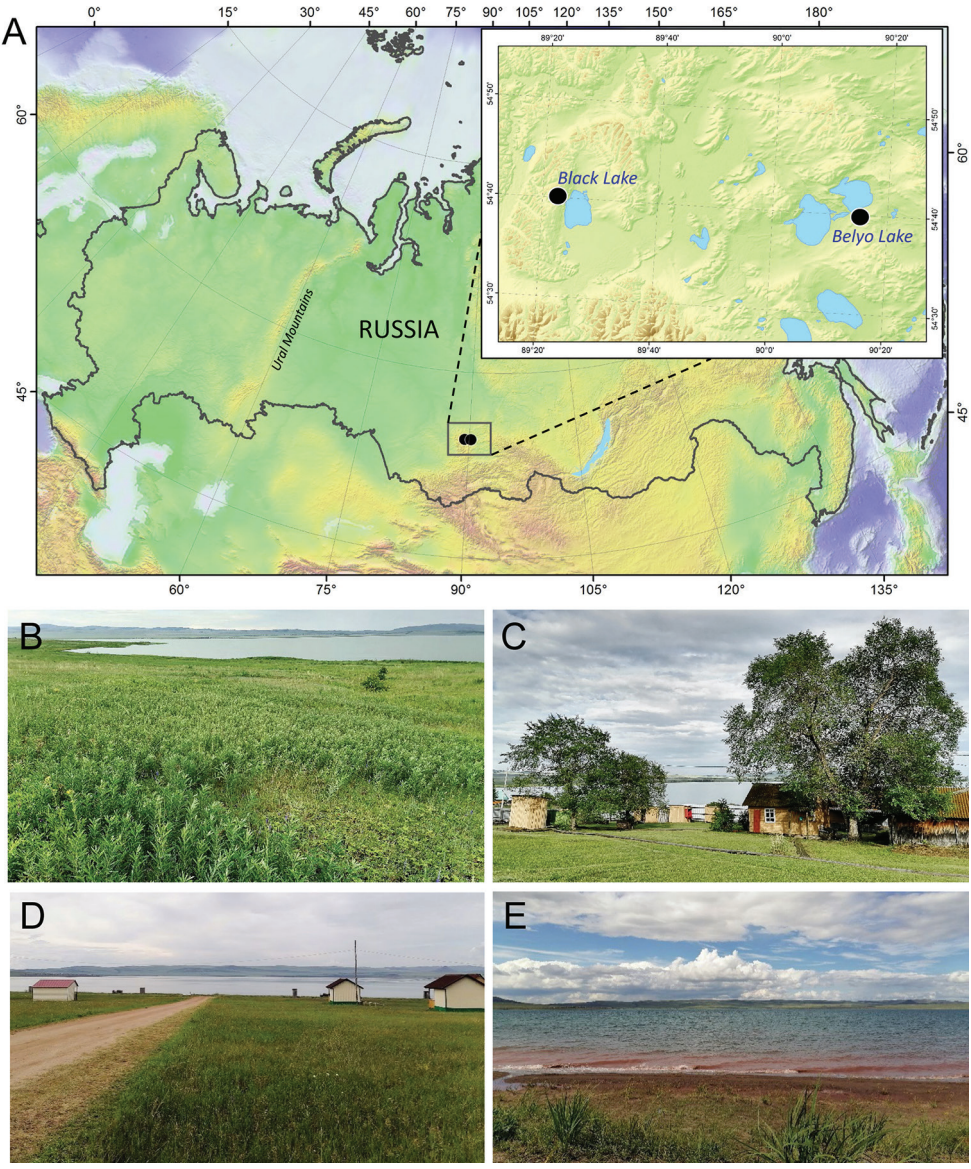

Figure 1. Sampling localities of *Micrurapteryx baranchikovi* sp. nov. in the Republic of Khakassia, Siberia, Russia **A** map of the sampled area (sampling localities are indicated by black dots) **B** type locality, bank of the Black Lake **C** the Black Lake field station of SIF SB RAS **D, E** bank of the Belyo Lake, beach "Majorca".

laboratory conditions (temperature 23 °C, humidity 70%) after two months, i.e., the first batch of dishes was taken out from the fridge on November 1st and the second on December 20th. The dishes were monitored every day to collect emerged adult moths and parasitoids. Adults were pinned and stored in a dry collection (53 adult moths), parasitoid adults were preserved in 95% ethanol for further morphological and molecular genetic analyses.

DNA barcoding

DNA barcoding of *Micrurapteryx baranchikovi* sp. nov. was performed to define its genetic relatedness to other species of *Micrurapteryx* and assess the DNA barcoding gap (the difference between the largest intraspecific and the smallest interspecific distances). In total, seven specimens of *M. baranchikovi* were involved in the genetic analysis (Suppl. material 1: Table S1); one larva (collected in 2019, as mentioned in the Introduction), two larvae and four adults (collected in 2020). DNA was extracted from whole bodies of larvae and hind legs of adults and sequenced at the Canadian Centre for DNA Barcoding (CCDB, Biodiversity Institute of Ontario, University of Guelph, Ontario, Canada) using primer set C_LepFolF/C_LepFolR, following the standard high-throughput protocol (de Waard et al. 2008). The same protocol was applied for sequencing three specimens of parasitoid wasps: two Ichneumonidae (sample IDs NK-20-32 ♀, NK-20-33 ♂) and one Braconidae (sample ID NK-20-34 ♀) that emerged from pupae of *M. baranchikovi.* The hind legs of parasitoids were used for DNA barcoding; the vouchers were saved for morphological identification. The specimen data of all sequenced material are given in Suppl. material 1: Table S1.

The sequences, trace files, biogeographic data and photographs of the vouchers were deposited in the Barcode of Life Data Systems (BOLD) (Ratnasingham and Hebert 2007; www.barcodinglife.org); the original sequences were also submitted to NCBI (National Centre for Biotechnology Information) to obtain GenBank accessions. All data are publicly available in BOLD (dx.doi.org/10.5883/DS-MICKHA).

For phylogenetic analysis, 38 sequences of five other *Micrurapteryx* species, showing close genetic and/or morphological relatedness to the new species, were involved in the analysis: three from Eurasia, *M. caraganella* (21 sequences), *M. gradatella* (eight), *M. kollariella* (three), and two species from North America: *M. occulta* (three sequences) and *M. salicifoliella* (three) (Suppl. material 1: Table S1). The majority of specimens of those species were sequenced for a previous study (Kirichenko et al. 2016), and some specimens of *M. salicifoliella* were DNA barcoded and published by Hebert et al. (2016).

For analysing genetic distances of parasitoids associated with *M. baranchikovi*, we additionally borrowed eight public sequences of the three species from BOLD: *Campoplex multicinctus* (six sequences), *C. borealis* (one) and *Agathis* sp. (one) (Suppl. material 1: Table S1).

Barcode Index Numbers (BINs) were retrieved for each species in BOLD (Ratnasingham and Hebert 2013). The sequences were aligned in BioEdit 7.2.5 (Jeanmougin et al. 1998). Maximum likelihood (ML) trees were constructed in MEGA X (Kumar et al. 2018) using Kimura 2-parameter model and bootstrap analysis (1000 iterations). Intra- and interspecific genetic distances were estimated using the same model.

The DNA barcodes of *Parectopa ononidis* (Zeller, 1839) (Lepidoptera: Gracillariidae) and *Metallus albipes* (Cameron, 1875) (Hymenoptera: Tenthredinidae), earlier obtained by NK (Suppl. material 1: Table S1), were used for rooting the respective phylogenetic trees.

Morphology

The external morphology of *Micrurapteryx baranchikovi* was examined based on 51 adult specimens. Thirteen adults (three males and ten females) were dissected; genitalia dissections and slide mounts were prepared following Robinson (1976). For comparison, the drawing of the male genitalia of *M. sophorivora* was reproduced from the paper by Kuznetzov and Tristan (1985). For genitalia, the terminology follows Klots (1970) and Kristensen (2003).

The braconid parasitoids reared from the pupae of *M. baranchikovi* were identified based on their morphological characters using the following keys: Tobias et al. (1986), Kotenko (2007), Simbolotti and van Achterberg (1999).

Imaging

The sampling localities and mined leaves were photographed by NK and EN using a digital camera Sony Nex3; the images of larvae, pupae and pinned adults of the moth were taken by the same camera through a Zeiss Stemi DV4 stereo microscope (Sukachev Institute of Forest SB RAS, Krasnoyarsk, Russia). Genitalia were photographed by PT with a Leica DFC 450 digital camera through Leitz Diaplan GMBH microscope (Museo Civico di Storia Naturale, Verona, Italy) and by EN and NK using a Canon EOS 650D mounted on Olympus CX41 microscope. The parasitoids were photographed by SAB using Olympus OM-D E-M1 digital camera mounted on Olympus SZX10 microscope (Zoological Institute RAS, Saint Petersburg, Russia). All digital photographs were edited and assembled into plates in Adobe Photoshop CS5 Extended.

Specimen depositories

SIF Sukachev Institute of Forest, Siberian Branch of the Russian Academy of Sciences, Krasnoyarsk, Russia (47 pinned moths, ethanol preserved larvae and pupae of the moth, 20 pressed leaves with the mines in herbarium);
MSNV Museo Civico di Storia Naturale, Verona, Italy (four pinned moths);
ZISP Zoological Institute of the Russian Academy of Sciences, Saint Petersburg, Russia (two pinned moths, 27 pinned parasitoid adults).

Results

Molecular data

***Micrurapteryx* spp.** The maximum likelihood tree based on COI sequences shows six clusters with 98–100 bootstrap support that match up with Barcode Index Numbers (BINs) (Fig. 2).

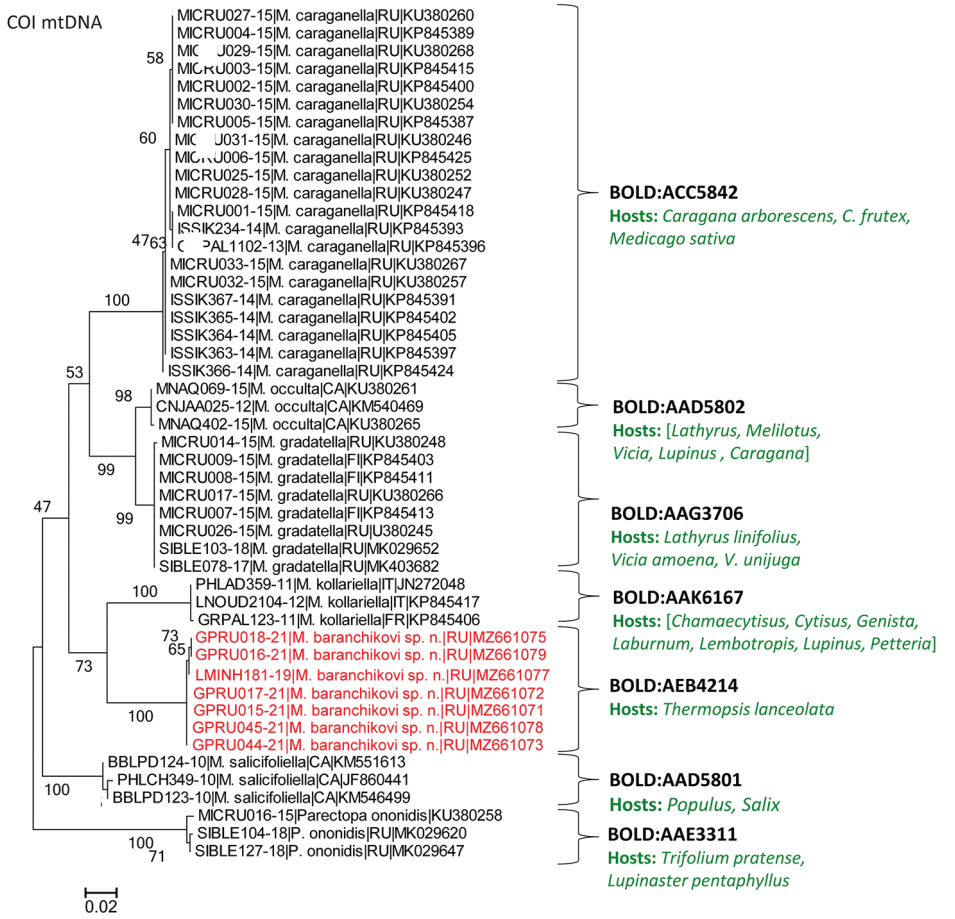

Figure 2. Maximum Likelihood tree showing the proximity of COI barcode sequences of *Micrurapteryx baranchikovi* sp. nov. (indicated in red) to other *Micrurapteryx* species. Each specimen is indicated by the BOLD process ID, followed by species name, country (CA Canada, FI Finland, FR France, IT Italy, RU Russia), and the GenBank accession number. Bootstrap values are indicated next to the corresponding branches. BIN numbers are given next to each cluster. The host plants are indicated in green; for the cases with no host plant species recorded, the list of host plant genera is provided in square parentheses (as per De Prins and De Prins 2021).

In the genus *Micrurapteryx*, the difference between the maximal intraspecific divergence (0.93% in *M. occulta*) and the minimal interspecific divergence (2.17% between *M. gradatella* and *M. occulta*) (Table 1) resulted in a DNA barcoding gap of 1.24%. Assigned to a unique BIN (BOLD:AEB4214), *Micrurapteryx baranchikovi* showed relatively low intraspecific variability (0.31%; N = 7) (Fig. 2, Table 1). Furthermore, it exhibited a pronounced DNA barcoding gap of 8.99% (the difference between the maximal intraspecific divergence in *M. baranchikovi*, 0.31%, and the minimal interspecific divergence in *M. baranchikovi* – *M. kollariella*, 9.30%; see Table 1).

Table 1. Intra- and interspecific divergences in COI mtDNA gene among *Micrurapteryx* spp. Minimal pairwise distances are given for each species pair; values in square brackets represent maximal intraspecific distances.

Species	*Micrurapteryx*					
	***baranchikovi* sp. nov.**	***kollariella***	***gradatella***	***caraganella***	***occulta***	***salicifoliella***
Micrurapteryx baranchikovi sp. nov.	[0.31]					
M. kollariella	9.30	[0.16]				
M. gradatella	10.23	10.08	[0.16]			
M. caraganella	10.23	11.01	8.53	[0.62]		
M. occulta	10.70	10.54	2.17	7.91	[0.93]	
M. salicifoliella	11.32	10.85	8.53	10.08	7.91	[0.47]

Micrurapteryx kollariella is the nearest neighbour to *M. baranchikovi*, with 59 diagnostic substitutions in the barcode fragment, as based on one studied population of *M. baranchikovi* in Khakassia (Suppl. material 2: Table S2). Notably, the North American *M. salicifoliella*, whose female genitalia have a high similarity to those of *M. baranchikovi* (see the analysis in Morphological section), formed the most distant genetic cluster with a minimal interspecific distance of 11.32% between these two species (Fig. 2, Table 1).

The specimens of the North American *M. occulta*, that might represent a *Thermopsis*-feeding *Micrurapteryx* originally described as *Gracilaria* [sic] *thermopsella* by Chambers in the USA (see the taxonomic note in Kirichenko et al. 2016), formed a distant cluster with a minimal interspecific distance of 10.70% to *M. baranchikovi* (Fig. 2, Table 1). In contrast, *M. occulta* sequences showed high similarity to the Eurasian *M. gradatella*, with a minimum genetic distance of 2.17% (Table 1); both species are known to attack *Lathyrus* in the continents where they occur.

Hymenopterous parasitoids. By DNA barcoding, the three sequenced specimens of parasitoids were identified as belonging to the two genera: *Campoplex* (Ichneumonidae: Campopleginae) (two specimens) and *Agathis* (Braconidae: Agathidinae) (one specimen). Sequences of two Khakassian specimens of *Campoplex* were identical (Suppl. material 3: Table S3).

In BOLD, the Khakassian *Campoplex* sp. aff. *borealis* showed little genetic divergence (0.39%) from *C. multicinctus* Gravenhorst sampled in Finland (process ID: ICHFI1691-13, BIN: BOLD:AAD1926) (Fig. 3, Suppl. material 1: Table S1). However, the latter seemed a clear misidentification as it joined a presumable cluster of *Campoplex borealis* in the analysed tree (Fig. 3). Furthermore, *Campoplex* sp. aff. *borealis* showed large genetic divergence (11.61%) from the cluster formed by five *C. multicinctus* from Finland, Belarus and Russia assigned to the BIN (BOLD:ACJ2277) (Fig. 3, Suppl. material 3: Table S3).

The genetic distance between the Khakassian *Campoplex* sp. aff. *borealis* and the only publicly available DNA barcode of morphologically related *Campoplex borealis* (from Germany, Process ID GMGMP3655-18, A. Hausman coll., BIN: BOLD:ACJ2208) reached 7.16% (Fig. 3; Suppl. material 3: Table S3).

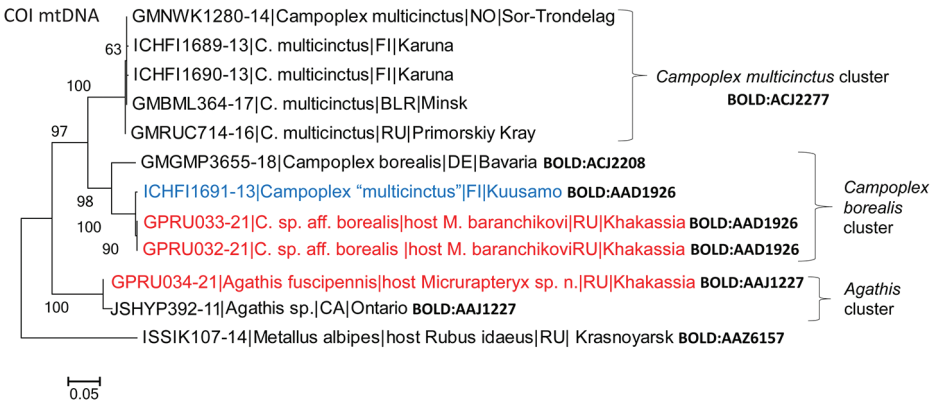

Figure 3. Maximum Likelihood tree showing the proximity of COI barcode sequences of the two hymenopteran parasitoids of *Micrurapteryx baranchikovi* sp. nov. (indicated in red) to the closest relatives in BOLD. As the specimen identity in BOLD (indicated in blue) is doubtful, the species name is given between quotes. Each specimen is indicated by the BOLD Process ID, followed by species name, host (where known), country (BLR Belarus, CA Canada, DE Germany, FI Finland, NO Norway, RU Russia), and sampling region. Bootstrap values are indicated next to the corresponding branches. BIN numbers are given in bold next to the clusters; if several BINs are known to one species, they are listed next to each specimen.

The only sequenced Khakassian specimen of a braconid wasp (NK-20-34 ♀, GPRU034-21) was identified in NCBI only to the genus level (97.92%), with the nearest neighbour *Agathis* sp. from Canada (Process ID JSHYP392-11, BIN: BOLD:AAJ1227; published in Hebert et al. (2016)) (Fig. 3). By morphology, we identified the braconid from Khakassia as *Agathis fuscipennis* (Zetterstedt, 1838). This species has been DNA barcoded for the first time.

In our study, no specimens of *Illidops subversor* (Tobias & Kotenko, 1986) (Braconidae: Microgastrinae) was DNA barcoded; the species was identified solely by morphology (see below).

New species taxonomy and biology

Family Gracillariidae Stainton, 1854
Subfamily Ornixolinae Kuznetzov & Baryshnikova, 2001
Genus *Micrurapteryx* Spuler, 1910

***Micrurapteryx baranchikovi* Kirichenko, Akulov & Triberti, sp. nov.**
http://zoobank.org/C30483F1-DA35-4BB8-983E-B79CB72FD9ED
Figs 4–9

Type material. ***Holotype*** ♂ (Fig. 4A, B): Republic of Khakassia, near the Black Lake field station of SIF SB RAS, along the lake bank, *Thermopsis lanceolata*; 28.VII.2020 coll. (mine), N. Kirichenko & E. Akulov coll, 08.XII.2020 emerged (hereafter indi-

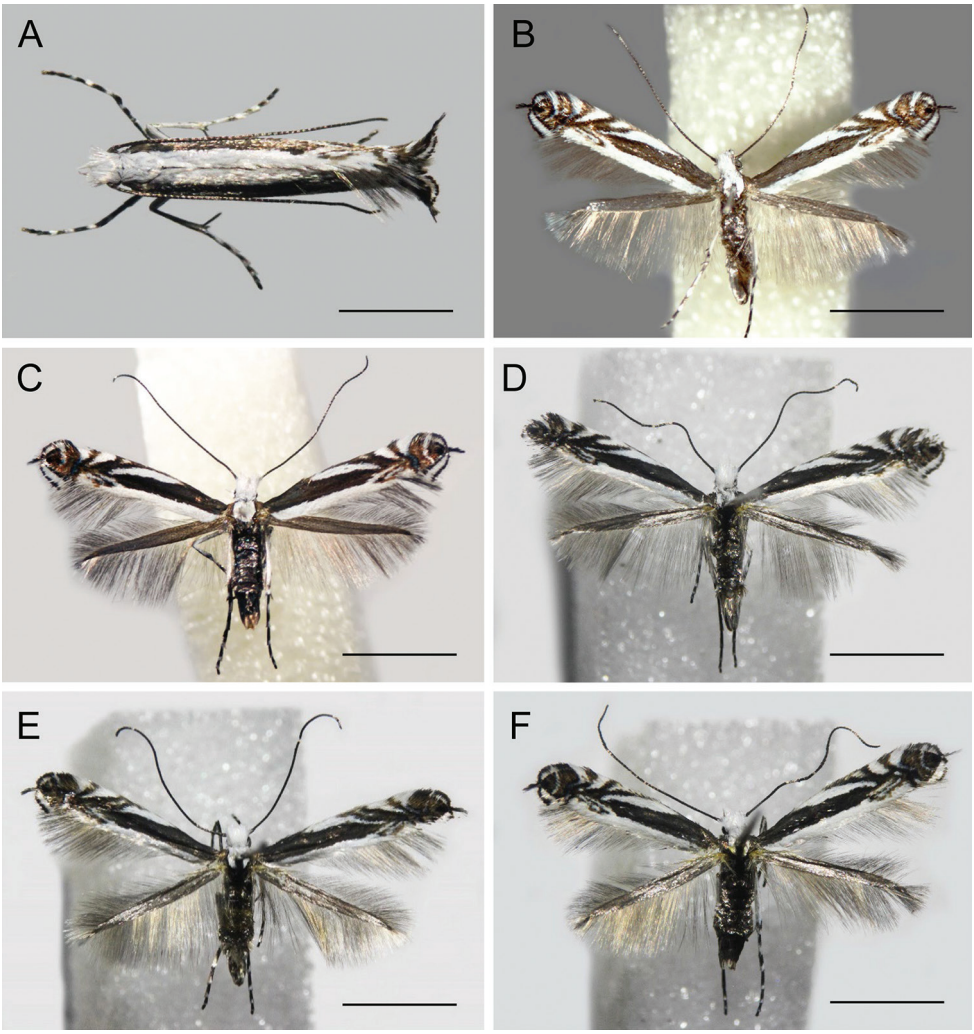

Figure 4. Adults of *Micrurapteryx baranchikovi* sp. nov. **A** resting posture **B** holotype, field no. NK-08.12-1 (♂), DNA barcoded, Process ID: GPRU015-21 **C** paratype, field no. NK-29.11-1 (♀), DNA barcoded, Process ID: GPRU016-21 **D** paratype, field no. NK-10-3 (♂) **E** paratype, field no. NK-11-3 (♂) **F** paratype, field no. NK-9-2 (♀). Scale bars: 2.5 mm.

cated as em.), field no. NK-08.12-1 (♂), genitalia slide NK-08.12-1♂, DNA barcoded (Process ID: GPRU015-21) (SIF). ***Paratypes.*** 15♂, 35♀ (Fig. 4C–F). Republic of Khakassia, near the Black Lake field station of SIF SB RAS, along the lake bank, *Thermopsis lanceolata*, 28.VII.2020 coll. (mine), Kirichenko N. coll., 14.I.2021 em., field no. NK-11-3, genitalia slide TRB4429♂ (MSNV); same label, but 17.I.2021 em. (from 2 mines), field nos NK-9-2, NK-10-3, genitalia slide TRB4425♀, TRB4428♂ (MSNV); 18.I.2021 em., field no. NK-11-4, genitalia slide TRB4430♀ (MSNV); 27.VII.2020 coll. (2 mines), 22.I.2021 em. 2♂, field nos NK-13-1 (♂), NK-13-3

(♂) (SIF); same label, but N. Kirichenko & E. Akulov coll., 28.VII.2020 coll. (mine), 26.XI.2020 em., field no. NK-26.11-1 (♀), genitalia slide NK-26.11-1♀ (SIF), DNA barcoded (Process ID: GPRU018-21); same label but 08.XII.2020 em., field no. NK-08.12-2 (♂), genitalia slide NK-08.12-2♀ (SIF), DNA barcoded (Process ID: GPRU017-21); same label but 29.XI.2020 em., field no. NK-29.11-1 (♀), genitalia slide NK-29.11-1♀, (SIF), DNA barcoded (Process ID: GPRU016-21); same label but 27.VII.2020 coll. (mine), 7.I.2021 em. 2♀, field nos NK-13-2 (♀), NK-10-1 (♀); same label but 28.VII.2020 coll. (mine), 24.XII.2020 em., field no. NK-11-1 (♀); 30.XII.2020 em., field no. NK-12-1 (♀);same label but 2.I.2021 em. 2♀, field nos NK-16-1 (♀), NK-11-5(♀); same label but 3.I.2021 em., 2♀, field nos NK-9-1 (♀), NK-12-3 (♀), genitalia slide NK-12-3♀; same label but 15.I.2021 em., field no. NK-10-2 (♀); same label but 19.I.2021 em., field no. NK-10-4 (♀); same label but 28.VII.2020 coll. (mine), 14.XI.2020 em. 4♀ & 1♂, field nos NK-14.11-1 (♀), NK-14.11-2 (♀), NK-14.11-3 (♀), NK-14.11-5 (♀), NK-14.11-4 (♂), genitalia slides NK-14.11-1♀, NK-14.11-2♀; same label but 26.XI.2020 em., field no. NK-08.12-3 (♀); same label but 3.XII.2020 em., field no. NK-03.12-1 (♀), genitalia slide NK-03.12-1♀; same label but 7.XII.2020 em. 3♀ & 1♂, field nos NK-07.12-1 (♀), NK-07.12-2 (♀), NK-07.12-3 (♀), NK-07.12-4(♂), genitalia slide NK-07.12-4♂; same label but 8.XII.2020 em., field no. NK-08.12-3 (♂); 15.XII.2020 em. 1♀ & 2♂, field nos NK-15.12-1 (♀), NK-15.12-2 (♂), NK-15.12-3 (♂); same label but 17.XII.2020 em. 3♀ & 1♂, field nos NK-17.12-1 (♀), NK-17.12-2 (♀), NK-17.12-3 (♀), NK-17.12-4 (♂); same label but 20.XII.2020 em. 2♂ & 2♀, field nos NK-20.12-1 (♂), NK-20.12-3 (♂), NK-20.12-2 (♀), NK-20.12-4 (♀), genitalia slide NK-20.12-2♀; same label but 25.XII.2020 em. 1♀ & 1♂, field nos NK-25.12-1 (♀), NK-25.12-2 (♂); same label but 26.XII.2020 em. 1♂ & 2♀, field nos NK-26.12-1 (♂), NK-26.12-2 (♀), NK-26.12-3 (♀), genitalia slide NK-26.12-3♀; 27.XII.2020 em. 1♂ & 2♀, field no. NK-27.12-1 (♂) (SIF).

Additional material examined. Pupa (2): Republic of Khakassia, near the Black Lake field station SIF SB RAS, along the lake bank, *Thermopsis lanceolata*, 28.VII.2020 coll. (2 mines), Kirichenko N. coll., field nos NK-28-1, NK-28-2. Larva (4): same label, (mine), filed no. Kh-NK-20-1, DNA barcoded (Process ID: GPRU044-21); same label but 27.VII.2020 coll. (2 mines), field nos NK-27-1, NK-27-2; same republic but Belyo Lake, along the lake bank, 7.VII.2020 coll. (mine), Kirichenko N. coll., filed no. Kh-NK-20-2, DNA barcoded (Process ID: GPRU045-21).

Diagnosis (Figs 4, 5). The forewing pattern of *M. baranchikovi* reflects the typical habits of the genus: a series of costal strigulae, a white band along the dorsal margin and a projection of the fringe line at apex (Fig. 4B–F). However, the genital structures allow easy identification. The male genitalia of *M. baranchikovi* are distinguished from congeners by the pointed and not rounded valvar tip (Fig. 5A, B). This character is present only in *M. sophorivora* Kuznetzov & Tristan, 1985 (Fig. 5E), which is widely distributed in central western Asia and whose larvae feed on *Sophora* and *Robinia* (Fabaceae) (Seven and Gençer 2009; De Prins and De Prins 2021). The two species are separable by the following characters in the male genitalia: (1) different inclination of

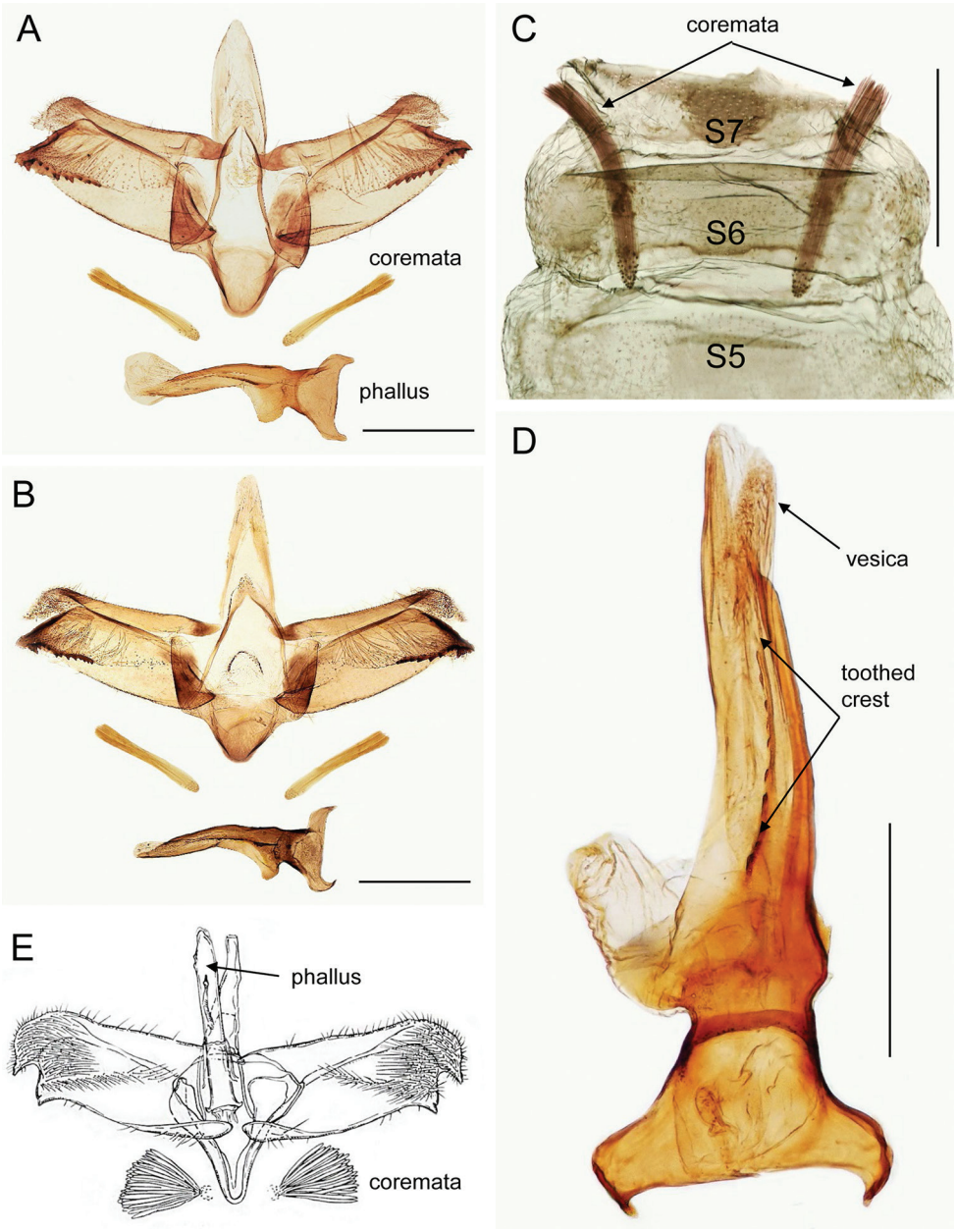

Figure 5. Male genitalia of *Micrurapteryx baranchikovi* sp. nov. **A** holotype, field no. NK-08.12-1 (♂) genitalia slide NK-08.12-1♂, DNA barcoded (Process ID: GPRU015-21) **B** paratype, field no. NK-07.12-4 (♂), genitalia slide NK-07.12-4♂ **C** paratype, field no. NK-11-3, genitalia slide TRB4428, coremata position in the abdominal segments (S) **D** paratype, field no. NK-11-3, genitalia slide TRB4428, zoomed phallus **E** male genitalia of *Micrurapteryx sophorivora* (drawing reproduced from Kuznetzov and Tristan (1985) with permission of the journal editor). Scale bars: 250 μm (**A–D**).

the valvar and saccular apices with respect to the horizontal axis of the valvae, at 90° in *M. sophorivora* versus at ca. 45° in *M. baranchikovi*; (2) straight phallus with a single and elongate cornutus, coremata wider and shorter than half phallus in *M. sophorivora* versus somewhat curved phallus, no cornuti, coremata longer than half phallus and thin in *M. baranchikovi* (Fig. 5A–E).

In the female genitalia, the differences are the following: thin ductus bursae and piriform corpus bursae with a group of thorn-like signa in *M. sophorivora*, while in *M. baranchikovi* ductus and corpus bursae are not differentiated and signa mostly absent or reduced to ca. ten microspines (Fig. 6A, D). These characters are present in the female genitalia of *M. salicifoliella*, but this species is easy distinguishable by the sclerotised section of antrum / ductus bursae protruding from the anterior margin of segment 7 (S7) (Kirichenko et al. 2016). The male genitalia of *M. baranchikovi* are very different from those of *M. salicifoliella* (see figs 28–29 in Kirichenko et al. 2016).

Description of adult (Figs 4–6). Male and female. Alar expanse 8.0–11.0 mm (51 specimens).

Head. Frons, vertex and palpi white with intermixture of dark scales around eyes. Labial palpus rather long and slender, slightly upturned; maxillary palpus ca. half of apical article of labial palpus. Antenna fuscous dorsally, scape, pedicel and ¼ of flagellum white ventrally, remaining articles ringed with paler colour; pecten absent.

Thorax. Dorsum white, ventral side and tegulae brownish grey. Legs white, fore, mid coxae and femurs dark brown outwardly, tibiae and tarsi annulated and of the same colour. Wing venation as in *M. kollariella* (see Vári 1961). Forewing dark brown in ground colour with white markings; costal margin with five white strigulae. First three strigulae almost parallel, oblique and bent outwards. First strigula very dilated on the costal margin and projected backwards, second often obsolescent, last two semi-circular, often both touching opposite margin or, in some specimens, fused apically. Fifth strigula with a dark apical dot. Dorsal margin white in basal 4/5 with two thin, linear projections distally, sometimes not connected to white margin. Cilia white around apex to tornus with dark brown tips interrupted by linear marking protruding from fringe line (not from dark apical dot). Hindwing grey ochreous, cilia pale grey.

Abdomen. Entirely brownish grey, last segments white ventrally, wider in male compared to female. A pair of thin coremata in the intersegmental membrane S5/S6, ca. half the width of S6 (Fig. 5C). S8 weakly sclerotised, tergum reduced to thin, narrow transverse band. In the female S6 shorter than or equal to preceding one and ca. a quarter of S7 long, sternum sclerotised, anterior margin with slight medial convexity (Fig. 6F).

Male genitalia. Tegumen short, subtriangular at apex, with long and thin pedunculi; tuba analis long and membranous, produced beyond tegumen, without suscaphium but with a pair of lateral lamellae, with no setae. Valva longitudinally cleft, costal region slightly concave, apex of cucullus pointed and inclined 45° with respect to longitudinal axis of valva; sacculus markedly developed, rectangular, apex produced into a pointed process with toothed margins, downward-oriented and almost parallel to cucullus (Fig. 5A, B). Phallus ca. 0.9 times length of valva, flattened, base bifurcate,

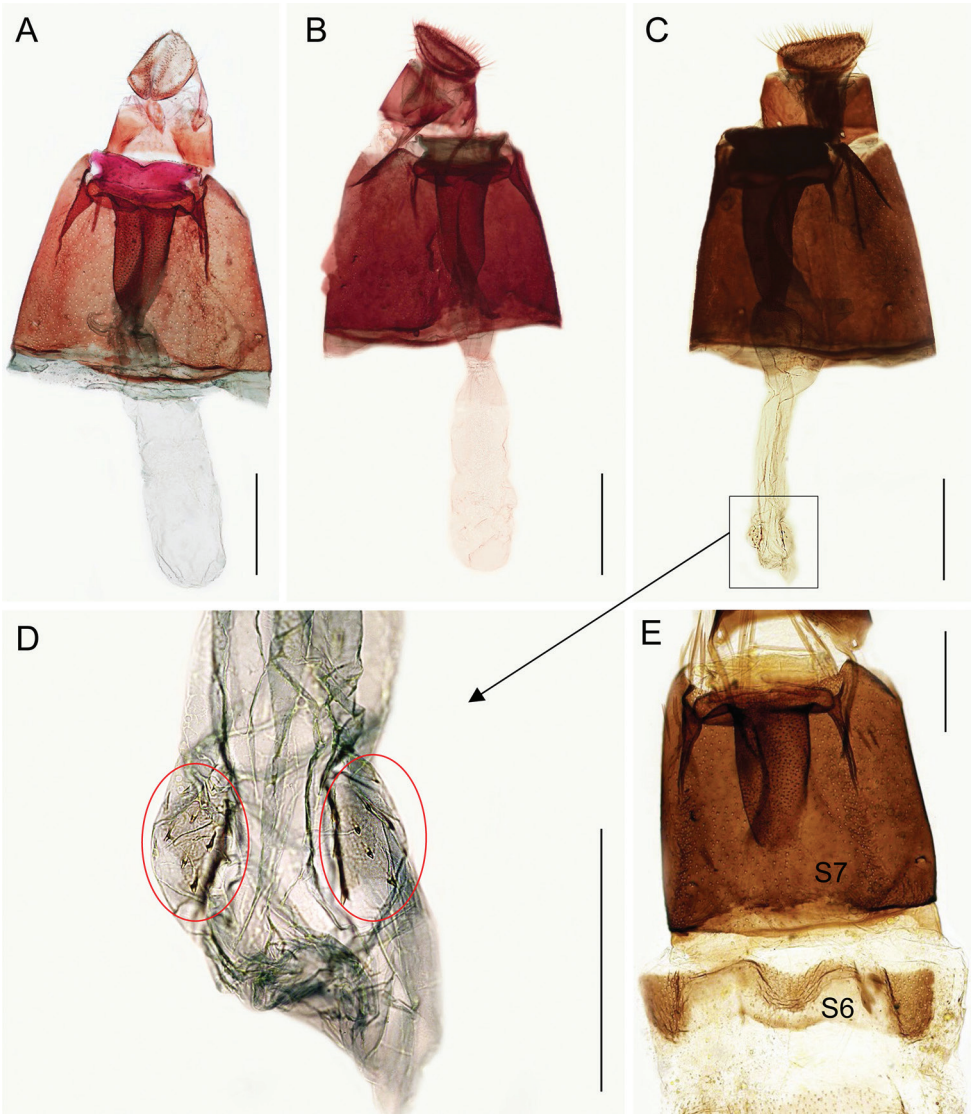

Figure 6. Female genitalia of *Micrurapteryx baranchikovi* sp. nov. **A** field no. NK-9-2 (♀), genitalia slide TRB4425 **B** field no. NK-08.12-2 (♀), genitalia slide NK-08.12-2♀, DNA barcoded (Process ID: GPRU017-21) **C** field no. NK-29.11-1 (♀), genitalia slide NK-29.11-1♀, DNA barcoded (Process ID: GPRU016-21) **D** enlarged part of bursa copulatrix with two fields of microspines (shown by red circles) **E** segments (S) 6 and 7. Scale bars 200 μm.

longitudinally a thin, mid-ventral toothed crest and a long, lateral thickening ending before a pointed apex, no cornuti (Fig. 5A, B, D).

Female genitalia. Posterior apophyses not spine-shaped but lamellar, anterior ones longer, linear, and thin. S8 short, ca. same length as posterior apophysis, weakly sclerotised. S7 ca. four times S8 long, sternum markedly sclerotised, elongate subrectangular,

its posterior margin modified in a membranous sector provided with a row of long and thin scales. This structure, supported by a sclerotised transverse bar, delimits a wide sinus vaginalis where, ventrally, the ostium bursae opens; opening of ostium is ca. half the width of S7 (Fig. 6E). Antrum and posterior section of ductus bursae undifferentiated, with dorsal wall strongly sclerotised for a length of just over half of S7 and covered with microspinules while the ventral one, membranous, bears a thin longitudinal thickening. Inception of ductus seminalis at anterior end of sclerotised section. Ductus and corpus bursae undifferentiated, signa mostly absent or reduced to ca. ten microspines. Ductus spermathecae with efferent canal forming three coils before vesicle (not shown).

Variability (Fig. 6). The new species exhibits considerable diversity in the structures of the bursa copulatrix. In most examined specimens (seven out of ten), ductus and corpus bursae are undifferentiated (Fig. 6A), in three other specimens, the ductus is narrower than corpus bursa (Fig. 6B, C). It could be due to individual variability; another explanation could be related to the method of dissection, in particular boiling, resulting in contraction of ductus in its apical part.

Another issue are microspines in the corpus bursae that were recorded in ca. half of all dissected females. In those females, two opposite weakly sclerotised plates containing ca. ten microspines were present, often hardly visible (Fig. 6C, D). Nevertheless, the adults with such variability did not differ in other morphological characters. The two females were DNA barcoded: one without microspines and another one with microspines in the corpus bursae (Fig. 6B, C); they showed very low genetic divergence (0.3%), leaving no doubt that they are one species.

Taxonomic remarks. Since it is still uncertain whether there is a separate *Thermopsis*-feeding species in North America *"Parectopa thermopsella*", here we examine the possibility that it could be conspecific with *M. baranchikovi*. To do this, we compared the Chambers's original description of *thermopsella* (Chambers 1875) with that of *M. baranchikovi.* In the genus *Micrurapteryx*, habitus is quite uniform and indistinguishable for many species (Kirichenko et al. 2016); therefore, any particular character can be important for species differentiation. We detected specific characters in adult morphology allowing to distinguish between *"Parectopa" thermopsella* and *M. baranchikovi.* These characters are listed below, with the original description of *thermopsella*'s characters italicised and provided word-by-word as it appeared in Chambers (1875), followed by the indication of differences in *M. baranchikovi*:

(1) *"Outer surface of the second joint of the palpi dark gray brown, inner surface white, third joint whitish with a brownish annulus before the tip."* In *M. baranchikovi*, labial palpi entirely white.

(2) *"Antennae dark gray brown annulated with white."* In *M. baranchikovi*, antennae with scape, pedicel and part of flagellum white ventrally, remaining articles ringed with paler colour.

(3) *"The dark brown of the disc is divided into three distinct spots by three short white streaks emitted from the white dorsal margin, and which pass a little obliquely backwards, the first placed before the middle, the second about the middle and the third behind it."* These markings are absent in the new species.

(4) *"In the grayish part of the wing are five white costal streaks; the first of these is long and narrow, beginning about the basal third of the wing length and passing obliquely backwards until it almost touches the white of the dorsal margin in the apical part of the wing, the second is wider and much shorter, the third shorter and narrower than the second, but both oblique; while the fourth is still shorter, and is nearly perpendicular to the margin."* In *M. baranchikovi*, the first streak is very dilated on the costal margin and projected backwards, while the third and fourth are well developed and almost similar, always wider than the second, which is almost obsolescent.

Larva. (Fig. 7A, C, E). The studied last instar larvae are tissue-feeders. The larva is yellow. It probably develops in five instars. The morphology does not show particular differences from *M. caraganella* (Kirichenko et al. 2016).

Pupa. (Figs 7B, D, F, 8). The young pupa is yellow, soon turns brownish; length 4.5–5.0 mm, width 0.7–1.0 mm. Frontal process (cocoon cutter) simple with pointed projection (Fig. 8); clypeal setae paired, very reduced and nearly contiguous; antenna and hindleg extended to S8; forewing to S5. Setae D1, L1 and SD1 present on S1–S7. Cremaster is very similar to *M. caraganella* (Kirichenko et al. 2016) consisting of a ring of five pairs of small spines, dorsal pair slightly enlarged, the two most ventral pairs are the smallest.

Etymology. The species is named in honour of Dr. Yuri N. Baranchikov, Russian forest entomologist and scientific supervisor of NK and EA, in recognition of his research in regional Lepidoptera and his effective 30-year heading the Black Lake field station of the V.N. Sukachev Institute of Forest SB RAS in Khakassia, around which the new *Micrurapteryx* species was discovered.

Bionomics (Figs 7G–M, 9). In Khakassia, *M. baranchikovi* develops in one generation annually. Adults are on wing in late May to early June. Oviposition takes place from early to mid-June. Eggs are laid on the lower surface of the leaves. Early instar larvae are found in the mines in late June to early July; late instar larvae in late July to early August. Pupation from early to late August; the pupae hibernate.

The mine (Fig. 9A) is similar to that of other *Micrurapteryx* species (Kirichenko et al. 2016). It starts on a lower side of the leaf (rarely on stipules) as a relatively long contorted well-visible tunnel in the epidermis (Fig. 9B). Soon the larva continues its development in a roundish or slightly branched blotch mine situated above the midrib of a leaflet (Fig. 9C, D). Older mines can occupy almost the complete leaflet (Fig. 9A). If several mines occur per leaflet, enlarging blotch mines merge and several larvae are found in one mine. Initially blotch mines are pale green, later yellowish or whitish. Severely damaged plants turn white (Fig. 9E, F); damaged leaves with abandoned mines soon turn brown and desiccate.

The blotch mines are nearly free of frass; larvae eject frass grains outside the mine by protruding the rear part of the body through a coarse slit that they gnaw in the lower epidermis. Often, frass can be found next to the slit; a few frass grains can be still seen inside the mines. Older larvae are able to vacate the mine and start a new one on a neighbouring leaflet or leaf by making a cut in the lower epidermis of leaf lamina and rapidly biting into the mesophyll.

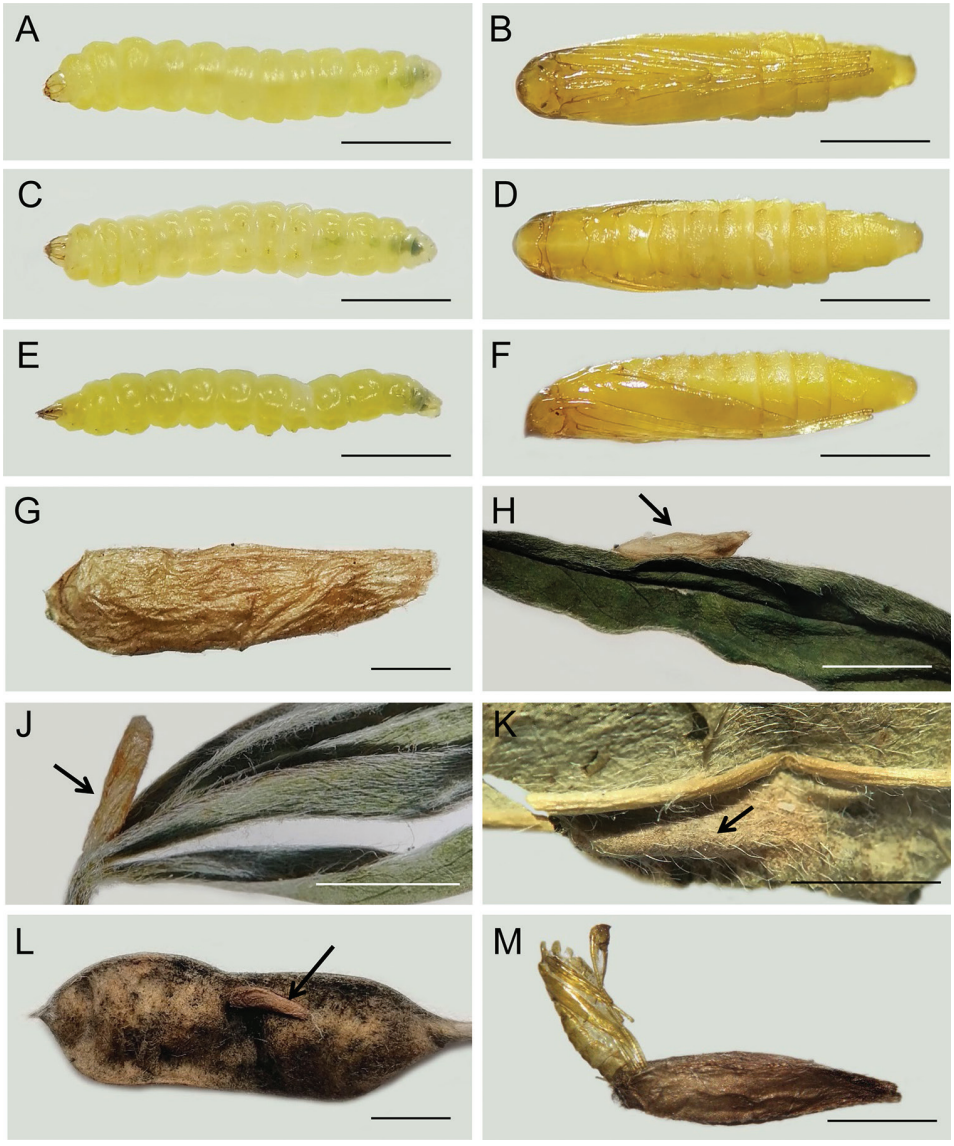

Figure 7. Premature stages of *Micrurapteryx baranchikovi* sp. nov. and pupation sites **A, C, E** mature larva before pupation [dorsal (**A**), ventral (**C**), lateral (**E**)] **B, D, F** pupa in few a hours after pupation [dorsal (**B**), ventral (**D**), lateral (**F**)] **G** cocoon **H** most common pupation site on the lower side of the leaf next to/or along the midrib. Rare pupation sites: **J** on the basis of the leaf **K** inside the leaf mine along the midrib **L** on legume surface **M** pupal exuviae protruding from cocoon. Arrows show the cocoon. Scale bars: 1.5 mm (**A–F**), 1.2 mm (**G**), 7 mm (**H–L**), 2.5 mm (**M**).

Pupation is external. The larva vacates the mine and moves to a neighbour or a distant leaf, where it spins a relatively thick cocoon (Fig. 7G). Most often pupation takes place on the lower side of the leaf lamina along the midrib (Fig. 7H). The colour and

the shape of the cocoon resembles the midrib, making it difficult to spot the cocoon. In dense populations, the pupation may occur in other places: on the upper side of the leaf next to the leaf edge, in the basis of the leaf (Fig. 7J), exceptionally inside the mine (Fig. 7K) or on a legume surface (Fig. 7L). The thick cocoon seems to help pupae to overwinter in the steppe with little or no snow cover. After adult emergence, the pupal exuviae (i.e., the 2/3 of its length) protrude through the opening of the cocoon (the least dense part of the cocoon) (Fig. 7M). In 2020, under laboratory conditions, the adults started emerging in ca. two weeks after they were moved from the fridge (where they overwintered for two month at a temperature of +3 °C) to room conditions (temperature + 23 °C, humidity 70%), and the emergence lasted for ca. one month.

Host plant. The host plant is the perennial legume herb, the lanceolate bush-pea, *Thermopsis lanceolata* (Fabaceae). The name *T. lanceolata* was proposed in 1811 by R. Brown for the plant from Siberia which was mistakenly determined in 1803 by P. Pallas under the name of *Sophora lupinoides* L. (Zhu and Kirkbride 2005). *Thermopsis lanceolata* grows in the steppe with chernozemic solonetzic and sandy soil, on stony and gravelly slopes, in meadows and agricultural fields, along lakes and rivers, as well as on disturbed areas and in/around settlements (Tolmachev 1974; Telyatiev 1985).

The plant is poisonous due to the high concentration of alkaloids (Telyatiev 1985). However, these alkaloids also make it a medical herb (Volynskiy et al. 1978). In Russia, the antitussive drugs produced from *T. lanceolata* have been utilised for decades to treat tracheitis, bronchitis and pneumonia (Telyatiev 1985; Lager 1988; Vidal Handbook 2021). Furthermore, the alcaloid cytisine extracted from *T. lanceolata* is a major component of respiratory analeptic drag against asphyxia (Telyatiev 1985). Finally, this alkaloid is also used for treating nicotine addiction (Telyatiev 1985; West et al. 2011; Hajek et al. 2013). *Thermopsis lanceolata* was reported to be weedy in some parts of Russia (Telyatiev 1985). Getting into hay, it can poison livestock, in particular horses (Telyatiev 1985; Minaeva 1991).

Distribution. The leaf mines of *Micrurapteryx baranchikovi* were found in the steppe area of the Republic of Khakassia (south-western Siberia) in two localities: around Black Lake (in 5 km from the Black Lake field station of SIF SB RA) and next to Belyo Lake (beach "Majorca"). The sampling area is situated in a temperate climatic zone (Grigoryev and Budyko 1960). Summers are dry and hot, with a number of sunny days in the republic, higher than in neighbouring regions; winters are cold, with little snow. The average air temperature in July is +18 °C, in January –19 °C (Samoilova et al. 2019). In the steppe area, the average annual precipitation is ca. 250 mm per year; up to 70% of precipitation falls in summer, of which 55% falls in August with rains and showers (Samoilova et al. 2019). The growing season lasts ca. 165 days (Samoilova et al. 2019).

It is highly likely that the moth is distributed across most of the republic where the host plant is present. Also, bearing in mind that *T. lanceolata* has rather extensive range in the Urals, in some other parts of Western and Eastern Siberia, as well as in Central Asia (Kazakhstan, Kyrgyzstan), Northern China and Mongolia (Kotunkov 1974; Telyatiev 1985; Lager 1988; Wu and Raven 2010), the occurrence of the moth in these regions is quite possible.

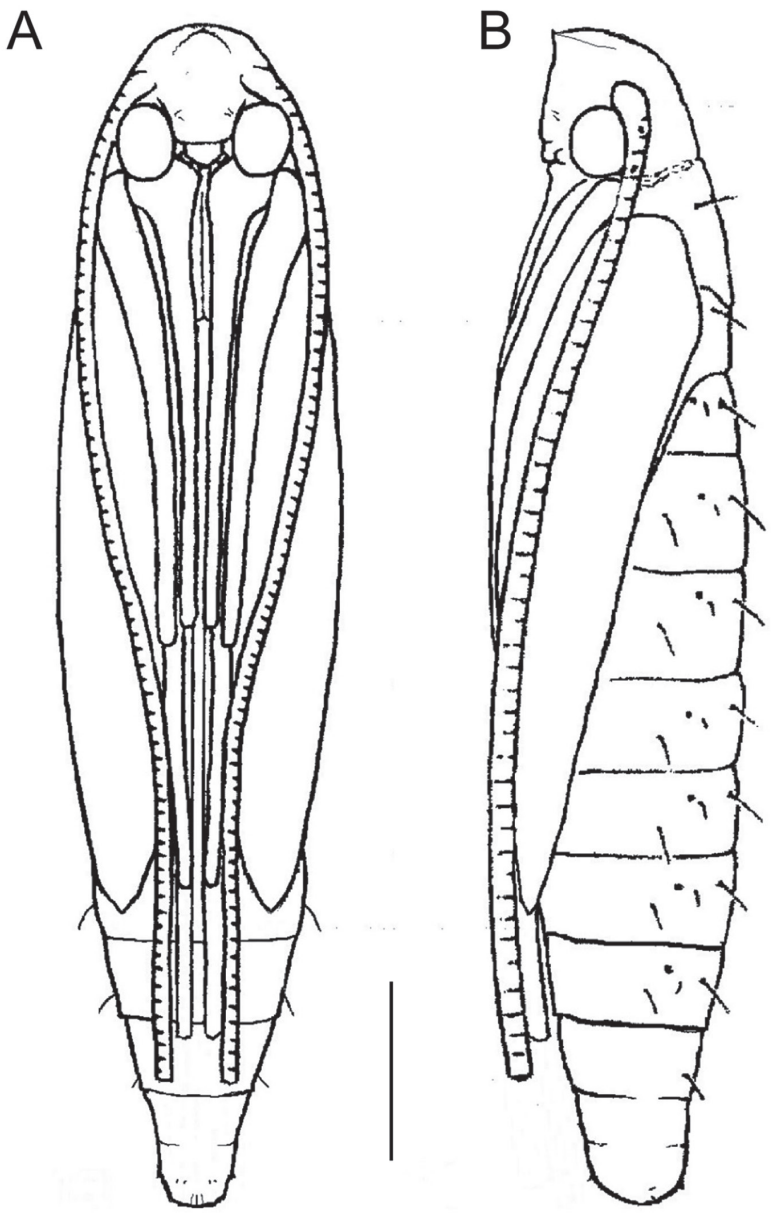

Figure 8. Pupa of *Micrurapteryx baranchikovi* sp. nov. **A** ventral view **B** lateral view. Scale bar: 0.8 mm.

Outbreak character. In July-August 2020, we recorded a local outbreak of the moth in the type locality, covering an area of ca. 500 m^2. Up to 15 mines per leaf and up to 57 mines per plant were documented. The damage peak occurred in late July to mid-August, i.e., when the leaf mines reached their maximal size (and some still con-

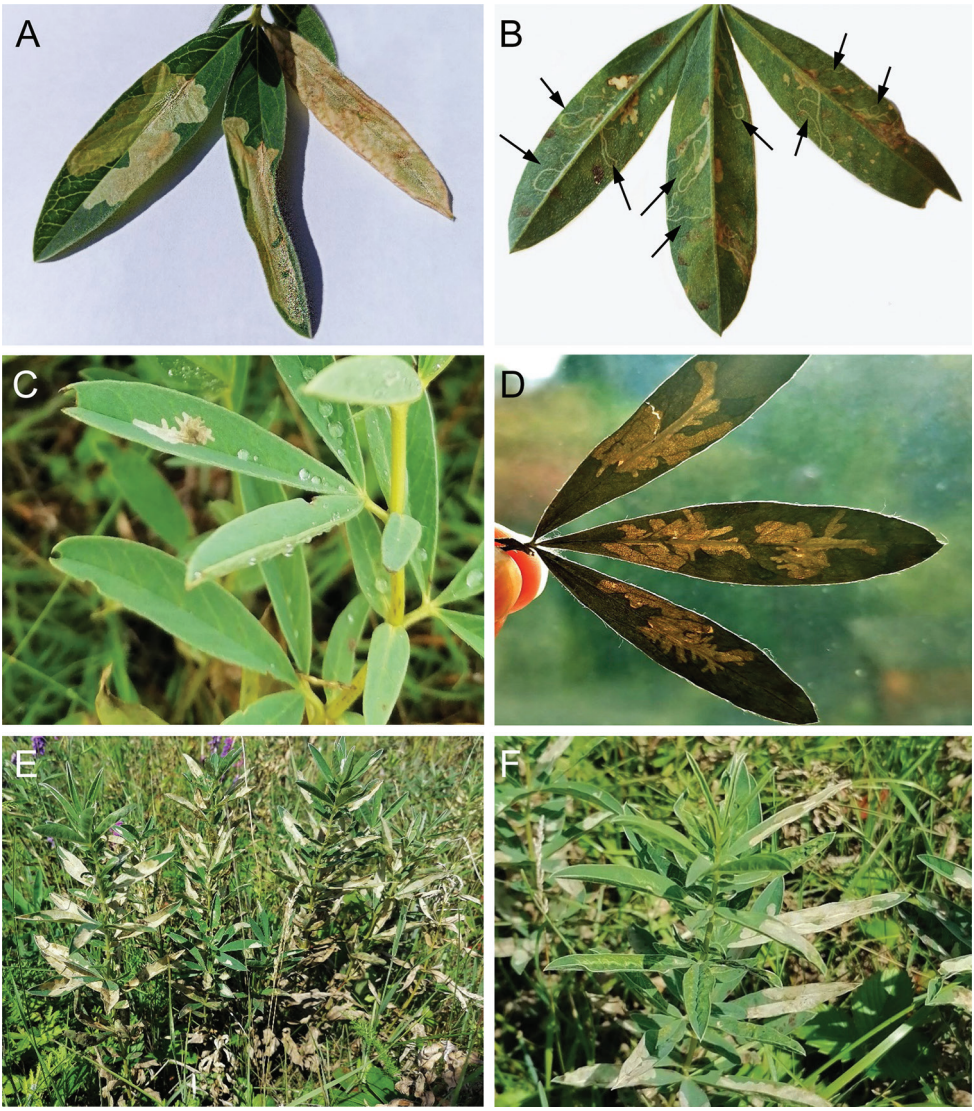

Figure 9. Leaf mines of *Micrurapteryx baranchikovi* on *Thermopsis lanceolata*, the Black Lake field station of SIF SB RAS, Khakassia, Russia **A** upper side blotch mines covering significant part of the leaflets **B** early mines (long narrow tunnels on the lower side of the leaf, the individual mines are indicated by arrows) **C** upper side branched blotch mine **D** multiple upper side branched mines in translucent light **E, F** damaged plants (with large whitish blotch mines on the leaves).

tained mature larvae) and the abandoned mines turned brown and dried out. Bearing in mind that *T. lanceolata* is used in Russia for medical purpose, severe damage caused by the new species may locally affect its harvesting in the Republic of Khakassia.

Indoor survival rate. In 2020, we obtained 53 moths from 300 pupae by indoor rearing; the survival rate of *Micrurapteryx baranchikovi* (at the pupal stage) was only

17.6% (53/300). Twenty seven out of 247 pupae were parasitised (see next section). The remaining 220 pupae (73.3%) did not succeed to develop to adults after hibernation.

Parasitoids. Overall, 27 parasitoid adults emerged from 300 pupae of *M. baranchikovi*, i.e., parasitism level was only 9% in 2020. Under laboratory conditions, the emergence of parasitoids lasted 12 days, from 10th to 21st of August.

The reared parasitoids were identified to three taxa: two braconids, *Agathis fuscipennis* (Zetterstedt, 1838) (Agathidinae) and *Illidops subversor* (Tobias & Kotenko, 1986) (Microgastrinae), and one ichneumonid *Campoplex* sp. aff. *borealis* (Zetterstedt, 1838) (Campopleginae). The identification of the first two species was done by external morphology; *A. fuscipennis* was additionally DNA barcoded, however, by its DNA barcode it was determined to genus level only. We failed to provide an exact identification of the Khakassian *Campoplex* neither by morphology nor by DNA barcoding. Morphologically, the examined specimens showed similarity to *Campoplex borealis* by colour of hind legs and shape of temple in dorsal view (see taxonomic note below).

All parasitoids reared from *M. baranchikovi* are solitary species. In our laboratory rearing, *A. fuscipennis* dominated and accounted for 18 out of 27 parasitoids (i.e., 67% of all emerged parasitoids), followed by *Campoplex* sp. aff. *borealis* (6 adults, 22%) and *I. subversor* (3 adults, 11%). They all represented novel records for the Republic of Khakassia and were documented as parasitoids of Gracillariidae for the first time.

Order Hymenoptera Linnaeus, 1758
Family Braconidae Nees, 1811
Subfamily Agathidinae Haliday, 1833
Genus *Agathis* Latreille, 1804

***Agathis fuscipennis* (Zetterstedt, 1838)**
Fig. 10

Material examined. 1♀, 1♂, Republic of Khakassia, near Black Lake field station of SIF SB RAS, 27.VII.2020 coll. (mine), 11–12.VIII.2020 em., Kirichenko N. coll, no. BL-14-20, host: *Micrurapteryx* sp. nov. (pupa), plant: *Thermopsis lanceolata*; Kirichenko N. det.; 1♀, 1♂, same labels, but 11–13.VIII.2020 em., no. BL-13-20; 1♀, same labels, but 27.VI.2020 coll. (mine), 17.VIII.2020 em., no. BL-16-20; 2♀, same labels, but 28.VII.2020 coll. (mine), 13–17.VIII.2020 em., no. BL-11-20; 1♂, same labels, but 28.VII.2020 coll. (mine), 14.VIII.2020 em., no. BL-1-20-2; 2♂, same labels, but 28.VII.2020 coll. (mine), 16–18.VIII.2020 em., no. BL-12-20; 1♀, 1♂, same labels, but 28.VII.2020 coll. (mine), 18–21.VII.2020 em., no. BL-9-20; 1♀, same labels, but VII.2020 coll. (mine), 17–19.VIII.2020 em. no. BL-8-20-1 (legs taken for DNA); 3♂, same labels, but 28.VII.2020 coll. (mine), 14–20.VIII.2020 em., no. BL-10-20; 2♂, same labels, but VII.2020 coll. (mine), 11–16.VIII.2020 em., no. BL-7-20-2. All deposited in ZISP.

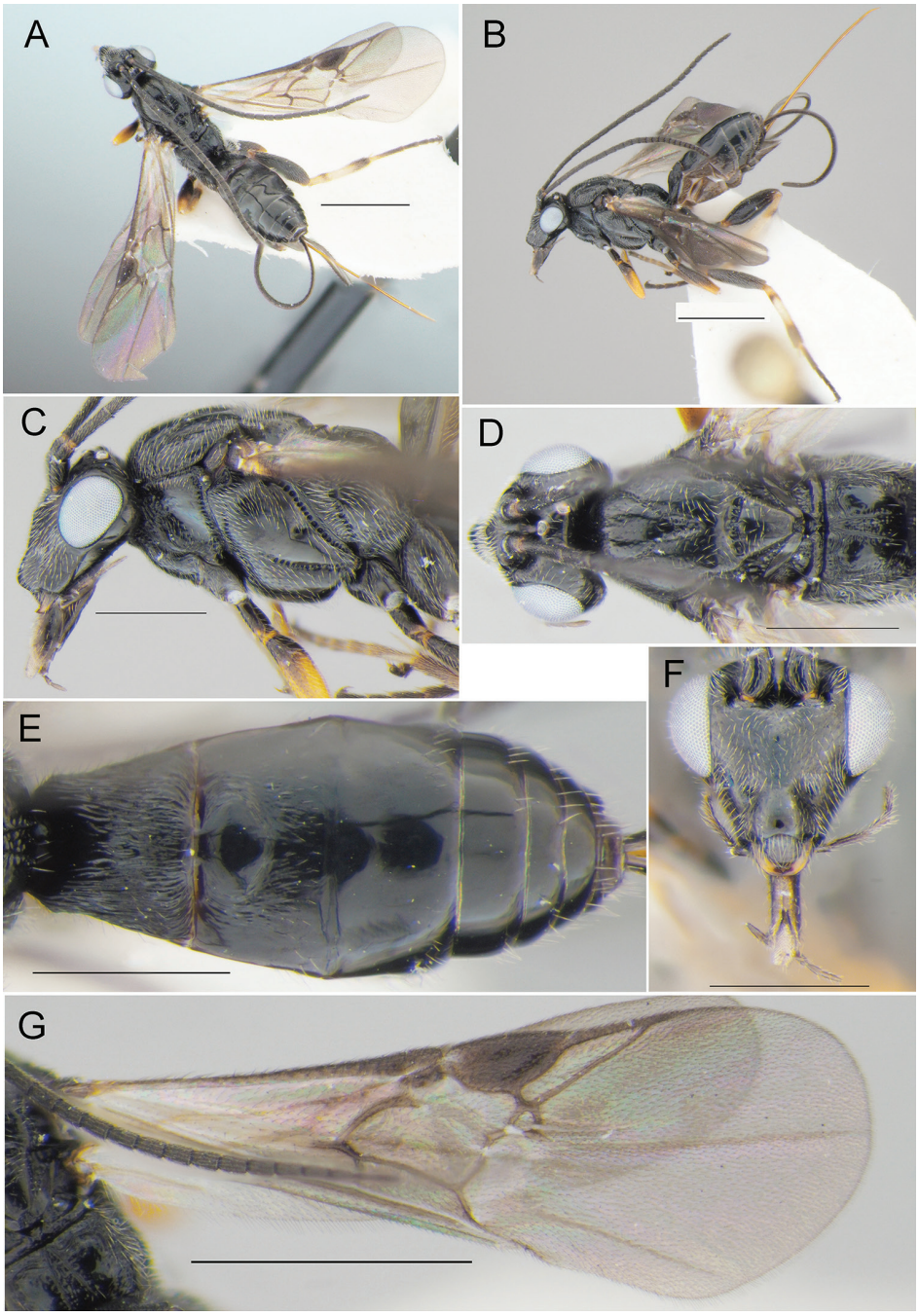

Figure 10. *Agathis fuscipennis* (Zetterstedt, 1838) (♀, reared specimen, 27.VII.2020 (mine) coll., 11-12.VIII.2020 em., no. BL-13-20, host: *Micrurapteryx baranchikovi* sp. nov., the Republic of Khakassia, Russia) **A** habitus, dorsal view **B** habitus, lateral view **C** head and mesosoma, lateral view **D** head and mesosoma, dorsal view **E** metasoma, dorsal view **F** head, front view **G** fore wing. Scale bars: 1 mm (**A, B, G**), 0.5 mm (**C–F**).

Hosts. (from Yu et al. 2016). **Lepidoptera, Coleophoridae**: *Coleophora albicostella* (Duponchel, 1842) [on *Potentilla* sp.: Rosaceae]; *C. albitarsella* Zeller, 1849 [on *Origanum vulgare*: Lamiaceae]; *C. artemisiae* Mühlig. 1864; *C. artemisicolella* Bruand, 1855; *C. chamaedriella* Bruand, 1852; *C. conspicuella* Zeller, 1849 [on *Aster linosyris*: Asteraceae]; *C. conyzae* Zeller, 1868 [on *Pulicaria dysenterica*: Asteraceae]; *C. cracella* (Vallot, 1835); *C. dianthi* Herrich-Schaffer, 1855; *C. follicularis* Vallot, 1802 [on *Pulicaria dysenterica*: Asteraceae]; *C. granulatella* Zeller, 1849; *C. inulae* Wocke, 1877 [on *Pulicaria dysenterica*: Asteraceae]; *C. linosyridella* Fuchs, 1880; *C. meridionella* Rebel, 1912; *C. salicorniae* Heinemann & Wocke, 1877; *C. salinella* Stainton, 1859; *C. vestianella* (Linnaeus, 1758). **Gelechiidae**: *Aproaerema anthyllidella* (Hübner, 1813) [on *Anthyllis* sp.: Fabaceae]; *Caryocolum saginella* (Zeller, 1868); *Chrysoesthia drurella* (Fabricius, 1775); *Ch. sexguttella* (Thunberg, 1794) [on *Chenopodium album*: Amaranthaceae]; *Scrobipalpa atriplicella* (Fischer v. Röslerstamm, 1841) [on *Chenopodium album*: Amaranthaceae]; *S. gallicella* (Constant, 1885); *S. ocellatella* (Boyd, 1858); *Thiotricha subocellea* (Stephens, 1834); *Tuta absoluta* (Meyrick, 1917) [on *Solanum nigrum*: Solanaceae]. **Gracillariidae:** *Micrurapteryx baranchikovi* sp. nov. [on *Thermopsis lanceolata*: Fabaceae] (**new record**). **Heliodinidae**: *Heliodines roesella* (Linnaeus, 1758) [on *Atriplex* sp.: Amaranthaceae]. **Epermeniidae**: *Ochromolopis ictella* (Hübner, 1813). **Tortricidae**: *Olethreutes arbutella* (Linnaeus, 1758); *Spilonota ocellana* (Denis & Schiffermüller, 1775).

Distribution. (according to Yu et al. 2016; Belokobylskij et al. 2019). Russia: Moscow Province, Perm Territory, Altai Territory, Krasnoyarsk Territory, the Republic of Khakassia (**new record**), Irkutsk Province, Zabaikalskiy Territory. Tunisia, Western and Central Europe, Armenia, Turkey, Iran, Kazakhstan, Uzbekistan, Tajikistan, Mongolia, Korea.

Remarks. The species from the Republic of Khakassia has been DNA barcoded for the first time. Given reliable species identification on morphology, the obtained sequence (process ID GPRU034-21) can be used as a reference DNA barcode for molecular-based identification of *Agathis fuscipennis.*

Subfamily Microgastrinae Foerster, 1863
Genus *Illidops* Mason, 1981

***Illidops subversor* (Tobias & Kotenko, 1986)**
Fig. 11

Apanteles subversor Tobias & Kotenko, 1986: 422; Yu et al. 2016.
Illidops subversor (Tobias & Kotenko, 1986): Kotenko 2007: 178; Belokobylskij et al. 2019: 296.

Material examined. 1♀, Republic of Khakassia, near Black Lake field station of SIF SB RAS, 27.VII.2020 coll. (mine), 10.VIII.2020 em., Kirichenko N. coll, no. BL-17-20, host: *Micrurapteryx* sp. nov. (pupa), plant: *Thermopsis lanceolata*, Kirichenko N.

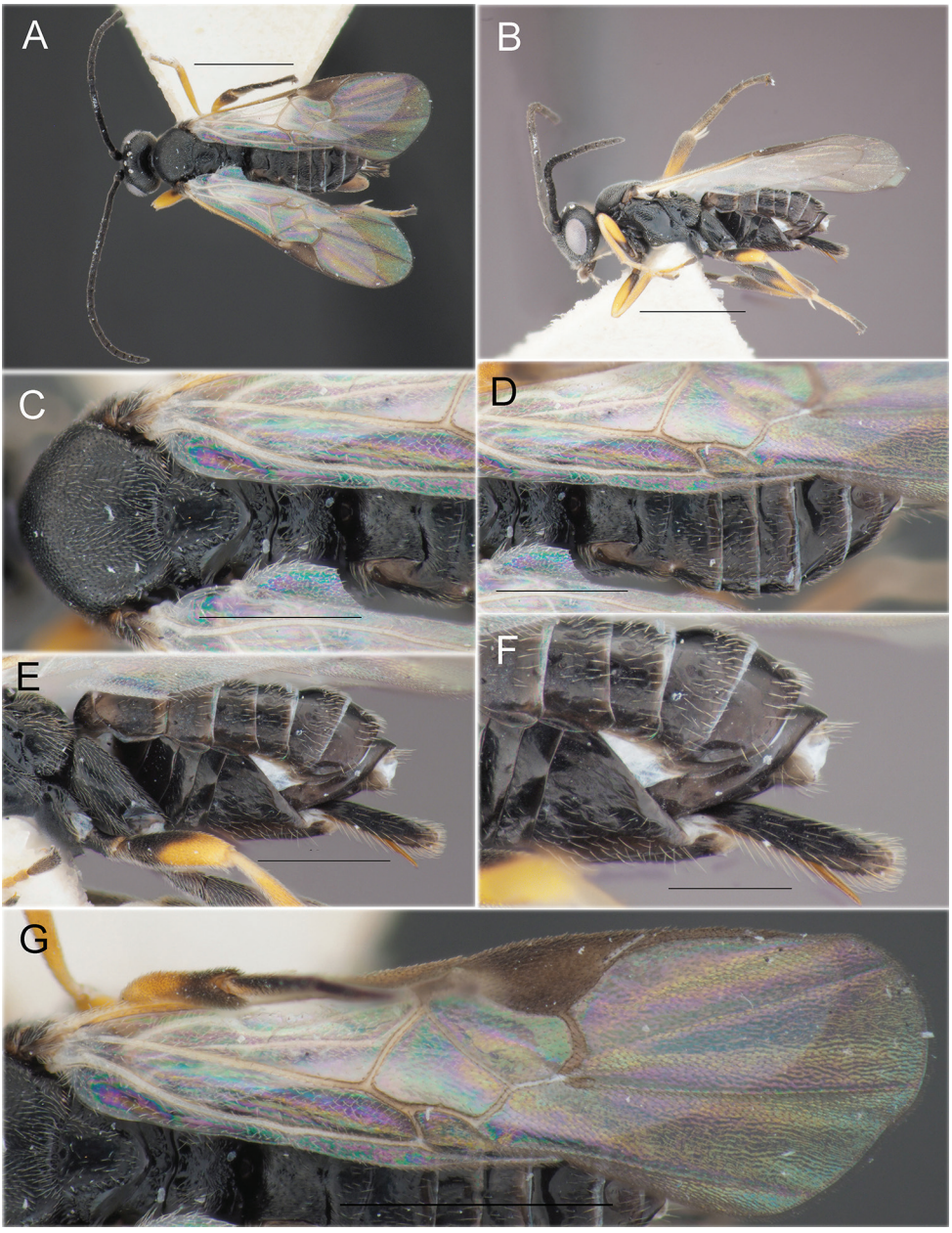

Figure 11. *Illidops subversor* (Tobias & Kotenko, 1986) (♀, reared specimen, 28.VII.2020 (mine) coll., 12.VIII.2020 em., no. BL-4-20, host: *Micrurapteryx baranchikovi* sp. nov., the Republic of Khakassia, Russia) **A** habitus, dorsal view **B** habitus, lateral view **C** mesosoma, dorsal view **D** metasoma, dorsal view **E** metasoma, lateral view **F** apical part of metasoma and ovipositor, lateral view **G** fore wing. Scale bars: 1 mm (**A, B, G**), 0.5 mm (**C–E**), 0.3 mm (**F**).

det.; 1♀, same labels, but 28.VII.2020 coll. (mine), 12.VIII.2020 em., no. BL-4-2; 1♂, same labels, but "7.VII.2020 coll. (mine), 18–23.VII.2020 em., no BL-0-20. All deposited in ZISP.

Hosts. Gracillariidae: *Micrurapteryx baranchikovi* sp. nov. [on *Thermopsis lanceolata* Brown: Fabaceae] (**new record**).

Distribution. (according to Belokobylskij et al. 2019). Russia: Novosibirsk Province, the Republic of Khakassia (**new record**).

Remarks. The specimens from Khakassia are very similar to the only known specimen, the holotype of *I. subversor* from the south of Western Siberia. However, in the holotype, the pterostigma is irregularly coloured, yellowish-brown medially and dark brown marginally, whereas in reared specimens of *I. subversor* from Khakassia, the pterostigma is mainly dark brown to almost black, but brownish yellow in a small basal spot (Fig. 11G). Such variation in pterostigma colour is known in parasitoids and may be related to specimen preservation.

Family Ichneumonidae Latreille, 1802
Subfamily Campopleginae Foerster, 1869
Genus *Campoplex* Gravenhorst, 1829

***Campoplex* sp. aff. *borealis* (Zetterstedt, 1838)**
Fig. 12

Material examined. 1♀, Republic of Khakassia, near Black Lake field station of SIF SB RAS, along the lake bank, 28.VII.2020 coll. (mine), 14.VIII.2020 em., Kirichenko N. coll., no. BL-1-20-1 (legs taken for DNA), host: *Micrurapteryx* sp. nov. (pupa), plant: *Thermopsis lanceolata*; Kirichenko N. det.; 1♀, same labels, but 15.VIII.2020 em., no. BL-3-20; 1♂, same labels, but 13–17.VIII.2020 em., no BL-11-20; 1♀, same labels, but 17.VIII.2020 em., no. BL-5-20; 1♂, same labels, but 18–21.VIII.2020 em., no. BL-9-20; 1♂, same labels, but VII.2020 coll. (mine), 11–16.VIII.2020 em., no. BL-7-20-1 (legs taken for DNA). All deposited in ZISP.

Hosts. *Micrurapteryx baranchikovi* sp. nov. (Gracillariidae).

Distribution. Republic of Khakassia.

Remarks. Morphologically, the specimens of *Campoplex* sp. aff. *borealis* from Khakassia are very similar to *Campoplex borealis* from the Western Palearctic (Zetterstedt, 1838) (Andrey I. Khalaim det.), with hind femur dark reddish brown to black, as was already recorded in the specimens from north-west of European Russia (Yu et al. 2016). However, DNA barcoding highlights a significant divergence (i.e., 7.3%) between the Khakassian specimens and *C. borealis* identified from Germany (Fig. 3, Suppl. material 3: Table S3). Such a divergence may suggest the presence of a cryptic species in Khakassia. To test this hypothesis, a special study, involving more sampling across the distributional range of *C. borealis*, would be needed.

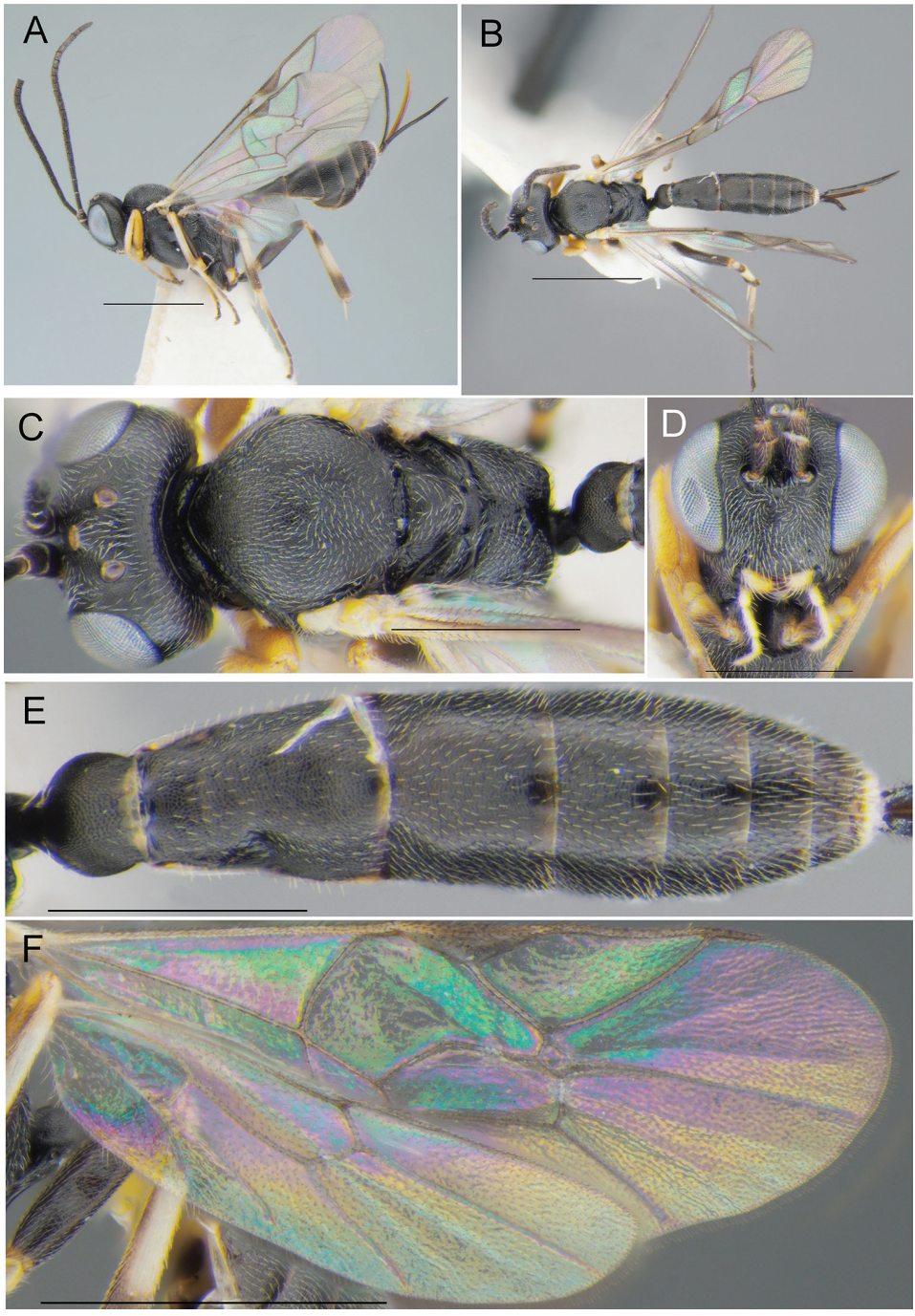

Figure 12. *Campoplex* sp. aff. *borealis* (Zetterstedt, 1838) (♀, reared specimen, 28.VII.2020 (mine) coll., 15.VIII.2020 em., no. BL-3-20, host: *Micrurapteryx baranchikovi*, the Republic of Khakassia, Russia) **A** habitus, lateral view **B** habitus, dorsal view **C** head and mesosoma, dorsal view **D** head, front view **E** metasoma, dorsal view **F** wings. Scale bars: 1 mm (**A, B, F**), 0.5 mm (**C–E**).

Discussion

Based on integrative taxonomy, we discovered a new species of gracillariid in the Republic of Khakassia (Siberia, Russia) that is described here as *Micrurapteryx baranchikovi* sp. nov. We showed that morphologically the male of the new species is somewhat similar to the Central Asian *M. sophorivora* feeding on *Sophora* (Fabaceae), whereas the female shows similarity to the North American *M. salicifoliella* feeding on *Salix* and *Populus* (Salicaceae). We highlighted the morphological characters differentiating *M. baranchikovi* from "*Parectopa*" *thermopsella* described in the XIX century in Colorado (USA) feeding on *Thermopsis* (Chambers 1875). Genetically, the new species is divergent from studied representatives of the genus *Micrurapteryx*, with 9.3% of interspecific divergence to the nearest neighbour *M. kollariella*. Morphologically, the latter is significantly different from *M. baranchikovi*. Furthermore, it feeds on a variety of Genisteae legumes, except *Thermopsis* (the tribe Sophoreae) (De Prins and De Prins 2021). The relatedness of *M. baranchikovi* to *Sophora*-feeding *Micrurapteryx* could be explained by the host plant phylogeny: *Thermopsis* (the host plant of *M. baranchikovi*) and *Sophora* (the host of *M. sophorivora*) are from one tribe Sophoreae, whereas Genisteae, on which *Micrurapteryx kollariella* feeds, is a genetically divergent tribe (Cardoso et al. 2013). This hypothesis will need further exploration for which molecular data of all Fabaceae-feeding *Micrurapteryx* would be required.

The new species has the ability to form outbreaks on *Thermopsis lanceolata*, as we documented for the Republic of Khakassia in 2020. This plant is harvested for medical purpose in some regions of Russia, including the Republic of Khakassia (Telyatiev 1985). For that purpose, all parts of the plant (except roots) are collected: green parts are harvested during the flowering period in June-July, whereas seeds are collected in August-September (Telyatiev 1985). As we showed in our study, the major damage caused by larvae of *M. baranchikovi* occurs in late July – mid August, which coincides with the harvesting period. The plants with damaged brownish leaves are not collected (Volynskiy et al. 1978). The natural population of *T. lanceolata* have declined due to exhaustive harvesting (Minaeva 1991), and the new moth may potentially affect the populations of this beneficial medical plant in the studied region.

In 2020, we documented a surprisingly low parasitism rate in the dense population of *M. baranchikovi*: only 9% of the pupae were infested by parasitoids. Furthermore, only three parasitoid species were found to attack the new moth species. Notably, before our study both braconids, *Agathis fuscipennis* and *Illidops subversor*, and the ichneumonid, *Campoplex* sp. aff. *borealis*, all reared from *M. baranchikovi* pupae, have never been reported as parasitoids of Gracillariidae.

In general, parasitoids associated with gracillariids are diverse and can be highly abundant; moreover, many parasitoid species are shared by different gracillariid species. For example, the parasitoid complex of the poplar leaf miner, *Phyllonorycter populifoliella*, a native outbreaking species in Russia, counts at least 68 species (Ermolaev 2019). In some years, the parasitoids are able to kill up to 77% of the moth's larvae and pupae (Belova 1994). Many of these native parasitoid species were recruited by the

East Asian *Phyllonorycter issikii* (Kumata, 1963) during its invasion to European Russia (Ermolaev et al. 2018).

So far, parasitoids have been known only for two *Micrurapteryx* species: *M. sophorivora* and *M. kollariella* (De Prins and De Prins 2021). As documented in Turkey, *M. sophorivora* is attacked exclusively by chalcidoids: *Baryscapus nigroviolaceus* (Nees, 1834), *Cirrospilus pictus* (Nees, 1834), *Necremnus croton* (Walker, 1839), *Neochrysocharis arvensis* Graham, 1963, *N. formosus* (Westwood, 1833), *Pnigalio* sp. (all from family Eulophidae) and *Pteromalus* sp. (Pteromalidae) (Gençer and Seven 2005). In Europe, for *M. kollariella* three parasitoids were recorded: one eulophid, *Pnigalio agraules* (Walker, 1839) and two ichneumonids, *Diadegma holopyga* (Thomson, 1887) and *Scambus annulatus* (Kiss, 1924) (Vidal and Buszko 1990; Sawoniewicz and Buszko 1994). The majority of these parasitoid species are also known in Europe on various gracillariids, in particular on the representatives of five subfamilies: *Cameraria*, *Phyllonorycter* (Lithocolletinae), *Caloptilia*, *Gracillaria* (Gracillariinae), *Parornix* (Parornichinae), *Metriochroa* (Oecophyllembiinae), and *Phyllocnistis* (Phyllocnistinae) (Kawahara et al. 2016). Surprisingly, in our study we found none of these species parasitising *M. baranchikovi*, despite that some occur in Russia (Belokobylskij et al. 2019).

Our study highlights the complexity of identifying the species of *Campoplex* from the Republic of Khakassia based on both morphology and DNA barcoding. Representatives of Campopleginae are still very scarcely studied in Russia (Belokobylskij et al. 2019). As a result, the Khakassian specimens are only preliminary determined here as *Campoplex* sp. aff. *borealis*. Furthermore, we noticed a mismatch in *C. multicinctus* identification in BOLD, and we suspect misidentification of one Finnish specimen of *C. multicinctus* on this platform that turned to be highly similar genetically to the Khakassian *C.* sp. aff. *borealis*. However, the latter morphologically and genetically is more similar to *C. borealis*, as we have shown in the study. We do not exclude that the Siberian *C.* sp. aff. *borealis* may represent a cryptic species.

Further study would be needed to define the range of the new moth and assess its potential impact on *T. lanceolata*, as well as to explore the complex of parasitoids associated with *M. baranchikovi* in Siberia and clarify their intraspecific divergence at morphological and molecular genetic levels.

Acknowledgements

We thank Jean-François Landry (Canada) and Charley Eiseman (USA) for fruitful discussions on *Thermopsis*-feeding *Micrurapteryx* and the comments on *M. occulta* and "*Parectopa" thermopsella*, Svetlana V. Shishova and Ekaterina A. Kirichenko (Krasnoyarsk, Russia) for assistance in the field, Dmitry R. Kasparyan and Andrei I. Khalaim (St. Petersburg, Russia) for consultation and determination of Campopleginae, Marko Mutanen (Finland), Torbjørn Ekrem (Norway), Evgeny V. Zakharov (Canada), Tatsiana Lipinskaya (Belarus), Caroline Chimeno (Germany)

for allowing us to use the sequences of parasitoid species, Irina A. Mikhailova (Krasnoyarsk, Russia) for helping with mapping, and Olga V. Kuznetsova (Siberian Federal University, Krasnoyarsk, Russia) for English language checking. Special thanks to Erik J van Nieukerken (the Netherlands), Camiel Doorenweerd (USA), and Tengteng Liu (China) for thoughtful revision of the manuscript. NK was partially supported by the Russian Foundation for Basic Research (project No. 19-04-01029-a) [field sampling, morphological and molecular genetic analysis] and the basic project of Sukachev Institute of Forest SB RAS, Krasnoyarsk, Russia (project No. 0287-2021-0011) [indoor rearing]. SAB received support from the Russian Foundation for Basic Research (project No. 19-04-00027) and the Russian State Research Project (No. AAAA–A19–119020690101–6). We also thank the team at the Biodiversity Institute of Ontario, University of Guelph (Ontario, Canada) for their great assistance in the production of DNA barcodes.

References

Bai HY (2013) A new species of *Micrurapteryx* Spuler (Lepidoptera: Gracillariidae) from Tibet, China. Entomological News 122(4): 324–327. https://doi.org/10.3157/021.122.0404

Belokobylskij SA, Samartsev KG, Il'inskaya AS [Eds] (2019) Annotated catalogue of the Hymenoptera of Russia. Volume II. Apocrita: Parasitica. Proceedings of the Zoological Institute Russian Academy of Sciences. Supplement 8. Zoological Institute RAS, St. Petersburg, 594 pp. https://doi.org/10.31610/trudyzin/2019.supl.8.5

Belova NK (1994) Pests of urban green spaces. Zashchita rasteniy (Plant protection) 8: 37–38. [In Russian]

Braun AF (1925) Microlepidoptera of northern Utah. Transactions of the American Entomological Society 51: 183–226.

Cardoso D, Pennington RT, de Queiroz LP, Boatwright JS, Van Wyk B-E, Wojciechowski MF, Lavin M (2013) Reconstructing the deep-branching relationships of the papilionoid legumes. South African Journal of Botany 89: 58–75. https://doi.org/10.1016/j.sajb.2013.05.001

Chambers VT (1875) Teneina [sic] of Colorado. The Cincinnati Quarterly Journal of Science 2(4): 289–305.

Davis DR (1983) Gracillariidae. In: Hodges RW (Ed.) Check list of the Lepidoptera of America North of Mexico including Greenland. EW Classey Ltd., Faringdon, and The Wedge Entomological Research Foundation, Washington, 9–11.

De Prins J, De Prins W (2021) Global Taxonomic Database of Gracillariidae (Lepidoptera). http://www.gracillariidae.net

de Waard JR, Ivanova NV, Hajibabaei M, Hebert PDN (2008) Assembling DNA barcodes: analytical methods. In: Cristopher M (Ed.) Methods in molecular biology: environmental genetics. Humana Press Inc., Totowa, USA, 275–293. https://doi.org/10.1007/978-1-59745-548-0_15

Eiseman C (2019) Leafminers of North America. Self-published e-book, clii + 1857 pp. [*Thermopsis*, 807–808.]

Ermolaev IV (2019) Ecological mechanisms of nonperiodical population wave: a case study of the poplar leafminer – *Phyllonorycter populifoliella* (Lepidoptera, Gracillariidae). Zhurnal Obshchei Biologii (Journal of General Biology) 80(6): 451–476. [In Russian] https://doi.org/10.1134/S0044459619060034

Ermolaev IV, Yefremova ZA, Domrachev TB (2018) The influence of parasitoids (Hymenoptera, Eulophidae) on the survival of the lime leafminer (*Phyllonorycter issikii*, Lepidoptera, Gracillariidae) in Udmurtia. Zoologicheskii Zhurnal (Zoological Journal) 97(4): 401–407. [In Russian] https://doi.org/10.1134/S0013873818040024

Gençer L, Seven S (2005) Chalcidoid parasitoids of *Micrurapteryx sophorivora* (Lepidoptera: Gracillariidae) in Kuluncak, Turkey. Phytoprotection 86: 133–134. https://doi.org/10.7202/012513ar

Grigoryev AA, Budyko MA (1960) Classification of the Climates of the USSR. Soviet Geography 1: 3–24. [In Russian] https://doi.org/10.1080/00385417.1960.10769843

Hajek P, McRobbie H, Myers K (2013) Efficacy of cytisine in helping smokers quit: systematic review and meta-analysis. Thorax 68 (11): 1037–1042. https://doi.org/10.1136/thoraxjnl-2012-203035

Hebert PDN, Ratnasingham S, Zakharov EV, Telfer AC, Levesque-Beaudin V, Milton MA, Pedersen S, Jannetta P, deWaard JR (2016) Counting animal species with DNA barcodes: Canadian insects. Philosophical Transactions of the Royal Society B 371: 20150333. https://doi.org/10.1098/rstb.2015.0333

Jeanmougin F, Thompson JD, Gouy M, Higgins DG, Gibson TJ (1998) Multiple sequence alignment with Clustal X. Trends in Biochemical Sciences 23: 403–405. https://doi.org/10.1016/S0968-0004(98)01285-7

Kawahara AY, Plotkin D, Ohshima I, Lopez-Vaamonde C, Houlihan PR, Breinholt JW, Kawakita A, Xiao L, Regier JC, Davis DR, Kumata T, Sohn JC, De Prins J, Mitter C (2017) A molecular phylogeny and revised higher-level classification for the leaf-mining moth family Gracillariidae and its implications for larval host-use evolution. Systematic Entomology 42(1): 60–81. https://doi.org/10.1111/syen.12210

Kirichenko N, Triberti P, Mutanen M, Magnoux E, Landry J-F, Lopez-Vaamonde C (2016) Systematics and biology of some species of *Micrurapteryx* Spuler (Lepidoptera, Gracillariidae) from the Holarctic Region, with re-description of *M. caraganella* (Hering) from Siberia. ZooKeys 579: 99–156. https://doi.org/10.3897/zookeys.579.7166

Klots A (1970) Lepidoptera. In: Tuxen SL (Ed.) Taxonomist's glossary of genitalia in insects. Munksgaard, Copenhagen, 115–139.

Kotenko AG (2007) Subfam. Microgastrinae. In: Lelej AS (Ed.) Key to insects of the Russian Far East. Vol. IV. Neuropteroidea, Mecoptera, Hymenoptera. Pt 5, Dalnauka, Vladivostok, 134–192. [In Russian]

Kotunkov GN (1974) The cultivated and wild medical plants: the handbook. Naukova Dumka, Kiev, 174 pp. [In Russian]

Kristensen NP (2003) Skeleton and muscles: adults. In: Kristensen NP (Ed.) Lepidoptera, Moths and Butterflies (Volume 2) – Morphology, physiology, and development. Handbook of Zoology 36(4), Walter de Gruyter, Berlin, 39–131. https://doi.org/10.1515/9783110893724.39

Kumar S, Stecher G, Li M, Knyaz C, Tamura K (2018) MEGA X: Molecular evolutionary genetics analysis across computing platforms. Molecular Biology and Evolution 35: 1547–1549. https://doi.org/10.1093/molbev/msy096

Kuznetzov VI, Tristan NI (1985) A review of the leaf blotch miners of the genus *Micrurapteryx* Spuler (Lepidoptera Gracillariidae) of the Palaearctic fauna. Entomologicheskoe Obozrenie 64(1): 177–192. [In Russian]

Lager AA (1988) Phytotherapy. Krasnoyarsk University, Krasnoyarsk, 272 pp. [In Russian]

McDunnough J (1939) Check list of the Lepidoptera of Canada and the United States of America. Part II. Microlepidoptera. Memoirs of the Southern California Academy of Sciences 2(1): 1–171.

Meyer CP, Paulay G (2005) DNA barcoding: Error rates based on comprehensive sampling. PLoS Biology 3: 2229–2238. https://doi.org/10.1371/journal.pbio.0030422

Minaeva VG (1991) The medical plants of Siberia. Nauka, Siberian branch, Novosibirsk, 431 pp. [In Russian]

Noreika R, Puplesis R (1992) Description of new species of moths of the family Gracillariidae (Lepidoptera) from Azerbaijan and Middle Asia and synonymy of *Gracillaria impictipennella* Grsm. Entomological Review 74(5): 43–51.

Ratnasingham S, Hebert PDN (2007) BOLD: The Barcode of Life Data System (http://www.barcodinglife.org). Molecular Ecology Notes 7: 355–364. https://doi.org/10.1111/j.1471-8286.2007.01678.x

Ratnasingham S, Hebert PDN (2013) A DNA-based registry for all animal species: the barcode index number (BIN) system. PLoS ONE 8(8): e66213. https://doi.org/10.1371/journal.pone.0066213

Robinson GS (1976) The preparation of slides of Lepidoptera genitalia with special reference to the Microlepidoptera. Entomologist´s Gazette 27: 127–132.

Samoylova GS, Goryachko MD, Kyzlasov IL, Torbostaev KM, Goryachko MD, Prokinova AN, Seleverstov VV, Kyzlasov IL (2019) Khakassia. Nature: climate. In: Kravets SL (Ed.) The Great Russian Encyclopedia. https://bigenc.ru/geography/text/5454659 [In Russian]

Sawoniewicz J, Buszko J (1994) Ichneumonidae (Hymenoptera) reared from mining Lepidoptera in Poland. Wiadomosci Entomologiczne 13(1): 55–61.

Seven S, Gençer L (2009) Contribution to the biology and distribution of the leaf-mining moth *Micrurapteryx sophorivora* Kuznetzov & Tristan, 1985 (Lepidoptera Gracillariidae). SHILAP 37: 511–514.

Simbolotti G, van Achterberg C (1999) Revision of the west Palaearctic species of the genus *Agathis* Latreille (Hymenoptera: Braconidae: Agathidinae). Zoologische Verhandelingen Leiden 325: 1–167.

Telyatiev VV (1985) Useful plants of Central Siberia. East Siberian publishing house, Irkutsk, 384 pp. [In Russian]

Tobias VI, Belokobylskij SA, Kotenko AG (1986) Fam. Braconidae. In: Medvedev GS (Ed.) Opredelitel Nasekomych Evrospeyskoy Chasti SSSR 3, Pereponchatokrylye 4. [Keys to insects of the European part of USSR. Hymenoptera.]. Nauka, Leningrad, 500 pp. [In Russian]

Tolmachev AI [Ed.] (1974) The key to the plants of Yakutia. Nauka, Novosibirsk, 543 pp. [In Russian]

Vári L (1961) South African Lepidoptera (Vol. I) – Lithocolletidae. Transvaal Museum Memoir 12: 1–238.

Vidal Handbook: Medical drugs in Russia (2021) Cough tablets (Antitussive pills): instructions for use. https://www.vidal.ru/drugs/antitussive_tablets__30376 [In Russian]

Vidal S, Buszko J (1990) Studies on the mining Lepidoptera of Poland. VIII. Chalcidoid wasps reared from mining Lepidoptera (Hymenoptera, Chalcidoidea). Polskie Pismo Entomologiczne 60: 73–103.

Vieira V, Karsholt O (2010) Lepidoptera, 219–221. In: Borges PAV, Costa A, Cunha R, Gabriel R, Gonçalves V, Martins AF, Melo I, Parente M, Raposeiro P, Rodrigues P, Santos RS, Silva L, Vieira P, Vieira V (Eds) A list of the terrestrial and marine biota from the Azores, Princípia, Cascais, 432 pp.

Volynskiy BG, Bender KI, Freidman SL, Bogoslovskaya SI, Voronona KV, Glazyrina GA, Kaprelova TS, Koloskova IG, Kuznetsova IG, Martynov LA (1978) Medical plants in traditional and folk medicine. 5th edn. Saratov University, Saratov, 360 pp. [In Russian]

West R, Zatonski W, Cedzynska M, Lewandowska D, Pazik J, Aveyard P, Stapleton J (2011) Placebo-controlled trial of cytisine for smoking cessation. New England Journal of Medicine 365(13): 1193–1200. https://doi.org/10.1056/NEJMoa1102035

Wu Z, Raven PH [Eds] (2010) Flora of China. Beijing, Science Press, St. Louis, Missouri Botanical Garden Press 10: 1–642.

Yu DSK, van Achterberg C, Horstmann K (2016) Taxapad 2016, Ichneumonoidea 2015. Database on flash-drive (CD). www.taxapad.com

Zhu X, Kirkbride Jr JH (2005) Proposal to conserve the names *Thermopsis lanceolata* and *Sophora lupinoides* with a conserved type (Leguminosae). Taxon 55(4): 1047–1049. https://doi.org/10.2307/25065715

Supplementary material 1

Table S1

Authors: Natalia I. Kirichenko, Evgeny N. Akulov, Paolo Triberti, Sergey A. Belokobylskij

Data type: Specimen data

Explanation note: The list of specimens of *Micrurapteryx* and parasitoid specied involved into molecular genetic analysis.

Link: https://doi.org/10.3897/zookeys.1061.70929.suppl1

Supplementary material 2

Table S2

Authors: Natalia I. Kirichenko, Evgeny N. Akulov, Paolo Triberti, Sergey A. Belokobylskij

Data type: Genetic data

Explanation note: The list of diagnostic substitutions in COI mtDNA gene in *Micrurapteryx baranchikovi* sp. nov. and *M. kollariella*.

Link: https://doi.org/10.3897/zookeys.1061.70929.suppl2

Supplementary material 3

Table S3

Authors: Natalia I. Kirichenko, Evgeny N. Akulov, Paolo Triberti, Sergey A. Belokobylskij

Data type: Genetic data

Explanation note: Genetic divergences in COI mtDNA gene in studied *Campoplex* parasitoids.

Link: https://doi.org/10.3897/zookeys.1061.70929.suppl3

ZooKeys 1061: 165–190 (2021)
doi: 10.3897/zookeys.1061.72235
https://zookeys.pensoft.net

RESEARCH ARTICLE

A peer-reviewed open-access journal
ZooKeys
Launched to accelerate biodiversity research

The *Herniosina* story continues in the Mediterranean: *H. calabra* sp. nov. from Calabria and *H. erymantha* Roháček, new female from the Peloponnese (Diptera, Sphaeroceridae)

Jindřich Roháček[1]

1 *Silesian Museum, Nádražní okruh 31, CZ-746 01 Opava, Czech Republic*

Corresponding author: Jindřich Roháček (rohacek@szm.cz)

Academic editor: Owen Lonsdale | Received 27 July 2021 | Accepted 30 August 2021 | Published 11 October 2021

http://zoobank.org/7D7A95CB-C84A-4729-A756-BB8615958E79

Citation: Roháček J (2021) The *Herniosina* story continues in the Mediterranean: *H. calabra* sp. nov. from Calabria and *H. erymantha* Roháček, new female from the Peloponnese (Diptera, Sphaeroceridae). ZooKeys 1061: 165–190. https://doi.org/10.3897/zookeys.1061.72235

Abstract

A study of recently acquired material of *Herniosina* Roháček, 1983 (Diptera: Sphaeroceridae: Limosininae) in the Mediterranean subregion revealed a new species, *H. calabra* **sp. nov.** (Italy: Calabria: Serre Calabresi Mts) and the first females of *H. erymantha* Roháček, 2016 (Greece: southern Peloponnese: Taygetos Mts). *Herniosina calabra* **sp. nov.** (both sexes) and the female of *H. erymantha* are described and illustrated in detail including structures of terminalia, their relationships are discussed and new information on their biology (habitat association) is given. An update of a key to all know species of *Herniosina* species is presented.

Keywords

Biology, distribution, Europe, *Herniosina* Roháček, key, Limosininae, relationships, taxonomy, terminalia

Introduction

The genus *Herniosina* Roháček, 1983 (Sphaeroceridae: Limosininae) has recently been reviewed by Roháček (2016), including all known species. In the latter study the genus was re-diagnosed without the Nearctic *H. voluminosa* Marshall, 1987 which has been removed so that the genus is monophyletic. *Herniosina voluminosa* was later transferred to a

monobasic genus *Voluminosa* Roháček & Marshall, 2017 because it lacks the majority of the defining apomorphies of the Palaearctic *Herniosina*, see Roháček and Marshall (2017).

Herniosina was originally described during the re-classification of the previous genus *Limosina* Macquart, 1835 by Roháček (1982, 1983) for two European species, *H. bequaerti* (Villeneuve, 1917) and *H. horrida* (Roháček, 1978). A third species, *H. pollex* Roháček, 1993, was added by Roháček (1993) from Central Europe and two more species, *H. erymantha* Roháček, 2016 and *H. hamata* Roháček, 2016 have recently been described from the E. Mediterranean area (Greece and Cyprus) by Roháček (2016). In addition, there is a record of an unnamed species of *Herniosina* (based on two females) from Israel (Papp and Roháček 1988: 89, as *Herniosina* sp. cf. *horrida*). Discovery of new *Herniosina* species in the eastern Mediterranean (Roháček 2016) indicated that there could also be undescribed species in other parts of the area, and, therefore, our subsequent collecting trips to the Mediterranean have been focused on the acquisition of further material of this largely terricolous and/or subterranean genus. These collecting efforts resulted in two series of *Herniosina* specimens, one from southern Peloponnese (Taygetos Mts) and the other from Calabria (Serre Calabresi Mts). While the former proved to belong to *H. erymantha* and includes the first known females of the species, the other has been recognised to represent an unnamed species morphologically somewhat intermediate between *H. erymantha* and *H. bequaerti*.

The genus *Herniosina* has been newly diagnosed by Roháček (2016: 74–75). This diagnosis does not need a revision after the inclusion of the new species being described below. *Herniosina* species can be most easily recognised by a combination of (largely apomorphic) features in the male abdomen and terminalia (postabdomen strongly down-curved, S1+2 more or less bulging, S5 strongly reduced, cerci modified to peculiar projections, both distiphallus and phallophore projecting posteroventrally) and the (largely plesiomorphic) structures of the female postabdomen (narrow and telescopic, sclerites of 6th and 7th segments and also 8th tergum well developed, no internal sclerites, cerci usually long and slender), however, with reduced S8 and S10.

Material and methods

Material

All the material examined (including specimens of *Herniosina bequaerti* used for illustrations but not listed below) is deposited in **SMOC**, Slezské zemské muzeum, Opava, Czech Republic.

Methods of preparation and study of postabdominal structures

Abdomens of some specimens were detached, cleared by boiling several minutes in 10% solution of potassium hydroxide (KOH) in water, then neutralised in 10% solution of acetic acid (CH_3COOH) in water, washed in water and subsequently transferred to glycerine. Postabdominal structures were dissected and examined in a drop of glycerine under binocular microscopes (Reichert, Olympus). Detailed examinations of genital structures

were performed with a compound microscope (Zeiss Jenaval). After examination, all dissected parts were put into small plastic tubes containing glycerine, sealed with hot forceps and pinned below the respective specimens. Specimens with abdomen removed and terminalia dissected are indicated in the list of material by the abbreviation **genit. prep.**

Drawing techniques and photography

Legs were drawn on squared paper using a Reichert binocular microscope with an ocular screen. Details of the male and female genitalia were drawn by means of Abbe's drawing apparatus on a compound microscope (Zeiss Jenaval) at larger magnification (130–500×). Wings were photographed on the compound microscope Olympus BX51 with an attached digital camera (Canon EOS 1200D). Whole adult (dry-mounted) specimens and wings were photographed by means of a digital camera Canon EOS 5D Mark III with a Nikon CFI Plan 10×/0.25NA 10.5 mm WD objective attached to a Canon EF 70–200 mm f/4L USM zoom lens. The specimen photographed by means of the latter equipment was repositioned upwards between each exposure using a Cognisys StackShot Macro Rail and the final photograph was compiled from multiple layers (20–40) using Helicon Focus Pro 7.0.2. The final images were edited in Adobe Photoshop CS6.

Measurements

Six main characteristics of the new species were measured: body length (measured from anterior margin of head to end of cercus, thus excluding the antenna), index t_2 : mt_2 (= ratio of length of mid tibia : length of mid basitarsus), wing length (from wing base to wing tip), wing width (maximum width), C-index (Cs_2 : Cs_3) (= ratio of length of 2nd costal sector : length of 3rd costal sector) and index rm\dm-cu : dm-cu (= ratio of length of section between rm and dm-cu on discal cell : length of dm-cu). All type specimens and also all newly collected specimens of *H. erymantha* were measured.

Presentation of faunistic data

Label data of primary-type specimens are presented strictly verbatim including information on form and colour of all associated labels. Data from paratypes of the new species and also from formerly unpublished non-type specimens are standardised and presented in full. Phenological and other biological information obtained from the material examined and literature are given in the Biology paragraph.

Morphological terminology

Morphological terminology follows that used for Sphaeroceridae by Roháček (1998) in the Manual of Palaearctic Diptera including terms of the male hypopygium. The "hinge" hypothesis of the origin of the eremoneuran hypopygium, re-discovered and documented by Zatwarnicki (1996), has been accepted and, therefore, the following synonymous terms of the male genitalia (emanating from other hypotheses) need to be listed (terms used first):

ejacapodeme = ejaculatory apodeme, epandrium = periandrium, medandrium = intraperiandrial sclerite, phallapodeme = aedeagal apodeme. Morphological terms of the male postabdomen and genitalia are depicted in Figs 3–13, those of the female postabdomen in Figs 17–19. Abbreviations of morphological terms used in text and illustrations are listed below.

Abbreviations of morphological terms used in text and/or figures

A_1 anal vein;
ac acrostichal (seta);
ads additional (setulae) on frons;
C costa;
ce cercus;
Cs_2, Cs_3 -2nd, 3rd costal sector;
CuA_1 cubitus;
dc dorsocentral (seta);
dm discal medial cell;
dm-cu discal medial-cubital (= posterior, tp) cross-vein;
dp distiphallus;
ea ejacapodeme;
ep epandrium;
f_1, f_2, f_3 fore, mid, hind femur;
g genal (seta);
gs gonostylus;
hu humeral (= postpronotal) (seta);
hy hypandrium;
ifr interfrontal (seta);
M media;
mt_2 mid basitarsus;
oc ocellar (seta);
occe outer occipital (seta);
occi inner occipital (seta);
ors fronto-orbital (seta);
pg postgonite;
pha phallapodeme;
pp phallophore;
pvt postvertical (seta);
R_1 1st branch of radius;
R_{2+3} 2nd branch of radius;
R_{4+5} 3rd branch of radius;
r-m radial-medial (= anterior, ta) cross-vein;
S1–S10 abdominal sterna;
sc scutellar (seta);
stpl sternopleural (= katepisternal) (seta);
T1–T10 abdominal terga;

t_1, t_2, t_3	fore, mid, hind tibia;
va	ventroapical seta on t_2;
vi	vibrissa;
vte	outer vertical (seta);
vti	inner vertical (seta).

Results

***Herniosina calabra* sp. nov.**
http://zoobank.org/54BE995C-8C1C-4A16-A968-9EF47B986734
Figs 1–20

Type material. ***Holotype*** ♂ labelled: "ITALY: W Calabria: Serre Calabresi Mts, Mongiana 2.4 km N, 38°32'05"N, 16°19'06"E", "1000 m, 25.5.2018, in tufts of *Juncus* in alder forest, J. Roháček leg.", "Holotypus ♂ *Herniosina calabra* sp. n., J. Roháček det. 2021" (red label). The specimen is dry-mounted on pinned triangular card, intact (SMOC 06/001/2018-1, Fig. 1). ***Paratypes*:** 8♂ 12♀ with same locality labels but with "Paratypus [♂ or ♀], *Herniosina calabra* sp. n., J. Roháček det. 2021" yellow labels; 3♂ 3♀ paratypes with abdomen detached, genitalia dissected and all removed parts preserved in glycerine in coalesced plastic tube pinned below the specimen, 1♂

Figure 1. *Herniosina calabra* sp. nov., male laterally (holotype). Body length ~ 2.3 mm.

Figure 2. *Herniosina calabra* sp. nov., wing (male paratype). Wing length ~ 2.1 mm.

with wing removed for photography and also preserved in glycerine in pinned plastic tube below the specimen (SMOC 06/001/2018-2 – 06/001/2018-21).

Etymology. The name of the new species is an adjective derived from Calabria (a region in southern Italy) where the type locality of the new species is situated.

Description. Male (Fig. 1). Total body length 2.06–2.46 mm; general colour blackish brown with mostly very sparse dark greyish brown microtomentum, hence body relatively shining. ***Head*** blackish brown to brown, lightest on gena. Frons blackish brown posteriorly to brown anteriorly, sparsely microtomentose and largely shining. Occiput blackish brown to black with sparse dark greyish brown microtomentum. Orbits, interfrontalia (very narrow, poorly delimited) and ocellar triangle also greyish brown to dark grey (orbits) microtomentose and duller than rest of frons; frontal triangle relatively narrow, glabrous and shining. Cephalic chaetotaxy: pvt absent, only minute adpressed postocellar setulae behind ocellar triangle; occe distinctly shorter than occi, the latter ~ 2/3 length of vte; vti longest among frontal setae, vte and oc slightly shorter than vti; two strongly exclinate and closely situated ors, posterior longer than anterior and both distinctly shorter than oc; 4 to (usually) 5 relatively short ifr, 1 or 2 middle pairs slightly longer than others; 4 very minute ads inside and below ors; g weak, hardly longer than anterior peristomal seta; vi long, ~ as long as vti. Frontal lunule short, wide, basally brown as anterior margin of frons, apically darkened. Face with cavities below antennae dark brown to black, shining despite sparse greyish microtomentum; medial carina distinct although slightly elevated. Gena high, brown in anterior half, blackish brown posteriorly, sparsely grey microtomentose. Eye relatively small; its longest diameter ~ 1.9 × as long as smallest genal height. Antenna relatively long, black or 3rd segment blackish brown; 3rd segment distinctly tapered apically both in dorsal and lateral view, with cilia on apex as long as those longest on arista. Arista long, ~ 3.8 × as long as antenna, in basal 1/4 short ciliate, otherwise moderately long ciliate.

Thorax dark brown to black, mesonotum relatively shining because of sparse microtomentum, pleuron more densely microtomentose and duller (Fig. 1). Some su-

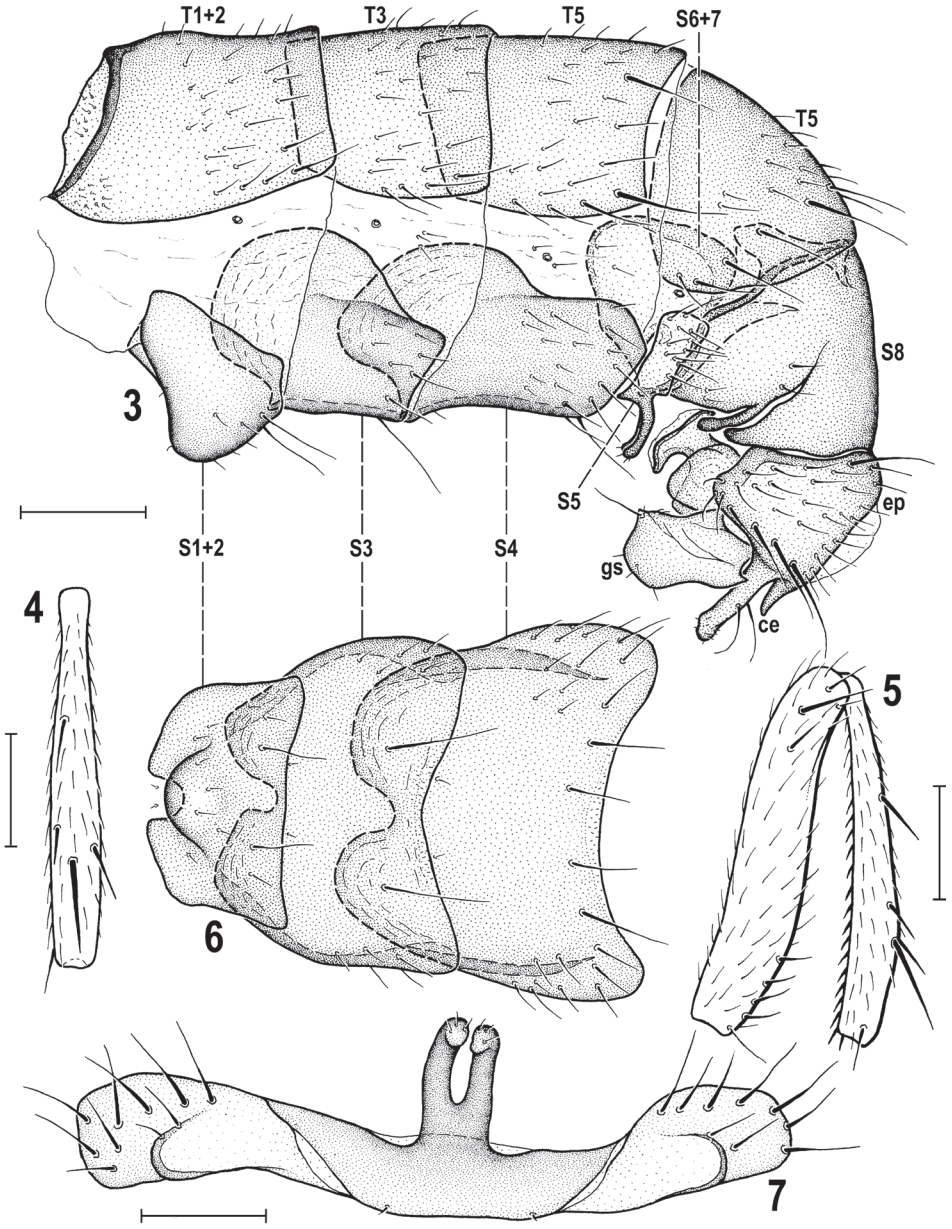

Figures 3–7. *Herniosina calabra* sp. nov. (male paratype). **3** Abdomen, laterally **4** mid tibia, dorsally **5** mid femur and tibia, anteriorly **6** preabdominal sterna, ventrally **7** S5, ventrally. Abbreviations: ce – cercus, ep – epandrium, gs – gonostylus, S – sternum, T – tergum. Scale bars: 0.2 mm (**3, 6**); 0.3 mm (**4, 5**); 0.1 mm (**7**).

tures between pleural sclerites pale brown. Scutellum relatively large and long, rounded triangular, with dorsal surface flat and finely microsculptured, duller than mesonotum. Thoracic chaetotaxy: 2 hu but internal reduced to microseta; 2 postsutural dc, anterior short and weak (only 2 × longer than dc microsetae), posterior strong, ~ as long as or

slightly shorter than basal sc; 8–10 rows of ac microsetae on suture; medial prescutellar ac pair somewhat prolonged and thickened but shorter than anterior dc; 2 strong sc, basal slightly longer than scutellum, apical (longest thoracic seta) ~ 1.5 × as long as basal; only 1 stpl because anterior stpl reduced to hardly discernible microseta.

Legs dark brown, coxae, trochanters, knees and tarsi brown to pale brown. f_1 with sparse and relatively short setae in posterodorsal and posteroventral rows. f_2 with a row of 4–6 curved but relatively short ventral setae in basal third (Fig. 5) in addition to the usual fine basal seta; t_2 ventrally with a long row of small dense spines terminated by a strongly reduced va seta (markedly shorter than anteroapical seta), see Fig. 5; dorsal chaetotaxy of t_2 as in congeners including relatively variable-in-length posterodorsal seta in apical fourth (Fig. 4). $t_2 : mt_2 = 1.91–2.02$.

Wing (Fig. 2) with pale brownish membrane and pale brown to blackish brown veins. C hardly produced beyond apex of R_{4+5}. R_{2+3} slightly sinuate to straight but apically distinctly upcurved to C; R_{4+5} sinuate but with apical half almost straight. Discal cell (dm) variable, relatively short to medium long, distally more or less tapered, usually with small process of M beyond dm-cu (venal fold of M continuing this process usually well visible); posterior outer corner of dm cell obtuse-angled, often with small to minute process of CuA_1 beyond dm-cu, rarely rounded (1 specimen). A_1 slightly sinuate; anal lobe well developed; alula narrow but not acute. Wing measurements: length 1.88–2.32 mm, width 0.77–0.97 mm, C-index = 0.87–1.17, rm\dm-cu : dm-cu = 2.87–3.67. Haltere with dirty yellow stem and dark brown knob.

Abdomen blackish brown to black, with only some postabdominal sclerites brown. Preabdominal terga (Figs 1, 3) large, shining, with only scarce greyish microtomentum, mostly sparsely and shortly setose (but with setae more numerous than in *H. erymantha*). T1+2 longest abdominal tergum. T4 distinctly longer than T3; T5 enlarged, although less than that of *H. bequaerti*, and postabdomen strongly down-curved (Fig. 3). T4 with 1 long seta in each posterior corner; T5 with 4–6 long setae at posterior margin (Fig. 3). Preabdominal sterna modified similarly as in relatives but differing in detail (Figs 3, 6): S1+2 strongly bulging (Fig. 3) and anteromedially narrowly desclerotised, appearing incised (Fig. 6); S3 and S4 deeply anteriorly emarginate due to enlarged posterolateral lobes (Fig. 6); however, these lobes can be smaller (weakly developed) in the smallest specimens; S1+2, S3 and S4 with sparse setae, largely at posterior and lateral margins; S1+2 and S3 with only 1 medial pair of setae long; S4 with 2 pairs of long setae at posterior margin. S5 (Fig. 7) reduced (shortened) and transversely strip-shaped, with pale-pigmented setose lateral parts as in relatives but with darker medial part provided with a long, somewhat flattened (in lateral view slightly bent, see Figs 3, 36) and deeply forked process carrying 2 or 3 setulae on apex of each digitiform lobe (Fig. 7). S6 and S7 coalesced to a complex asymmetrical sclerite hidden under T5 and S8 on left side of postabdomen, narrow ventrally and dorsally but laterally dilated and provided with several flat, keel-like internal lobes (Fig. 3). S8 as long as T5, somewhat tapered posteriorly, with 2 pairs of setulae and with a distinct slit left laterally, the margins of which terminate in 2 slender dark-pigmented digitiform lobes (see Fig. 3).

Genitalia. Epandrium (Figs 8, 9) slightly longer but narrower than that of *H. erymantha* although also angular dorsolaterally (see Fig. 9), with a group of longer and stronger setae laterally and lateroventrally (posterior seta longest and most robust) and

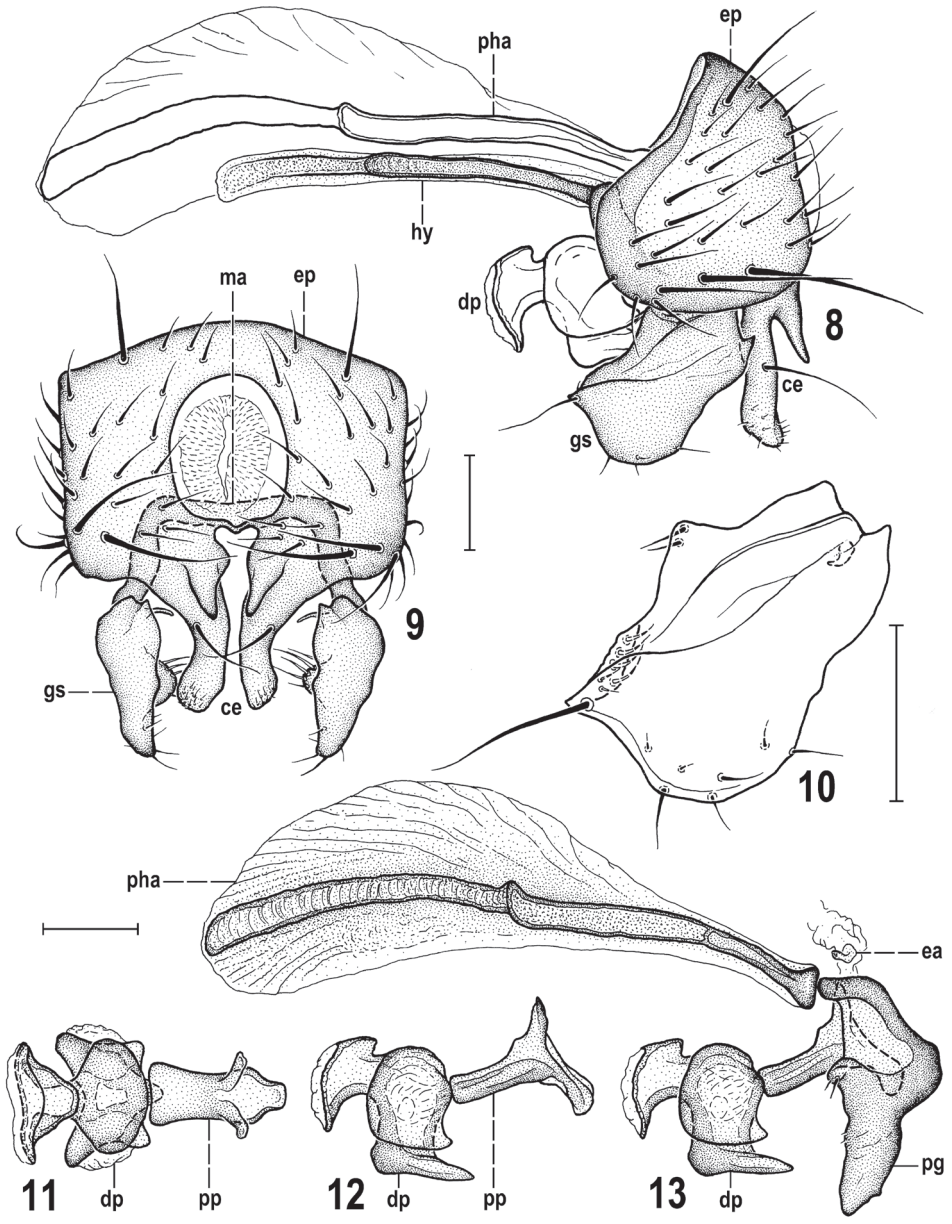

Figures 8–13. *Herniosina calabra* sp. nov. (male paratype). **8** Genitalia, laterally **9** external genitalia, caudally **10** gonostylus, laterally **11** aedeagus, dorsally **12** ditto, laterally **13** aedeagal complex, laterally. All scale bars 0.1 mm. Abbreviations: ce – cercus, dp – distiphallus, ea – ejacapodeme, ep – epandrium, gs – gonostylus, hy – hypandrium, ma – medandrium, pg – postgonite, pha – phallapodeme, pp – phallophore.

also dorsolaterally with 1 longer seta (as in *H. bequaerti*). Anal fissure narrower than high (Fig. 9), suboval, thus more resembling that of *H. bequaerti*. Cerci fused with epandrium, each posteroventrally projecting in 2 processes most similar to those of *H. erymantha*: one (more anterior) robust, almost as long as gonostylus and distally

slightly dilated and bearing 1 long seta in addition to series of microsetulae, the other (posterior and more medial) short, lengthwise conical, and bare (Figs 8, 9). Anterior process of cercus differing from that of *H. erymantha* in having distal half distinctly bent out (see Fig. 9). Medandrium low, somewhat reduced and connected by long internal arms with gonostyli (Fig. 9), and posteromedially fused with cerci. Hypandrium with long (though shorter than in *H. bequaerti* and *H. erymantha*) and slender anteromedial rod-like apodeme (Fig. 8). Gonostylus (Figs 8, 9, 10) sub-oblong in lateral view, most resembling that of *H. erymantha* but wider, posterodorsally bearing a distinct tooth (Fig. 10) and its slender dorsal internal process (visible on Fig. 9) short, slightly curved. Aedeagal complex (Figs 11–13) with large and long phallapodeme (as in both relatives) normally provided by large dorsal keel (as in *H. bequaerti*). However, size of phallapodeme and its keel can be reduced in small specimens. Aedeagus most similar to that of *H. bequaerti* because distiphallus is short, with both lateral lobes and an unpaired ventral process short (Figs 11, 12). Postgonite short and robust as that of *H. bequaerti*, differing mainly by robust and non-curved apex (Fig. 13). Phallophore resembling those of both relatives, anteriorly rod-like but dorsoventrally flattened (cf. Figs 11 and 12), posteriorly projecting ventrally and hence epiphallus-like. A minute, pale-pigmented ejacapodeme can be seen close to base of postgonites (Fig. 13).

Female (Fig. 14). Similar to male unless mentioned otherwise below. Total body length 2.10–2.78 mm. f_2 ventrally without curved setae, with only 1 fine basal seta; t_2 ventrally finely setulose and with 1 long va seta (Fig. 16); anteroapical seta and all setae on dorsal surface of t_2 somewhat longer (Fig. 15) than in male. $t_2 : mt_2$ = 1.63–1.95. Wing measurements: length 1.83–2.46 mm, width 0.77–1.05 mm, C-index = 0.87–1.06, rm\dm-cu : dm-cu = 2.85–3.75. Preabdominal terga shorter, more transverse and becoming narrower posteriorly, T1+2 widest and longest and with some microtomentum, while T3–T5 almost glabrous and strongly shining; T1+2–T4 similarly setose as in male; T5 unmodified, simply trapezoidal, with setae at posterior margin shorter. Preabdominal sterna unmodified, simple, sparsely and shortly setose and distinctly brownish grey microtomentose, subshiny. S1+2 smallest and dark pigmented only in posterior half; S3–S5 subequal in length but becoming wider posteriorly or S4 as broad as S5; S3 trapezoidal (wider posteriorly); S4 and S5 transversely sub-oblong; all these sclerites blackish brown and shining.

Postabdomen (Figs 17–19) telescopically retractable, basally (6th segment) markedly narrower than preabdomen at 5th segment. 6th segment (both T6 and S6) distinctly wider than 7th segment in contrast to those of *H. bequaerti*. T6 wide and short, transversely trapezoidal, with pale-pigmented anterior and (wider) posterior marginal stripe (Fig. 17), setose at lateral and posterior margins, with longest setae in posterior corners; T7 distinctly narrower than T6 and reaching farther onto lateral side (Fig. 19), with small unpigmented anteromedial area and setosity restricted to posterior margin (Fig. 17). T8 as long as T7 but dorsomedially narrowly depigmented and appearing divided into two dark sclerites (Fig. 17), in contrast to T8 of both *H. bequaerti* and *H. erymantha*. T10 transversely subtriangular (Fig. 17), shorter than those of *H. bequaerti* and *H. erymantha*), pigmented (darkest anterolaterally) except for posterior corner,

Figure 14. *Herniosina calabra* sp. nov., female laterally (paratype). Body length ~ 2.2 mm.

with a pair of long setae, some fine setulae and micropubescent on almost entire surface. S6 somewhat wider, shorter (more transverse), slightly paler and more setulose than S7 (Fig. 18). S7 dark-pigmented except for posterior marginal stripe and with 4 longer and several short setae at posterior margin. S8 (Figs 18, 19) reduced, short but wider than those of *H. bequaerti* and *H. erymantha*, strikingly convex at anterior margin where densely micropubescent (cf. Fig. 19), otherwise with only 6–8 short setae. S10 reduced to distinctive transverse (in ventral view sinuous) sclerite, being medially depigmented (Fig. 18) but laterally blackish brown and posterodorsally rectangularly incised (Fig. 19), which is also visible in dorsal view (Fig. 17). S10 densely micropubescent and with a few setae including 1 long pair. Spermathecae 2+1 (Fig. 20) blackish brown, pyriform with conical bases, most resembling those of *H. erymantha*, sharing with the latter distally ringed conical bases, dark thickened apex and terminal parts of ducts of paired spermathecae connected rather far from their bodies; however, spermathecae of *H. calabra* are more robust, with wider basal conical parts. Cerci (Figs 17–19) more robust than those of *H. bequaerti* but much longer and narrower than

those of *H. erymantha*, each bearing 1 dorsal preapical and 1 apical setae, both very long and sinuate, apart from other shorter setosity and dense micropubescence.

Remarks. *Herniosina calabra* sp. nov. seems to be morphologically intermediate between *H. bequaerti* and *H. erymantha*. Although seemingly more similar to *H. erymantha* (smaller body size, shorter male T5 and S8, male S5 with deeply forked medial process, anterior process of male cercus long and robust, gonostylus ventrally rounded, not emarginate, spermathecae with conical basal part distally ringed) it is probably most closely related to *H. bequaerti*. Sister-species relationship of *H. calabra* and *H. bequaerti* seems to be particularly demonstrated by the following putative synapomorphies: very similar construction of the male aedeagal complex, including the short distiphallus (with both lateral lobes and unpaired ventral process short) and surprisingly similarly formed, short and robust postgonite. In the female postabdomen there is also a shared synapomorphy: the modified (posterodorsally more or less incised) lateral part of S10 (cf. Fig. 19 and Fig. 42).

The new species can be easily separated from all known congeners only by postabdominal characters. The most species-specific are as follows: the long, slender and deeply forked medial process of male S5 (Fig. 7); the male S8 with digitiform lobes on both sides of lateral slit (Fig. 3); the gonostylus with a posteromedial tooth (Fig. 10), the male cercus with anterior (more lateral) lobe with apex bent outwards (Fig. 9); the postgonite short and with robust apex (Fig. 13); the lateral part of female S10 dark-pigmented and with posterodorsal rectangular incision (Fig. 19). Moreover, the combination of female T8 medially narrowly depigmented with short T10 and relatively long slender cerci (see Fig. 17) is also very characteristic.

Biology. The entire type series of *H. calabra* sp. nov. (21 specimens) was collected (aspirated by a pooter) in May under *Juncus* tufts (Fig. 22) growing under alder trees surrounding a small creek in a montane meadow (Fig. 21). The sphaerocerid community co-occurring with *H. calabra* in and under these tufts of rush (based on collected specimens) proved to be relatively rich and contained the following 15 species: Copromyzinae: *Lotophila atra* (Meigen, 1830) 2♂3♀, Sphaerocerinae: *Sphaerocera curvipes* Latreille, 1805 2♂2♀, Limosininae: *Gigalimosina flaviceps* (Zetterstedt, 1847) 2♂, *Limosina silvatica* (Meigen, 1830) 5♂3♀, *Opacifrons coxata* (Stenhammar, 1855) 1♀, *Pteremis fenestralis* (Fallén, 1820), 4♂4♀, *Pullimosina* (*Pullimosina*) *heteroneura* (Haliday, 1836) 2♀, *P.* (*P.*) *pullula* (Zetterstedt, 1847) 3♀, *P.* (*P.*) *vulgesta* Roháček, 2001 1♂, *Puncticorpus cribratum* (Villeneuve, 1918) 1♂1♀, *Spelobia clunipes* (Meigen, 1830) 2♂, *S. palmata* (Richards, 1927) 1♀, *S. talparum* (Richards, 1927) 1♂1♀, *S.* sp. cf. *talis* Roháček, 1983 1♂ and *Terrilimosina schmitzi* (Duda, 1918) 1♀. This assemblage included largely saprophagous terricolous species (such as *H. calabra*, *G. flaviceps*, *Limosina silvatica*, *Pteremis fenestralis*, *Pullimosina* species, *Puncticorpus cribratum*, *T. schmitzi*) but also a few microcavernicolous species (*Spelobia talparum*, *S.* sp. cf. *talis*) and some ubiquitous, predominantly coprophagous, species (*Lotophila atra*, *Sphaerocera curvipes*, *Spelobia clunipes*). The presence of the latter two groups indicates that there could also be some droppings of small mammals in the detritus. This is for the first time that a species of *Herniosina* has been found under tufts of a graminoid plant. However, rotting leaves of alder were also present under tufts of *Juncus* sp. ex-

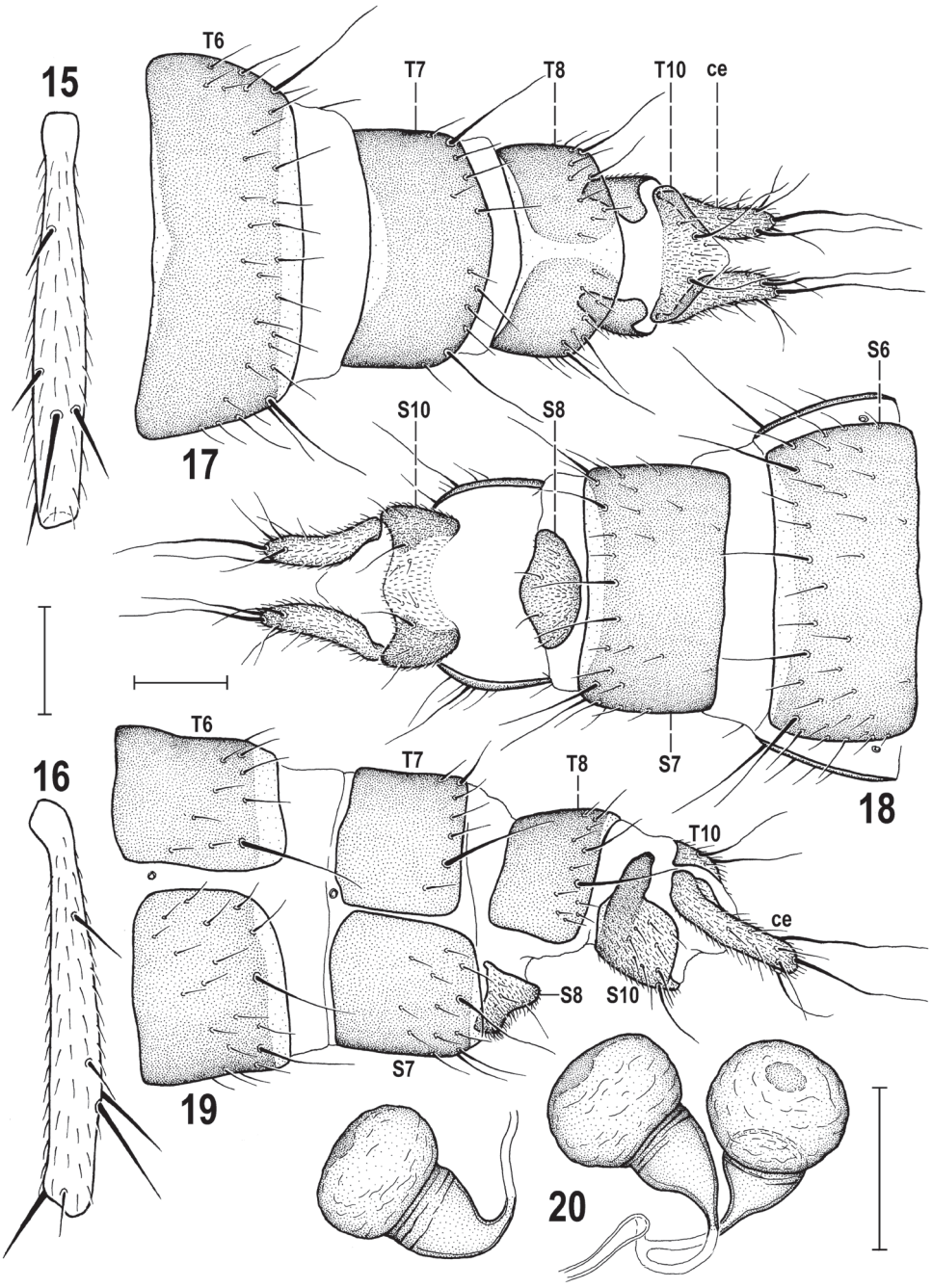

Figures 15–20. *Herniosina calabra* sp. nov., female paratypes. **15** Mid tibia, dorsally **16** ditto, anteriorly **17** postabdomen, dorsally **18** ditto, ventrally **19** ditto, laterally **20** spermathecae. Abbreviations: ce – cercus, S – sternum, T – tergum. Scale bars: 0.3 mm (**15, 16**); 0.1 mm (**17–20**).

Figures 21–22. Habitat of *Herniosina calabra* sp. nov. **21** General view of the habitat in Serre Calabresi at Mongiana, alder trees and herbaceous undergrowth surrounding a small creek (25.v.2018) **22** *Juncus* tuft, a microhabitat of the species.

amined (see Fig. 22), which indicate more resemblance to a leaf-litter association as known in most other *Herniosina* species (cf. Roháček 2016).

Distribution. Hitherto only known from S. Italy (Calabria).

***Herniosina erymantha* Roháček, 2016**
Figs 23–30

Herniosina erymantha Roháček, 2016: 80 [male only, phylogenetic notes, illustr.]. Type locality: Greece, Peloponnese, Alepochori 0.5 km SE.

Type material. ***Holotype*** ♂ labelled: "GREECE: NW Peloponnese: Alepochori 0.5 km SE 37°58'57"N, 21°48'10"E", "590 m, 27.5.2015, sifting leaves under *Platanus*, J. Roháček leg.", "Holotypus ♂ *Herniosina erymantha* sp. n., J. Roháček det. 2016" (red label). The specimen is dry-mounted on pinned triangular card, with left wing and abdomen detached, genitalia dissected and all removed parts preserved in glycerine in coalesced plastic tube pinned below the specimen (SMOC).

Other material examined. Greece: SW Peloponnese: Taygetos Mts, Nedousa 0.5 km W, 37°08'35"N, 22°13'42"E, 665 m, sweeping vegetation along brook & spring, 5.x.2017, 1♂ 3♀, 9.x.2017, 1♀ (genit. prep.); Taygetos Mts, Artemisia 3 km NW, Nedonas River, 37°07'01"N, 22°12'17"E, 390 m, sweeping riverside vegetation, 5.x.2017, 2♂ (1♂ genit. prep.); Taygetos Mts, Artemisia 1 km E, 37°05'47"N, 22°14'27"E, 655 m, sweeping vegetation along brook, 7.x.2017, 1♂, 9.x.2017, 1♀ (genit. prep.); Taygetos Mts, Saidona 1.5 km NE, 36°53'16"N, 22°17'59"E, 820 m, sweeping vegetation along brook, 8.x.2017, 1♂ (genit. prep.), all J. Roháček leg. (SMOC).

Supplementary description. Male (Fig. 23). Total body length 1.79–2.46 mm. ***Head.*** Cephalic chaetotaxy: 3 or 4 relatively short ifr, subequal in length or the middle pair longer. Gena high, usually reddish-brown only anteriorly, sometimes on most of genal surface. Third antennal segment with ciliation on apex as long as longest cilia on arista.

Thorax. Scutellum relatively large and long (1.5 ~ as wide as long), rounded triangular, with dense fine microsculpture on flat dorsal surface. Thoracic chaetotaxy: 1 or 2 stpl, posterior long, anterior reduced to microseta or absent.

Legs. f_2 with a long row of 6–8 curved but relatively short ventral setae in basal half to two-thirds. $t_2 : mt_2 = 1.83–1.90$.

Wing. Discal cell (dm) variable, relatively short to medium long, distally usually less tapered than in most relatives, with small process of M beyond dm-cu being continued by a venal fold; posterior outer corner of dm obtuse-angled to rounded, sometimes with small remnant of CuA_1. Wing measurements: length 1.87–2.38 mm, width 0.77–1.01 mm, C-index = 0.88–1.09, rm\dm-cu : dm-cu = 2.62–3.15.

Abdomen. Male S5 (Fig. 37) with medial forked process in lateral view knob-like, distinctly shorter but much more robust (Fig. 38) than that of *H. calabra* (Fig. 36).

Genitalia. Epandrium besides a group of longer and stronger setae laterally and lateroventrally usually also with 1 longer dorsolateral seta which can sometimes be reduced (as is in the holotype, see Roháček 2016: figs 20, 21). Gonostylus (Fig. 41) with posterodorsal corner broadly rounded, never tooth-like and projecting.

Female (Fig. 24). Similar to male unless mentioned otherwise. Total body length 2.06–2.52 mm. f_2 ventrally without thicker curved setae, simply setose including 1 long fine basal seta; also t_2 ventrally finely setulose but with 1 long va seta and anter-

Figure 23. *Herniosina erymantha* Roháček, 2016, male laterally (Greece: Peloponnese). Body length ~ 2.4 mm.

oapical seta longer than in male (Fig. 25) and longer than in female *C. calabra*; setae on dorsal surface of t_2 (Fig. 26) also longer than in male, particularly as regards distal posterodorsal seta. t_2 : mt_2 = 1.71–1.80. Wing measurements: length 1.91–2.34 mm, width 0.83–0.99 mm, C-index = 0.94–1.07, rm\dm-cu : dm-cu = 2.92–3.46. Preabdominal terga shorter, more transverse and becoming narrower posteriorly, similarly setose as in male. T1+2 widest and longest, covered by sparse but distinct microtomentum apart from posterior marginal stripe; T3–T5 subequal in length, strongly shining because T3 and T4 are glabrous and T5 has microtomentum reduced. Preabdominal sterna unmodified, simple, sparsely and shortly setose and distinctly brownish grey microtomentose, hence less shining than in male. S1+2 smallest, less transverse than S3–S5, darker pigmented only in posterior two-thirds (one fourth to half); S3 and S4 becoming slightly wider posteriorly (S4 largest) and both slightly trapezoidal (wider

Figure 24. *Herniosina erymantha* Roháček, 2016, female laterally, with a mite on thoracic pleuron (Greece: Peloponnese). Body length ~ 2.2 mm.

posteriorly); S5 transversely suboblong, somewhat narrower and shorter than S4; all these sclerites dark brown.

Postabdomen (Figs 27–29) telescopically retractable but broader than in *H. bequaerti* or *H. calabra*, particularly as regards 7th and 8th segments when compared with width of 5th abdominal segment. T6 wide and short, transversely oblong, with pale-pigmented posterior marginal stripe (Fig. 27), sparsely setose at posterior and lateral margin, with 1 long seta in each posterior corner; T7 only slightly narrower than T6 (Fig. 27) but reaching farther onto lateral side (Fig. 29), sparsely setose only at posterior margin and with very narrowly unpigmented posterior margin. T8 shorter and narrower than T7, all dark-pigmented or only narrowly paler at posterior margin medially (Fig. 27). T10 shortly pentagonal, rounded laterally, less transverse than that of *H. calabra* but shorter than that of *H. bequaerti*, pale-pigmented only anteriorly and laterally, and dorsally with a pair of long setae, a few fine setulae and entirely covered by micropubescence (Fig. 27). S6 wider, more transverse and more densely setulose than S7, dark-pigmented except for posterior margin (Fig. 28), with 4 or 6 long posterior setae. S7 also dark but with narrowly unpigmented anterior margin (Fig. 28) and with 4 long (those in medial pair close to each oth-

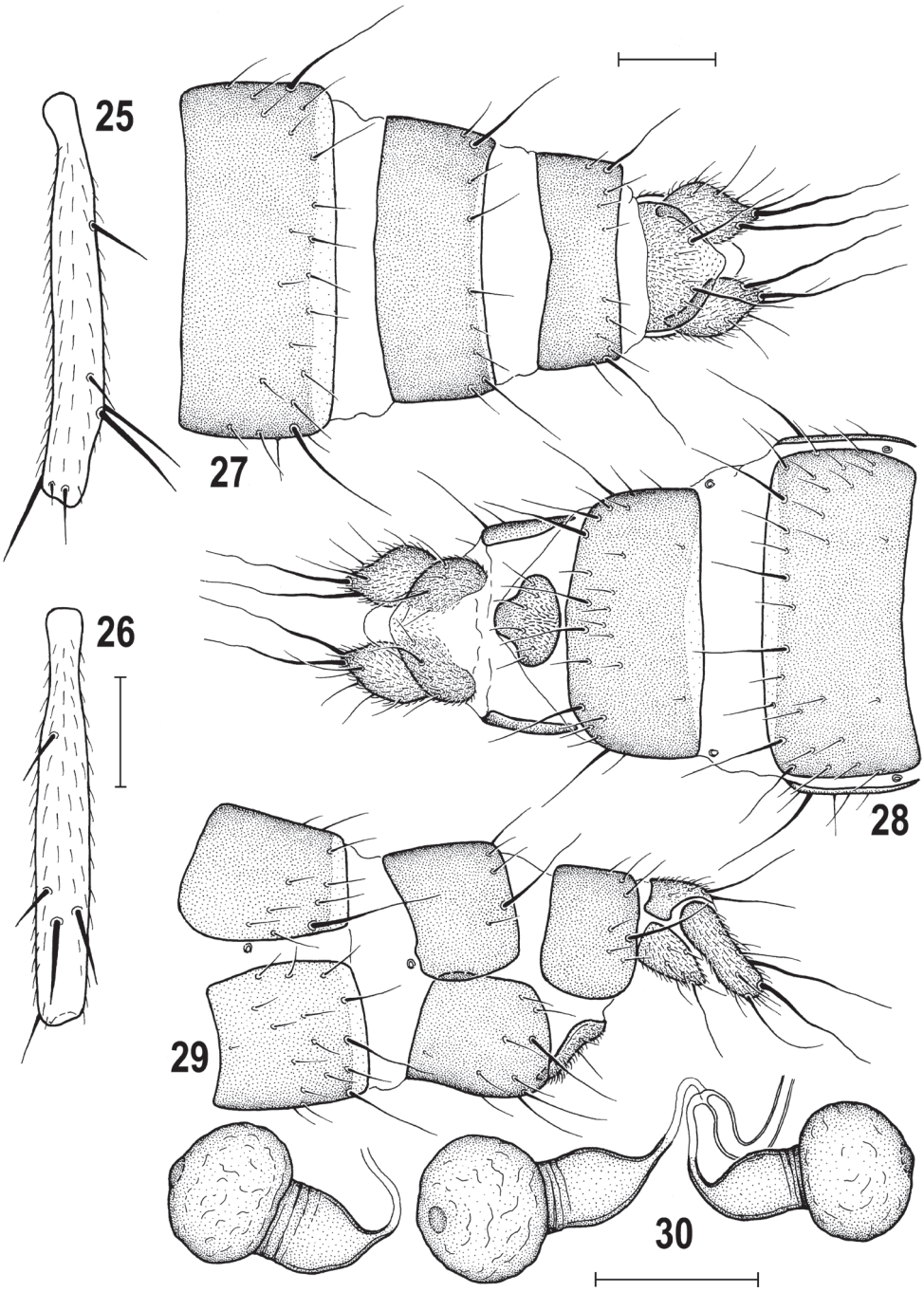

Figures 25–30. *Herniosina erymantha* Roháček, 2016, female (Greece: Peloponnese). **25** Mid tibia, anteriorly **26** Ditto, dorsally **27** postabdomen, dorsally **28** ditto, ventrally, **29** ditto, laterally, **30** spermathecae. Scale bars: 0.3 mm (**25, 26**); 0.1 mm (**27–30**).

Figures 31–32. Habitat of *Herniosina erymantha* Roháček, 2016. **31** valley of montane brook surrounded by *Platanus* trees near Nedousa village in Taygetos Mts (Greece: Peloponnese) (5.x.2017) **32** *Platanus* growth near brook near Artemisia village in Taygetos Mts with the Czech dipterists J. Starý (on left) and M. Vála (on right) in foreground (9.x.2017).

er) setae in addition to sparse short setae in posterior half. S8 (Figs 28, 29) small, narrower than that of *H. calabra*, having posterior half tapered, with several fine setae (4 longer) and distinctive micropubescence, particularly anteromedially. S10 reduced to short, V-shaped, micropubescent and setose sclerite being medially depigmented to interrupted (Fig. 28), with lateral pigmented parts simple (Fig. 29) in contrast to those of *H. calabra*. Spermathecae 2+1 (Fig. 30) blackish brown, elongate pyriform, most resembling those of *H. calabra* but with basal conical parts narrower. Cerci (Figs 27–29) markedly different from those of both *H. calabra* and *H. bequaerti*, unusually short and robust (more so than in *H. hamata* Roháček, 2016), apically conical and dorsoventrally somewhat flattened, each with 1 dorsal preapical and 1 apical seta long sinuate and 1 ventral preapical seta curved (apart form a number of shorter setae), and with dense micropubescence.

Remarks. *Herniosina erymantha* sp. nov. has only been known from the male holotype (Roháček 2016). A series of specimens recorded here enabled the description of the male to be supplemented and to add the first description of the female. As mentioned above (see Remarks under *H. calabra*), *H. erymantha* seems to be most closely allied to the sister-pair *H. bequaerti* – *H. calabra*. This relationship can now also be confirmed by the female postabdominal characters, including the similar formation of female S8 and, particularly, by the medially depigmented (to almost interrupted) S10 (cf. Fig. 28).

On the other hand, female *H. erymantha* can be easily distinguished from females of both its relatives (and also from all other congeners) by the unusually robust cerci (Fig. 27) and the detailed shape of S8 and S10 (Fig. 28).

Biology. Almost all newly obtained specimens of *H. erymantha* were swept from above decaying leaf-litter and sparse vegetation under *Platanus* trees in valleys of montane brooks in the Taygetos Mts (Figs 31, 32), usually mostly in humid places (shores of brooks, springs). Because the holotype was sifted from dead leaves of *Platanus* in a similar montane habitat in the Erimanthos Mts (see Roháček 2016) it is very probable that its larvae develop in this microhabitat. Adults are now known to occur in May (Roháček 2016) and October (present data).

Distribution. Hitherto only known from Greece: Peloponnese.

An updated key to the identification of *Herniosina* species

1 Male **2**
– Female **7**
2(1) S1+2 with a strong protruding bulge (Figs 3, 23). **3**
– S1+2 only slightly protruding (Roháček 2016: figs 41, 47, 51). **6**
3(2) S5 with a single long medial process that is apically more or less forked (Figs 33, 35, 37); gonostylus in lateral view sub-oblong (Figs 39–41), at most ventrally emarginate (Fig. 39); phallapodeme and hypandrial rod long to very long (Figs 8, 13); posteromedial process of cercus small, with apex more acute (Figs 8, 9); funnel-shaped apex of distiphallus more robust and postgonite with apex simple (Figs 12, 13) **4**
– S5 with 2 small digitiform medial processes (Roháček 2016: fig. 36); gonostylus in lateral view with large posteroventral lobe (Roháček 2016: figs 28, 29); both

phallapodeme and hypandrial rod short (Roháček 2016: fig. 28); posteromedial process of cercus robust, with apex bluntly rounded (Roháček 2016: figs 28, 30); funnel-shaped apex of distiphallus slender and postgonite with apex curved medially (Roháček 2016: fig. 27)..... ***H. horrida*** **(Roháček, 1978)**

4(3) S5 with medial process long and robust, in lateral view sinuous (Fig. 34), elongate, conical and apically shortly forked (Fig. 33); gonostylus ventrally emarginate (Fig. 39, arrow); cercus with both processes relatively short and both apically pointed (Roháček 2016: figs 4, 5)..... ***H. bequaerti*** **(Villeneuve, 1917)**

– S5 with medial process either short and in lateral view pestle-shaped (Fig. 38) or slender and in lateral view recurved (Fig. 36), always more or less flattened and apically deeply forked (Figs 35, 37); gonostylus ventrally slightly to distinctly rounded (Figs 40, 41); cercus with only medial process short and somewhat pointed; its lateral process very long and robust, apically slightly dilated in lateral view (Roháček 2016: figs 20, 21, Figs 8, 9)..... **5**

5(4) S5 with medial forked process short and robust, pestle-shaped in lateral view (Figs 37, 38); gonostylus without acute posterodorsal corner (Fig. 41) but with long slender curved internal projection (Roháček 2016: fig. 22, Fig. 41 arrow); distiphallus with ventral and lateral lobes relatively long (Roháček 2016: fig. 26) and postgonite longer, slender, with bent but blunt apex (Roháček 2016: fig. 24); f_3 with long row of 6–8 ventrobasal curved setae (Roháček 2016: fig. 18). ..... ***H. erymantha*** **Roháček, 2016**

– S5 with medial forked process long and slender (Fig. 35), digitiform and recurved in lateral view (Fig. 36); gonostylus with acute posterodorsal corner (Figs 10, 40, arrow) and with short internal projection (cf. Figs 9, 40); distiphallus with ventral and lateral lobes short (Fig. 12) and postgonite short, robust (Fig. 13); f_3 with short row of 4–6 ventrobasal curved setae (Fig. 5) .. ..***H. calabra*** **sp. nov.**

6(2) Preabdominal sterna sparsely setose (Roháček 2016: fig. 41); cercus with medial process very long, robust, digitiform and projecting posteroventrally; its lateral process distally slender and laterally provided with a robust long seta arising on small lobe (Roháček 2016: figs 37, 38); gonostylus with lobe-like posteroventral part and internally with a small keel-like process (Roháček 2016: fig. 39); phallophore anteriorly slender, ventromedial lobe of distiphallus simple (unmodified) and postgonite rather straight, with simple apex (Roháček 2016: fig. 40). ..... ***H. pollex*** **Roháček, 1993**

– Preabdominal sterna more densely setose (Roháček 2016: fig. 51); cercus without medial process and its lateral process long, slender, apically somewhat dilated, with long seta arising more basally (Roháček 2016: figs 49, 50); gonostylus with a robust posterior internal hook-like process directed ventrally and its posteroventral lobe smaller, knob-like (Roháček 2016: fig. 56); phallophore anteriorly thicker and short, ventromedial lobe of distiphallus projecting far posteriorly and of unusual shape (Roháček 2016: fig. 52) and postgonite proximally dilated and with curved apex (Roháček 2016: fig. 55)..... ***H. hamata*** **Roháček, 2016.**

7(1) T6, T7, S6 and S7 shorter and more transverse (Roháček 2016: figs 58, 62); T8 dorsomedially interrupted into 2 lateral sclerites (Roháček 2016: fig. 58); S8 with membranous window in posterior half (Roháček 2016: figs 62, 64); spermathecae bulbous, without separate basal conical part (Roháček 2016: figs 59, 60)..... ***H. hamata*** **Roháček, 2016**

– T6, T7, S6 and S7 longer, narrower, less transverse (Figs 17, 19, 27, 29); T8 dorsomedially complete (Figs 27, 42), at most medially depigmented (Fig. 17); S8 entirely sclerotised and pigmented (Figs 18, 28); spermathecae pyriform, with distinct basal conical part (Figs 20, 30)..... **8**

8(7) S10 divided into 2 lateral sclerites (Roháček 2016: fig. 8) or medially desclerotised and depigmented (Figs 18, 28); S8 smaller, of various shape (Roháček 2016: fig. 8, Figs 18, 28)..... **9**

– S10 undivided, horseshoe-shaped (Roháček 2016: figs 33, 46); S8 larger, simple, plate-shaped (Roháček 2016: figs 33, 46)..... **11**

9(8) Cerci short and robust (Figs 27, 28); lateral part of S10 simple, posterodorsally without emargination or incision (Fig. 29). .... ***H. erymantha*** **Roháček, 2016**

– Cerci long and slender (Figs 17, 19, 42, 43); lateral part of S10 posterodorsally emarginated to incised (Figs 19, 42)..... **10**

10(9) T6 narrow, hardly wider than T7 (Roháček 2016: fig. 7); T8 dorsomedially simply pigmented, at most with small anteromedial pale-pigmented area (Fig. 43); T10 longer triangular (Fig. 43); lateral parts of S10 posterodorsally slightly emarginated (Figs 42, 43); spermatheca with conical base not ringed distally and its apex with small invagination (Fig. 44) ....***H. bequaerti*** **(Villeneuve, 1917)**

– T6 broad, wider than T7 (Fig. 17); T8 dorsomedially narrowly depigmented (Fig. 17); T10 short, transversely subtriangular (Fig. 17); lateral parts of S10 posterodorsally with rectangular incision (Fig. 19); spermatheca with conical base distally ringed and its apex with only terminal thickening (Fig. 20)..... .....***H. calabra*** **sp. nov.**

11(8) T10 longer, elongately triangular (Roháček 2016: fig. 32); S8 transversely suboval, with only 1 pair of setae (Roháček 2016: fig. 33); cercus longer (Roháček 2016: fig. 34). .....***H. horrida*** **(Roháček, 1978)**

– T10 shorter, transversely subtriangular (Roháček 2016: fig. 43); S8 more trapezoidal and with 1 pair of longer plus 1–2 pairs of short setae (Roháček 2016: fig. 46); cercus shorter (Roháček 2016: fig. 45) ..... ***H. pollex*** **Roháček, 1993**

Discussion

The monophyly of *Herniosina* was demonstrated by Roháček (2016) and its affiliation within the *Limosina* group of genera (sensu Roháček 1982) was confirmed by Roháček and Marshall (2017). Although its closest relationships with *Apteromyia* Vimmer, 1929 (suggested by Roháček 2016: 102) is somewhat questioned by a conflict of the pres-

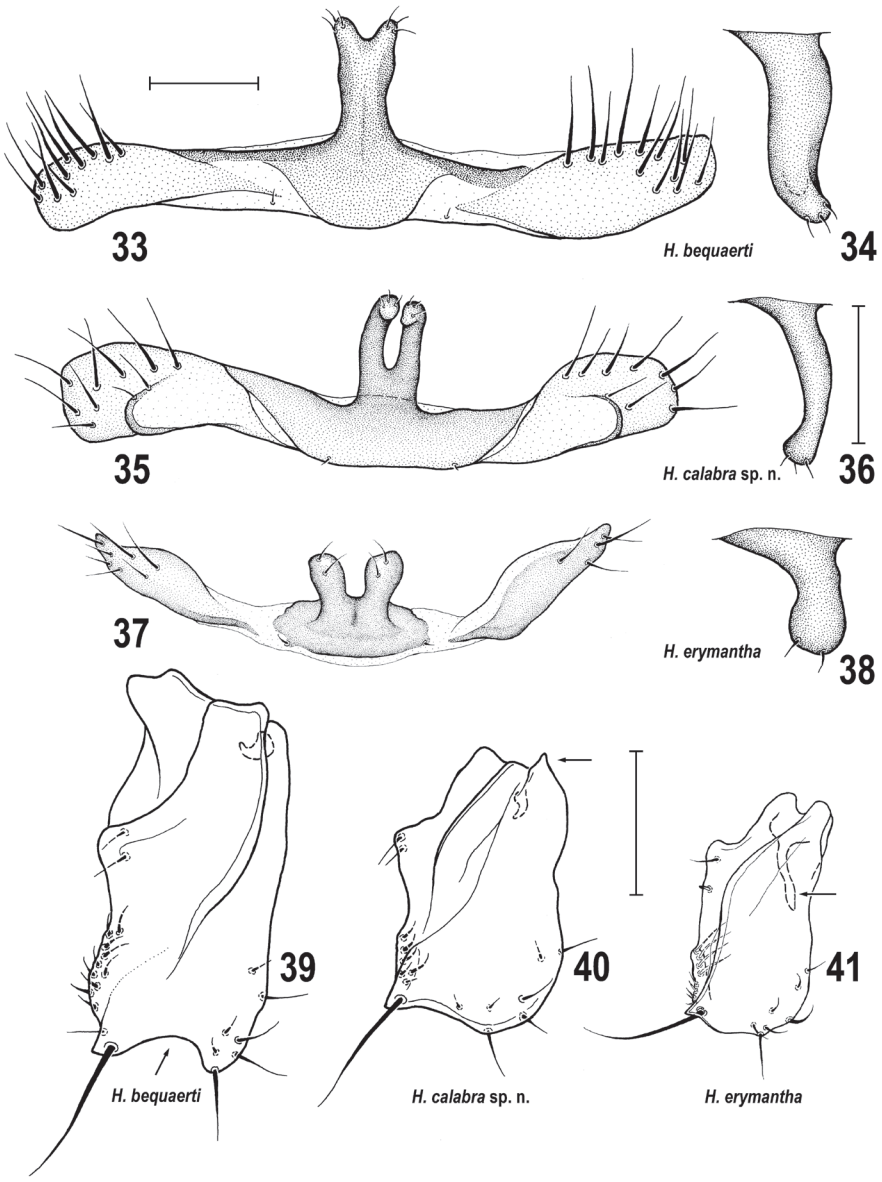

Figures 33–41. *Herniosina* species, comparison of male characters. **33** *H. bequaerti*, S5, ventrally, **34** same species, process of S5, laterally **35** *H. calabra* sp. nov., S5, ventrally **36** same species, process of S5, laterally **37** *H. erymantha*, S5, ventrally **38** same species, process of S5, laterally **39** *H. bequaerti*, gonostylus, laterally **40** *H. calabra* sp. nov., gonostylus, laterally **41** *H. erymantha*, gonostylus, laterally. All scale bars 0.1 m.

ence of some putative synapomorphies of *Volumosina* Roháček & Marshall, 2017 and *Apteromyia* (cf. Roháček and Marshall 2017: 459), the sister group relationship of *Herniosina* and *Apteromyia* remains as the most probable (Roháček 2016). Particularly, the peculiar modifications of the aedeagal complex (distiphallus with unpaired

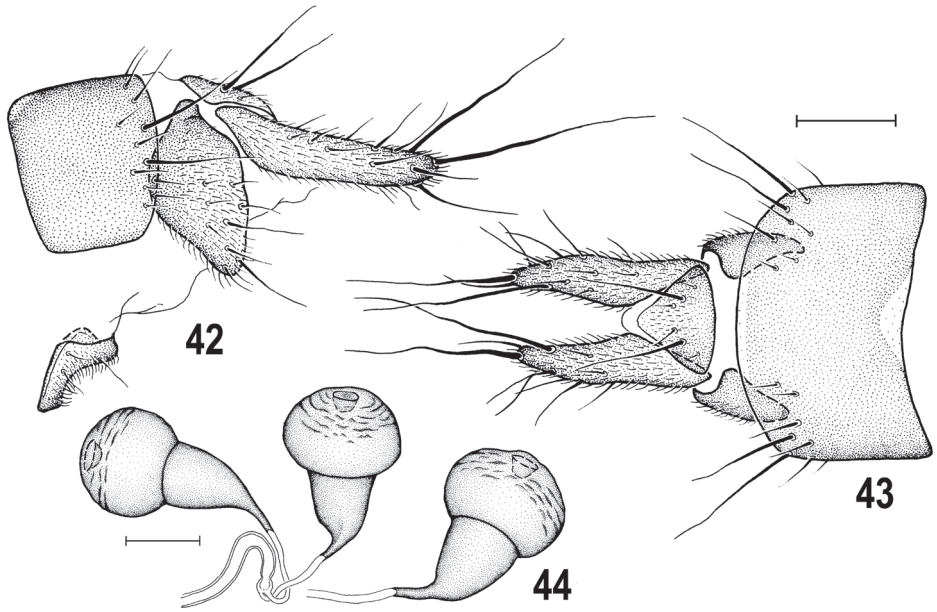

Figures 42–44. *Herniosina bequaerti* (Villeneuve, 1917), female (Czech Republic: Bohemia). **42** Apex of postabdomen, laterally **43** ditto, dorsally **44** spermathecae. Scale bars: 0.1 mm (**42, 43**); 0.05 mm (**44**).

ventromedial lobe projecting posteriorly; phallophore anteriorly slender and elongate, projecting, movably attached to dorsal side of distiphallus) and the male cerci (formed as robust compact processes below anal fissure) are possible unique synapomorphies of these two genera.

The addition of *Herniosina calabra* sp. nov. did not affect the concept of the genus which remains a compact group of similar species, differing mainly by the structures of the male and female terminalia. This new species seems to be most closely allied to *H. bequaerti* and *H. erymantha*, and, consequently the hypothesis of the relationships of species within *Herniosina* has to be changed as follows. *Herniosina hamata* is considered a sister-taxon to the five other congeners which belong to a monophyletic group supported by the following putative synapomorphies: male preabdominal sclerites with setosity reduced; male cercus modified to 2 (lateral and medial) processes; gonostylus with dorsal internal projection; spermathecae pyriform, with distinct conical basal part. *Herniosina pollex*, with the bulge of the male S1+2 small (a plesiomorphy shared with *H. hamata*) is considered a sister-group to a clade with *H. horrida*, *H. erymantha*, *H. calabra* and *H. bequaerti* being supported by 2 synapomorphies (male S1+2 strongly bulging; gonostylus with slender dorsal internal projection). *Herniosina horrida* (having male S5 with a pair of small posteromedial projections = a plesiomorphy shared with *H. hamata* and *H. pollex*) seems to branch off the remaining triplet formed by *H. erymantha*, *H. calabra*, and *H. bequaerti*. The close alliance of these three species

is supported not only by 3 synapomorphic features in the male terminalia (S5 with posteromedial distally forked projection; medial process of cercus small and apically pointed; funnel-shaped apex of distiphallus short and robust) but also by female S10 medially desclerotised or divided. Finally, *H. erymantha* is considered a sister-group to *H. calabra* – *H. bequaerti* pair, the latter being supported by similar formation of the aedeagal complex (distiphallus shortened, postgonite short and robust) and modified female S10 having lateral parts posterodorsally emarginated to incised.

Discovery of the new species, *H. calabra*, added new information to the general distribution of the genus *Herniosina*. The currently known distribution of the genus ranges from Spain in the west to Russia (Kabardino-Balkariya) in the east and from Iceland and Fennoscandia in the north to Spain, S. Italy, Cyprus and Israel in the south (Roháček et al. 2001; Marshall et al. 2011, present data). The formerly recognised distribution of *Herniosina* in the eastern Mediterranean, viz. in S. Greece (Roháček 2016: *H. erymantha* in northern Peloponnese), Cyprus (Roháček 2016: *H. hamata* in Troodos Mts), and Israel (Papp and Roháček 1988: *Herniosina* sp. in Mt. Hermon) is confirmed by new records of *H. erymantha* from southern Peloponnese (Taygetos Mts) and there is a new occurrence in the middle Mediterranean, viz. from S. Italy (*H. calabra* in Calabria: Serre Calabresi Mts). *Herniosina bequaerti* remains the most widely distributed species occurring throughout Europe (including Iceland) but obviously absent in southeastern parts (cf. Séguy 1963; Roháček 2016). *Herniosina pollex* seems also to be widespread because it is known not only from Central Europe (Czech Republic, Slovakia) but also from the Russian Caucasus (Kabardino-Balkariya), see Roháček (2016). Other known species are probably more restricted. *Herniosina horrida* is to date only known from central Europe, *H. calabra* from Italy (Calabria), *H. erymantha* from Greece (Peloponnese), *H. hamata* from Cyprus, and *Herniosina* sp. from Israel. Nevertheless, it is probable that these species are in fact more widespread. Because they are terricolous and cavernicolous, all *Herniosina* species are seldom collected by non-specialists, and, therefore, they are poorly represented in the museum collections. This is particularly true for the Mediterranean and other southern parts of the W. Palaearctic region.

Acknowledgements

It is an agreeable duty to thank my companions on collecting trips to the Calabria (2018) and Peloponnese (2017), M. Vála and J. Starý (Olomouc, Czech Republic) (see Fig. 32), for their kind assistance during field work in these parts of the Mediterranean. I am also grateful to P. Chandler (Melksham, England) for comments and English corrections of this paper and to both reviewers for helpful criticism. This research of Sphaeroceridae was financially supported by the Ministry of Culture of the Czech Republic by institutional financing of long-term conceptual development of research institution (the Silesian Museum, MK000100595).

References

Marshall SA, Roháček J, Dong H, Buck M (2011) The state of Sphaeroceridae (Diptera: Acalyptratae): a world catalog update covering the years 2000–2010, with new generic synonymy, new combinations, and new distributions. Acta Entomologica Musei Nationalis Pragae 51(1): 217–298. https://www.aemnp.eu/data/article-1323/1304-51_1_217.pdf

Papp L, Roháček J (1988) The Sphaeroceridae (Diptera) of Israel. Israel Journal of Entomology 21(1987): 77–109.

Roháček J (1982) A monograph and re-classification of the previous genus *Limosina* Macquart (Diptera, Sphaeroceridae) of Europe. Part I. Beiträge zur Entomologie, Berlin 32: 195–282. https://www.contributions-to-entomology.org/article/view/1178/1177

Roháček J (1983) A monograph and re-classification of the previous genus *Limosina* Macquart (Diptera, Sphaeroceridae) of Europe. Part II. Beiträge zur Entomologie, Berlin 33: 3–195. https://www.contributions-to-entomology.org/article/view/1184/1183

Roháček J (1993) *Herniosina* Roháček and *Minilimosina* Roháček of Europe: two new species, new records and taxonomic notes (Insecta, Diptera: Sphaeroceridae). Entomologische Abhandlungen, Staatliches Museum für Tierkunde in Dresden 55: 185–203.

Roháček J (1998) 3.43. Family Sphaeroceridae. In: Papp L, Darvas B (Eds) Contributions to a Manual of Palaearctic Diptera. Vol. 3., Higher Brachycera. Science Herald, Budapest, 463–496.

Roháček J (2016) *Herniosina* Roháček: revised concept, two new species, new key and atlas of male and female terminalia (Diptera, Sphaeroceridae). ZooKeys 609: 69–106. https://doi.org/10.3897/zookeys.609.9459

Roháček J, Marshall SA (2017) *Volumosina*, a new Nearctic genus for the rare old-growth forest fly *Herniosina voluminosa* Marshall (Diptera: Sphaeroceridae). Canadian Entomologist 149: 444–460. https://doi.org/10.4039/tce.2017.21

Roháček J, Marshall SA, Norrbom AL, Buck M, Quiros DI, Smith I (2001) World catalog of Sphaeroceridae (Diptera), Slezské zemské muzeum, Opava, 414 pp.

Séguy E (1963) Diptères hypogés recueillis par M. Paul A. Remy en Yugoslavie. Mémoires du Muséum National d'Histoire Naturelle, Paris (n.s.) (A) 18: 187–229. https://www.biodiversitylibrary.org/page/57329122#page/1/mode/1up

Zatwarnicki T (1996) A new reconstruction of the origin of eremoneuran hypopygium and its implications for classification (Insecta: Diptera). Genus 7: 103–175.